



"A STUDY OF SOME TETRAAZAMACROCYCLIC
COMPLEXES OF NICKEL(II) AND COPPER(II)"

A Thesis presented for the degree of
DOCTOR OF PHILOSOPHY
in THE UNIVERSITY OF ADELAIDE

by

DEWAN M.M. ABDUL HADI

B.Sc. (Hons.), University of Dacca, 1969

M.Sc., University of Dacca, 1970.

Department of Physical and Inorganic Chemistry,
University of Adelaide, Adelaide, S.A. 5001, Australia

MAY, 1981

TO

MY PARENTS

DECLARATION

This thesis contains no material previously submitted for a degree or diploma in any University, and to the best of my knowledge and belief, contains no material previously published or written by another person, except where due reference is given in the text.

(DEWAN M.M. ABDUL HADI)
May, 1981

ACKNOWLEDGEMENTS

I would like to thank my supervisor Dr. S.F. Lincoln and co-supervisor Dr. J.H. Coates for their interest, encouragement, guidance, help and criticisms during the course of this research work at the University of Adelaide.

Thanks to Dr. G.H. Searle for his encouragement and enlightening discussions during the preparation of ligands, to Dr. J.R. Rodgers and Dr. M.R. Snow for the structure determination of $[\text{Ni}(\text{Me}_4\text{12aneN}_4)\text{N}_3]\text{ClO}_4$ and $[\text{Ni}(\text{Me}_4\text{12aneN}_4)](\text{ClO}_4)_2$ and to Mr. E. Horn for the encouragement and reading the manuscript.

Thanks to Dr. J.P. Hunt and Dr. H.W. Dodgen for Oxygen-17 n.m.r. water exchange kinetic studies of the $[\text{Ni}(\text{12aneN}_4)(\text{OH}_2)_2]^{2+}$ system.

The assistance and friendship of my fellow research workers over the years have been greatly appreciated.

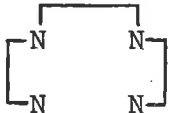
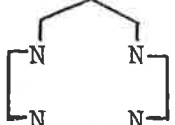
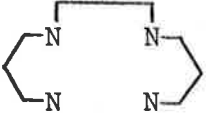
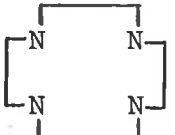
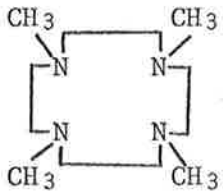
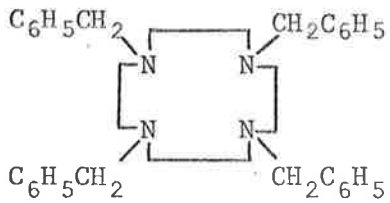
I am also thankful for the help from the workshop personnel of this department towards maintenance of apparatus.

A Commonwealth Postgraduate Scholarship is greatly acknowledged.

I am heavily indebted to my parents whose sacrifices and devotion during these years made this work possible.

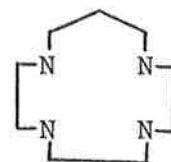
Finally, I wish to thank Miss K.A. Jones and Mrs. M. Wyatt for the quick and excellent typing of this thesis.

Glossary of Abbreviations for Ligands, Solvents etc.

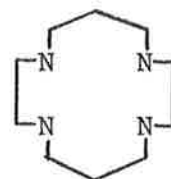
Abbreviations	Name	Structure or Formula
1. Me	methyl	-CH ₃
2. tb	tetrabenzyl	(C ₆ H ₅ CH ₂ -) ₄
3. tren	2,2',2''-triamino triethylamine	N(CH ₂ CH ₂ NH ₂) ₃
4. Me ₆ tren	2,2',2''-tri(N,N- dimethylamino) triethyl- amine	N(CH ₂ CH ₂ NMe ₂) ₃
5. dmf	N,N'-dimethylformamide	HCON(CH ₃) ₂
6. 2,2,2-tet or trien	1,4,7,10-tetra-azadecane	
7. 2,3,2-tet	1,4,8,11-tetra-aza- undecane	
8. 3,2,3-tet	1,5,8,12-tetra-aza- dodecane	
9. 12aneN ₄	1,4,7,10-tetra-azacyclo- dodecane	
10. Me ₄ 12aneN ₄	1,4,7,10-tetramethyl-1,4, 7,10-tetra-azacyclododecane	
11. tb12aneN ₄	1,4,7,10-tetrabenzyl-1,4, 7,10-tetra-azacyclododecane	

Abbreviations	Name	Structure or Formula
---------------	------	----------------------

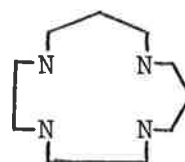
12. 13aneN₄ 1,4,7,10-tetra-azacyclo-
tridecane



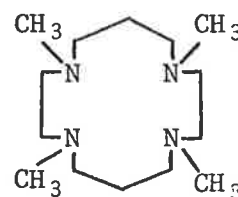
13. 14aneN₄ 1,4,8,11-tetra-azacyclo-
tetradecane



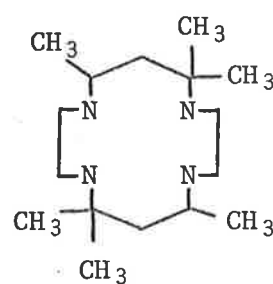
14. iso14aneN₄ 1,4,7,11-tetra-azacyclo-
tetradecane



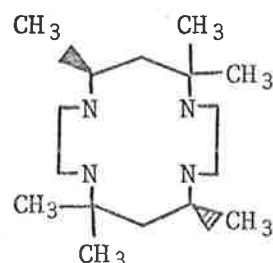
15. Me₄14aneN₄ 1,4,8,11-tetramethyl-
1,4,8,11-tetra-azacyclo-
tetradecane

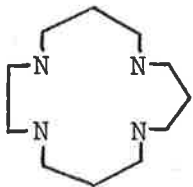
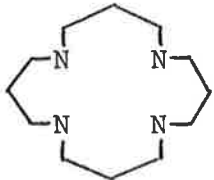
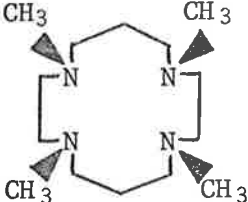
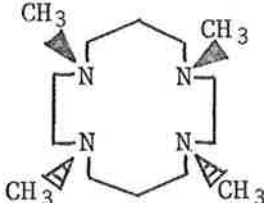


16. 1,7-CTH 5,7,7,12,14,14-hexa-
methyl-1,4,8,11-tetra-
azacyclo-tetradecane



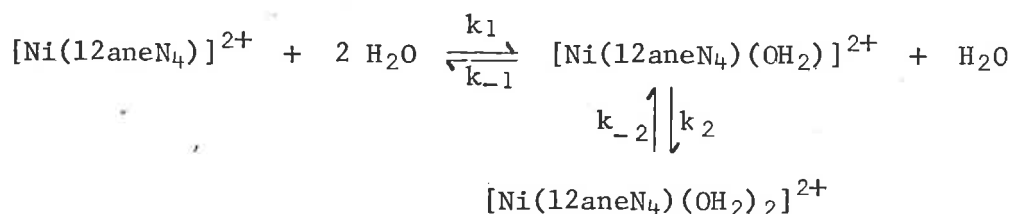
17. tet-a or meso 1,7-CTH meso-5,7,7,12,14,14-hexa-
methyl-1,4,8,11-tetra-
aza-cyclotetradecane



Abbreviations	Name	Structure or Formula
18. DMSO	dimethylsulphoxide	$(\text{CH}_3)_2\text{SO}$
19. k_{obs}	observed rate constant	-
20. n.m.r.	nuclear magnetic resonance	-
21. 15aneN ₄	1,4,8,12-tetraazacyclopentadecane	
22. 16aneN ₄	1,5,9,13-tetraazacyclohexadecane	
23. R.S.R.S.- Me ₄ 14aneN ₄	1,4,8,11-tetraazacyclopentadecane (four methyl groups on the same side of the macrocyclic plane)	
24. R.S.S.R.- Me ₄ 14aneN ₄	1,4,8,11-tetraazacyclopentadecane (two methyl groups on either side of the macrocyclic plane)	

ABSTRACT

The temperature and ionic strength dependence of high spin - low spin equilibrium constants of $[\text{Ni}(\text{12aneN}_4)](\text{ClO}_4)_2$, $[\text{Ni}(\text{Me}_4\text{12aneN}_4)](\text{ClO}_4)_2$, $[\text{Ni}(\text{13aneN}_4)](\text{ClO}_4)_2$ and $[\text{Ni}(\text{Me}_4\text{14aneN}_4)](\text{ClO}_4)_2$ are studied using uv/visible spectrophotometry and the results are reported. The temperature dependence of magnetic moments (using Evans method) of $[\text{Ni}(\text{12aneN}_4)](\text{ClO}_4)_2$ in 4.0 mol dm^{-3} aqueous LiClO_4 consistent with high spin - low spin equilibrium are also reported. The kinetic study of the system



in aqueous LiClO_4 solution is reported and k_1/k_{-1} is found to be rate determining in the establishment of the overall equilibrium between the square planar and octahedral species. Oxygen-17 n.m.r. water exchange kinetic studies (data obtained from J.P. Hunt and H.W. Dodgen) of the $[\text{Ni}(\text{12aneN}_4)(\text{OH}_2)_2]^{2+}$ system at 5.75, 11.5 and 13.2 MHz in 3.00 mol dm^{-3} aqueous LiClO_4 solution are summarised here. The high spin - low spin interconversion of $[\text{Ni}(\text{Me}_4\text{12aneN}_4)](\text{ClO}_4)_2$, $[\text{Ni}(\text{13aneN}_4)](\text{ClO}_4)_2$ and $[\text{Ni}(\text{Me}_4\text{14aneN}_4)](\text{ClO}_4)_2$ systems are studied in aqueous LiClO_4 solution using temperature jump technique. The temperature dependence of uv/visible spectral change of $[\text{Ni}(\text{tb12aneN}_4)\text{Cl}]\text{Cl}$ and $[\text{Ni}(\text{tb12aneN}_4)\text{NO}_3]\text{NO}_3$ systems are also reported. In the case of $[\text{Ni}(\text{Me}_4\text{12aneN}_4)](\text{ClO}_4)_2$ and $[\text{Ni}(\text{Me}_4\text{14aneN}_4)](\text{ClO}_4)_2$ systems in high aqueous LiClO_4 concentrations, the temperature dependence of spectral changes is explained in terms of isomerisations.

The stoichiometry of the complex formation between metal ions and ligands in water and N,N' -dimethylformamide (here after dimethylformamide) are studied using Job's method of continuous variation and one to one complex formation

is established in all cases except $[\text{Cu}(\text{tb}12\text{aneN}_4)_2](\text{ClO}_4)_2$ formation in dimethylformamide in which case one metal ion combines with two molecules of the ligand. The pK_a values of macrocyclic ligands and complexes as well as equilibrium constants between complexes and monodentate ligands are reported. Substitution reactions of different complexes with N_3^- are also studied.

The acid dissociations of $[\text{Ni}(12\text{aneN}_4)](\text{ClO}_4)_2$, $[\text{Cu}(12\text{aneN}_4)](\text{ClO}_4)_2$ and $[\text{Cu}(\text{Me}_412\text{aneN}_4)](\text{ClO}_4)_2$ are studied using uv/visible spectrophotometry and the curvature of the plot of k_{obs} VS $[\text{H}^+]$ in each case is explained in terms of the formation of different protonated species in the course of the acid dissociation. Different protonated species are expected to dissociate at different rates with the higher protonated species dissociating faster.

The rate of formation of $[\text{Ni}(12\text{aneN}_4)(\text{OH}_2)_2]^{2+}$ from $[\text{Ni}(\text{OH}_2)_6]^{2+}$ and 12aneN₄ is studied using uv/visible spectrophotometry and the possibility of an I_d mechanism is discussed. The reaction of $[\text{Ni}(12\text{aneN}_4)(\text{OH}_2)_2]^{2+}$ with NaOH is studied using stopped flow spectrophotometry and the results are discussed in terms of an isomerisation.

The rates of formation of $[\text{Ni}(\text{Me}_412\text{aneN}_4)]^{2+}$, $[\text{Ni}(\text{Me}_414\text{aneN}_4)]^{2+}$, $[\text{Cu}(\text{Me}_412\text{aneN}_4)]^{2+}$, $[\text{Cu}(\text{Me}_414\text{aneN}_4)]^{2+}$ and $[\text{Co}(\text{Me}_414\text{aneN}_4)]^{2+}$ in dimethylformamide are studied using stopped flow spectrophotometry. In the case of the $[\text{Ni}(\text{Me}_414\text{aneN}_4)]^{2+}$ system, the possibility of an I_d mechanism is discussed. In all cases, the first metal-nitrogen bond formation is expected to be rate determining followed by the other (three) metal-nitrogen bond formation.

The temperature dependence of high spin - low spin equilibrium constants of different nickel(II) complexes are studied in dimethylformamide and acetonitrile, and the results are compared with similar aqueous studies.

Different isomers of nickel(II) complexes with $\text{Me}_412\text{aneN}_4$ and $\text{Me}_414\text{aneN}_4$ are prepared under different conditions and their properties are studied in different solvents using uv/visible spectrophotometry. The molecular structures of $[\text{Ni}(\text{Me}_412\text{aneN}_4)\text{N}_3]\text{ClO}_4$ and $[\text{Ni}(\text{Me}_412\text{aneN}_4)](\text{ClO}_4)_2$,

related to this project, were determined by John R. Rodgers and the results are discussed.

Different macrocyclic ligands and their complexes with nickel(II) and copper(II) are prepared and characterised using infra-red spectral analysis, metal analysis, elemental analysis and n.m.r. spectral analysis. The magnetic moments in the solid state and in nitromethane solution of some of the nickel(II) complexes are measured using the Gouy method.

CONTENTS

CHAPTER ONE

Introduction

Page No.

1.1	Formation and Dissociation Reactions of Macrocyclic Complexes	2
1.1.1	The Macrocyclic Effect	2
1.1.2	Formation of Macrocyclic Complexes	4
1.1.3	Dissociation of Macrocyclic Complexes	9
1.2	High Spin-Low Spin Equilibrium	11
1.3	Substitution Reactions	19
1.4	Isomerisation	21
1.5	Kinetic Terminology	22
1.6	Objective of this Project	24
	References	26

CHAPTER TWO

Preparative Chemistry and Characterisation

2.1	Reagents and Materials	32
2.2	Preparation of Ligands:-	
	(a) 12aneN ₄	33
	(b) Me ₄ 12aneN ₄	36
	(c) tb12aneN ₄	39
	(d) 13aneN ₄	40
	(e) 14aneN ₄ and Me ₄ 14aneN ₄	42

2.3.1	Preparation of Complexes:-	
	(a) $[\text{Ni}(\text{12aneN}_4)](\text{ClO}_4)_2$	42
	(b) $[\text{Ni}(\text{Me}_4\text{12aneN}_4)](\text{ClO}_4)_2$ (ethanol water preparation)	43
	(c) $[\text{Ni}(\text{Me}_4\text{12aneN}_4)](\text{ClO}_4)_2$ (ethanol preparation)	43
	(d) $[\text{Ni}(\text{Me}_4\text{12aneN}_4)](\text{ClO}_4)_2$ (ethanol preparation using triethylorthoformate)	43
	(e) $[\text{Ni}(\text{Me}_4\text{12aneN}_4)(\text{dmf})](\text{ClO}_4)_2$ (dmf preparation)	44
	(f) $[\text{Ni}(\text{tb12aneN}_4)\text{Cl}]\text{Cl}$	44
	(g) $[\text{Ni}(\text{tb12aneN}_4)\text{NO}_3]\text{NO}_3$	44
	(h) $[\text{Ni}(\text{13aneN}_4)](\text{ClO}_4)_2$	44
	(i) $[\text{Ni}(\text{Me}_4\text{14aneN}_4)](\text{ClO}_4)_2$ (ethanol water preparation)	44
	(j) $[\text{Ni}(\text{Me}_4\text{14aneN}_4)](\text{ClO}_4)_2$ (ethanol preparation using triethylorthoformate)	44
	(k) $[\text{Ni}(\text{Me}_4\text{14aneN}_4)(\text{dmf})](\text{ClO}_4)_2$ (dmf preparation)	45
	(l) $[\text{Cu}(\text{12aneN}_4)](\text{ClO}_4)_2$	45
	(m) $[\text{Cu}(\text{Me}_4\text{12aneN}_4)](\text{ClO}_4)_2$ and $[\text{Cu}(\text{tb12aneN}_4)](\text{ClO}_4)_2$	45
	(n) $[\text{Ni}(\text{tb12aneN}_4)](\text{ClO}_4)_2$	45
	(o) $[\text{M}(\text{dmf})_6](\text{ClO}_4)_2$ (where M = nickel(II), copper(II) and cobalt(II))	45
	(p) $[\text{Ni}(\text{Me}_4\text{12aneN}_4)\text{N}_3]\text{ClO}_4$	46
	(q) $[\text{Ni}(\text{Me}_4\text{12aneN}_4)\text{NCS}]\text{NCS}$	46
2.3.2	Ligand Extraction from $[\text{Ni}(\text{13aneN}_4)](\text{ClO}_4)_2$	46
2.4	Characterisation of Compounds:-	
	(a) Infra-red Spectral Measurements	46
	(b) Metal Analysis	51
	(c) The Elemental Analysis (C, H and N)	54
	(d) N.m.r. Spectral Analysis	54
2.5.1	Determination of pKa Value of 12aneN ₄ and Me ₄ 12aneN ₄	54
2.5.2	Potentiometric and Spectrophotometric Titration of Metallo-Macrocyclic Complexes	55

2.5.3	Determination of Stoichiometry and Equilibrium Constants:-	
	(a) $[\text{Ni}(\text{Me}_4\text{12aneN}_4)\text{N}_3]^+$ System	65
	(b) $[\text{Ni}(\text{Me}_4\text{14aneN}_4)\text{N}_3]^+$ System	68
2.5.4	Substitution Reactions in an Aqueous Medium:-	
	(a) $[\text{Ni}(\text{Me}_4\text{14aneN}_4)](\text{ClO}_4)_2/\text{NaN}_3$ System	72
	(b) $[\text{Cu}(\text{12aneN}_4)](\text{ClO}_4)_2/\text{NaN}_3$ and $[\text{Cu}(\text{Me}_4\text{12aneN}_4)](\text{ClO}_4)_2/\text{NaN}_3$ Systems	76
	(c) $[\text{Ni}(\text{12aneN}_4)](\text{ClO}_4)_2/\text{NaN}_3$ and $[\text{Ni}(\text{13aneN}_4)](\text{ClO}_4)_2/\text{NaN}_3$ Systems	76
2.5.5	Uv/visible Spectroscopic Method of Equilibrium Constants Determination in an Aqueous Medium:-	
	(a) $[\text{Cu}(\text{12aneN}_4)\text{X}]^+$ ($\text{X} = \text{N}_3^-, \text{SCN}^-$ or OCN^-) Formation	76
	(b) $[\text{Cu}(\text{Me}_4\text{12aneN}_4)\text{X}]^+$ ($\text{X} = \text{N}_3^-, \text{SCN}^-$ or OCN^-) Formation	81
	(c) $[\text{Ni}(\text{12aneN}_4)\text{N}_3]^+$ and $[\text{Ni}(\text{13aneN}_4)\text{SCN}]^+$ Formation	82
2.5.6	Solid State Magnetic Moments by the Gouy Method	83
2.6.1	Isomeric Properties of $[\text{Ni}(\text{Me}_4\text{12aneN}_4)]^{2+}$ Complexes	83
2.6.2	Isomeric Properties of $[\text{Ni}(\text{Me}_4\text{14aneN}_4)]^{2+}$ Complexes	85
2.6.3	Red to Green Colour Change of a Mixture of $[\text{Ni}(\text{dmf})_6](\text{ClO}_4)_2$ and $\text{Me}_4\text{14aneN}_4$ in dmf	88
	References	95

CHAPTER THREE

Molecular Structure

3.1	Introduction	98
3.2	The Molecular Crystal Structure of $[\text{Ni}(\text{Me}_4\text{12aneN}_4)\text{N}_3]\text{ClO}_4$	98
3.3	The Molecular Crystal Structure of $[\text{Ni}(\text{Me}_4\text{12aneN}_4)](\text{ClO}_4)_2$	102
3.4	Discussion	106
	References	108

CHAPTER FOUR

High Spin-Low Spin Equilibria of Nickel(II) Systems in Aqueous Solution

4.1	Introduction	110
4.2.1	The $[\text{Ni}(\text{12aneN}_4)](\text{ClO}_4)_2$ System	113
4.2.2	Magnetic Moment Measurements by the Gouy Method and the Evans Method	114
4.2.3	The Temperature and Ionic Strength Dependence of Equilibrium Constants	118
4.2.4	The Temperature Jump Kinetic Study	121
4.2.5	^{17}O N.m.r. Water Exchange Kinetic Study	128
4.3.1	The $[\text{Ni}(\text{Me}_4\text{12aneN}_4)](\text{ClO}_4)_2$ System	136
4.3.2	Magnetic Moment Measurements by the Gouy Method	136
4.3.3	The Temperature and Ionic Strength Dependence of Equilibrium Constants	137
4.3.4	The Temperature Jump Kinetic Study	142
4.4.1	The $[\text{Ni}(\text{tb12aneN}_4)\text{Cl}]\text{Cl}$ and $[\text{Ni}(\text{tb12aneN}_4)\text{NO}_3]\text{NO}_3$ Systems	144
4.4.2	The Temperature Dependence of Uv/visible Spectral Change	144
4.5.1	The $[\text{Ni}(\text{13aneN}_4)](\text{ClO}_4)_2$ System	148
4.5.2	The Temperature and Ionic Strength Dependence of Equilibrium Constants	149
4.5.3	The Temperature Jump Kinetic Study	149
4.6.1	The $[\text{Ni}(\text{Me}_4\text{14aneN}_4)](\text{ClO}_4)_2$ System	152
4.6.2	Magnetic Moment Measurements by the Gouy Method	153
4.6.3	The Temperature and Ionic Strength Dependence of Equilibrium Constants	153
4.6.4	The Temperature Jump Kinetic Study	158
4.7.1	General Discussion	159
	References	166

CHAPTER FIVE

Formation and Dissociation of Macrocyclic Complexes in Aqueous Solution

5.1	Introduction	170
5.2	Determination of the Stoichiometry of $[\text{Ni}(\text{12aneN}_4)(\text{OH}_2)_2]^{2+}$ Formation	172
5.3	Formation Rate Constants of $[\text{Ni}(\text{12aneN}_4)(\text{OH}_2)_2]^{2+}$	173
5.4	The Effect of Hydrogen Ion Concentration and Temperature on the Rates of Dissociation of $[\text{Ni}(\text{12aneN}_4)](\text{ClO}_4)_2$, $[\text{Cu}(\text{12aneN}_4)](\text{ClO}_4)_2$ and $[\text{Cu}(\text{Me}_4\text{12aneN}_4)](\text{ClO}_4)_2$	182
5.5	The Effect of Ionic Strength on the Rates of Dissociation of $[\text{Ni}(\text{12aneN}_4)](\text{ClO}_4)_2$, $[\text{Cu}(\text{12aneN}_4)](\text{ClO}_4)_2$ and $[\text{Cu}(\text{Me}_4\text{12aneN}_4)](\text{ClO}_4)_2$	195
5.6	The Reaction of $[\text{Ni}(\text{12aneN}_4)(\text{OH}_2)_2]^{2+}$ with Sodium Hydroxide	197
5.7	General Discussion	199
	References	203

CHAPTER SIX

Non-Aqueous Chemistry

6.1	Introduction	207
6.2	Determination of the Stoichiometry of the Metal-Macrocyclic Complexes in dmf	208
6.3	Rate Measurements on the Formation of	
6.3.1	$[\text{Ni}(\text{Me}_4\text{14aneN}_4)]^{2+}$ Complex	216
6.3.2	$[\text{Ni}(\text{Me}_4\text{12aneN}_4)]^{2+}$ Complex	223
6.3.3	$[\text{Cu}(\text{Me}_4\text{12aneN}_4)]^{2+}$ Complex	228
6.3.4	$[\text{Cu}(\text{Me}_4\text{14aneN}_4)]^{2+}$ Complex	228
6.3.5	$[\text{Co}(\text{Me}_4\text{14aneN}_4)]^{2+}$ Complex	233
6.4	The Temperature Dependence of the Spin-Equilibria of Nickel(II) Complexes.	233

6.5	General Discussion	244
	References	248

CHAPTER SEVEN

Experimental Techniques

7.1	Spectrophotometric Measurements and pH Determinations	252
7.2	Magnetic Moment Measurements:-	
	(a) The Gouy Method	252
	(b) The Evans' Method	253
7.3	Job's Method of Continuous Variation	254
7.4	Oxygen-17 n.m.r. Measurements	255
7.5	The Temperature Jump Method:-	
	(a) The Relation between Relaxation Time and Rate Constants	256
	(b) The Magnitude of the Displacement of Equilibrium Concentrations	259
	(c) Experimental Considerations	260
	(d) Analysis of the Photographs	263
7.6	The Stopped Flow Method:-	
	(a) Principle of the Stopped Flow Method	264
	(b) The Stopped Flow Apparatus	266
	(c) Analysis of Stopped Flow Traces	267
	(d) Estimation of the rate constant for the First Order Process	269
	(e) Estimation of the Apparatus Dead Time	271
	(f) Second Variety of Stopped Flow Apparatus	272
	References	275
	Publication From This Work	277

CHAPTER ONE

Introduction

Contents

- 1.1 Formation and dissociation reactions of macrocyclic complexes
 - 1.1.1 The macrocyclic effect
 - 1.1.2 Formation of macrocyclic complexes
 - 1.1.3 Dissociation of macrocyclic complexes
- 1.2 High spin-low spin equilibrium
- 1.3 Substitution reactions
- 1.4 Isomerisation
- 1.5 Kinetic terminology
- 1.6 Objective of this report



Introduction

The research described in this thesis is mainly concerned with:-

- i. Formation and dissociation reactions of macrocyclic complexes of nickel(II) and copper(II).
- ii. High spin-low spin equilibria of macrocyclic complexes of nickel(II).
- iii. Isomerisation and substitution reactions of macrocyclic complexes of nickel(II).

Therefore, a general review of these topics especially with respect to macrocyclic complexes of metal ions is presented here.

1.1 Formation and Dissociation Reactions of Macrocyclic Complexes

1.1.1 The Macrocyclic Effect:-

Cabiness and Margerum¹ introduced the term "macrocyclic effect" in 1969 to highlight the large increase in stability constants of the macrocyclic complex compared to an open chain analogue. They observed a large difference in the stability constants for the formation of $[\text{Cu}(\text{tet-a})]^{2+}$ and $[\text{Cu}(2,3,2\text{-tet})]^{2+}$ in an aqueous solution. In principle the "macrocyclic effect" refers to the decrease in the Gibbs energy, ΔG° , for the metathetic reaction²



(T = non-cyclic ligand, L = cyclic ligand and M = metal ion).

Macrocyclic complexes play an important role in many naturally occurring systems and as for the chelate effect before it, considerable attention has been directed towards separating ΔG° into its component enthalpic and entropic parts in order to understand the origin of the enhanced stability of macrocyclic complexes. Moreover, the rate of formation of metallo-macrocyclic complexes in an aqueous medium or the rate of their dissociation in an acidic medium is very slow. There are many excellent review articles^{3,4,5} treating various aspects of metallo-macrocyclic complexes. However, the discussion here will be limited mainly to the nitrogen containing macrocyclic complexes of metal ions. A clear understanding of the macrocyclic effect should indicate why these complexes are so stable and kinetic studies should help shed light on these enhanced stabilities

Although the existence of macrocyclic effect has been accepted, controversy has arisen over its specific thermodynamic origin. It has been established that the chelate effect is of largely entropic origin⁶, but no agreement has been reached as to whether the macrocyclic effect is of enthalpic or entropic origin in the macrocyclic ligand reactions.

Cabiness and Margerum¹ rejected the possibility of explaining its origin in terms of entropy. They proposed that two important factors contribute to the macrocyclic effect, the configuration and solvation of a free macrocyclic ligand compared to its non-cyclic analogue. Later on with a detailed study Hinz and Margerum⁷ found that the ΔH° and $T\Delta S^\circ$ values are -129.7 ± 2.5 and 2.5 kJ/mol for the $[\text{Ni}(\text{14aneN}_4)]^{2+}$ formation in an aqueous solution whereas these values correspond to -70.3 ± 2 and 17.2 kJ/mol for the $[\text{Ni}(2,3,2\text{-tet})]^{2+}$ formation at 298.2K (ionic strength 0.1). They proposed that the macrocyclic effect is due to the large negative ΔH° value for the formation of $[\text{Ni}(\text{14aneN}_4)]^{2+}$ complex. They reasoned⁸ that the smaller desolvation that occurs in the macrocyclic complexes leads to a more favourable enthalpy change for a macrocycle compared to a linear molecule.

Paoletti and co-workers⁹ reported the preliminary results of a study of copper(II)tetraamine complexes. They proposed that the origin of the macrocyclic effect is a combination of enthalpy and entropy factors. After an extensive study and reassessment of the results, however, it was found that only the entropy factor was important¹⁰. Fabrizzi, Paoletti and Lever¹⁰ reported that the ΔH° and $T\Delta S^\circ$ values are -90.4 and 24.3 kJ/mol for the formation of the $[\text{Cu}(2,2,2\text{-tet})]^{2+}$ complex at 298.2K in an aqueous solution. Kodama and Kimura^{11,12} found that these ΔH° and $T\Delta S^\circ$ values correspond to -76.6 and 64 kJ/mol for the formation of the $[\text{Cu}(\text{12aneN}_4)]^{2+}$ complex. They compared these results with those of Fabbrizzi, Paoletti and Lever¹⁰ and concluded that the macrocyclic effect is due to the favourable changes in ΔS° and that the apparent contrast between their results with $[\text{Cu}(\text{12aneN}_4)]^{2+}$ and those of Hinz and Margerum⁷ with $[\text{Ni}(\text{14aneN}_4)]^{2+}$ is not fully explained by differences between ring sizes and metal ions.

Fabbrizzi and co-workers² estimated that the ΔH° and $T\Delta S^\circ$ values are

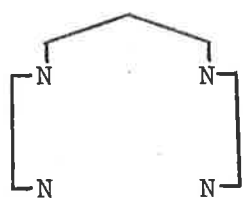
-84.9 and 41.8 kJ/mol, respectively, for $[\text{Ni}(\text{14aneN}_4)]^{2+}$ formation whereas these values correspond to -77.8 and 14 kJ/mol, respectively, for $[\text{Ni}(2,3,2\text{-tet})]^{2+}$ formation at 298.2K in an aqueous solution. Therefore they considered that the macrocyclic effect in the $[\text{Ni}(\text{14aneN}_4)]^{2+}$ complex is due to the favourable change in ΔS° .

Kodama and Kimura¹³ determined the equilibria and kinetics of reaction of zinc(II), cadmium(II) and lead(II) with 12 to 15-membered macrocyclic tetraamines in an aqueous solution using polarographic methods. The stability constants of the zinc complexes hardly change with macrocyclic ring size unlike the copper(II) system. The much larger cadmium(II) and lead(II) form complexes only with 12aneN₄. The 10^3 - 10^5 times greater stabilities of the macrocyclic complexes compared with the related complexes of linear tetraamines are all due to favourable entropy change regardless of the metal ion size.

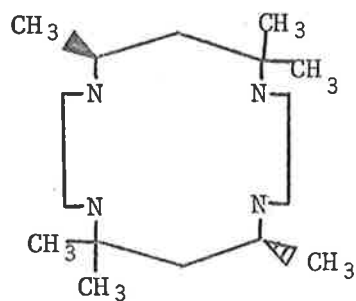
So systems have been reported in which the macrocyclic effect is a result of enthalpic stabilization or entropic stabilization. However, it is necessary to study more comparable systems using a variety of solvents in order to establish the thermodynamic origin of the macrocyclic effect.

1.1.2 Formation of Macrocyclic Complexes:-

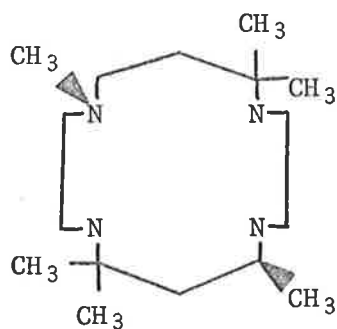
Cabbiness and Margerum¹⁴ reported kinetic studies on the complexation of copper(II) with meso-1,7-CTH, rac-1,7-CTH, 1,7-CT, 2,3,2-tet and porphyrin ligand (see Figure 1.1) in both acidic and basic solutions. In acid solutions the aliphatic macrocyclic ligands react much slower with $[\text{Cu}(\text{OH}_2)_6]^{2+}$ than do the porphyrin. In 0.5 mol dm⁻³ NaOH, the 14-membered macrocycles (meso-1,7-CTH, rac-1,7-CTH and 1,7-CT) react more slowly than the open chain ligand 2,3,2-tet by factors of 10^3 - 10^4 . The more rigid porphyrin ring was found to be less reactive than 2,3,2-tet by a factor of 10^9 . All reactions are kinetically second order and the products are believed to be square planar complexes of copper. The porphyrin structure because of its rigidity, has the greatest tendency to force a mechanism of multiple desolvation of the metal ion and the open chain polyamine can cause a serial displacement of the co-ordinated solvent. In the case of 14-membered macrocycles, Cabbiness and Margerum suggested that both paths must be considered since these ligands are



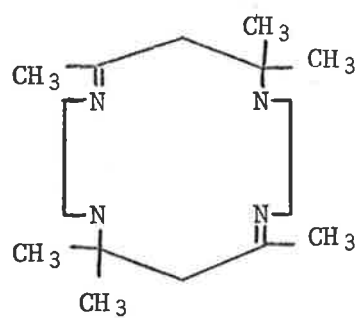
2,3,2-tet



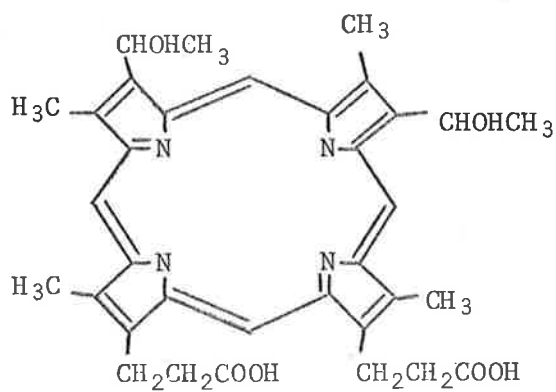
tet a or meso-1,7-CTH



Tet b or rac-1,7-CTH



trans[14]diene or 1,7-CT



hematoporphyrin IX

Figure 1.1

not very flexible. The factors which suggest that twisting or folding of these cyclic ligands may be important are:- 1. their much greater reactivity compared to the porphyrin molecule, 2. the formation of intermediate structural isomers, 3. the fact that subtle changes in structure, as in meso-1,7-CTH compared to rac-1,7-CTH cause noticeable changes in the rate constants. Models indicate that some degree of multiple desolvation is necessary in the co-ordination of the third and fourth nitrogens. However, the rate determining steps may still occur earlier in the co-ordination process i.e. first or second metal-nitrogen bond formation. Cabiness and Margerum also treated the problem of protonation of the nitrogen atoms in acidic solution. They found that the observed 1st order rate constant increases with increase of pH. The resolved rate constant for the reaction of $[\text{Cu}(\text{OH}_2)_6]^{2+}$ with monoprotinated meso-1,7-CTH is $7.6 \times 10^3 \text{ mol}^{-1} \text{ dm}^3 \text{ s}^{-1}$ and the value for the rate constant with diprotinated meso-1,7-CTH must be less than $10^{-5} \text{ mol}^{-1} \text{ dm}^3 \text{ s}^{-1}$. The macrocyclic structure causes the two protons in $(\text{meso-1,7-CTH})\text{H}_2^{+2}$ to be nearer one another than would be the case in an open chain molecule. The fact that the pK_2 value is as large as 10.4 ($\text{pK}_1 = 12.6$) suggests that hydrogen bonding compensates for electrostatic repulsion of the two protons and therefore it is kinetically difficult for $[\text{Cu}(\text{OH}_2)_6]^{2+}$ to react with $(\text{meso-1,7-CTH})\text{H}_2^{+2}$. The porphyrins do not add protons in the ring until pH 4-5 and therefore their rates are less drastically affected by acid.

Hertli and Kaden¹⁵ reported that formation kinetics of copper(II), nickel(II), cobalt(II) and zinc(II) with $\text{Me}_4\text{14aneN}_4$ in an aqueous solution using a pH-stat technique. Stability constants were calculated from the formation and dissociation rates, and they observed no macrocyclic effect. The kinetics of complex formation between $\text{Me}_4\text{14aneN}_4$ and cobalt(II) or zinc(II) were found to be directly proportional to $[\text{M}^{2+}]_{\text{tot}}$, to $[\text{Me}_4\text{14aneN}_4]_{\text{tot}}$ and inversely proportional to $[\text{H}^+]$ (see equation 1.2).

$$\frac{d[\text{ML}]}{dt} = k_+ [\text{M}^{2+}]_{\text{tot}} [\text{Me}_4\text{14aneN}_4]_{\text{tot}} / [\text{H}^+] \quad 1.2$$

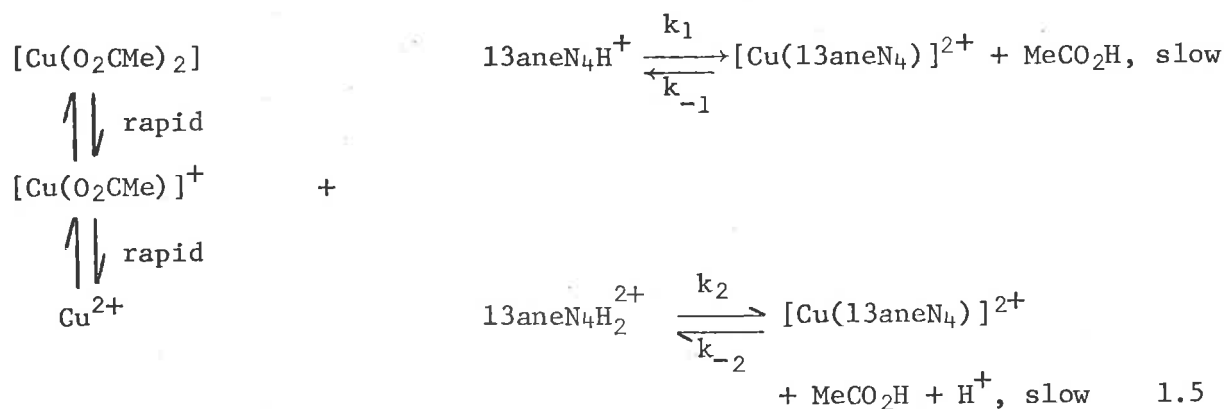
diprotonated species reacts suggests that the rate determining step is an associative process, probably proton loss preceding second bond formation.

Kodama and Kimura¹³ measured the rate constants for formation of complexes of zinc(II), cadmium(II) and lead(II) with 12aneN₄, 13aneN₄, 14aneN₄, 15aneN₄ and their non-cyclic analogues in acetate buffers. They proposed that the rate law for complex formation of all the metal ions in acetate buffer is

$$\frac{d[ML^{2+}]}{dt} = k_H [M(O_2CMe)^+] [LH^+] + k_{2H} [M(O_2CMe)^+] [LH_2^{2+}] \quad 1.4$$

(M = metal ion, L = ligand, k_H = formation rate constant with monoprotonated ligand and k_{2H} = formation rate constant with diprotonated ligand). The kinetic behaviour of these complexes in acetate buffer is identical to those found for the copper(II) system^{12,17}.

Kodama and Kimura¹⁷ also reported polarographic studies of [Cu(13aneN₄)]²⁺ complexation in acetate buffer. The proposed mechanism, similar to that of the 12aneN₄^{11,12} system, is shown below (see equation 1.5)



The rate of complexation depends upon the protonation of the ligand but not as much as for the 12aneN₄ system. They suggested that this may be due to less significant proximity effect of the 13-membered ring structure.

Further studies of complex formation with macrocyclic ligands are also reported in the literatures¹⁸⁻²⁵.

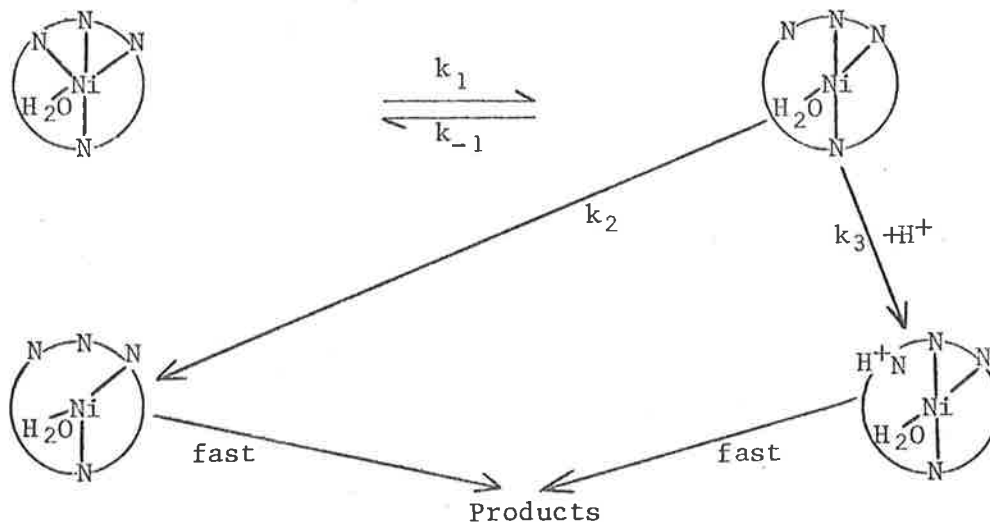
1.1.3 Dissociation of Macrocyclic Complexes:-

Cabbiness and Margerum¹⁴ reported that the kinetics of dissociation of the more stable macrocyclic ligands require high acidities to cause the reaction to occur at a conveniently measurable rate. The observed first order dissociation rate constants for $[\text{Cu}(\text{teta})]^{2+}$ (red) and $[\text{Cu}(2,3,2\text{-tet})]^{2+}$ complexes in 6.1 mol dm^{-3} HCl at 298.2K are 3.6×10^{-7} and 4.1 s^{-1} , respectively. The factor of 10^7 in the relative reactivity gives an indication of the large effects which macrocyclic structures have on the dissociation kinetics.

Hertli and Kaden¹⁵ studied the dissociation kinetics of the penta co-ordinated copper(II), nickel(II), cobalt(II) and zinc(II) complexes with $\text{Me}_4\text{14aneN}_4$ at acid pH (spectrophotometrically). The rate law is shown by equation (1.6),

$$-\frac{d[\text{ML}]}{dt} = k^{\text{ML}} [\text{ML}] + k_{\text{H}}^{\text{ML}} [\text{ML}][\text{H}^+] + k_{\text{H}^2}^{\text{ML}} [\text{ML}][\text{H}^+]^2 \quad 1.6$$

(where k^{ML} , k_{H}^{ML} and $k_{\text{H}^2}^{\text{ML}}$ are dissociation rate constants, M = metal ion and L = ligand). For M = zinc(II) and cobalt(II) only the term proportional to $[\text{H}^+]$ was observed, whereas for M = copper(II) both $k_{\text{H}^2}^{\text{ML}}$ and k_{H}^{ML} and for M = nickel(II) k^{ML} and k_{H}^{ML} were involved. The dissociation of $[\text{Ni}(\text{Me}_4\text{14aneN}_4)]^{2+}$ complex was studied in more detail over a broad range of proton concentrations. They assumed that the dissociation for the penta co-ordinated nickel(II) complex with $\text{Me}_4\text{14aneN}_4$ proceeds by the generally accepted dissociation mechanism for chelate compounds²⁶ as shown in Figure 1.2



Scheme for the dissociation of $[\text{Ni}(\text{Me}_4,14\text{aneN}_4)]^{2+}$

Figure 1.2

If it is assumed that $k_{-1} \gg k_2 + k_3[H^+]$, the rate equation can be expressed as

$$-\frac{d\ln[\text{ML}]}{dt} = \frac{k_1}{k_{-1}} (k_2 + k_3[H^+]) \quad 1.7$$

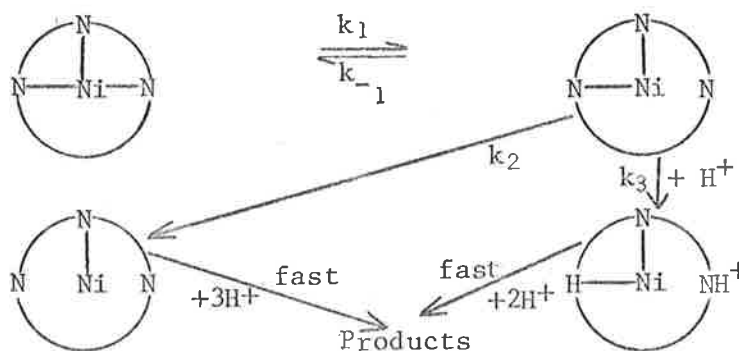
In the case of $[\text{Ni}(\text{Me}_4,14\text{aneN}_4)]^{2+}$ system equation 1.6 becomes

$$-\frac{d[\text{ML}]}{dt} = k^{\text{ML}} [\text{ML}] + k_{\text{H}}^{\text{ML}} [\text{ML}][\text{H}^+]$$

or

$$-\frac{d\ln[\text{ML}]}{dt} = (k^{\text{ML}} + k_{\text{H}}^{\text{ML}} [\text{H}^+]) \quad 1.7a$$

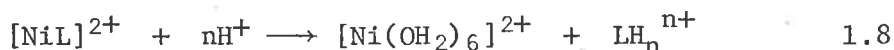
Equations 1.7 and 1.7a are of similar form. The mechanism proposed by Hertli and Kaden for the dissociation of $[\text{Ni}(\text{Me}_4,14\text{aneN}_4)]^+$ is very similar to the one observed for the dissociation of the nickel(II) complex with *cis,cis*-1,3,5-triaminocyclohexane²⁷ as shown below (Figure 1.3)



Scheme for the dissociation of $[\text{Ni}(\text{cis,cis-1,3,5-triaminocyclohexane})]^{2+}$

Figure 1.3

In a review by D.H. Busch⁴, the acid dissociation reaction of the macrocyclic complexes is shown by the equation 1.8



(L = macrocyclic ligand)

The hydrogen ion concentration dependence of dissociation rate constants makes comparison between systems difficult. However, the dissociation rates obtained under identical conditions clearly indicate the relative labilities of the complexes. The dissociation rate constants were found to be $2 \times 10^{-5} \text{ s}^{-1}$ for $[\text{Ni}(\text{12aneN}_4)]^{2+}$, $6.4 \times 10^{-5} \text{ s}^{-1}$ for $[\text{Ni}(\text{15aneN}_4)]^{2+}$ and $1.9 \times 10^{-1} \text{ s}^{-1}$ for $[\text{Ni}(\text{16aneN}_4)]^{2+}$ in 0.3 mol dm^{-3} aqueous HClO_4 at 298.2K and ionic strength 0.5. The $[\text{Ni}(\text{14aneN}_4)]^{2+}$ complex is stable for many months under these conditions. Kinetics of dissociation of nickel(II) complexes of O_2N_2 donor macrocycles in acid are also reported^{28,29}.

In this thesis, the rate of formation of $[\text{Ni}(\text{12aneN}_4)(\text{OH}_2)_2]^{2+}$ in aqueous solution is reported. The acid dissociations of $[\text{Ni}(\text{12aneN}_4)]^{2+}$, $[\text{Cu}(\text{12aneN}_4)]^{2+}$ and $[\text{Cu}(\text{Me}_4\text{12aneN}_4)]^{2+}$ are also reported together with the reaction of $[\text{Ni}(\text{12aneN}_4)]^{2+}$ in aqueous sodium hydroxide. The rate of formation of nickel(II) and copper(II) complexes with $\text{Me}_4\text{12aneN}_4$ and $\text{Me}_4\text{14aneN}_4$ in dmf are presented here. Kinetics and mechanism of formation of nickel(II) complexes of O_2N_2 donor macrocyclic ligands in methanol were reported³⁰ but there appears to be no study of complexation in dmf using tetra-azamacrocyclic ligands.

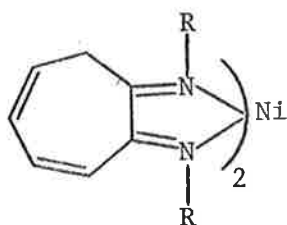
1.2 High Spin-Low Spin Equilibria

A number of first row transition metal complexes exhibit magnetic susceptibility and uv/visible spectral change consistent with a thermal equilibrium between two states of differing spin multiplicity. A variety of systems in which the spin equilibrium is present in solution³¹⁻³⁶ are reported.

In solution it is possible to measure spin state lifetime and rate constants using rapid perturbation-relaxation kinetics³⁷⁻³⁹. Such kinetic

studies of spin equilibrium processes should result in an understanding of these phenomenon. Chemical modification of ligands, ionic strength, temperature and pressure are some of the important factors⁴⁰ which may influence an equilibrium between high spin and low spin states. Paramagnetic susceptibility, n.m.r. spectra, electronic spectra and infra red spectra are some of the important physical properties⁴⁰ of the molecules exhibiting spin equilibria. Among these properties, temperature and pressure dependence magnetic susceptibility and uv/visible spectral change are commonly employed to characterise spin equilibrium processes.

Eaton and colleagues⁴¹ reported the diamagnetic-paramagnetic equilibrium in nickel(II)aminotroponeimineates (see Figure 1.4) using

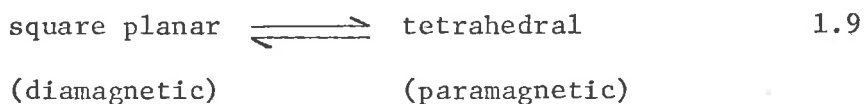


where R = -CH₃, CH₃CH₂-, C₆H₅- etc.

Ni(II) N,N'dialkyl(or diaryl)aminotroponeimineates

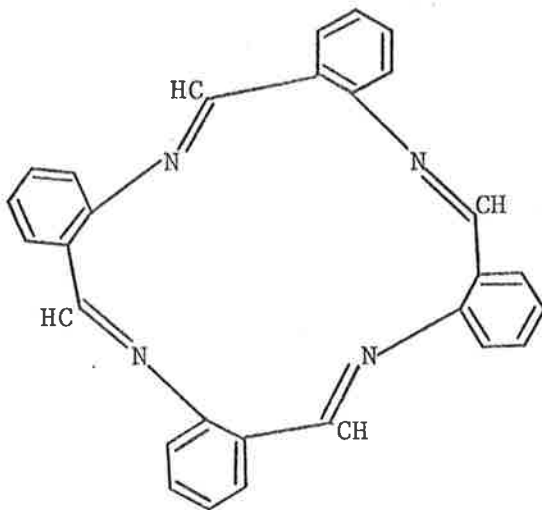
Figure 1.4

magnetic susceptibility, electronic spectra and n.m.r. experiments. The equilibrium 1.9 was found



to be markedly dependent upon temperature, solvent and the structure of the ligand. The diamagnetic form was identified with a square planar configuration and the paramagnetic form, with an approximately tetrahedral configuration. The parameters associated with these solution equilibria were derived from temperature dependences of n.m.r. contact shifts, magnetic susceptibilities and spectral intensities.

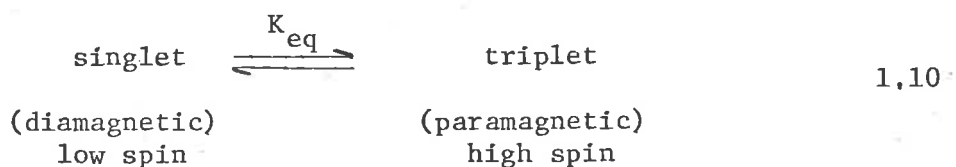
Busch and Melson⁴² assumed an equilibrium between singlet and triplet states to explain temperature dependence magnetic properties of the chloride and bromide salts of nickel(II) complexes containing a macrocyclic ligand, tetrabenzo[b,f,j,n][1,5,9,13]tetraazacyclohexadecine (see Figure 1.5).



tetrabenzo[b,f,j,n,][1,5,9,13]tetraazacyclohexadecine

Figure 1.5

With ClO_4^- , BF_4^- and $\text{B}(\text{C}_6\text{H}_5)_4^-$, the resultant complexes are diamagnetic in the solid state and therefore have singlet ground states. With I^- , NO_3^- and NCS^- , the resultant complexes exhibit magnetic moments consistent with triplet ground states in the solid state. The equilibrium arising from thermal distribution between singlet and triplet states can be written as

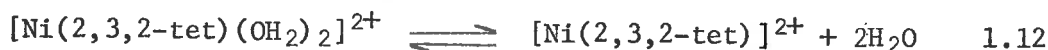


The equilibrium constant, $K_{\text{eq}} = \frac{N_{\text{H}}}{N_{\text{L}}}$ where N_{L} and N_{H} represent the mol fractions of the low spin and high spin forms, respectively. These mol fractions can be estimated from the measured magnetic moment at any temperature, assuming the moment of the compound in the high spin state to be 3.2 B.M., (i.e. moment at room temperature for the high spin thiocyanate complex) and that of the substance in the low spin state to be 0.5 B.M. (i.e. moment at room temperature for the perchlorate complex). The thermodynamic parameters were calculated using equation 1.11

$$-RT \ln K_{\text{eq}} = \Delta H^\circ - T\Delta S^\circ \quad 1.11$$

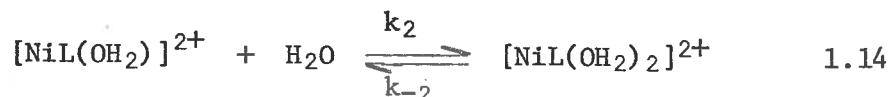
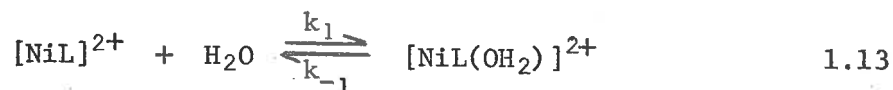
Wilkins and co-workers⁴³ observed that the $[\text{Ni}(2,3,2\text{-tet})]^{2+}$ complex exists in dilute aqueous solution (298.2K and ionic strength 0.5) as a mixture of approximately 25% planar $[\text{Ni}(2,3,2\text{-tet})]^{2+}$ and 75% octahedral

$[\text{Ni}(2,3,2\text{-tet})(\text{OH}_2)_2]^{2+}$, the latter is probably a mixture of cis and trans diaquo forms^{44,45}. The equilibrium 1.12 is shifted to form more of the planar species on addition of inert electrolytes,



particularly NaClO_4 , or by an increase in temperature.

Ivin and co-workers⁴⁶ followed the kinetics of planar-octahedral interconversion in a $[\text{Ni}(2,3,2\text{-tet})]^{2+}$ system using neodymium laser radiation technique. In aqueous solution this complex exists mainly as the trans configuration in equilibrium⁴³ with the yellow, square planar configuration. They observed that the relaxation time was independent of the complex concentration over the range 0.05 to 0.2 mol dm^{-3} but varied (0.3 to 0.09 μsec) with temperature (285.2 to 331.2K). They proposed two step mechanisms



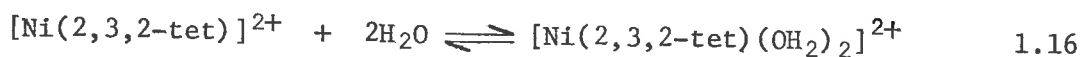
(L = 2,3,2-tet)

as proposed for the octahedral-tetrahedral interconversion in $[\text{Co}(\text{py})_4\text{Cl}_2]$ complex⁴⁷ (py = pyridine). Considerations of the stereochemistry and the extent of d-orbital perturbation expected to be caused by water ligands^{47a} indicate that the penta co-ordinated intermediate, $[\text{NiL}(\text{OH}_2)]^{2+}$, is also likely to be a high spin species, so that step 1 (equation 1.13) involving a change of spin is likely to be rate controlling according to these authors. The following expression for the relaxation time τ was derived⁴⁷

$$\tau^{-1} = k_1[\text{H}_2\text{O}](1 + K) \quad 1.15$$

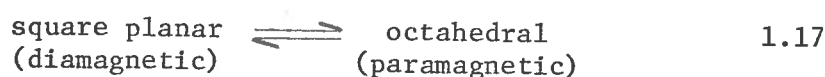
where $K = [\text{NiL}^{2+}]/[\text{NiL}(\text{OH}_2)_2^{2+}]$. They have also observed similar effect in aqueous solution of $[\text{Ni}(\text{trien})]^{2+}$ complex. The relaxation times were about a factor of 2 slower than in the $[\text{Ni}(2,3,2\text{-tet})]^{2+}$ system.

Creutz and Sutin⁴⁸ also reported that the $[\text{Ni}(2,3,2\text{-tet})]^{2+}$ complex exists as an equilibrium mixture of low spin planar and high spin octahedral forms in aqueous solution at room temperature^{43,49} (see equation 1.16).

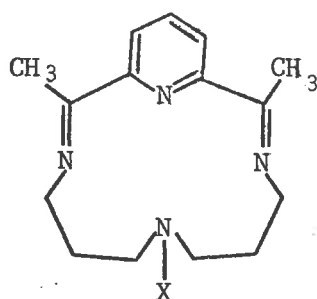


They observed a rapid increase in absorbance followed by a slower absorbance decrease using a neodymium laser technique. The relaxation time for this decrease is $0.30 \pm 0.02 \mu\text{sec}$ at 296.2K and independent of the concentration of the nickel complex, in accord with the previously reported results⁴⁶.

Jordan and Rusnak⁵⁰ investigated the temperature dependence of the diamagnetic paramagnetic equilibrium (1.17) of nickel(II)



complex of 2,12-dimethyl-3,7,11,17-tetraazabicyclo[11.3.1]heptadeca-1(17), 2,11,13,15-pentaene and its methylated analogue (see Figure 1.6).



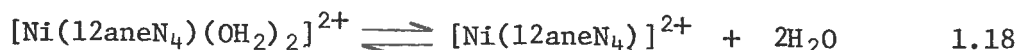
2,12-dimethyl-3,7,11,17-tetraazabicyclo[11.3.1]heptadeca-1(17), 2,11,13,15-pentaene (when $X = \text{H}$) and its methylated analogue (when $X = \text{CH}_3$)

Figure 1.6

in water, methanol, dmf, DMSO and acetonitrile. They observed that the diamagnetic form of the complex is thermodynamically favoured at high temperatures. The equilibrium constants ($[\text{paramagnetic species}]/[\text{diamagnetic species}]$) have been determined from the studies of the temperature dependence of the magnetic susceptibility and of the ligand proton chemical shifts. They have also estimated ΔH° and ΔS° values for the square planar octahedral equilibrium.

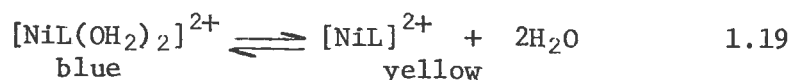
Fabbrizzi⁵¹ reported that an aqueous solution of $[\text{Ni}(\text{12aneN}_4)]^{2+}$ is blue and its electronic spectrum is typical of a presumably cis-diaquo high spin octahedral complex. An increase in either inert electrolyte concentrations

or temperature increases the intensity of a new absorption band at 435 nm. The intensity of the other bands (355 and 555 nm) simultaneously decreases. The absorption band at 477-435 nm is typical of a yellow diamagnetic nickel(II) complex. The reaction of interest is shown by equilibrium 1.18. But Fabbrizzi could not



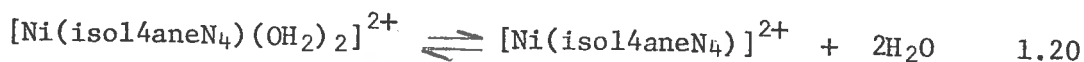
assess the thermodynamic parameters because of the impossibility of reaching 100% of the yellow species and determining its limiting spectrum.

Fabbrizzi and colleagues⁵² have made a thermodynamic study of the blue-to-yellow conversion of the nickel(II) complexes of 14aneN₄ and its linear analogue 2,3,2-tet and 3,2,3-tet. The formation of low spin species is favoured by increasing either the temperature or the ionic strength in all cases and the equilibrium is shown by equation 1.19. In aqueous 0.1 mol dm⁻³



NaClO₄ at 298.2K, [Ni(14aneN₄)]²⁺, [Ni(2,3,2-tet)]²⁺ and [Ni(3,2,3-tet)]²⁺ exist as 71%, 22% and 8% of the yellow forms, respectively. The ΔS° values for the blue-to-yellow conversion of nickel(II) complexes with 14aneN₄, 2,3,2-tet and 3,2,3-tet are 83.7, 37.7 and 41.8 (error ±8) J K⁻¹ mol⁻¹, respectively. While the ΔH° values for these complexes are 22.6, 14.2 and 18.4 (error ±1.7) kJ/mol, respectively. The [Ni(14aneN₄)]²⁺ system exhibits the greatest proportion of the yellow form at equilibrium. Of these three systems the formation of the yellow form from the blue form is the most endothermic for the [Ni(14aneN₄)]²⁺ system. This enhanced stability must therefore depend on a very favourable entropy term. Finally, it was concluded that the ability of 14aneN₄ to stabilise the yellow form relative to that of its linear analogues does not result from any special cyclic effect but depends only on the steric interactions which are also present in the appropriate linear ligands.

Sabatini and Fabbrizzi⁵³ reported that [Ni(isol4aneN₄)]²⁺ exists in aqueous solution as a mixture of blue, octahedral (high spin) and yellow, planar (low spin) species (see equation 1.20). The



equilibrium 1.20 was found to be displaced to the right both by increasing temperature and by increasing supporting electrolyte concentrations. The thermodynamic parameters for the blue-to-yellow conversion are given in Table 1.1.

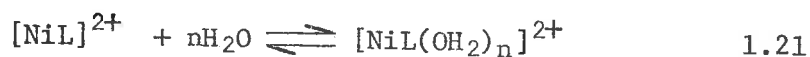
Table 1.1

Thermodynamic quantities for the blue-to-yellow conversion of nickel(II) complexes with cyclic and non-cyclic tetraamines at 298.2K in aqueous 0.1 mol dm⁻³ NaClO₄.

ligand	ΔH° , kJ mol ⁻¹	ΔS° , J K ⁻¹ mol ⁻¹
isol4aneN ₄	22.2±0.4	78.2±2.1
14aneN ₄ ⁵²	22.6±1.7	83.7±8.4
2,3,2-tet ^{8,52}	14.2±1.7	37.7±8.4
3,2,3-tet ⁵²	18.4±1.7	41.8±8.7
2,2,2-tet ⁸	14.2	12.6

They compared the thermodynamic quantities of nickel(II) complexes with different ligands as shown in Table 1.1 and concluded that the entropy term is specially favourable for the enhanced stabilities of the macrocyclic complexes. The blue-to-yellow conversion is more endothermic for cyclic ligands than for their open chain counter parts but this enthalpic disadvantage is more compensated by the entropy term.

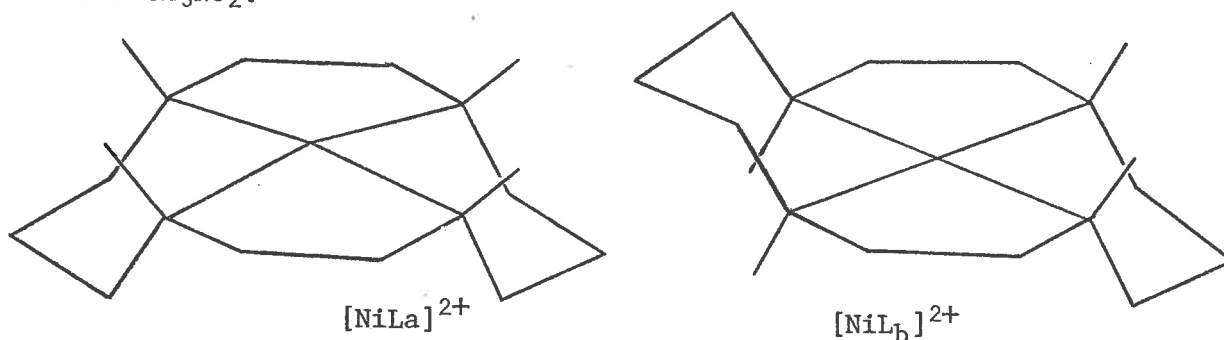
Moore and Herron⁵⁴ have made assessment of equilibrium constants and related thermodynamic parameters associated with diamagnetic paramagnetic equilibria of $[\text{Ni}(\text{Me}_4\text{14aneN}_4)]^{2+}$ and $[\text{Ni}(\text{14aneN}_4)]^{2+}$ complexes in aqueous solution from visible spectra and magnetic susceptibility measurements. The reaction of interest is shown by equation 1.21.



(L = ligand)

Two isomers of $[\text{Ni}(\text{Me}_4\text{14aneN}_4)]^{2+}$ (see Figure 1.7) and a single isomer of

$[\text{Ni}(\text{14aneN}_4)]^{2+}$ have also been investigated in $\text{HCON}(\text{CH}_3)_2$, $(\text{CH}_3)_2\text{SO}$, CH_3CN and CH_3NO_2 .



Two isomers of $[\text{Ni}(\text{Me}_4\text{14aneN}_4)]^{2+}$

Figure 1.7

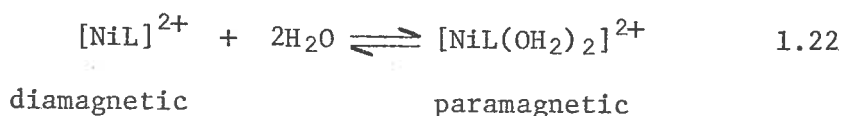
All three complexes, $[\text{NiLa}]^{2+}$, $[\text{NiLb}]^{2+}$ and $[\text{Ni}(\text{14aneN}_4)]^{2+}$ dissolve in water to give a mixture of diamagnetic square planar and paramagnetic solvated species. Thermodynamic parameters for the diamagnetic to paramagnetic conversion of all three nickel(II) complexes are given in Table 1.2 and this will allow an estimation of the effects of macrocyclic conformation and ligand structure on the equilibrium 1.21.

Table 1.2

Thermodynamic parameters at 298K (ionic strength 0.2) for the diamagnetic to paramagnetic conversion of nickel(II) complexes in aqueous solution using visible spectra.

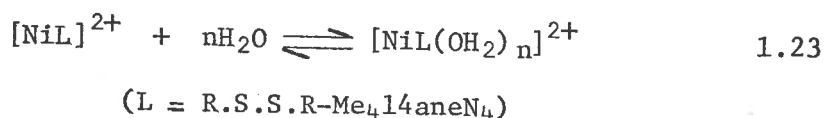
system	K (equilibrium constant)	$-\Delta H^\circ$, kJ mol^{-1}	$+\Delta S^\circ$, $\text{J K}^{-1} \text{mol}^{-1}$
$[\text{NiLa}]^{2+}$	1.05	12.2 ± 1.6	-41 ± 9
$[\text{NiLb}]^{2+}$	1.14	43.8 ± 1.6	-146 ± 10
$[\text{Ni14aneN}_4]^{2+}$	0.25	24.0 ± 1.5	-91 ± 8

Watkins and colleagues⁵⁵ reported the solvent adduct study of $[\text{Ni}(\text{14aneN}_4)]^{2+}$ with co-ordinating solvents CH_3CN , $\text{HCON}(\text{CH}_3)_2$, $(\text{CH}_3)_2\text{SO}$ and H_2O using optical and n.m.r. techniques. The reaction of interest is given by



The thermodynamic parameters for each solvent system were determined and the stability order for solvent adduct formation (solvated paramagnetic species) was found to be $\text{HCON}(\text{CH}_3)_2 > \text{CH}_3\text{CN} > (\text{CH}_3)_2\text{SO} > \text{H}_2\text{O}$ over the investigated temperature range for each solvent system.

Moore and co-workers⁵⁶ reported that an aqueous solution of $[\text{Ni}(\text{R.S.S.R-Me}_4\text{14aneN}_4)](\text{ClO}_4)_2$ exists as an equilibrium between unsolvated planar diamagnetic and the disolvated pseudo octahedral paramagnetic form (see equation 1.23)



as a result of their variable-temperature and variable-pressure ¹H n.m.r. studies. Thermodynamic functions were also assessed by them. More spin equilibrium systems are also reported in the literatures⁵⁷⁻⁶⁰.

In this thesis, the spin equilibria of $[\text{Ni}(\text{12aneN}_4)]^{2+}$, $[\text{Ni}(\text{Me}_4\text{12aneN}_4)]^{2+}$, $[\text{Ni}(\text{13aneN}_4)]^{2+}$ and $[\text{Ni}(\text{Me}_4\text{14aneN}_4)]^{2+}$ systems in aqueous and non-aqueous solvents are reported. The temperature dependence of magnetic moments (using Evans method) of $[\text{Ni}(\text{12aneN}_4)](\text{ClO}_4)_2$ in 4.0 mol dm^{-3} aqueous LiClO_4 consistent with high spin-low spin equilibrium are also presented. The relaxation time of the spin equilibrium systems are studied in aqueous solution using the temperature jump technique. The temperature dependent uv/visible spectral change of $[\text{Ni}(\text{tb12aneN}_4)\text{Cl}]\text{Cl}$ and $[\text{Ni}(\text{tb12aneN}_4)\text{NO}_3]\text{NO}_3$ complexes are reported. The results of the ⁰17 n.m.r. studies of $[\text{Ni}(\text{12aneN}_4)(\text{OH}_2)_2]^{2+}$ are also summarised.

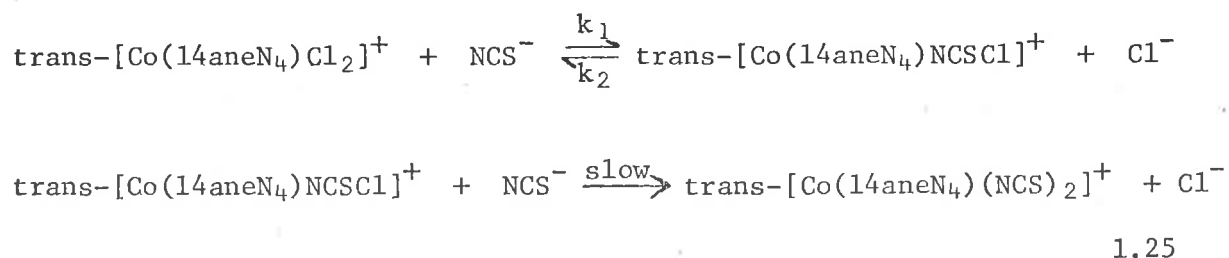
1.3 Substitution Reactions:-

Ligand substitution reactions of metal tetra-azamacrocyclic complexes were studied only with a few systems. McAuley and associates⁶¹ studied the kinetics of the reaction of $[\text{Ni}(\text{14aneN}_4)(\text{OH}_2)_2]^{3+}$ with Cl^- , Br^- and NCS^- in aqueous perchloric acid medium using spectrophotometric and stopped flow techniques. The observed rate law in the reaction with NCS^- , carried out in excess $[\text{Ni}(\text{14aneN}_4)(\text{OH}_2)_2]^{3+}$ is shown in equation 1.24.

$$\frac{d[\text{Ni}(\text{14aneN}_4)(\text{NCS})^{2+}]}{dt} = k_{\text{obs}} [\text{Ni}(\text{14aneN}_4)(\text{OH}_2)_2^{3+}] [\text{NCS}^-] \quad 1.24$$

The rate was found to be independent of acid concentration and the product spectrum is consistent with the formation of a one to one complex under the conditions used. They proposed a dissociative mechanism for all the three systems ($[\text{Ni}(\text{14aneN}_4)(\text{OH}_2)_2]^{3+}$ with Cl^- , Br^- and NCS^-) studied. The general mechanism for many trivalent metal complexes (especially aquo ions) is an associative interchange type⁶².

Poon and Tobe⁶³ reported the kinetics of the reactions of $[\text{Co}(\text{14aneN}_4)(\text{Cl}_2)]^+$ with Cl^- , N_3^- , NO_2^- and NCS^- . The rate constants for the Cl^- substitution and NCS^- substitution were found to be independent of Cl^- and NCS^- concentration over the range studied. In the reaction with NCS^- , the rate of reaction was independent of pH within the pH range 2-3 and the replacement of the first chloride ligand was very much faster ($t_{1/2} = 2.5$ h) than the replacement of the second ($t_{1/2} = 60$ h) at 333.7K. In order to see the environmental effect on the rate constant, they have also studied the entry of NCS^- in an environment of excess chloride. They found that the reactions were slowed down in presence of excess chloride. They proposed that the change were consistent with the following scheme (see equation 1.25).



Poon and Andrew⁶⁴ studied the ligand substitution reactions of low spin $\text{trans-}[\text{Fe}(\text{14aneN}_4)(\text{NCS})\text{X}]^+$ complexes ($\text{X} = \text{Cl}^-$, Br^- , $\text{CH}_2\text{ClCOO}^-$, $\text{CHCl}_2\text{COO}^-$) by thiocyanate and $\text{trans-}[\text{Fe}(\text{14aneN}_4)(\text{NCS})_2]^+$ by a series of nucleophiles in aqueous acidic solution. The rate constants are strongly dependent on the nature of the leaving ligands but are independent of the nature and concentration of the entering groups. They proposed a dissociative mechanism for

the substitution reactions of these low-spin iron(III)-amine complexes.

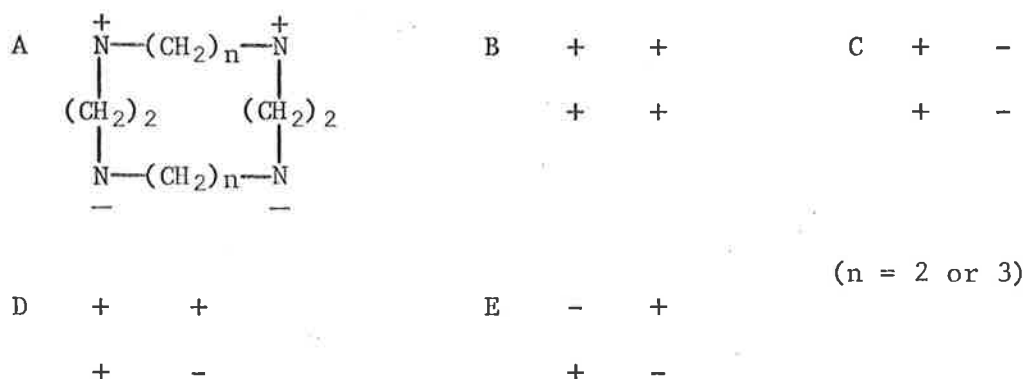
In this thesis, substitution reactions of metal tetra-azamacrocyclic complexes with azide are reported together with the results of equilibrium constant for $[\text{Cu}(\text{12aneN}_4)\text{X}]^+$ and $[\text{Cu}(\text{Me}_4\text{12aneN}_4)\text{X}]^+$ formation (where $\text{X} = \text{N}_3^-$, NCS^- or OCN^-).

1.4 Isomerisation:-

Bosnich and co-workers^{65,66} have discussed the stereochemistry of 14aneN_4 macrocycle. They pointed out the possible existence of five basic structural forms, as determined by the distribution of nitrogen atom configurations with respect to five and six-membered chelate rings.

Busch and Warner⁶⁷ reported that the complex ion $[\text{Ni}(\text{1,7-CTH})]^{2+}$ can exist in twenty possible isomeric forms depending on the configurations of the two asymmetric carbon centres and the four asymmetric nitrogen centres. They have characterised three isomers. Isomerism of nickel(II) and copper(II) macrocyclic complexes are also reported in the literature⁶⁸.

In case of co-ordinated $\text{Me}_4\text{12aneN}_4$ and $\text{Me}_4\text{14aneN}_4$, theoretically there could be five possible sets of nitrogen configurations for a coplanar array of nitrogen donors as shown below:-



In these diagrams a plus refers to a methyl group above the plane and a minus methyl group below the plane of the four nitrogens. The number of carbon atom in the linking chain are also represented. The configurations of a general nature of the co-ordinated ligand are discussed in the literature^{67,69}. The complex prepared by adding hydrated nickel(II) perchlorate to one equivalent $\text{Me}_4\text{14aneN}_4$ was shown to have the stereochemistry (B) where all four methyl groups lie on the same side of the macrocyclic plane⁷⁰. The complex produced

by direct methylation of $[\text{Ni}(\text{14aneN}_4)](\text{ClO}_4)_2$ possesses the stereochemistry (A) where two methyl groups lie above the macrocyclic plane and the other two below⁷¹. The complex of stereochemistry (B) shows a marked propensity towards five co-ordination^{70,72,73}, a fifth unidentate ligand (e.g. solvent or halide ion or azide) co-ordinating on the same side of the macrocycle as the four methyl groups, thereby pulling the metal atom out of the plane and forcing the complex to adopt either a square based pyramidal or trigonal-bipyramidal⁷⁴ structure. The sixth co-ordination in such complexes is hindered by the folded alkyl backbone of the macrocyclic ring and octahedral complexes are therefore rare. The complex of stereochemistry (A), however, frequently tends to form an octahedral complex, although five co-ordinate species are also known with strong ligands such as cyanide or hydroxide ions⁷¹.

As a further exploration of the effects of macrocyclic ligands upon the properties of complexes, nickel(II) complexes of $\text{Me}_4\text{12aneN}_4$ and $\text{Me}_4\text{14aneN}_4$ were prepared under different conditions (see section 2.3) expecting different sets of nitrogen donor configurations and their properties were investigated in different solvents. The results of these studies are reported in this thesis.

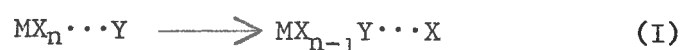
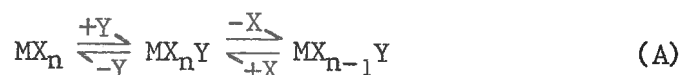
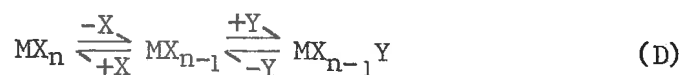
1.5 Kinetic Terminology:-

The possible mechanistic pathways can be categorised into three main processes⁷⁵.

- i. $\text{S}_{\text{N}}1$ (lim), dissociative (D)
- ii. $\text{S}_{\text{N}}1$ (I_{d}) or $\text{S}_{\text{N}}2$ (I_{a}) and
- iii. $\text{S}_{\text{N}}2$ (lim), associative (A).

During a dissociative process, the leaving ligand is lost in the first step producing an intermediate of reduced co-ordination number which undergoes rapid association with the incoming ligand. In the process, therefore, the reaction rate is dependent on the rate of dissociation and the nature of the leaving group. But, the rate is independent of the nature of the incoming ligand (neglecting solvent effects etc.) and concentration of the incoming ligand at excess ligand concentration. The associative process involves the

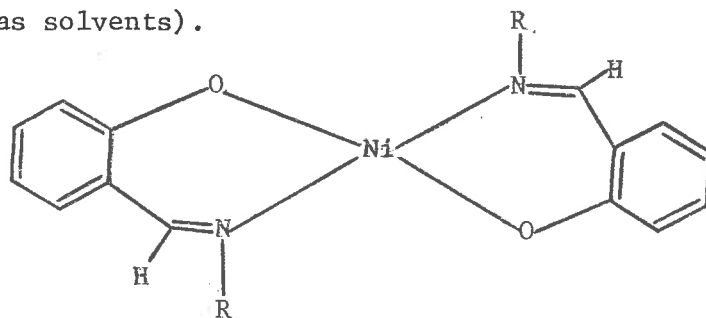
addition of the entering ligand during the first step, resulting in an intermediate of increased co-ordination number. Here the reaction rate is dependent on the nature and concentration of the entering group. The rate should show a first order dependence on the concentration of the entering ligand. Furthermore, since both entering and leaving groups are involved in the transition state, their nature will, therefore, determine its activation energy. During an interchange (I) process the leaving group moves from the inner to the outer co-ordination sphere, while the incoming group moves from the outer to the inner. When in an I mechanism the two groups are only weakly bonded in a D like transition state, then the reaction rate is only slightly dependent on the nature of the entering group and hence the process is described as a dissociative interchange (I_d). The reaction rate of an I_d process is independent of the ligand concentration at high ligand concentrations where all the ligand exists in the ion pair complex. Although many salts may be regarded as almost completely ionized at all reasonable concentration in solution, the ions are not necessarily free to move independently. As a result of electrostatic attraction, ions of opposite charge may form a certain proportion of what are termed ion pairs; these are not definite molecules, but they behave as if they were non-ionized molecules. Any particular ion-pair has a temporary existence only, for there is a continual interchange between the various ions in the solution. In the A like transition state of an I process, substantial bonding to both the entering and leaving groups occurs, hence they have a large influence on the activation energy. Such processes are called associative interchange (I_a). The main pathways mentioned above can be illustrated by the following equations:



where, X represents the leaving group and Y the entering group, while $\text{MX}_n \cdots \text{Y}$ represents an out-sphere complex.

1.6 Objective of this Project:-

Metal complexes of naturally occurring macrocyclic ligands have been known for more than fifty years but synthetic macrocyclic ligands and their metal complexes have been the subject of extensive research over the last sixteen years. The significance of macrocyclic ligands and their metal complexes is most obvious as it relates to such naturally occurring macrocycles as the metallo-porphyrins, vitamin B₁₂ and chlorophyl. The possibility of using synthetic macrocyclic complexes as models for more intricate biological macrocyclic systems, has been recognised^{3-5,76}. Tetra-azamacrocycles are able to induce strong ligand field effects⁷⁷ and stabilise unusually high oxidation states of metals⁷⁸. The useful and unusual thermodynamic¹ and kinetic⁷⁹ stabilities of the metal complexes of the new synthetic macrocyclic ligands make them ideal systems for studying a great variety of chemical phenomenon such as ligand substitution reactions, unusual redox behaviour and solution characteristics. A particular spin state may be often essential for the functional behaviour of several naturally occurring ring systems such as porphyrins and corrins which contain metal ions as macrocyclic complexes. Spin-state isomerism in the case of nickel(II) complex has been a subject of interest and contention over a number of years. Maki⁸⁰ first observed this phenomenon for salicylaldehyde complexes (see Figure 1.8) in 1958 (chloroform, pyridine etc. as solvents).



Ni bis salicylaldimines

- (a) R = OH; salicylaldoxime
- (b) R = CH₃; N-methyl salicylalimine

Figure 1.8

However, to date the study with metallo-macrocyclic complexes is by no means as yet exhaustive. Therefore, the complexes and methods as presented in this thesis were chosen to increase the knowledge and understanding of this field.

The main object of this study was to prepare a number of nickel(II) complexes with different macrocyclic ligands and study spin equilibrium processes as a function of temperature, ionic strength, solvent type and the structure of the ligand. It was desirable to gain an insight into the factors which control the lability of these equilibria and to determine which of them embraces the rate determining step for the low spin to high spin interconversion. Another objective was to study acid dissociation reactions of nickel(II) and copper(II) macrocyclic complexes to see the factors affecting the rate of dissociation and possibly to propose a mechanism for their dissociation. It was also proposed to study the kinetics of formation of nickel(II), copper(II) and cobalt(II) macrocyclic complexes in aqueous and non-aqueous solvents to gain an insight into the factors controlling the rate of formation and possibly to propose a mechanism for their formation. It was anticipated that different isomers of nickel(II) complexes of $\text{Me}_4\text{12aneN}_4$ and $\text{Me}_4\text{14aneN}_4$ may be prepared under different conditions expecting different sets of nitrogen donor atoms configuration and the aim was to characterise the different isomers. A further objective was to study substitution reactions of nickel(II) and copper(II) macrocyclic complexes with monodentate ligands in aqueous solution with a view to establishing the mechanism of such substitution processes and to gain an insight into the factors controlling the lability of these complexes. For these objectives, the experimental techniques were chosen to be mainly uv/visible spectrophotometry, temperature jump spectrophotometry and stopped flow spectrophotometry.

References for Chapter One

1. D.K. Cabbiness and D.W. Margerum, *J.A.C.S.*, 91, 6540 (1969).
2. L. Fabbrizzi, P. Paoletti and R.M. Clay, *Inorg. Chem.*, 17, 1042 (1978).
3. G.A. Melson, "Co-ordination Chemistry of Macrocyclic Compounds", Plenum Press, New York (1979).
4. D.H. Busch, *Acc. Chem. Res.*, 11, 392, (1978).
5. R.M. Izatt and J.J. Cristensen, "Synthetic Multidentate Macrocyclic Compounds", Academic Press, New York (1978).
6. D. Munro, *Chem. Br.*, 13, 100 (1977).
7. F.P. Hinz and D.W. Margerum, *J.A.C.S.*, 96, 4993 (1974).
8. F.P. Hinz and D.W. Margerum, *Inorg. Chem.*, 13, 2941 (1974).
9. P. Paoletti, L. Fabbrizzi and R. Barbucci, *Inorg. Chem.*, 12, 1961 (1973)
10. L. Fabbrizzi, P. Paoletti and A.B.P. Lever, *Inorg. Chem.*, 15, 1502 (1976).
11. M. Kodama and E. Kimura, *J. Chem. Soc., Chem. Comm.*, 326 (1975).
12. M. Kodama and E. Kimura, *J. Chem. Soc., Dalton Trans.*, 116 (1976).
13. M. Kodama and E. Kimura, *J. Chem. Soc., Dalton Trans.*, 2269 (1977).
14. D.K. Cabbiness and D.W. Margerum, *J.A.C.S.*, 92, 2151 (1970).
15. L. Hertli and T.A. Kaden, *Helv. Chim. Acta.*, 57, 1328 (1974).
16. M. Eigen, *Pure App. Chemistry*, 6, 105 (1963).
17. M. Kodama and E. Kimura, *J. Chem. Soc., Chem. Comm.*, 891 (1975).
18. Chin-Tung Lin, D.B. Rorabacher, G.R. Cayley and D.W. Margerum, *Inorg. Chem.*, 14, 919 (1975).
19. R. Buxtorf, W. Steinmann and T.A. Kaden, *Chimia*, 28, 15 (1974).
20. M. Kodama and E. Kimura, *J. Chem. Soc., Dalton Trans.*, 1081 (1978).
21. M. Kodama and E. Kimura, *J. Chem. Soc., Dalton Trans.*, 2335 (1976).
22. A.P. Leugger, L. Hertli and T.A. Kaden, *Helv. Chim. Acta.*, 61, 2296 (1978).
23. Bih-Fong Liang and Chun-Sun Chung, *J. Chem. Soc., Dalton Trans.*, 1349 (1980).
24. R. Buxtorf and T.A. Kaden, *Helv. Chim. Acta.*, 57, 1035 (1974).

25. P.S. Grunow and T.A. Kaden, *Helv. Chim. Acta*, 61, 2291 (1978).
26. F. Basolo and R. Pearson, "Mechanism of Inorganic Reactions", John Wiley and Sons Inc., New York, 216 (1967).
27. R.F. Childers and R.A.D. Wentworth, *Inorg. Chem.*, 8, 2218, (1969).
28. L.F.L. and R.J.S., *J.A.C.S.*, 101, 4014 (1979).
29. A. Ekstrom, L.F. Lindoy and R.J. Smith, *Inorg. Chem.*, 19, 724 (1980).
30. A. Ekstrom, L.F. Kondoy, H.C. Lip, R.J. Smith, H.J. Goodwin, M. McPartlin and P.A. Tasker, *J. Chem. Soc., Dalton Trans.*, 1027 (1979).
31. J.P. Jesson, S. Trofimenko and D.R. Eaton, *J.A.C.S.*, 89, 3158 (1967).
32. M.A. Hoselton, L.J. Wilson and R.S. Drago, *J.A.C.S.*, 97, 1722 (1975).
33. L.J. Wilson, D. Georges and M.A. Hoselton, *Inorg. Chem.*, 14, 2968 (1975).
34. M.F. Tweedle and L.J. Wilson, *J.A.C.S.*, 98, 4824 (1976).
35. E.V. Dose, K.M.M. Murphy and L.J. Wilson, *Inorg. Chem.*, 15, 2622 (1976).
36. M.G. Simmons and L.J. Wilson, *Inorg. Chem.*, 16, 126 (1977).
37. D.H. Turner, G.W. Flynn, N. Sutin and J.V. Beitz, *J.A.C.S.*, 94, 1554 (1972).
38. J.K. Beattie, N. Sutin, D.H. Turner and G.W. Flynn, *J.A.C.S.*, 95, 2052 (1973).
39. M.A. Hoselton, R.S. Drago, L.J. Wilson and N. Sutin, *J.A.C.S.*, 98, 6967 (1976).
40. R.L. Martin and A.H. White in "Transition Metal Chemistry" edited by R.L. Carlin, vol. 4 (1968).
41. D.R. Eaton, W.D. Philips and D.J. Caldwell, *J.A.C.S.*, 85, 397 (1963).
42. G.A. Melson and D.H. Busch, *J.A.C.S.*, 86, 4830 (1964).
43. R.G. Wilkins, R. Yelin, D.W. Margerum and D.C. Weatherburn, *J.A.C.S.*, 91, 4326 (1969).
44. D.F. Cook and E.D. McKenzie, *Inorg. Chim. Acta*, 29, 193 (1978).
45. E.J. Billo, *Inorg. Chim. Acta*, 37, L533 (1979).
46. K.J. Ivin, R. Jamison and J.J. McGarvey, *J.A.C.S.*, 94, 1763 (1972).
47. R.D. Farina and J.H. Swinehart, *J.A.C.S.*, 91, 568 (1969).
- 47a. E.K. Barefield, D.H. Busch and S.M. Nelson, *Quart. Rev. Chem. Soc.*, 22, 483 (1968).

48. C. Creutz and N. Sutin, *J.A.C.S.*, 95, 7177 (1973).
49. B. Bosnich, R.D. Gillard, E.D. McKenzie and G.A. Webb, *J. Chem. Soc. A*, 1331 (1966).
50. L. Rusnak and R.B. Jordan, *Inorg. Chem.*, 10, 2199 (1971).
51. L. Fabbrizzi, *Inorg. Chem.*, 16, 2667 (1977).
52. A. Anichini, L. Fabbrizzi, P. Paoletti and R.M. Clay, *Inorg. Chim. Acta*, 24, L21 (1977).
53. L. Sabatini and L. Fabbrizzi, *Inorg. Chem.*, 18, 438 (1979).
54. N. Herron and P. Moore, *Inorg. Chim. Acta*, 36, 89 (1979).
55. G.S. Vigee, C.L. Watkins and H.F. Bowen, *Inorg. Chim. Acta*, 35, 255 (1979).
56. A.E. Merbach, P. Moore and K.E. Newman, *J. Mag. Resonance*, 41, 30 (1980).
57. L. Fabbrizzi, *J. Chem. Soc., Dalton Trans.*, 1857 (1979).
58. A.M. Greenaway, C.J. O'Connor, A. Schrock and E. Sinn, *Inorg. Chem.*, 18, 2692 (1979).
59. D.F. Evans and T.A. James, *J. Chem. Soc., Dalton Trans.*, 723 (1979).
60. J.R. Ferraro, L.J. Basile and L. Sacconi, *Inorg. Chim. Acta*, 35, L317 (1979).
61. R.I. Haines and A. McAuley, *Inorg. Chem.*, 19, 719 (1980).
62. T.W. Swaddle, *Co-ord. Chem. Rev.*, 14, 217 (1974).
63. C.K. Poon and M.L. Tobe, *Co-ord. Chem. Rev.*, 1, 81 (1966).
64. C.K. Poon and Andrew W.M. To, *Inorg. Chem.*, 18, 1277 (1979).
65. B. Bosnich, M.L. Tobe and G.A. Webb, *Inorg. Chem.*, 4, 1102 (1965).
66. B. Bosnich, R. Mason, P. Pauling, G.B. Robertson and M.L. Tobe, *J. Chem. Soc., Chem. Comm.*, 97 (1965).
67. L.G. Wagner and D.H. Busch, *J.A.C.S.*, 91, 4092 (1969).
68. N.F. Curtis, D.A. Swann, T.N. Waters and I.E. Maxwell, *J.A.C.S.*, 91, 4588 (1969).
69. B. Bosnich, C.K. Poon and M.L. Tobe, *Inorg. Chem.*, 4, 1102 (1965).
70. M.J. D'Aniello, M.T. Mocella, F. Wagner, E.K. Barefield and I.C. Paul, *J.A.C.S.*, 97, 192 (1975).

71. F. Wagner and E.K. Barefield, *Inorg. Chem.*, 15, 408 (1976).
72. E.K. Barefield and F. Wagner, *Inorg. Chem.*, 12, 2435 (1973).
73. K.D. Hodges, R.G. Wollmann, E.K. Barefield and D.N. Hendrickson, *Inorg. Chem.*, 16, 2746 (1977).
74. N.W. Alcock, N. Herron and P. Moore, *J. Chem. Soc., Dalton Trans.*, 1282 (1978).
75. C.H. Langford and H.B. Gray, "Ligand Substitution Processes", W.A. Benjamin, Inc., New York (1965).
76. L.F. Lindoy, *Chem. Soc. Rev.*, 14, 421 (1975).
77. D.H. Busch, K. Farmery, W.L. Goedken, V. Katovic, A.C. Melnyk, C.R. Sperati and N. Tokel, *Adv. Chem. Ser.*, 100, 44 (1971).
78. F.V. Lovecchio, E.S. Gore and D.H. Busch, *J.A.C.S.*, 96, 3109 (1974).
79. C.T. Lin, D.B. Rorabacher, G.R. Cayley and D.W. Margerum, *Inorg. Chem.*, 14, 919 (1975).
80. G. Maki, *J. Chem. Phys.*, 29, 1129 (1958).

CHAPTER TWO

Preparative Chemistry and Characterisation

Contents

2.1 Reagents and Materials

2.2 Preparation of Ligands:-

- (a) 12aneN₄
- (b) Me₄12aneN₄
- (c) tb12aneN₄
- (d) 13aneN₄
- (e) 14aneN₄ and Me₄14aneN₄

2.3.1 Preparation of Complexes:-

- (a) [Ni(12aneN₄)](ClO₄)₂
- (b) [Ni(Me₄12aneN₄)](ClO₄)₂ (ethanol water preparation)
- (c) [Ni(Me₄12aneN₄)](ClO₄)₂ (ethanol preparation)
- (d) [Ni(Me₄12aneN₄)](ClO₄)₂ (ethanol preparation using triethyl-orthoformate)
- (e) [Ni(Me₄12aneN₄)(dmf)](ClO₄)₂ (dmf preparation)
- (f) [Ni(tb12aneN₄)Cl]Cl
- (g) [Ni(tb12aneN₄)NO₃]NO₃
- (h) [Ni(13aneN₄)](ClO₄)₂
- (i) [Ni(Me₄14aneN₄)](ClO₄)₂ (ethanol water preparation)
- (i) [Ni(Me₄14aneN₄)](ClO₄)₂ (ethanol preparation using triethyl-orthoformate)
- (k) [Ni(Me₄14aneN₄)(dmf)](ClO₄)₂ (dmf preparation)
- (l) [Cu(12aneN₄)](ClO₄)₂
- (m) [Cu(Me₄12aneN₄)](ClO₄)₂ and [Cu(tb12aneN₄)](ClO₄)₂
- (n) [Ni(tb12aneN₄)](ClO₄)₂
- (o) [M(dmf)₆](ClO₄)₂ (where M = nickel(II), copper(II) and cobalt(II))
- (p) [Ni(Me₄12aneN₄)N₃] ClO₄
- (q) [Ni(Me₄12aneN₄)NCS]NCS

Contents (cont.)

- 2.3.2 Ligand Extraction from $[\text{Ni}(\text{13aneN}_4)](\text{ClO}_4)_2$
- 2.4 Characterisation of Compounds:-
- Infra-red Spectral Measurements
 - Metal Analysis
 - The elemental analysis (C, H and N)
 - N.m.r. Spectral Analysis
- 2.5.1 Determination of pKa Value of 12aneN₄ and Me₄12aneN₄
- 2.5.2 Potentiometric and Spectrophotometric Titration of Metallo-Macro-cyclic Complexes
- 2.5.3 Determination of Stoichiometry and Equilibrium Constants:-
- $[\text{Ni}(\text{Me}_4\text{12aneN}_4)\text{N}_3]^+$ system
 - $[\text{Ni}(\text{Me}_4\text{14aneN}_4)\text{N}_3]^+$ system
- 2.5.4 Substitution Reactions in an Aqueous Medium:-
- $[\text{Ni}(\text{Me}_4\text{14aneN}_4)](\text{ClO}_4)_2/\text{NaN}_3$ system
 - $[\text{Cu}(\text{12aneN}_4)](\text{ClO}_4)_2/\text{NaN}_3$ and $[\text{Cu}(\text{Me}_4\text{12aneN}_4)](\text{ClO}_4)_2/\text{NaN}_3$ systems
 - $[\text{Ni}(\text{12aneN}_4)](\text{ClO}_4)_2/\text{NaN}_3$ and $[\text{Ni}(\text{13aneN}_4)](\text{ClO}_4)_2/\text{NaN}_3$ systems
- 2.5.5 Uv/visible Spectroscopic Method of Equilibrium Constants Determination in an Aqueous Medium
- $[\text{Cu}(\text{12aneN}_4)\text{X}]^+$ ($\text{X} = \text{N}_3^-, \text{SCN}^-$ or OCN^-) formation
 - $[\text{Cu}(\text{Me}_4\text{12aneN}_4)\text{X}]^+$ ($\text{X} = \text{N}_3^-, \text{SCN}^-$ or OCN^-) formation
 - $[\text{Ni}(\text{12aneN}_4)\text{N}_3]^+$ and $[\text{Ni}(\text{13aneN}_4)\text{SCN}]^+$ formation
- 2.5.6 Solid State Magnetic Moments by the Gouy Method
- 2.6.1 Isomeric Properties of $[\text{Ni}(\text{Me}_4\text{12aneN}_4)]^{2+}$ complexes
- 2.6.2 Isomeric Properties of $[\text{Ni}(\text{Me}_4\text{14aneN}_4)]^{2+}$ complexes
- 2.6.3. Red to Green Colour Change of a Mixture of $[\text{Ni}(\text{dmf})_6](\text{ClO}_4)_2$ and Me₄14aneN₄ in dmf

CHAPTER TWO

Preparative Chemistry and Characterisation2.1 Reagents and Materials:-

All chemicals used were analytical grade except for preparative chemistry where reagent grade chemicals without further purification were used. All volumetric glassware used were A-grade. Doubly distilled water was used to prepare all solutions. Ionic strength was adjusted either with NaClO_4 or LiClO_4 and pH was adjusted using NaOH and HClO_4 . HClO_4 was standardised against NaOH which was standardised against potassium hydrogen phthalate. In non-aqueous study, all manipulations were carried out in a dry box which was kept dry by nitrogen (continuous flow) and phosphorous pentoxide. Molecular sieves (BDH 4A) were used to dry the solvents. Ether was dried with sodium wire and filtered to remove any NaOH formed. Commercial deuterated nitromethane was doubly distilled, dried by molecular sieves and purity checked by ^1H n.m.r. using a T60 spectrometer. A large quantity of dmf was distilled¹. About 10 grams of anhydrous copper sulfate was added to 2.5 litres dmf and the mixture was left stoppered for at least three days with shaking twice a day. Dmf was distilled at 314K under vacuum using an oil pump and a nitrogen leak tube. It was then stored over molecular sieves under nitrogen in the refrigerator. The purity was checked by ^1H n.m.r. using a T60 Spectrometer. Dmf was distilled and dried to remove any hydrolysis products (e.g. dimethyl amine). Methanol was distilled under normal conditions and used to wash and dry the spectrophotometer cells. Distilled acetone was used to rinse the glassware before drying in the oven at 388K. Deacon 90, detergents, perchloric acid-sulphuric acid mixture and chromic acid mixture were used to clean the glassware. Spectrophotometer cells were cleaned by Deacon 90.

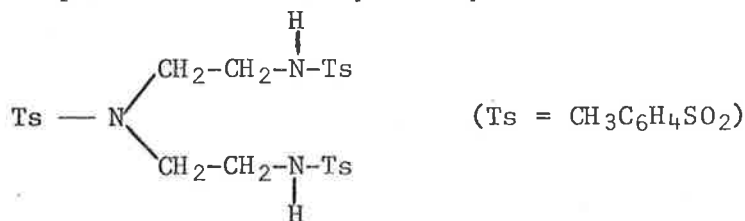
All the compounds, including ligands and complexes, were dried either by a vacuum line or in a vacuum dessicator over phosphorus pentoxide and silica gel.

2.2 Preparation of Ligands:-

(a) 12aneN₄:-

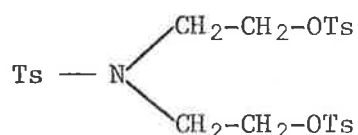
The preparation of 12aneN₄ was carried out by modification of reported²⁻⁵ methods.

(i) Preparation of tritosyldiethylenetriamine:-



A solution of diethylene triamine (10.3 gm) and sodium hydroxide (12.0 gm) in 100 cm³ of water was placed in a 1000 cm³ beaker and stirred magnetically. A solution of p-toluene sulphonyl chloride (57.2 gm, recrystallised from χ_4 petroleum ether) in 300 cm³ of solvent ether was added dropwise to the above solution. The mixture was stirred for half an hour. A white precipitate was formed and about 150 cm³ methanol was added to coagulate the products. Stirring was continued for a further half an hour. The crystals were filtered, washed with water followed by ethanol (and then dried in a vacuum dessicator using silica gel). A yield of 71% was obtained (melting point range of 443 to 448K). Several batches were prepared similarly and the yield varied from 65 to 85%.

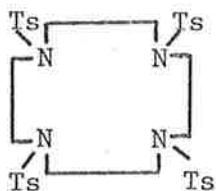
(ii) Preparation of tritosyldiethanolamine:-



Diethanolamine (21 gms) and dry pyridine (192 cm³) were placed in a 4-necked, 2 litre flask equipped with a mechanical teflon stirrer, thermometer, nitrogen inlet tube and a separating funnel. The reaction mixture was cooled and solid p-toluene sulphonyl chloride (115 gm) was added slowly keeping the temperature below 283K (using a crude sodium chloride ice bath). The mixture was stirred (mechanical stirrer with electric motor) for two and a half hours in the ice bath. A solution of hydrochloric acid (600 cm³ of 2.9 mol dm⁻³) was added dropwise from a separating funnel maintaining the

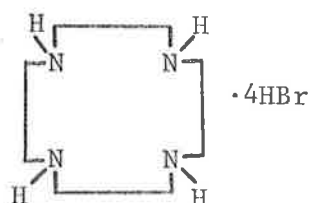
temperature below 283K. After the addition was complete, the flask was allowed to stand overnight resulting in the formation of yellow crystals. The crystals were filtered, crushed in a mortar, washed sequentially with water, ethanol, ether and finally dried in a vacuum desiccator using silica gel. Several batches were prepared using this method and the yield varied from 60 to 70% (melting point range of 346 to 348K).

(iii) Preparation of tetratosyl 12aneN₄:-



About 15 gm sodium hydride (50% in oil) was added slowly to magnetically stirred solution of tritosyldiethylenetriamine (56.5 gm) in 1 litre of dmf in a 3 litre conical flask. The solution was stirred for more than one hour, until the evolution of hydrogen gas ceased. A solution of tritosyldiethanolamine (56.8 gm) in dmf (500 cm³) was slowly added to the stirred solution at 383K (oil bath used) over a period of two and a half hours. The resulting solution was stirred for a further period of one hour before cooling to room temperature, and an addition of approximately 12 litres of water caused crystals to precipitate. The solutions were stirred for more than three hours and allowed to stand overnight. The crystals were filtered, washed with water followed by a small amount of ethanol and minimum amount of ether. The colour of the compound is light yellow and it decomposes at 513K. The compound can be recrystallised from chloroform. Several batches were prepared and the yield varied from 62 to 75%.

(iv) Preparation of 12aneN₄·hydrobromide:-



Tetratosyl·12aneN₄ (50.5 gm), mixture of 47% hydrobromic acid (700 cm³) and acetic anhydride (550 cm³), phenol (140 gm) and anti-bumping granules were added to a 2 litre three necked round bottom flask fitted with condensers (two, one above the other). A mixture of hydrobromic acid and acetic anyhydride (about 30% HBr/ACOH) was prepared by adding acetic anhydride to hydrobromic acid very slowly. Phenol was used to increase the solubility of tetratosyl·12aneN₄. The solution was then refluxed for approximately 50 hours using a heating mantle. The reaction mixture was then concentrated to about 60 cm³ by a rotatory evaporator. About 100 cm³ water was added and the solution was washed several times with chloroform using a separating funnel. The bottom layer was drained off and the aqueous layer was collected after filtering through glass wool. This solution, after adding about 20 cm³ acetic anhydride, was then concentrated to about 20 cm³ by a rotatory evaporator. Some yellowish white crystals were formed. About 1 litre of ethanol was added to the solution and allowed to stand overnight. The crystals were filtered, washed with ethanol and dried in a vacuum dessicator. Glacial acetic acid may be used instead of ethanol. The compound decomposes at about 513K. Several batches were prepared and the yield varied from 45 to 55%.

(v) Free ligand extraction:-

About 12 gm of 12aneN₄·hydrobromide was dissolved in a minimum amount of water and was neutralised with excess sodium hydroxide solution over the stoichiometric amount. Several extractions were carried out with chloroform. The chloroform was flashed off using a rotatory evaporator, ether was added and also flashed off leaving behind the solid ligand. The 12aneN₄ ligand was dissolved in minimum amount of distilled water, filtered through millipore filter paper (plastic syringe) and recrystallised. The purity was checked by ¹³C and ¹H n.m.r. spectrophotometers (tables 2.1 and 2.2). The melting point range is 343 to 346K. Several batches were prepared and the yield varied from 55 to 68%.

The Me₄12aneN₄ ligand was prepared

Table 2.1

¹³C n.m.r. Chemical Shifts (ppm)

Compounds	Solvent	Shift (w.r.t. TMS*)	Shift (w.r.t. TB [#])	Assignment
1 12aneN ₄	D ₂ O		14.2	>N-CH ₂ -
2 12aneN ₄ ·hydrobromide	D ₂ O		13.54	>N-CH ₂ -
3 Me ₄ 12aneN ₄	CDCl ₃	44.5		>N-CH ₃
		55.9		>N-CH ₂ -
4 N-benzylaziridine	CDCl ₃	27.6		$\overset{\wedge}{\text{N}}\text{-CH}_2$
		65.2		N-CH ₂ -Ar
		126.8		-Ar (p)
		128.0		-Ar (o)
		128.5		-Ar (m)
		140.5		-Ar (tertiary)
5 tb12aneN ₄	CDCl ₃	53.1		>N-CH ₂ -
		60.3		>N-CH ₂ -Ar
		126.7		-Ar (p)
		128.2		-Ar (o)
		129.2		-Ar (m)
		140.4		-Ar (tertiary)
6 13aneN ₄	D ₂ O		-3.3	$\text{>N}-\overset{ }{\text{C}}-\text{CH}_2-\overset{ }{\text{C}}-\text{N}<$
			15.4	$\text{>N}-\text{CH}_2-\overset{ }{\text{C}}-\overset{ }{\text{C}}-\text{N}<$
			15.7	
			16.5	$\text{>N}-\text{CH}_2-\overset{ }{\text{C}}-\text{N}<$
			16.7	
7 14aneN ₄	CDCl ₃	29.5		$\text{>N}-\overset{ }{\text{C}}-\text{CH}_2-\overset{ }{\text{C}}-\text{N}<$
		49.8		$\text{>N}-\text{CH}_2-\overset{ }{\text{C}}-\overset{ }{\text{C}}-\text{N}<$
		50.8		$\text{>N}-\text{CH}_2-\overset{ }{\text{C}}-\text{N}<$

Table 2.1 (cont.)

compounds	solvent	shift (w.r.t. TMS*)	shift (w.r.t. TB#)	assignment
8 Me ₄ 14aneN ₄	CDCl ₃	24.8		$>N-\overset{ }{\underset{ }{C}}-CH_2-\overset{ }{\underset{ }{C}}-N<$
		43.5		$>N-CH_3$
		54.4		$-CH_2-\overset{ }{\underset{ }{N}}-\overset{ }{\underset{ }{C}}-$
9 [Ni(13aneN ₄)](ClO ₄) ₂	CD ₃ NO ₂		-4.41	$>N-\overset{ }{\underset{ }{C}}-CH_2-\overset{ }{\underset{ }{C}}-N<$
			17.07	$>N-CH_2-\overset{ }{\underset{ }{C}}-C-N<$
			18.02	$>N-CH_2-\overset{ }{\underset{ }{C}}-N<$
			18.98	
			22.95	

N.B. The chemical shifts of the carbon atoms containing hydrogen are given in Table 2.1.

* = internal reference

= external reference

TB = tertiary butanol

TMS = tetramethylsilane

Ar = aromatic

o = ortho

m = meta

p = para

Table 2.2

 ^1H n.m.r. Chemical Shifts (ppm)

compounds	shift	assignment
1 12aneN ₄	2.71	$>\text{N}-\text{CH}_2-\overset{\text{I}}{\underset{\text{I}}{\text{C}}}-\text{N}<$
	4.73	$>\text{N}-\text{H}$
2 Me ₄ 12aneN ₄	2.24	$>\text{N}-\text{CH}_3$
	2.54	$>\text{N}-\text{CH}_2-\overset{\text{I}}{\underset{\text{I}}{\text{C}}}-\text{N}<$
3 N-benzyl aziridine	1.15	$\begin{array}{c} \text{CH}_2 \\ \diagup \\ >\text{N}-\text{C}< \end{array}$
	1.73	$\begin{array}{c} < \\ \text{N} \\ \diagdown \\ \text{CH}_2 \end{array}$
	3.30	$>\text{N}-\text{CH}_2-\text{Ar}$
	7.31	C_6H_5-
4 tb12aneN ₄	2.68	$>\text{N}-\text{CH}_2-\overset{\text{I}}{\underset{\text{I}}{\text{C}}}-\text{N}<$
	3.43	$>\text{N}-\text{CH}_2-\text{Ar}$
	7.30	C_6H_5-
5 14aneN ₄	2.25	$>\text{N}-\overset{\text{I}}{\text{C}}-\text{CH}_2-\overset{\text{I}}{\text{C}}-\text{N}<$
	2.82	$>\text{N}-\text{H}$
	2.69	$>\text{N}-\text{CH}_2-\overset{\text{I}}{\underset{\text{I}}{\text{C}}}-\text{N}<$
	2.76	$>\text{N}-\text{CH}_2-\overset{\text{I}}{\text{C}}-\overset{\text{I}}{\text{C}}-\text{N}<$
6 Me ₄ 14aneN ₄	1.68	$>\text{N}-\overset{\text{I}}{\text{C}}-\text{CH}_2-\overset{\text{I}}{\text{C}}-\text{N}<$
	2.22	$>\text{N}-\text{CH}_3$
	2.43	$>\text{N}-\text{CH}_2-\overset{\text{I}}{\underset{\text{I}}{\text{C}}}-\text{N}<$
	2.51	$>\text{N}-\text{CH}_2-\overset{\text{I}}{\text{C}}-\overset{\text{I}}{\text{C}}-\text{N}<$

N.B. Ar = aromatic, solvent = CDCl_3 with tetramethylsilane as reference.

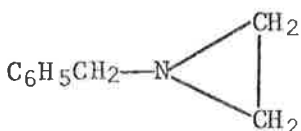
The chemical shifts of the proton or protons attached to the carbon atom or nitrogen atom are given in Table 2.2.

for the first time by a method⁶ similar to the preparation of $\text{Me}_4\text{14aneN}_4$. About 9 gm of 12aneN_4 , 60 cm^3 of formic acid (98-100%), 15 cm^3 of formaldehyde (37-40%), 6 cm^3 of water and antibumping granules were added to a 500 cm^3 two necked round bottom flask fitted with a condenser. The reaction mixture was refluxed for more than 30 hours using a heating mantle and then transferred to a 500 cm^3 beaker. A concentrated solution of sodium hydroxide was added dropwise to the cooled and stirred reaction mixture until the pH became greater than 12. Several extractions were carried out with chloroform and the chloroform was flashed off by a rotatory evaporator leaving behind an oily liquid. The oily liquid was transferred to a pear shaped distilling flask with a little chloroform and distilled at about 363K at 0.1 mm pressure to a clear oily liquid. The purity was checked by ^{13}C and ^1H n.m.r. spectrophotometers (Tables 2.1 and 2.2). Mass spectral analysis⁷ indicated the parent molecule ion at 228. Several batches were prepared and the yield varied from 40 to 66%. The fraction of the distillate collected separately at 333 to 343K and 0.15 mm pressure was discarded.

(c) tbl2aneN_4 :-

The tbl2aneN_4 ligand was prepared according to the following procedure⁸⁻¹²:-

(i) Preparation of N-benzyl aziridine:-



About 50 gm (0.33 mol) of 2-benzylaminoethanol and 18.3 cm^3 of 98% H_2SO_4 (0.33 mol, sp. gr. = 1.84) were separately diluted with half their weight of water. The acid was taken in a two necked round bottom flask fitted with thermometer and cooled in an ice bath. The amine was added slowly to the acid with constant stirring. The reaction mixture was then heated to boil under reduced pressure. Some

antibumping granules were used to prevent bumping. The solution was heated just to keep it boiling until a definite white turbidity appeared between 413 to 423K. Suddenly crystallization took place and the temperature rose up to 458K. The white crystals of 2-benzylaminoethyl-sulphuric acid were collected, washed with ethanol and dried. The yield was 95%.

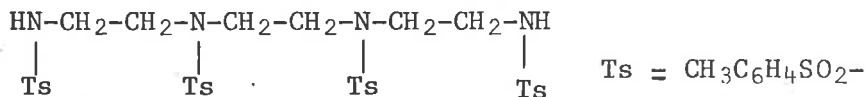
The mixture of 2-benzylaminoethyl sulphuric acid (72.6 gm), water (126 cm³) and sodium hydroxide (55 gm) was heated very close to boiling point (about 373K) in a two necked round bottom flask fitted with a thermometer and a condenser. The cyclization took place before the boiling point was reached and heating was stopped at that time. Two layers were obtained on cooling. The upper imine layer was taken up in ether and mechanically separated from the reaction mixture using a separating funnel. Ether was evaporated off using a water pump leaving behind N-benzyl aziridine. The pure compound was finally obtained by vacuum distillation (353 to 355K, 7 mm pressure). The purity was checked by ¹³C and ¹H n.m.r. spectra (Tables 2.1 and 2.2). The yield was only 20%. A fraction collected at 463 to 473K was discarded.

(ii) The tbl2aneN₄ ligand was prepared by refluxing a mixture of N-benzyl aziridine (5 gm) and p-toluenesulfonic acid (0.025 gm) in 98% ethanol (38 cm³) for more than six hours. On cooling, the white solid ligand was collected by filtration and recrystallised from absolute alcohol. The yield was 50% and the melting point was 413K. The purity of the ligand was checked by ¹³C and ¹H n.m.r. spectra (Tables 2.1 and 2.2).

(d) l3aneN₄:-

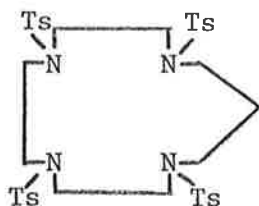
This ligand was prepared by modification of methods^{2,3,13,14} as follows:-

(i) Preparation of tetra-p-toluene sulfonyl derivatives of triethyl-enetetramine:-

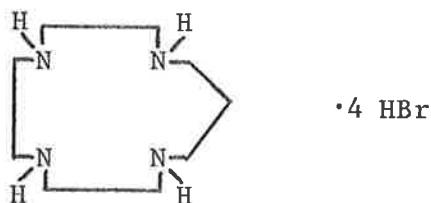


To a stirred solution of triethylenetetramine (29.3 gm) and sodium hydroxide (32 gm) in 216 cm³ water, a solution of p-toluene sulfonyl chloride (153 gm) in 800 cm³ of ether was added dropwise with stirring. The mixture was then stirred for about an hour and a paste like substance was obtained after decantation. This substance was digested with 1 litre of methanol and filtered to get tosylated linear tetramine. Two batches were prepared and the yield was 40% and 45%, respectively. The compound starts decomposing at 488K.

(ii) Preparation of tetratosyl 1,3-diazetaneN₄:-



About 15 gm of 50% sodium hydride was added slowly to a magnetically stirred solution of tosylated linear tetramine (92 gm) in 2.3 litres dmf in a 3 litre conical flask. The solution was then stirred until the evolution of hydrogen ceased. A solution of 1,3 dibromopropane (25 gm) in 500 cm³ dmf was slowly added to the stirred solution at 393K over a period of 3 hours. The resulting solution was stirred for a further period of two hours. The addition of water (approximately 12 litres) to the cooled solution caused crystals to precipitate. The solutions were stirred for more than three hours and allowed to stand overnight. The crystals were filtered, washed with water, small amount of ethanol and dried. The colour of the compound is light yellow and it starts decomposing at about 483K. The yield was 72%.

(iii) Preparation of 13aneN₄ hydrobromide:-

The 13aneN₄ hydrobromide was prepared by exactly the same method as that used in the preparation of 12aneN₄ hydrobromide. Two batches were prepared and the yield was 50% and 45%, respectively.

(iv) Free ligand extraction:-

The ligand was extracted by exactly the same procedure used for the extraction of 12aneN₄. The purity was checked by ¹³C n.m.r. spectrum (Table 2.1). Two batches were prepared and the yield was 63% and 55%. The ligand is an oily liquid.

(e) 14aneN₄ and Me₄14aneN₄:-

These ligands were purchased from Strem chemicals, recrystallised from water and the purity was checked by ¹³C and ¹H n.m.r. spectra (Tables 2.1 and 2.2).

2.3.1 Preparation of Complexes:-

The complexes were prepared by methods similar to those in the literature^{2,6,15-18}.

(a) [Ni(12aneN₄)](ClO₄)₂:-

About 5.8 gm of [Ni(ClO₄)₂], 6H₂O was dissolved in 40 cm³ of absolute ethanol and filtered. About 2.8 gm 12aneN₄ was dissolved in 20 cm³ absolute ethanol. To the hot and stirred ethanolic solution of [Ni(ClO₄)₂], 6H₂O, the ligand solution was added dropwise and after completion of addition, the reaction mixture was refluxed for 15 minutes. The solution was then cooled, filtered through millipore filter paper and evaporated to dryness by rotatory evaporator. The brownish yellow product was dried in a vacuum dessicator and digested by four 30 cm³ lots of dry chloroform to remove chloroform soluble impurities and excess ligand. The

last traces of water was finally removed by digestion in triethylorthoformate for about two hours. The product was then filtered and washed with dry chloroform under dry nitrogen atmosphere and finally dried in a vacuum dessicator and characterised. A few batches were prepared and the yield varied from 75-80%.

(b) [Ni(Me₄12aneN₄)](ClO₄)₂ (ethanol water preparation):-

About 8.1 gm of [Ni(ClO₄)₂], 6H₂O was dissolved in 100 cm³ of water and filtered. About 5.1 gm of Me₄12aneN₄ was dissolved in 50 cm³ of ethanol. To the hot and stirred solution of nickel(II), ligand solution was added dropwise. The reaction mixture was refluxed for four hours and left overnight at room temperature with stirring to ensure completion of the reaction. The solution was then filtered through millipore filter paper and evaporated to dryness by rotatory evaporator. The orange crystals were washed several times with dry ethanol, dried in a vacuum dessicator and finally characterised. The yield was 80%.

(c) [Ni(Me₄12aneN₄)](ClO₄)₂ (ethanol preparation):-

To the hot and stirred ethanolic solution of [Ni(ClO₄)₂], 6H₂O (1.1 gm in 30 cm³), ligand solution (0.7 gm in 20 cm³) was added dropwise and the reaction mixture was refluxed for about 10 minutes. The pink crystals were collected by filtration, washed with ethanol, dried in a vacuum dessicator and finally characterised. The yield was 78%.

(d) [Ni(Me₄12aneN₄)](ClO₄)₂ (ethanol preparation using triethylorthoformate):-

About 0.8 gm of [Ni(ClO₄)₂], 6H₂O was dissolved in 20 cm³ ethanol containing 9 gm of triethylorthoformate and filtered. The ligand solution (0.5 gm in 10 cm³ ethanol with a little triethylorthoformate) was added dropwise to the hot and stirred solution of [Ni(ClO₄)₂], 6H₂O. The reaction mixture was refluxed at 328K (a silica gel drying tube was inserted into the top of the reflux condenser) for about an hour and then filtered to obtain light orange crystals. The crystals were washed several times with dry chloroform, left overnight by passing nitrogen through the complex inside a dry box, dried under a vacuum line and finally characterised. The

yield was 68%.

(e) $[\text{Ni}(\text{Me}_4\text{12aneN}_4)(\text{dmf})](\text{ClO}_4)_2$ (dmf preparation):-

The ligand solution (1 gm in 10 cm³ dmf) was added dropwise to the filtered and stirred solution of $[\text{Ni}(\text{dmf})_6](\text{ClO}_4)_2$ (3 gm in 20 cm³ dmf) inside a dry box. The reaction mixture was left overnight with stirring and then evaporated to dryness by a rotatory evaporator. The green complex was washed with ether, dried under nitrogen and in a vacuum dessicator before characterisation. The yield was 92%.

(f) $[\text{Ni}(\text{tb12aneN}_4)\text{Cl}]\text{Cl}^{16}$:-

To the filtered, hot and stirred ethanolic solution of $[\text{NiCl}_2] \cdot 6\text{H}_2\text{O}$ (0.3 gm in 20 cm³), the ligand solution (0.3 gm in 50 cm³) was added dropwise. The reaction mixture was refluxed for 15 minutes, cooled and filtered. The yellow-green crystals were washed with ethanol, ether and dried in a vacuum dessicator before characterisation. The yield was 60%.

(g) $[\text{Ni}(\text{tb12aneN}_4)\text{NO}_3]\text{NO}_3^{16}$:-

This complex was prepared by exactly the same way used for preparing $[\text{Ni}(\text{tb12aneN}_4)\text{Cl}]\text{Cl}$. The colour of the complex is blue and the yield was 68%.

(h) $[\text{Ni}(\text{13aneN}_4)](\text{ClO}_4)_2$:-

This complex was prepared by exactly the same way used for preparing $[\text{Ni}(\text{12aneN}_4)](\text{ClO}_4)_2$. The colour of the complex is yellow and the yield was 78%.

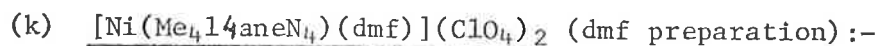
(i) $[\text{Ni}(\text{Me}_4\text{14aneN}_4)](\text{ClO}_4)_2$ (ethanol water preparation):-

The same preparative method was employed as used in the case of $[\text{Ni}(\text{Me}_4\text{12aneN}_4)](\text{ClO}_4)_2$ (ethanol water preparation). The colour of the complex is red and the yield was 96%.

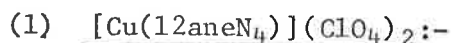
(j) $[\text{Ni}(\text{Me}_4\text{14aneN}_4)](\text{ClO}_4)_2$ (ethanol preparation using triethylorthoformate):-

The method used for the preparation of $[\text{Ni}(\text{Me}_4\text{12aneN}_4)](\text{ClO}_4)_2$ (ethanol preparation using triethylorthoformate) is also used for preparing N.B. Hereafter, unless otherwise mentioned, the $[\text{Ni}(\text{Me}_4\text{12aneN}_4)](\text{ClO}_4)_2$ and $[\text{Ni}(\text{Me}_4\text{14aneN}_4)](\text{ClO}_4)_2$ complexes are from ethanol water preparation.

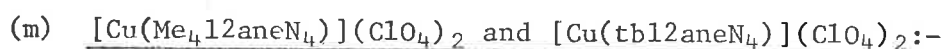
this complex. The colour of the complex is red and the yeild was 82%.



This complex was prepared by the method used for the preparation of $[\text{Ni}(\text{Me}_4\text{12aneN}_4)(\text{dmf})](\text{ClO}_4)_2$ except that in this case solid ligand was added slowly to the metal ion solution. The colour of the complex is green and the yield was 93%.



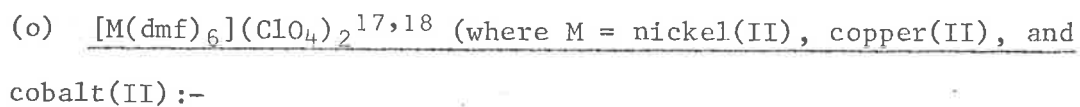
To the filtered, hot and stirred ethanolic solution of $[\text{Cu}(\text{ClO}_4)_2]$, 6 H₂O (3 gm in 20 cm³), the ligand solution (1.4 gm in 10 cm³) was added dropwise. The reaction mixture was refluxed for another 15 minutes and cooled to obtain purple crystals which were washed several times with ethanol to remove excess ligand. The complex was dissolved in water, filtered through a millipore filter, evaporated to dryness by a rotatory evaporator and dried in a vacuum dessicator before characterisation. The yield was 65%.



These two complexes were prepared by the method used for the preparation of $[\text{Cu}(\text{12aneN}_4)](\text{ClO}_4)_2$. The colour of both the complexes are blue. The yield was 92% and 68% for $[\text{Cu}(\text{Me}_4\text{12aneN}_4)](\text{ClO}_4)_2$ and $[\text{Cu}(\text{tb12aneN}_4)](\text{ClO}_4)_2$ respectively.



An attempt to prepare this complex was unsuccessful. Ethanolic solution of tb12aneN₄ (0.2 gm in 50 cm³) was added dropwise to the filtered, hot and stirred solution of $[\text{Ni}(\text{ClO}_4)_2]$, 6H₂O (0.12 gm in 10 cm³). No reaction was occurred even after refluxing for more than one hour.



A mixture of 0.039 mol of $[\text{M}(\text{ClO}_4)_2]$, 6H₂O, 27.5 × 0.039 mols of triethylorthoformate and 0.028 mol of dmf was refluxed at 328K under silica gel drying tube for about two hours. The product was filtered, washed several times with ether inside a dry box, left to dry overnight under nitrogen and

finally dried under a vacuum line. The yield varied from 80 to 90%.

(p) [Ni(Me₄12aneN₄)N₃] ClO₄ :-

About 0.3 gm of NaN₃ and 2.0 gm of [Ni(Me₄12aneN₄)](ClO₄)₂ (2.3b) were dissolved separately in a minimum amount of water. To the stirred solution of the complex, NaN₃ solution was added dropwise and then filtered. The green crystals were washed with ethanol and dried in a vacuum dessicator and characterised. The yield was 74%.

(q) [Ni(Me₄12aneN₄)NCS]NCS :-

This complex was prepared by the method employed for the preparation of [Ni(Me₄12aneN₄)](ClO₄)₂ (ethanol water preparation). The colour of the complex is green and the yield was 75%.

2.3.2 Ligand Extraction from [Ni(13aneN₄)](ClO₄)₂ :-

It became necessary to synthesis a small amount of the 13aneN₄ ligand and the ligand was therefore synthesised from pure [Ni(13aneN₄)](ClO₄)₂ in the following way^{13,14} which is a standard procedure for extraction of ligand from metal complexes. A strong solution of sodium hydroxide was prepared in water and added to 2.5 gm of NaCN so that aqueous NaCN solution is basic. The [Ni(13aneN₄)](ClO₄)₂ complex (2 gm) was added slowly to the aqueous solution of NaCN with stirring and refluxed for more than two hours. The reaction mixture was cooled and pH was adjusted to above 12 with sodium hydroxide solution. Several extractions were carried out with chloroform which was flashed off using a rotatory evaporator leaving behind the oily ligand. The purity of the ligand was checked by ¹³C n.m.r. spectrum (Table 2.1) and the chemical shifts were found similar to those obtained previously using the ligand mentioned in section 2.2. The yield was 70%.

2.4 Characterisation of Compounds :-

(a) Infra-red spectral measurements :-

A qualitative infra-red spectral analysis was employed to detect the presence of co-ordinated water, bound or free perchlorate and the general characteristic of the compounds. The measurements were recorded on a Perkin Elmer 457 grating infra-red spectrophotometer using NaCl windows

with nujol as the mulling agent (0.05 mm polystyrene film as reference). The I.R. frequencies of the compounds assigned according to the literature¹⁹⁻²³ are given in Table 2.3

Table 2.3
I.R. Spectral Data

Compounds	Substituents	I.R. Frequencies (cm ⁻¹)
1 12aneN ₄	HO-H	3560(msh), 3400(bs)
	>NH, HO-H	3330(msp), 3280(mwsp)
	$\begin{array}{l} \text{>CN<} \\ \text{>C-C<} \end{array}$	1130(m), 1125(s), 1082(msh), 1053(m), 1040(m), 1020(w), 1012(w)
	>N(CH ₂) ₂ N<	962(ms), 946(s), 890(bm), 860(s), 762(s), 725(w)
2 Me ₄ 12aneN ₄	HO-H	3300(bs)
	>NCH ₂	2760(s)
	$\begin{array}{l} \text{>CN<} \\ \text{>C-C<} \end{array}$	1140(msh), 1105(s), 1065(s), 1030(s)
	>N(CH ₂) ₂ N<	970(s), 894(m), 880(ms), 815(wsh), 770(w), 745(s)
3 tb12aneN ₄	HO-H	3400(bm)
	>NCH ₂	2710(w)
	Ar. rings	1600(w)
	$\begin{array}{l} \text{>CN<} \\ \text{>C-C<} \end{array}$	1153(w), 1138(w), 1130(w), 1080(m), 1060(m), 1043(m)
	>N(CH ₂) ₂ N<	985(m), 970(m doublet), 925(m), 903(w), 882(w), 825(w), 795(m), 760(m), 728(s), 690(s), 660(w)

Compounds	Substituents	I.R. Frequencies (cm ⁻¹)
4 Tetratosyl·12aneN ₄	HO-H	3280(bw)
	Ar. rings	1595(m)
	-SO ₂ -N<	1342(ms), 1164(s)
	>N(CH ₂) ₂ N<	975(m), 900(m), 818(ms), 770(msh), 720(s)
5 Ni(12aneN ₄)(ClO ₄) ₂	>NH, HO-H	3322(m), 3255(s)
	ClO ₄ ⁻	ν ₃ 1085(bvs), ν ₁ 960(ms), ν ₄ 628(s)
	>N(CH ₂) ₂ N<	925(w), 870(w), 810(m), 728(ms)
6 [Ni(Me ₄ 12aneN ₄)](ClO ₄) ₂ (ethanol water preparation) (KBr plate used)	HO-H	3520(bm)
	ClO ₄ ⁻	ν ₃ 1075(bs), ν ₁ 965(m), ν ₄ 616(s)
	Ni-N	520(mw)
	>N(CH ₂) ₂ N<	915(m), 802(w), 750(ms), 720(wsh)
7 [Ni(Me ₄ 12aneN ₄)](ClO ₄) ₂ (ethanol preparation)	HO-H	3460(bm)
	ClO ₄ ⁻	ν ₃ 1080(bs), ν ₄ 618(m)
	>N(CH ₂) ₂ N<	780(bw), 740(msh), 715(m)
8 [Ni(Me ₄ 12aneN ₄)](ClO ₄) ₂ (ethanol preparation using triethylorthoformate)	ClO ₄ ⁻	ν ₃ 1089(s), ν ₁ 960(w), ν ₄ 620(ms),
	>N(CH ₂) ₂ N<	918(w), 755(ms), 719(ws), 663(w)
9 [Ni(Me ₄ 12aneN ₄)(dmf)] (ClO ₄) ₂ (dmf preparation)	$\text{H}-\overset{\text{O}}{\parallel}{\text{C}}-\text{N}(\text{CH}_3)_2$	1670(s)
	ClO ₄ ⁻	ν ₃ 1091(vs), ν ₁ 963(m), ν ₄ 622(ms)
	>N(CH ₂) ₂ N<	904(m), 795(w), 748(m), 725(w), 622(vw)

Compounds	Substituents	I.R. Frequencies (cm ⁻¹)
10 [Ni(tb12aneN ₄) NO ₃] NO ₃	HO-H	3400(bw)
	>NCH ₂	2720(mw)
	-O-NO ₂	ν ₅ 1305(m), ν ₁ 1278(m), ν ₂ 1023(m) ν ₄ 720(ms), 700(m) (split)
	>N(CH ₂) ₂ N<	780(m), 745(w), 720(s), 700(m) doublet), 660(msp)
11 [Ni(tb12aneN ₄) Cl]Cl	HO-H	3400(bw)
	>NCH ₂	2720(mw)
	Ar. rings	1580(vw)
	>N(CH ₂) ₂ N<	780(msp), 743(m), 723(ms) 700(s), 660(ms)
12 [Ni(13aneN ₄)](ClO ₄) ₂	HO-H	3460(bw)
	>NH, HO-H	3200(ms)
	ClO ₄ ⁻	ν ₃ 1075(bs), ν ₁ 965(m), ν ₄ 615(w)
	>N(CH ₂) ₂ N<	715(s), others vw
	>N(CH ₂) ₃ N<	
13 [Ni(Me ₄ 14aneN ₄)](ClO ₄) ₂ (ethanol water preparation) (KBr plate used)	HO-H	3440(vw)
	ClO ₄ ⁻	ν ₃ 1075(bs), ν ₁ 950(m), ν ₄ 618(s) ν ₂ 47(vw)
	Ni-N	528(w)
	>N(CH ₂) ₂ N<	925(mw), 902(w), 868(w), 802(ms), 733(m), 715(wsh)
	>N(CH ₂) ₃ N<	

Compounds	Substituents	I.R. Frequencies (cm ⁻¹)
14 [Ni(Me ₄ 14aneN ₄)](ClO ₄) ₂ (ethanol preparation using triethylortho- formate)	ClO ₄ ⁻ >N(CH ₂) ₂ N< >N(CH ₂) ₃ N<	ν ₃ 1082(bs), ν ₁ 980(m), ν ₄ 622(s) 927(mw), 905(w), 870(vw), 805(ms), 758(m), 735(m)
15 [Ni(Me ₄ 14aneN ₄)(dmf)] (ClO ₄) ₂ (dmf preparation)	$\text{H}-\overset{\text{O}}{\parallel}{\text{C}}-\text{N}(\text{CH}_3)_2$ ClO ₄ ⁻ >N(CH ₂) ₂ N< >N(CH ₂) ₃ N<	1670(s) ν ₃ 1090(bs), ν ₁ 960(m), ν ₄ 620(s) 928(mw), 896(w), 868(vw), 803(ms), 756(w), 727(m), 700(m)
16 [Ni(Me ₄ 12aneN ₄)N ₃] ClO ₄	HO-H N ₃ ⁻ ClO ₄ ⁻ >N(CH ₂) ₂ N<	3325(bw) 2045(ssp) ν ₃ 1080(vs), ν ₁ 963(m) ν ₄ 621(ms) 905(m), 795(w), 749(ms), 718(w), 660(vw)
17 [Cu(12aneN ₄)](ClO ₄) ₂	HO-H >NH ClO ₄ ⁻ >N(CH ₂) ₂ N<	3480(bm) 3280(sps) ν ₃ 1090(bs), ν ₁ 980(m), ν ₄ 630(mw) 925(w), 912(w), 875(m), 812(m), 728(m)
18 [Cu(Me ₄ 12aneN ₄)](ClO ₄) ₂	HO-H ClO ₄ ⁻ >N(CH ₂) ₂ N<	3360(bw) ν ₃ 1070(bs), ν ₁ 960(m), ν ₄ 617(mw) 902(m), 865(w), 749(m), 715(ms)

Compounds	Substituents	I.R. Frequencies (cm ⁻¹)
19 [Cu(tbl2aneN ₄)](ClO ₄) ₂	HO-H	3330(vw)
	>N-CH ₂	2720(mw)
	Ar. rings	1580(vw)
	ClO ₄ ⁻	v ₃ 1075(bs), v ₁ 938(m), v ₄ 612(mw)
	>N(CH ₂) ₂ N<	780(m), 750(m), 720(s doublet), 702(ssh)

N.B. ClO₄⁻ = ionic perchlorate

-O-NO₂ = unidentate

v₁ = symmetrical stretching

v₂ = symmetrical bending

v₃ = asymmetrical stretching

v₄ = asymmetrical bending

Ar. = aromatic

s = strong

m = medium

w = weak

sp = sharp

sh = shoulder

b = broad

v = very

(b) Metal analysis:-

Ion exchange method²⁴ was carried out using Dowex 50W cation exchange resin in the hydrogen form for a quantitative determination of metal ion content and stoichiometry for each of the complexes prepared. A known amount of dry complex was dissolved in distilled water and eluted through the resin. The acidic effluent was then titrated against standardised sodium hydroxide using bromothymol blue indicator. The results of the metal analysis are given in Table 2.4.

Table 2.4

Microanalysis and Metal Analysis Data

Compound	% C required	% C found	% H required	% H found	% N required	% N found	% metal required	% metal found
1 12aneN ₄ ·hydrobromide	19.39	18.62	4.88	4.92	11.30	11.36	-	-
2 tb12aneN ₄	81.16	80.97	8.32	8.08	10.52	10.44	-	-
3 [Ni(12aneN ₄)](ClO ₄) ₂	22.35	21.90	4.69	4.71	13.03	12.52	13.66	13.45
4 [Ni(Me ₄ 12aneN ₄)](ClO ₄) ₂ (ethanol water preparation)	29.66	29.97	5.81	5.97	11.53	10.75	12.08	11.93
5 [Ni(Me ₄ 12aneN ₄)](ClO ₄) ₂ (ethanol preparation using triethylorthoformate)	29.66	28.44	5.81	5.62	11.53	10.68	12.08	11.40
6 [Ni(Me ₄ 12aneN ₄)(dmf)](ClO ₄) ₂ (dmf preparation)	32.28	32.16	6.32	6.38	12.55	12.43	10.52	10.39
7 [Ni(Me ₄ 12aneN ₄)](ClO ₄) ₂ (ethanol preparation)	-	-	-	-	-	-	12.08	11.62
8 [Ni(Me ₄ 12aneN ₄)N ₃] ClO ₄	33.64	33.80	6.59	6.87	22.88	22.93	13.70	13.43
9 [Ni(Me ₄ 12aneN ₄)NCS]NCS, H ₂ O	39.89	38.55	7.12	6.50	19.94	18.23	-	-
10 [Ni(tb12aneN ₄)Cl]Cl	64.40	63.10	6.61	5.82	8.35	7.84	8.86	8.67

Table 2.4 (cont.)

Compound	% C required	% C found	% H required	% H found	% N required	% N found	% metal required	% metal found
11 [Ni(tb12aneN ₄)NO ₃] ₂ NO ₃	59.68	58.33	6.26	5.83	11.60	10.88	8.21	8.02
12 [Ni(13aneN ₄)](ClO ₄) ₂	24.35	24.83	5.00	5.20	12.62	12.72	13.23	13.08
13 [Ni(Me ₄ 14aneN ₄)](ClO ₄) ₂ (ethanol water preparation)	32.72	32.47	6.28	6.03	10.90	11.10	11.42	11.36
14 [Ni(Me ₄ 14aneN ₄)](ClO ₄) ₂ (ethanol preparation using triethylorthoformate)	32.72	32.73	6.29	6.19	10.90	10.76	11.42	11.32
15 [Ni(Me ₄ 14aneN ₄)(dmf)](ClO ₄) ₂ (dmf preparation)	34.79	34.65	6.70	6.69	11.93	11.82	10.00	10.01
16 [Cu(12aneN ₄)](ClO ₄) ₂	22.11	22.49	4.64	4.64	12.89	12.71	14.50	14.62
17 [Cu(Me ₄ 12aneN ₄)](ClO ₄) ₂	28.30	29.68	5.90	6.37	11.01	10.30	12.33	12.49
18 [Cu(tb12aneN ₄)](ClO ₄) ₂	54.37	53.50	5.58	5.76	7.05	7.15	7.99	7.75

(c) The Elemental Analysis (C, H and N):-

The analysis was carried out by the C.S.I.R.O. Microanalytical Division in Melbourne. The results of the analysis are given in Table 2.4.

(d) N.m.r. Spectral Analysis:-

^{13}C n.m.r. spectra²⁵ were recorded either on a Bruker WP80 (80 Mhz for ^1H and 20.1 Mhz for ^{13}C) or HX90E (90 Mhz for ^1H and 22.63 for ^{13}C) to characterise the ligands and also complex. A Varian T60 (^1H n.m.r.) was also used whenever appropriate. Deuterated solvents and 10 mm n.m.r. tubes were used. The results of ^{13}C n.m.r. and ^1H n.m.r. are given in Tables 2.1 and 2.2, respectively.

The ^{13}C n.m.r. peaks were assigned according to intensity, multiplicity and in consultation with the literature^{19,26-28}. In $\text{Me}_4\text{14aneN}_4$, three peaks were observed instead of theoretically expected four peaks because of two different carbon environments having the same chemical shift. The peaks of other compounds are consistent with those expected. The chemical shifts differ due to solvent and functional group.

All the ^1H n.m.r. spectra were run in CDCl_3 with tetramethylsilane as reference. The peaks were assigned according to intensity, multiplicity and in consultation with the literature^{19,26-28}. The number of peaks found in each case are consistent with those theoretically expected.

2.5.1 Determination of pKa Value of 12aneN₄ and Me₄12aneN₄:-

In theory, the presence of four amine groups in 12aneN₄ creates the possibility that each ligand molecule may accept four protons and that such behaviour does occur is shown by the isolation of 12aneN₄·4HBr (see section 2.2). The pKa value of 12aneN₄ at 298.2K and ionic strength 1.0 (adjusted with NaClO₄) was found to be 10.1 ± 0.2 by potentiometric titration. Only one equivalence point was observed which is consistent with two protonations (characterised by similar pKa's of 12aneN₄). Experimentally 5.0 cm³ of 4.88×10^{-2} mol dm⁻³ 12aneN₄ in 1.0 mol dm⁻³ NaClO₄ (nitrogen gas bubbling through the solution) was titrated with 1.0 mol dm⁻³ HClO₄ using a calibrated micro-meter syringe and the pH was recorded after each addition. Blank 1.0 mol dm⁻³

NaClO_4 was also titrated under identical conditions for pH correction. Figure 2.1 shows the plot of pH (after correction for the blank titration) against the number of mmols of acid added. The end point observed at pH 5.0 indicate that two protonation of 12aneN_4 occurs each characterised by similar pK_a (≈ 10.1) values. The pK_a values of $\text{Me}_412\text{aneN}_4$ in 1.0 mol dm^{-3} NaClO_4 and 298.2K were determined under conditions identical to those for 12aneN_4 . Two equivalence points were observed (Figure 2.2) indicating that at equilibrium the ligand exists as $\text{Me}_412\text{aneN}_4\text{H}_2^{2+}$. The two pK_a values are approximately 11.4 and 9.2.

Protonation of the three $-\text{N}(\text{CH}_3)_2$ and three $-\text{NH}_2$ groups of the ligands Me_6tren and tren , respectively, results in a single equivalence point^{29, 30} because of similar pK_a 's in each case. In the case of the 12aneN_4 ligand two intramolecular hydrogen bonds probably form, each involving two nitrogen and one hydrogen atoms. Hence, leaving only two nitrogen lone pairs easily accessible for protonation. This would explain why two protons are accepted by 12aneN_4 during titration with acid. The titration of $\text{Me}_412\text{aneN}_4$ with acid results in the protonation of only two of the nitrogen atoms, hence allowing similar hydrogen bonding as for the 12aneN_4 ligand. The 14aneN_4 and $\text{Me}_414\text{aneN}_4$ ligands also only accept two protons in two well separated steps and the same explanations were given in the literature³¹.

2.5.2 Potentiometric and Spectrophotometric Titration of Metal Macrocyclic Complexes:-

Aqueous 1.0 mol dm^{-3} NaClO_4 with and without the $[\text{Ni}(12\text{aneN}_4)]^{2+}$ complex was titrated against 0.20 mol dm^{-3} NaOH and 0.20 mol dm^{-3} HClO_4 (ionic strength 1.0 adjusted with NaClO_4) separately at 298.2K . The titration curves did not show any equivalence point and the curves looked like the titration curve of pure water. The $[\text{Ni}(13\text{aneN}_4)](\text{ClO}_4)_2$, $[\text{Ni}(\text{Me}_414\text{aneN}_4)](\text{ClO}_4)_2$ and $[\text{Cu}(12\text{aneN}_4)](\text{ClO}_4)_2$ complexes were also titrated under conditions identical to those for the $[\text{Ni}(12\text{aneN}_4)]^{2+}$ complex with the same result.

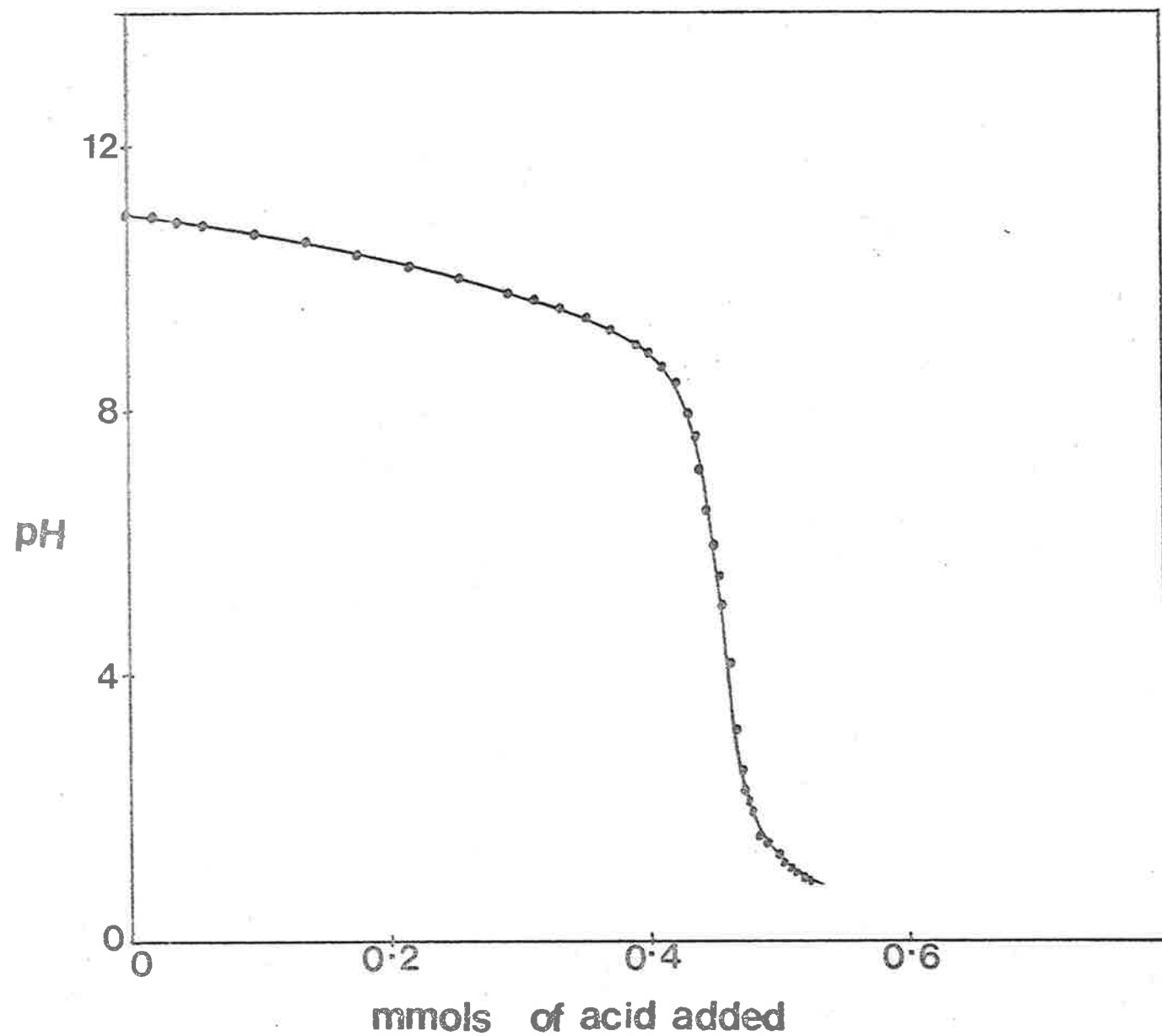


Figure 2.1

Potentiometric pH titration curve for the determination of pKa of 12aneN₄ at 298.2 K. An aqueous solution (5 cm³) of 4.88 × 10⁻² mol dm⁻³ ligand (ionic strength adjusted to 1 with NaClO₄) was titrated against 1 mol dm⁻³ HClO₄ from calibrated micrometer syringe.

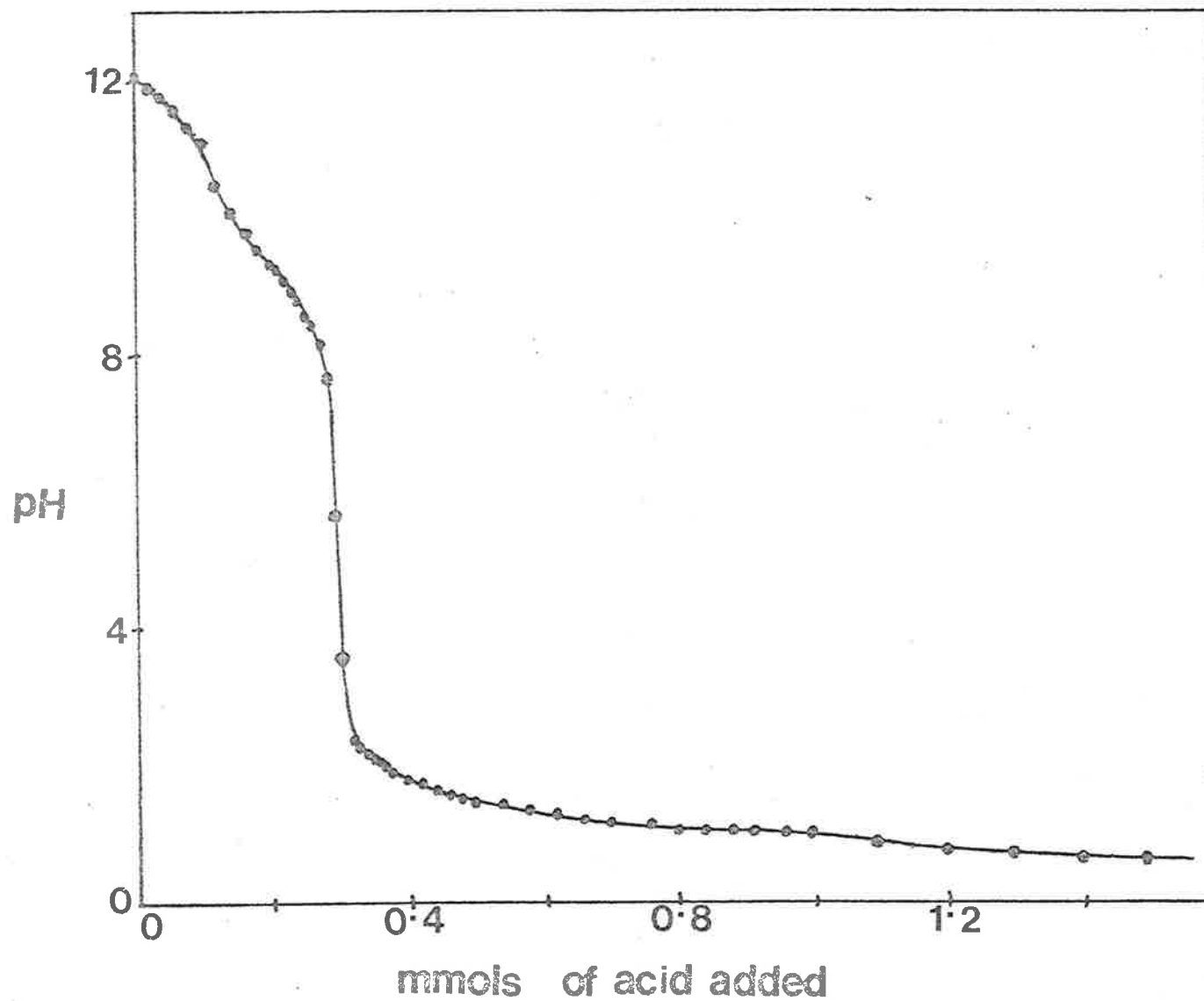


Figure 2.2

Potentiometric pH titration curve for the determination of pKa values of Me₄12aneN₄ at 298.2 K. An aqueous solution (5 cm³) of 3.08 × 10⁻² mol dm⁻³ ligand (ionic strength adjusted to 1 with NaClO₄) was titrated against 1 mol dm⁻³ HClO₄ from calibrated micrometer syringe.

Therefore spectrophotometric pH titration with NaOH was employed to determine the pKa values of these complexes. Experimentally, 2.0 cm³ solution of known concentration of a complex was taken in a spectrophotometer cell and the spectrum was run using a uv/visible spectrophotometer after recording the pH of the solution. A known quantity of aqueous sodium hydroxide solution (micrometer syringe used) was added to the solution in the cell and the solution was stirred with a teflon plunger mounted on a thin platinum wire. The pH and the spectrum of the solution were recorded after each addition. The new concentration of the complex was calculated in each case. The molar extinction coefficient at a particular wavelength was then plotted against pH. The results of the pH titration of different complexes are given in Table 2.5. Figures 2.3 and 2.4, 2.5 and 2.6, and 2.7 and 2.8 show the spectrophotometric pH titration of [Ni(Me₄12aneN₄)](ClO₄)₂, [Ni(Me₄14aneN₄)](ClO₄)₂ and [Cu(Me₄12aneN₄)](ClO₄)₂ in 0.5 mol dm⁻³ LiClO₄ at 293.2K, respectively. No isosbestic point was observed in the case of [Ni(12aneN₄)]²⁺ and [Ni(13aneN₄)]²⁺ complexes after constructing the spectra for the same concentration in each case and this implies that the molar extinction coefficient of aquo and hydroxo complexes are different at all wavelengths examined. At the end of the titration, the purple-blue solution of [Ni(12aneN₄)]²⁺ turns blue, the yellow solution of [Ni(13aneN₄)]²⁺ turns yellow-green, the reddish solution of [Ni(Me₄12aneN₄)]²⁺ turns greenish, the red solution of [Ni(Me₄14aneN₄)]²⁺ turns green and the blue solution of [Cu(Me₄12aneN₄)]²⁺ turns light blue but the original colour reappears on addition of HClO₄ in all cases. The results of spectrophotometric pH titration of [Ni(Me₄14aneN₄)]²⁺ are consistent with those of a recent publication³². For example, the pKa value of 10.7 compares with 10.8 of the literature³². (The results discussed here were obtained prior to the appearance of reference 32). The pKa values were taken as the pH at which the spectral change was half way between the limiting spectra observed at

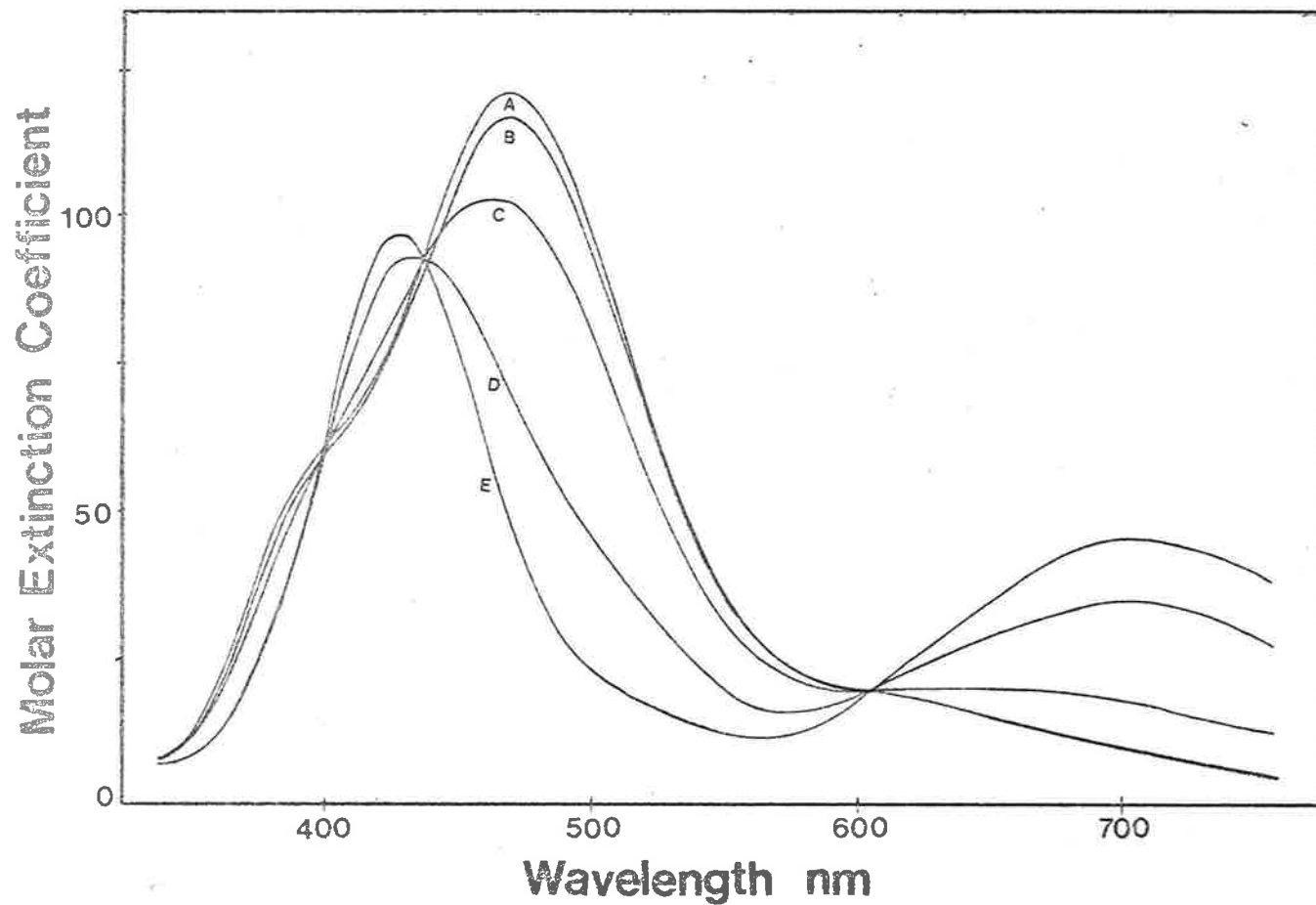


Figure 2.3

Spectrophotometric pH titration of aqueous $2.78 \times 10^{-3} \text{ mol dm}^{-3}$ $[\text{Ni}(\text{Me}_4\text{12aneN}_4)](\text{ClO}_4)_2$ solution against NaOH (ionic strength adjusted to 0.5 with LiClO_4) at 293.2 K. pH 6.30, 8.38, 9.66, 10.46 and 11.45 for the spectra from A to E.

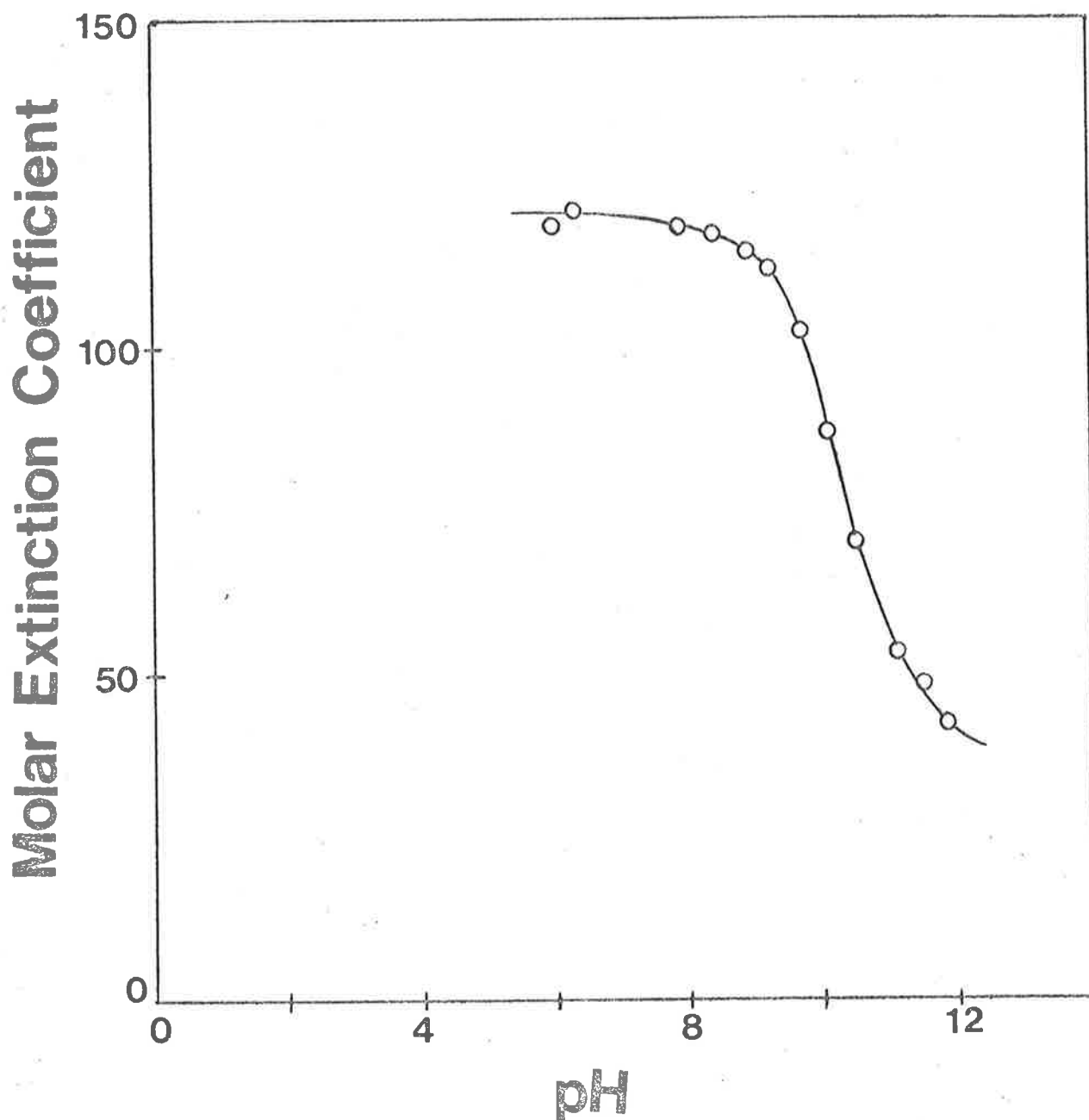
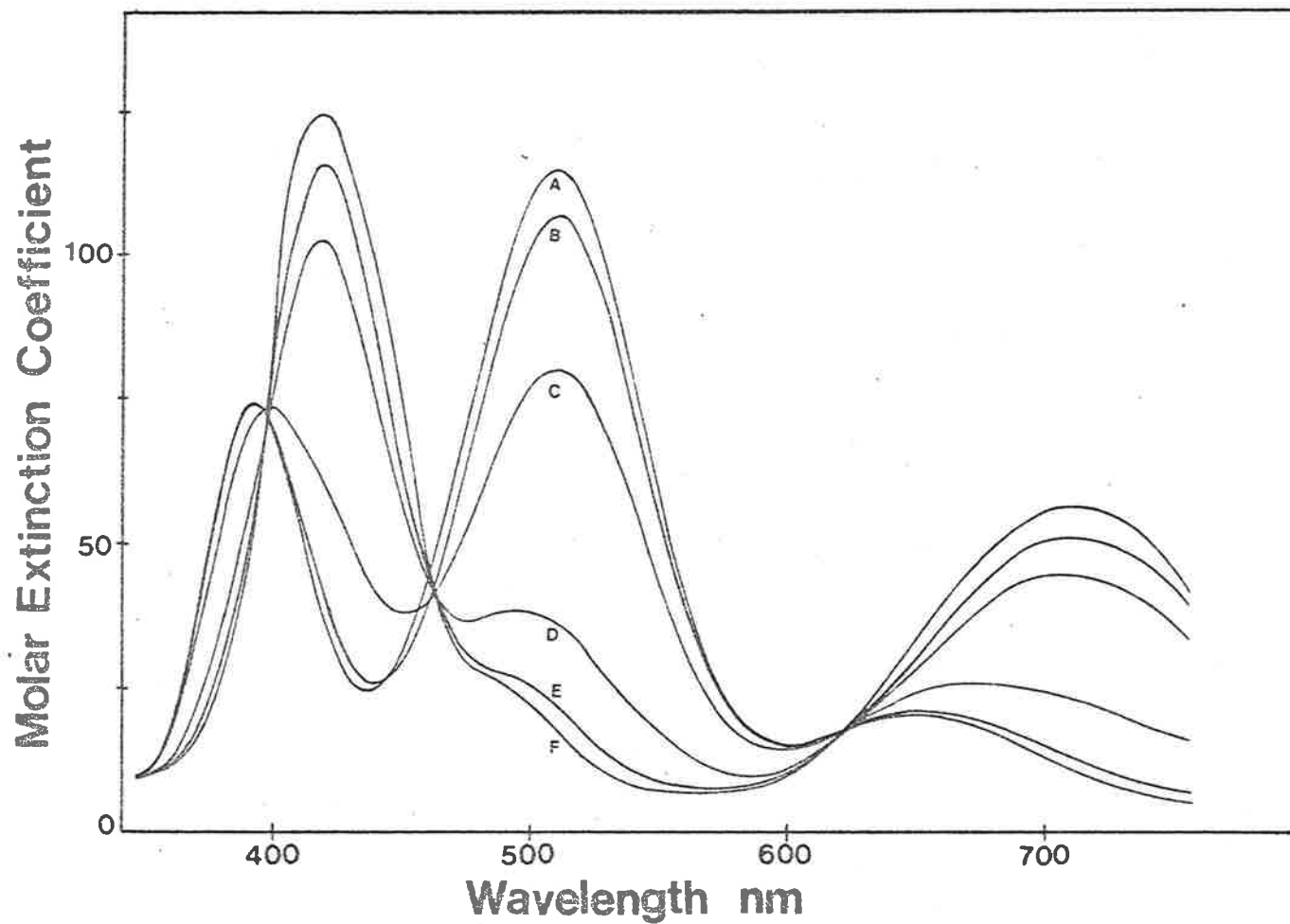


Figure 2.4

Spectrophotometric pH titration curve of aqueous $2.78 \times 10^{-3} \text{ mol dm}^{-3}$ $[\text{Ni}(\text{Me}_4\text{12aneN}_4)](\text{ClO}_4)_2$ solution against NaOH at 293.2 K and $\lambda = 468 \text{ nm}$ (ionic strength adjusted to 0.5 with LiClO_4). Further addition of base does not cause a significant spectral change. Some datum points are obtained from Figure 2.3

Figure 2.5

Spectrophotometric pH titration of aqueous $2.80 \times 10^{-3} \text{ mol dm}^{-3}$ $[\text{Ni}(\text{Me}_4\text{14aneN}_4)](\text{ClO}_4)_2$ solution against NaOH (ionic strength adjusted to 0.5 with LiClO_4) at 293.2 K. pH 7.54, 9.28, 10.21, 11.05, 11.52 and 11.85 for the spectra from A to F.



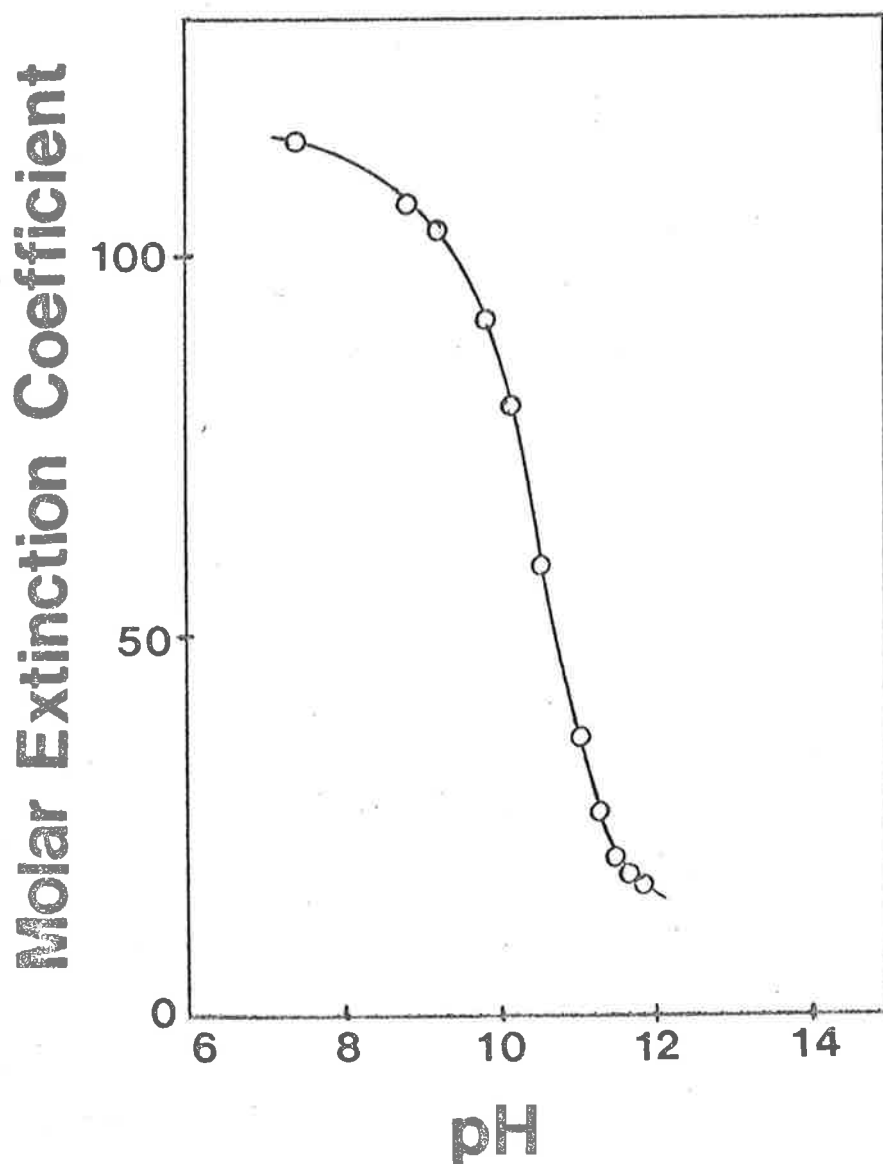
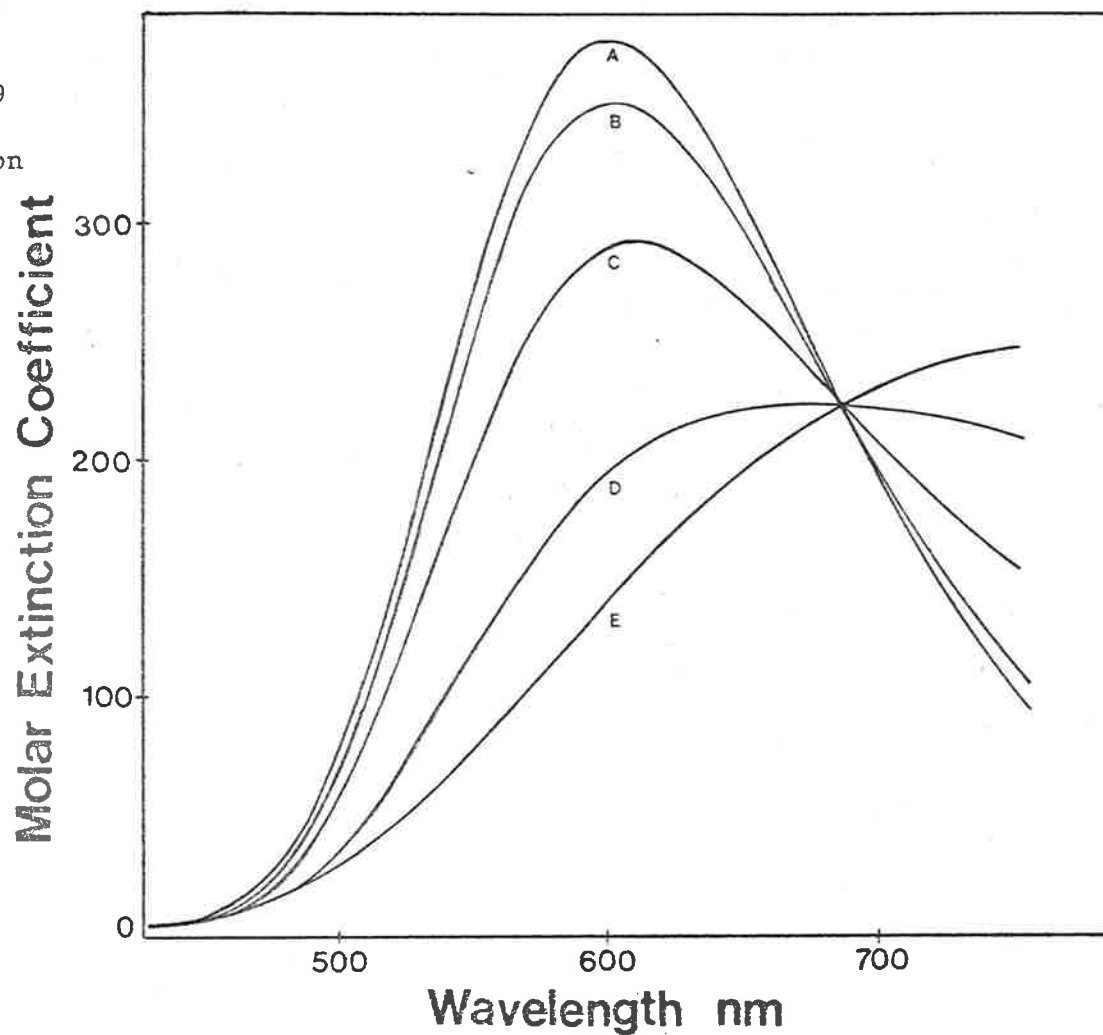


Figure 2.6

Spectrophotometric pH titration curve of aqueous $2.80 \times 10^{-3} \text{ mol dm}^{-3}$ $[\text{Ni}(\text{Me}_4\text{14aneN}_4)](\text{ClO}_4)_2$ solution against NaOH at 293.2 K and $\lambda = 514 \text{ nm}$ (ionic strength adjusted to 0.5 with LiClO_4). Further addition of base does not cause a significant spectral change. Some datum points are obtained from Figure 2.5.

Figure 2.7

Spectrophotometric pH titration of aqueous $1.09 \times 10^{-3} \text{ mol dm}^{-3}$ $[\text{Cu}(\text{Me}_4\text{12aneN}_4)](\text{ClO}_4)_2$ solution against NaOH (ionic strength adjusted to 0.5 with LiClO_4) at 293.2 K. pH 6.28, 11.32, 11.83, 12.12 and 12.27 for the spectra from A to E.



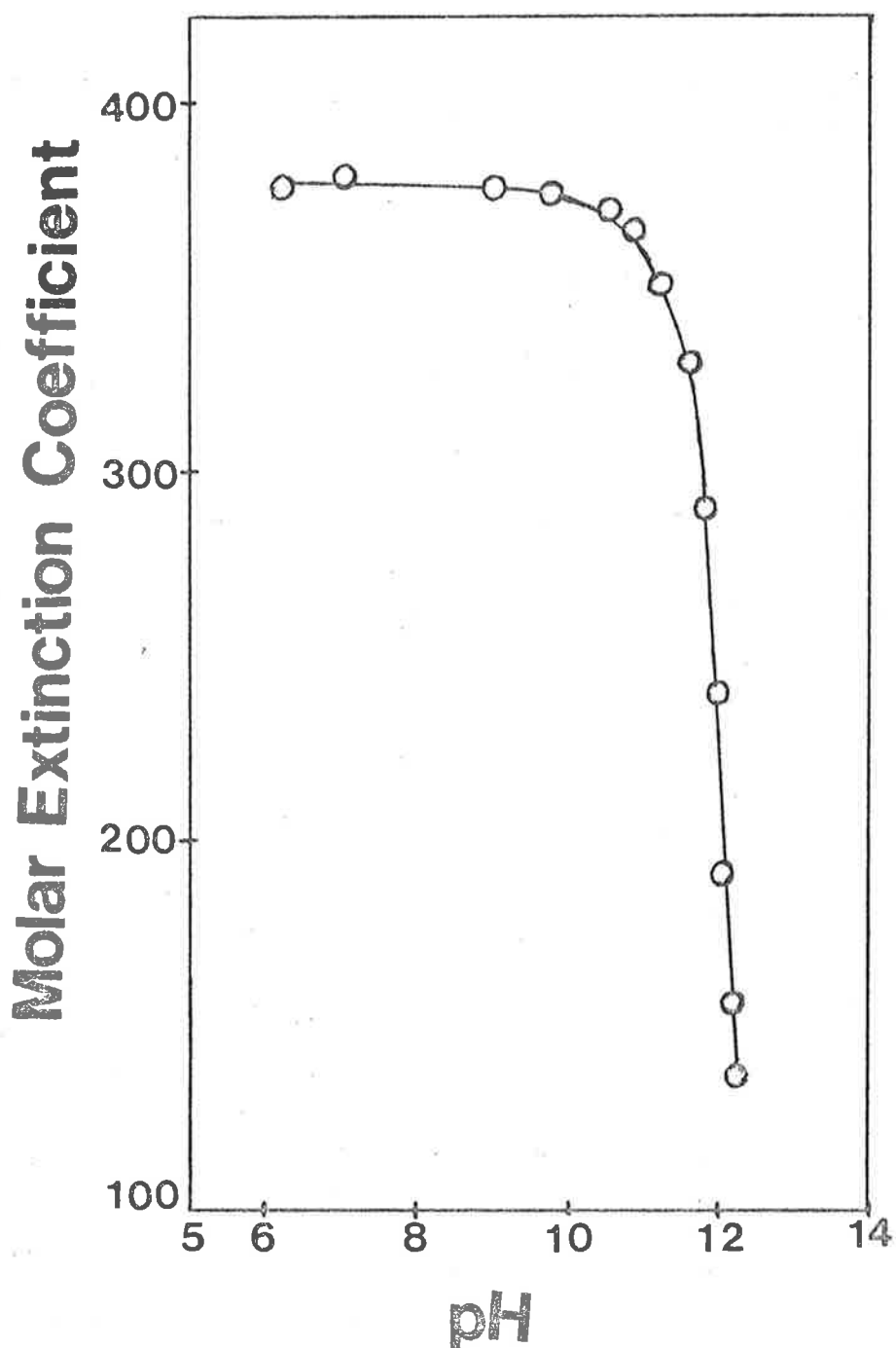


Figure 2.8

Spectrophotometric pH titration curve of aqueous $1.08 \times 10^{-3} \text{ mol dm}^{-3}$ $[\text{Cu}(\text{Me}_4\text{12aneN}_4)](\text{ClO}_4)_2$ solution against NaOH at 293.2 K and $\lambda = 600 \text{ nm}$ (ionic strength adjusted to 0.5 with LiClO_4). Some datum points are obtained from Figure 2.7. Further addition of base does not cause a significant spectral change.

low and high pH. The spectrophotometric pH titration was carried out to estimate the pKa of the co-ordinated water molecules in the aquo complexes. The value of pKa for the aquo complex is a thermodynamic measure of the ease with which a proton is transferred to water from that complex.

Table 2.5
Spectrophotometric pH Titration Data at 293.2K

Complex	isosbestic points, nm	wavelength, nm	pKa	ionic strength
1 [Ni(12aneN ₄)](ClO ₄) ₂	x	355	8.0	1.0
2 [Ni(Me ₄ 12aneN ₄)](ClO ₄) ₂	400, 438 and 610	468	10.2	0.5
3 [Ni(13aneN ₄)](ClO ₄) ₂	x	350	8.4	1.0
4 [Ni(Me ₄ 14aneN ₄)](ClO ₄) ₂	398, 462 and 626	514	10.7	0.5
5 [Cu(Me ₄ 12aneN ₄)](ClO ₄) ₂	688	600	12.0	0.5

2.5.3 Determination of Stoichiometry and Equilibrium Constants:-

(a) [Ni(Me₄12aneN₄)N₃]⁺ System:-

Qualitatively, when NaN₃ is added to the aqueous reddish solution of [Ni(Me₄12aneN₄)](ClO₄)₂, the solution turns green and the reddish colour reappears on dilution. Aqueous solutions of 2.93×10^{-3} mol dm⁻³ in [Ni(Me₄12aneN₄)](ClO₄)₂ and 3.05×10^{-3} mol dm⁻³ in NaN₃ were prepared separately with 1.0 mol dm⁻³ in NaClO₄ for Job's method (see section 7.3) of continuous variation (all reaction mixtures are reddish) at 298.2K. Figure 2.9 shows the plot of Y (A_{measured} - A_{calculated}) at 346 nm against the mol fraction of NaN₃. The molar extinction coefficients of [Ni(Me₄12aneN₄)](ClO₄)₂ and NaN₃ at 346 nm are 6.83 and 0.33 mol⁻¹ dm³ cm⁻¹, respectively. The [Ni(Me₄12aneN₄)N₃]ClO₄ species absorbs strongly at 346 nm allowing Job's plot calculation. The solid lines in Figure 2.9 are least squares linear regression lines for datum points 2, 3, 4, and

Figure 2.9

$A_{\text{measured}} - A_{\text{calculated}}$ ($\lambda = 346$ nm and cell path = 1 cm) vs mol fraction of NaN_3 for Job's method of continuous variation for the determination of stoichiometry of $[\text{Ni}(\text{Me}_4\text{12aneN}_4)\text{N}_3]^+$ formation at 298.2 K. Stock solutions of aqueous 2.93×10^{-3} mol dm^{-3} $[\text{Ni}(\text{Me}_4\text{12aneN}_4)](\text{ClO}_4)_2$ and 3.05×10^{-3} mol dm^{-3} NaN_3 were used (ionic strength adjusted to 1 with NaClO_4).

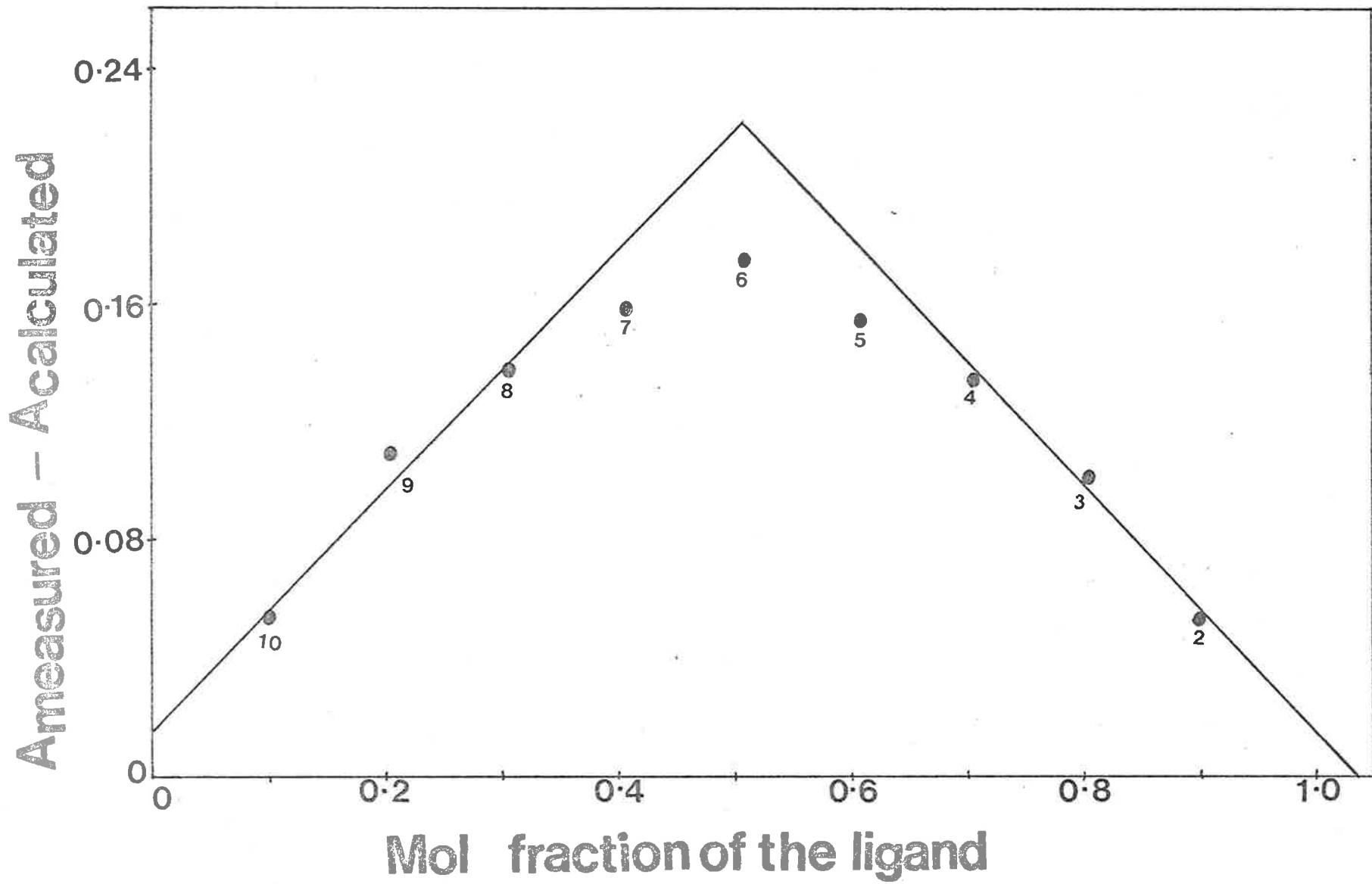


Figure 2.9

10, 9, 8, respectively. The peak appears at 0.51 mol fraction of NaN_3 showing a one to one complex formation. The molar extinction coefficient of $[\text{Ni}(\text{Me}_4\text{12aneN}_4)](\text{ClO}_4)_2$ is $139.8 \text{ mol}^{-1} \text{ dm}^3 \text{ cm}^{-1}$, and the absorbance of $[\text{Ni}(\text{Me}_4\text{12aneN}_4)\text{N}_3]\text{ClO}_4$ at 466 nm is negligible. Therefore, the equilibrium constants (i.e. $[\text{Ni}(\text{Me}_4\text{12aneN}_4)\text{N}_3^+]_{\text{eq}}/([\text{Ni}(\text{Me}_4\text{12aneN}_4)^{2+}]_{\text{eq}} [\text{NaN}_3]_{\text{eq}})$) were calculated at 466 nm for the solution mixtures 8, 7, 6, 5, and 4 (see Figure 2.9) and found to be 54.4, 60.4, 39.4, 59.1 and 56.6 $\text{mol}^{-1} \text{ dm}^3$. The spectrum of the azide complex in 0.5M NaN_3 (ionic strength 1.0 adjusted with NaClO_4) is shown in Figure 2.10.

(b) $[\text{Ni}(\text{Me}_4\text{14aneN}_4)\text{N}_3]^+$ System:-

Qualitatively, when NaN_3 is added to the red aqueous solution of $[\text{Ni}(\text{Me}_4\text{14aneN}_4)](\text{ClO}_4)_2$, the solution turns green and the red colour reappears on dilution. Aqueous solutions of $5.19 \times 10^{-3} \text{ mol dm}^{-3}$ $[\text{Ni}(\text{Me}_4\text{14aneN}_4)](\text{ClO}_4)_2$ and $5.48 \times 10^{-3} \text{ mol dm}^{-3}$ NaN_3 were prepared for Job's method of continuous variation at 298.2K (ionic strength 1.0 adjusted with NaClO_4). Figure 2.11 shows the plot of Y ($A_{\text{measured}} - A_{\text{calculated}}$) at 351 nm against the mol fraction of NaN_3 . The molar extinction coefficients of $[\text{Ni}(\text{Me}_4\text{14aneN}_4)](\text{ClO}_4)_2$ and NaN_3 at 351 nm are 7.3 and 0.37 $\text{mol}^{-1} \text{ dm}^3 \text{ cm}^{-1}$, respectively. A Job's plot was constructed at 351 nm. The points 5, 6 and 7 are not included in the least squares linear regression lines (solid lines). The occurrence of a peak at 0.49 mol fraction of NaN_3 indicates the formation of a one to one complex. The molar extinction coefficient of $[\text{Ni}(\text{Me}_4\text{14aneN}_4)](\text{ClO}_4)_2$ at 510 nm is $142.4 \text{ mol}^{-1} \text{ dm}^3 \text{ cm}^{-1}$ and the absorbance of $[\text{Ni}(\text{Me}_4\text{14aneN}_4)\text{N}_3]\text{ClO}_4$ at 510 nm is negligible. Therefore, the equilibrium constants were calculated at 510 nm for the solution mixtures 4, 5, 6, 7 and 8 (see Figure 2.11) and found to be 57.9, 53.5, 64.4, 48.8 and 70.2 $\text{mol}^{-1} \text{ dm}^3$, respectively. The spectrum of the azide complex in 0.5 mol dm^{-3} NaN_3 (ionic strength 1.0 adjusted with NaClO_4) is shown in Figure 2.10.

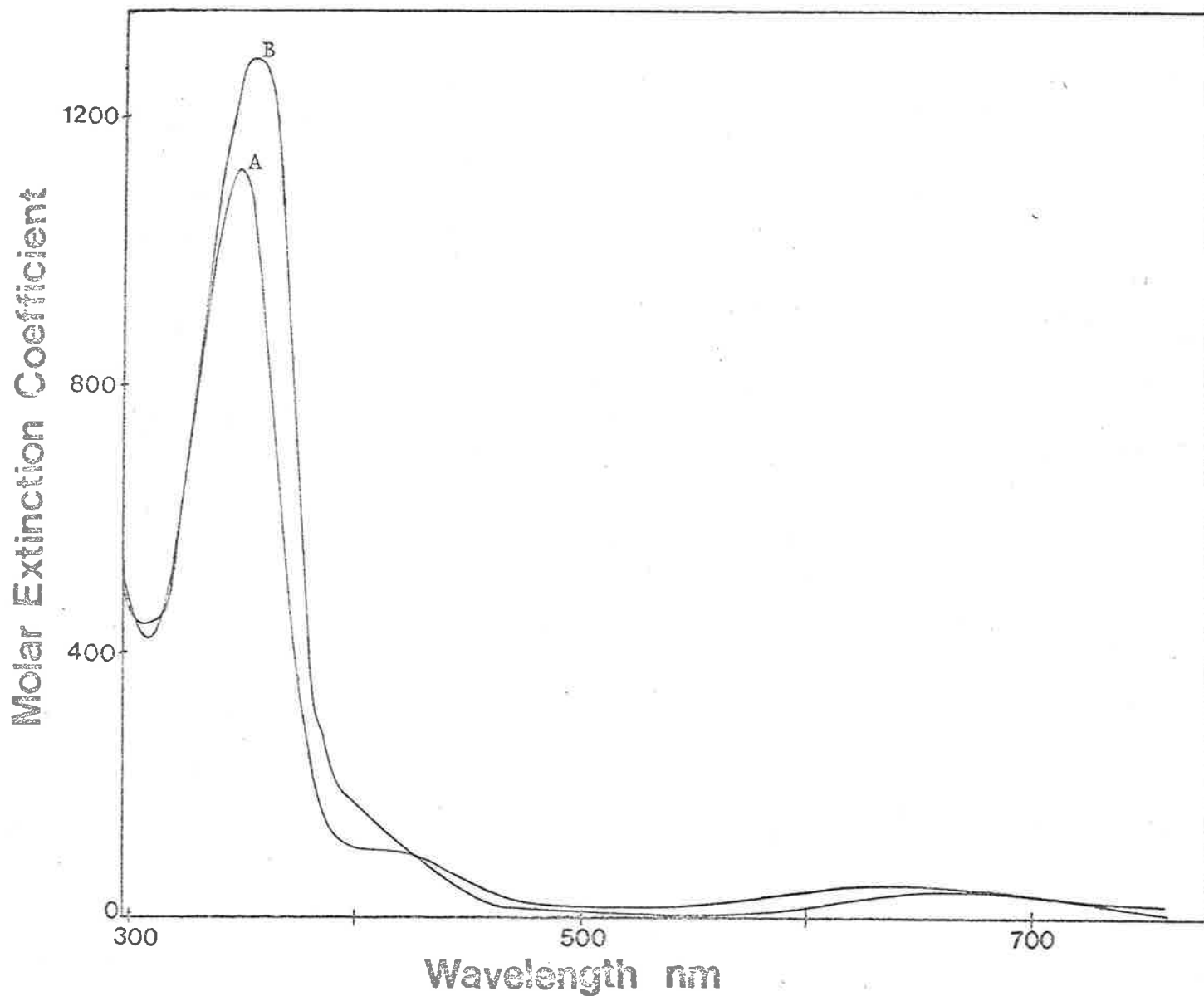


Figure 2.10

Uv/visible spectra of aqueous $1.46 \times 10^{-3} \text{ mol dm}^{-3} [\text{Ni}(\text{Me}_4\text{12aneN}_4)](\text{ClO}_4)_2$ (spectrum A) and aqueous $1.46 \times 10^{-3} \text{ mol dm}^{-3} [\text{Ni}(\text{Me}_4\text{14aneN}_4)](\text{ClO}_4)_2$ (spectrum B) complexes in $0.5 \text{ mol dm}^{-3} \text{ NaN}_3$ at 298.2K (ionic strength adjusted to 1 with NaClO_4).

Figure 2.11

$A_{\text{measured}} - A_{\text{calculated}}$ ($\lambda = 351$ nm and cell path = 1 cm) vs mol fraction of NaN_3 for Job's method of continuous variation for the determination of stoichiometry of $[\text{Ni}(\text{Me}_4\text{14aneN}_4)\text{N}_3]^+$ formation at 298.2 K. Stock solutions of aqueous 5.19×10^{-3} mol dm^{-3} $[\text{Ni}(\text{Me}_4\text{14aneN}_4)](\text{ClO}_4)_2$ and aqueous 5.48×10^{-3} mol dm^{-3} NaN_3 were used (ionic strength adjusted to 1 with NaClO_4).

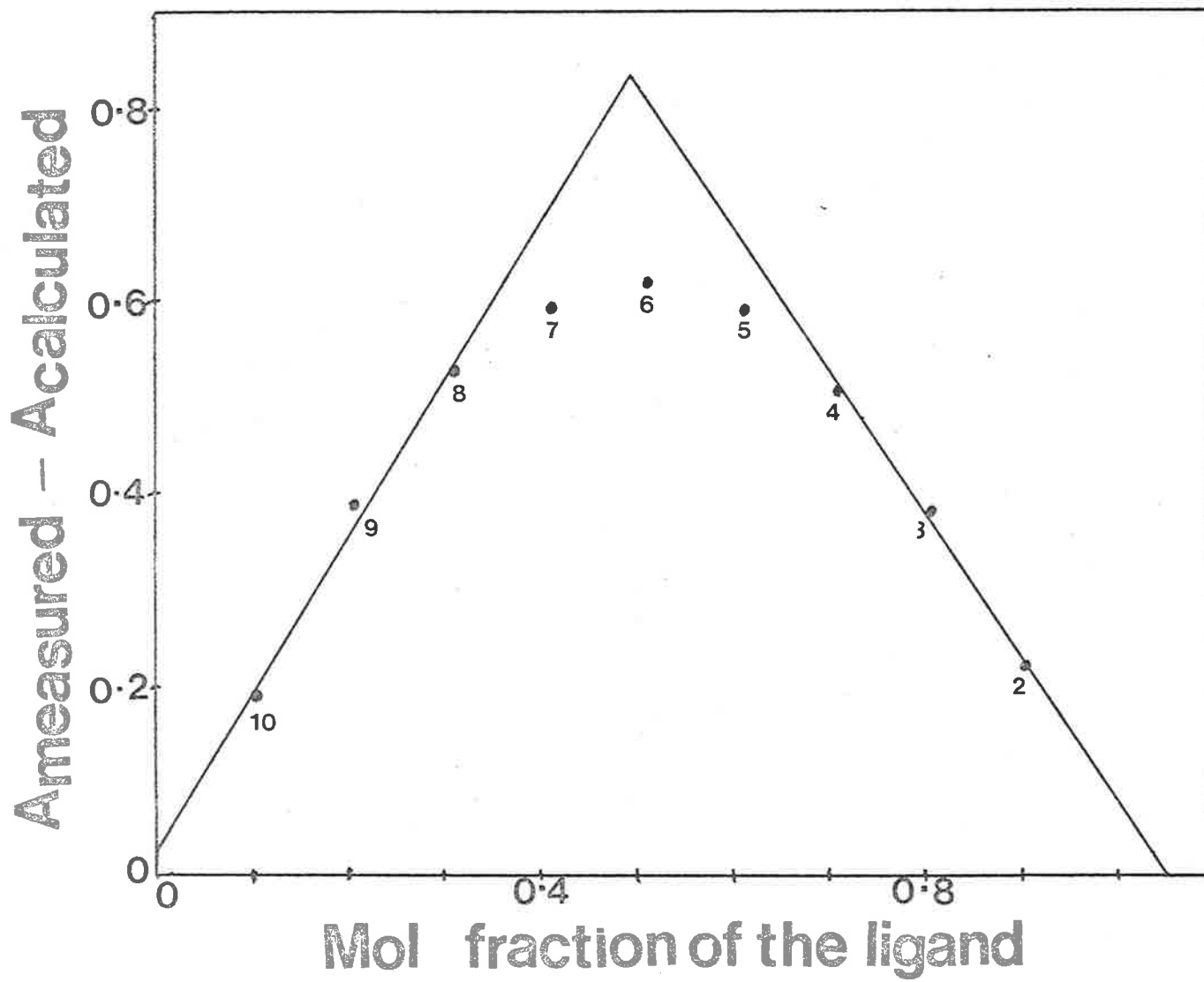
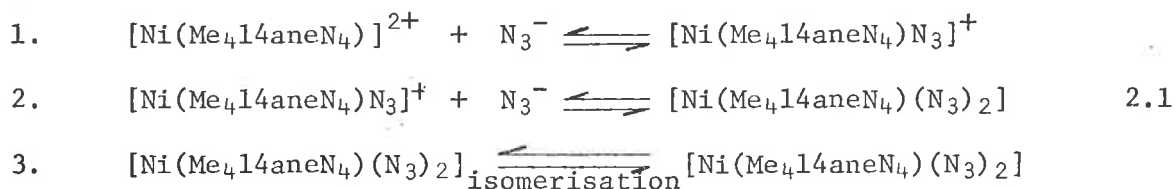


Figure 2.11

2.5.4 Substitution Reactions in an Aqueous Medium:-

(a) [Ni(Me₄14aneN₄)](ClO₄)₂/N₃⁻ System:-

With the [Ni(Me₄14aneN₄)](ClO₄)₂/N₃⁻ system the stopped flow technique was employed at the wavelength of 350 nm and the pseudo 1st order kinetic condition was attained by the use of high azide concentration (0.25 and 0.5 mol dm⁻³, ionic strength 1.0). Under these conditions three kinetic processes were observed as shown in Figure 2.12. However, with low azide concentration (0.05 mol dm⁻³) and under otherwise identical conditions only one fast process was observed (t_{1/2} ≈ 0.12 s). Three kinetic processes were again observed when a solution of 2.06 × 10⁻⁴ mol dm⁻³ [Ni(Me₄14aneN₄)](ClO₄)₂ and 0.05 mol dm⁻³ NaN₃ was mixed with an equi-volume solution of NaN₃ giving an azide concentration of 0.525 mol dm⁻³. At 298.2K and a concentration of 0.5 mol dm⁻³ NaN₃ the half lives were found to be approximately 0.0016, 0.08 and 8.0 seconds for the first, second and third processes, respectively. The above observations can be explained by the following reaction sequence (see equation 2.1):-



In the first reaction a five co-ordinate species forms on the addition of the first azide. While, on addition of the second azide a six co-ordinate complex forms in the second reaction. Six co-ordinate complexes of the type [Ni(Me₄14aneN₄)X₂] (where X = N₃⁻, OCN⁻, CN⁻ or SCN⁻) can be formed by addition of a two-fold excess of the appropriate sodium salt to an aqueous solution of the perchlorate salt^{33,34}. In section 2.5.3, the formation of [Ni(Me₄14aneN₄)N₃]⁺ was established by Job's method of continuous variation. The present kinetic study was performed in large excess concentration of azide and therefore a six co-ordinate complex, [Ni(Me₄14aneN₄)(N₃)₂] can be formed. The third process may be understood by an isomerisation step (reaction three) in which inversion of the

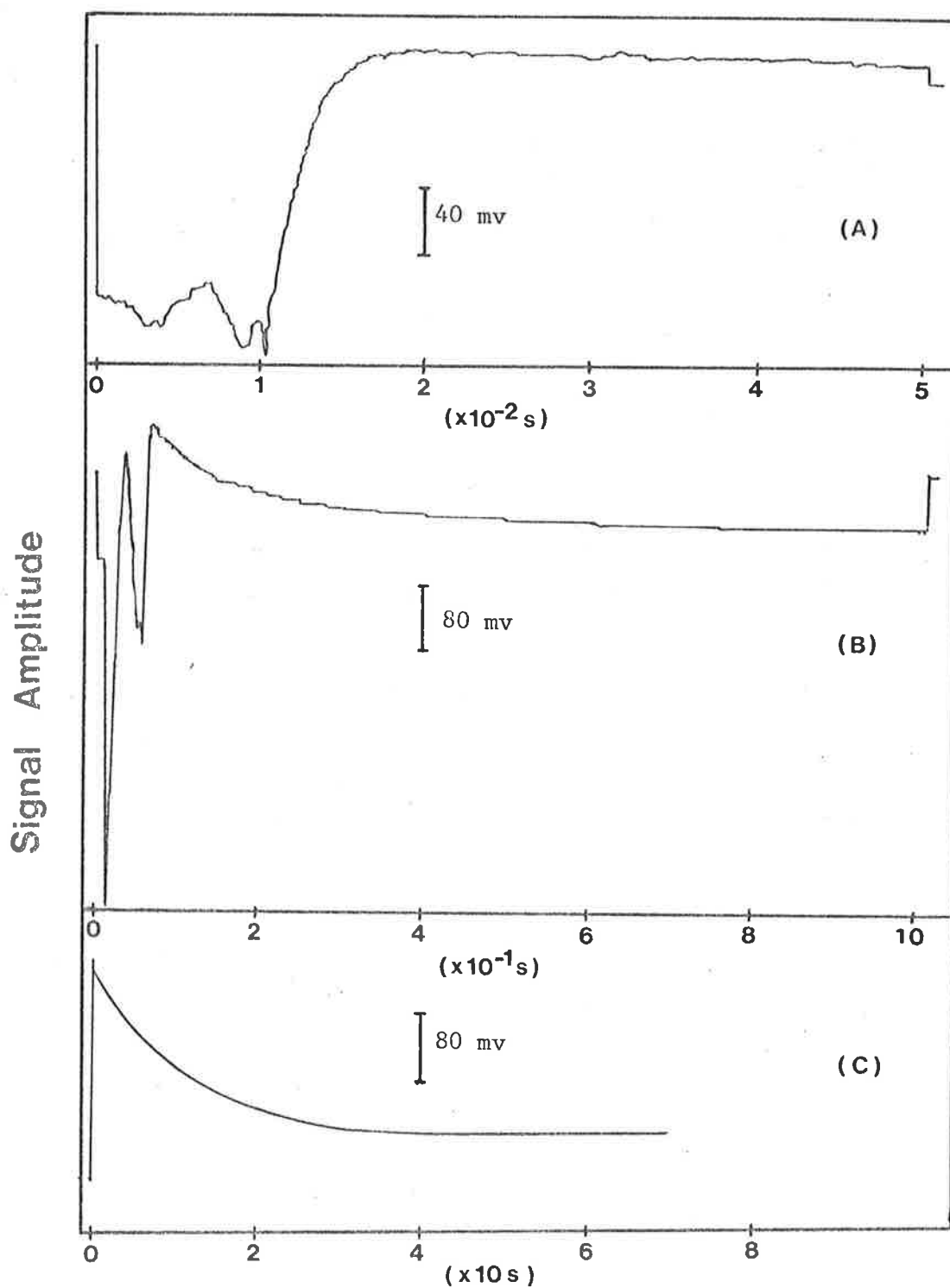


Figure 2.12

Three kinetic processes for the reaction of aqueous $2.06 \times 10^{-4} \text{ mol dm}^{-3}$ $[\text{Ni}(\text{Me}_4\text{14aneN}_4)](\text{ClO}_4)_2$ with 0.5 mol dm^{-3} NaN_3 at 298.2 K and $\lambda = 350 \text{ nm}$ (ionic strength adjusted to 1 with NaClO_4). In process (A), the first $1 \times 10^{-2} \text{ s}$ is due to solutions flowing after mixing before the flow has stopped and in process (B), the first $0.6 \times 10^{-1} \text{ s}$ is due to the flowing solution and process (A). Process (C) was obtained using the chart recorder without using Oscilloscope and Data Lab.

nitrogen atoms of the ligand is required to attain a thermodynamic equilibrium. In principle four such isomers may arise (see Chapter 1):-

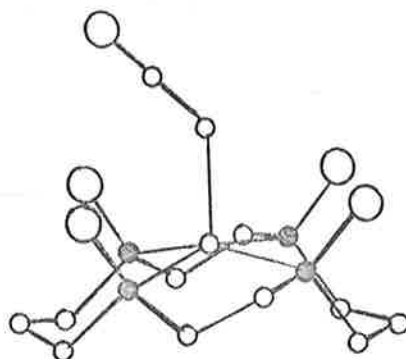
- i) four methyl groups on the same side of the ring
- ii) three methyl groups on the same side
- iii) two methyl groups on either side (cis) and
- iv) two methyl groups on either side (trans).

The available data cannot be used to distinguish between these possibilities. The $[\text{Ni}(\text{Me}_4\text{14aneN}_4)](\text{ClO}_4)_2$ complex may exist as one of the two square planar isomers (boat, R.S.R.S. and chair, R.S.S.R.) discussed in the literature^{33,34}. Figure 2.13 shows crystal structure³⁵ of $[\text{Ni}(\text{Me}_4\text{14aneN}_4)\text{N}_3]\text{ClO}_4$ where all four methyl groups lie on the same side of the macrocyclic plane. The crystal structure of $[\text{Ni}(\text{Me}_4\text{14aneN}_4)_2(\text{N}_3)_3]^+$ was also reported³⁶ where two methyl groups lie on either side of the macrocyclic plane (see Figure 2.14).

A solution of $2.93 \times 10^{-3} \text{ mol dm}^{-3}$ $[\text{Ni}(\text{Me}_4\text{14aneN}_4)](\text{ClO}_4)_2$ with 0.01 mol dm^{-3} NaN_3 (ionic strength 1.0) was also studied at 298.2K using the temperature jump technique ($\lambda = 510 \text{ nm}$) and two processes were observed. The fast process occurred within the heating time of the solution which is about $4 \mu\text{s}$ and the second process was accompanied by a small absorbance change. So no kinetic data were obtained from this study. However, these two processes may be attributed to the formation of a six co-ordinate species and the isomerisation discussed earlier.

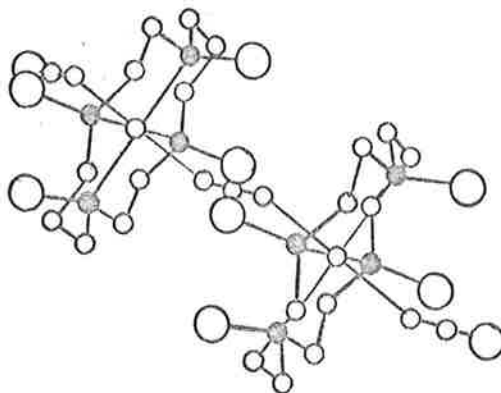
The kinetics of substitution reactions of $[\text{Ni}(\text{Me}_4\text{14aneN}_4)(\text{OH}_2)_2]^{3+}$ and $[\text{Fe}(\text{14aneN}_4)(\text{NCS})\text{X}]^+$ with halide and thiocyanate ions in an aqueous medium using stopped flow technique were recently reported^{37,38} and are consistent with a dissociative mechanism. The study of the water exchange rate constant on $[\text{Ni}(\text{Me}_4\text{14aneN}_4)(\text{OH}_2)_2]^{2+}$ is in progress³⁹ and the results may be useful in interpreting the observations reported here for the reaction of $[\text{Ni}(\text{Me}_4\text{14aneN}_4)(\text{OH}_2)_2]^{2+}$ with azide.

Figure 2.13

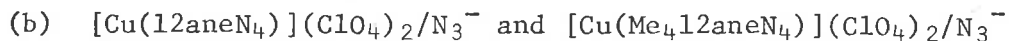


Crystal structure of $[\text{Ni}(\text{Me}_4,14\text{aneN}_4)\text{N}_3]^+$ where all four methyl groups lie on the same side of the macrocyclic plane (diagram from reference 35). The filled small circles represent nitrogen atoms and the attached large circles represent methyl groups.

Figure 2.14

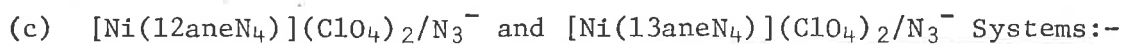


Crystal structure of $[\text{Ni}_2(\text{Me}_4,14\text{aneN}_4)_2(\text{N}_3)_3]^+$ where two methyl groups lie on either side of the macrocyclic plane (diagram from reference 36). The filled small circles represent nitrogen atoms and the attached large circles represent methyl groups.



Systems:-

These systems were studied at 298.2K and a wavelength of 620 nm under pseudo first order condition with excess azide (ionic strength 1.0). The kinetic processes were too fast to be detected by either the stopped flow or the temperature jump technique.

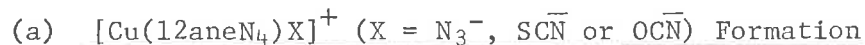


The $[\text{Ni}(\text{12aneN}_4)](\text{ClO}_4)_2/\text{N}_3^-$ system was found to be too fast to be studied under pseudo first order condition with excess N_3^- using the stopped flow technique (560 nm, 298.2K and ionic strength 1.0). The water exchange rate constant on $[\text{Ni}(\text{12aneN}_4)(\text{OH}_2)_2]^{2+}$ is very fast (see Chapter 4) and the substitution reaction is also expected to be fast. While, the $[\text{Ni}(\text{12aneN}_4)](\text{ClO}_4)_2/\text{NH}_2(\text{CH}_2)_2\text{NH}_2$ system could not be studied because of precipitation in presence of electrolyte (i.e. NaClO_4).

Qualitatively, the absorbance of an aqueous solution of $[\text{Ni}(\text{13aneN}_4)](\text{ClO}_4)_2$ changes slowly on addition of N_3^- . Quantitative studies using uv/visible spectrophotometry were carried out under pseudo first order condition with excess azide at 288.6K and 500 nm (ionic strength 1.0 and pH 7.0). Only one process was observed. The half life of this kinetic process was found to be 19.11 and 19.58 minutes with 0.06 and 0.07 mol dm^{-3} NaN_3 , respectively. It is not clear whether slow substitution occurs or isomerisation due to inversion of the nitrogen atoms of the ligand to achieve thermodynamic equilibrium as discussed in section 2.5.4 (a) (also see Chapter 1).

2.5.5 Uv/visible Spectroscopic Method for the Determination of Equilibrium

Constants in an Aqueous Medium:-



To a fixed volume of the $[\text{Cu}(\text{12aneN}_4)]^{2+}$ complex a solution containing the ligand ($\text{N}_3^-, \text{SCN}^-$ or OCN^-) was added from a calibrated Finn pipette. The solution was stirred with a teflon plunger mounted on a thin

platinum wire and a spectrum was recorded after each addition. The concentrations of both the complex and the ligand were calculated after each addition. Let M = complex, L = ligand, ML = complex formed, ϵ_I = molar extinction coefficient of M, ϵ_{II} = molar extinction coefficient of ML, ϵ = experimental molar extinction coefficient ($\frac{A}{[M]_0}$) and A = absorbance. Then, at equilibrium for a 1 cm path length cell

$$A = \epsilon_I [M]_{eq} + \epsilon_{II} [ML]_{eq} \quad 2.2$$

$$[M]_0 = [M]_{eq} + [ML]_{eq} \quad 2.3$$

and $[L]_{eq} = [L]_0 - [ML]_{eq} \quad 2.4$

$$A = \epsilon_I ([M]_0 - [ML]_{eq}) + \epsilon_{II} [ML]_{eq} \quad 2.5$$

$$= \epsilon_I [M]_0 + (\epsilon_{II} - \epsilon_I) [ML]_{eq}$$

$$\therefore \epsilon [M]_0 = \epsilon_I [M]_0 + (\epsilon_{II} - \epsilon_I) [ML]_{eq}$$

$$\therefore [ML]_{eq} = \frac{(\epsilon - \epsilon_I)}{(\epsilon_{II} - \epsilon_I)} [M]_0 \quad 2.6$$

$$[M]_{eq} = [M]_0 - [ML]_{eq}$$

$$= [M]_0 - \frac{\epsilon - \epsilon_I}{\epsilon_{II} - \epsilon_I} [M]_0$$

and $[L]_{eq} = [L]_0 - \frac{\epsilon - \epsilon_I}{\epsilon_{II} - \epsilon_I} [M]_0 \quad 2.7$

$$\therefore K_{eq} = \frac{[ML]_{eq}}{[M]_{eq} [L]_{eq}}$$

$$\therefore K_{eq} = \frac{\frac{(\epsilon - \epsilon_I)}{(\epsilon_{II} - \epsilon_I)} [M]_0}{\left([M]_0 - \frac{(\epsilon - \epsilon_I)}{(\epsilon_{II} - \epsilon_I)} [M]_0\right) [L]_{eq}} \quad 2.8$$

$$\therefore (\epsilon - \epsilon_I)^{-1} = (\epsilon_{II} - \epsilon_I)^{-1} + (\epsilon_{II} - \epsilon_I)^{-1} [L]_{eq}^{-1} K_{eq}^{-1} \quad 2.9$$

A plot of $(\epsilon - \epsilon_I)^{-1}$ against $[L]_{eq}^{-1}$ gives

$$K_{eq} \text{ as } \frac{\text{intercept}}{\text{slope}}$$

To obtain $(\epsilon_{II} - \epsilon_I)^{-1}$ for the $[L]_{eq}$ calculation (equation 2.7), $(\epsilon - \epsilon_I)^{-1}$ is plotted against $[L]_o^{-1}$ giving the intercept equal to $(\epsilon_{II} - \epsilon_I)^{-1}$ since at high $[L]_o$ values, $[L]_o$ is approximately equal to $[L]_{eq}$. Equation 2.9 is derived⁴⁰ for a one to one complex formation. Knowing the value of ϵ_I , the value of ϵ_{II} can be obtained from the intercept of the plot of $(\epsilon - \epsilon_I)^{-1}$ against $[L]_o^{-1}$. Thus knowing the value of ϵ_{II} , the K_{eq} values can be calculated individually by solving the simultaneous equations 2.2, 2.3 and 2.4. The K_{eq} values were determined using both methods and are comparable to within 10%. Subsequently equation 2.9 was used for all determinations of K_{eq} . The K_{eq} values (ionic strength 1.0 and pH 7.0) were determined at three different temperatures. The K_{eq} , ΔH° and ΔS° values are given in Table 2.6. Figure 2.15 shows the spectrophotometric titration of $[\text{Cu}(\text{12aneN}_4)]^{2+}$ with N_3^- at 297.9K. All the spectra shown were constructed for $1.20 \times 10^{-2} \text{ mol dm}^{-3}$ $[\text{Cu}(\text{12aneN}_4)]^{2+}$ and one isosbestic point occurs at 606 nm.

Figure 2.15

Spectrophotometric titration of aqueous $1.20 \times 10^{-2} \text{ mol dm}^{-3}$ $[\text{Cu}(\text{12aneN}_4)](\text{ClO}_4)_2$ solution against NaN_3 at 297.9 K and $\text{pH} = 7.01$ (ionic strength adjusted to 1 with NaClO_4). $[\text{NaN}_3] = 0, 0.019, 0.056, 0.090, 0.122$ and $0.166 \text{ mol dm}^{-3}$ for the spectra from 1 to 6.

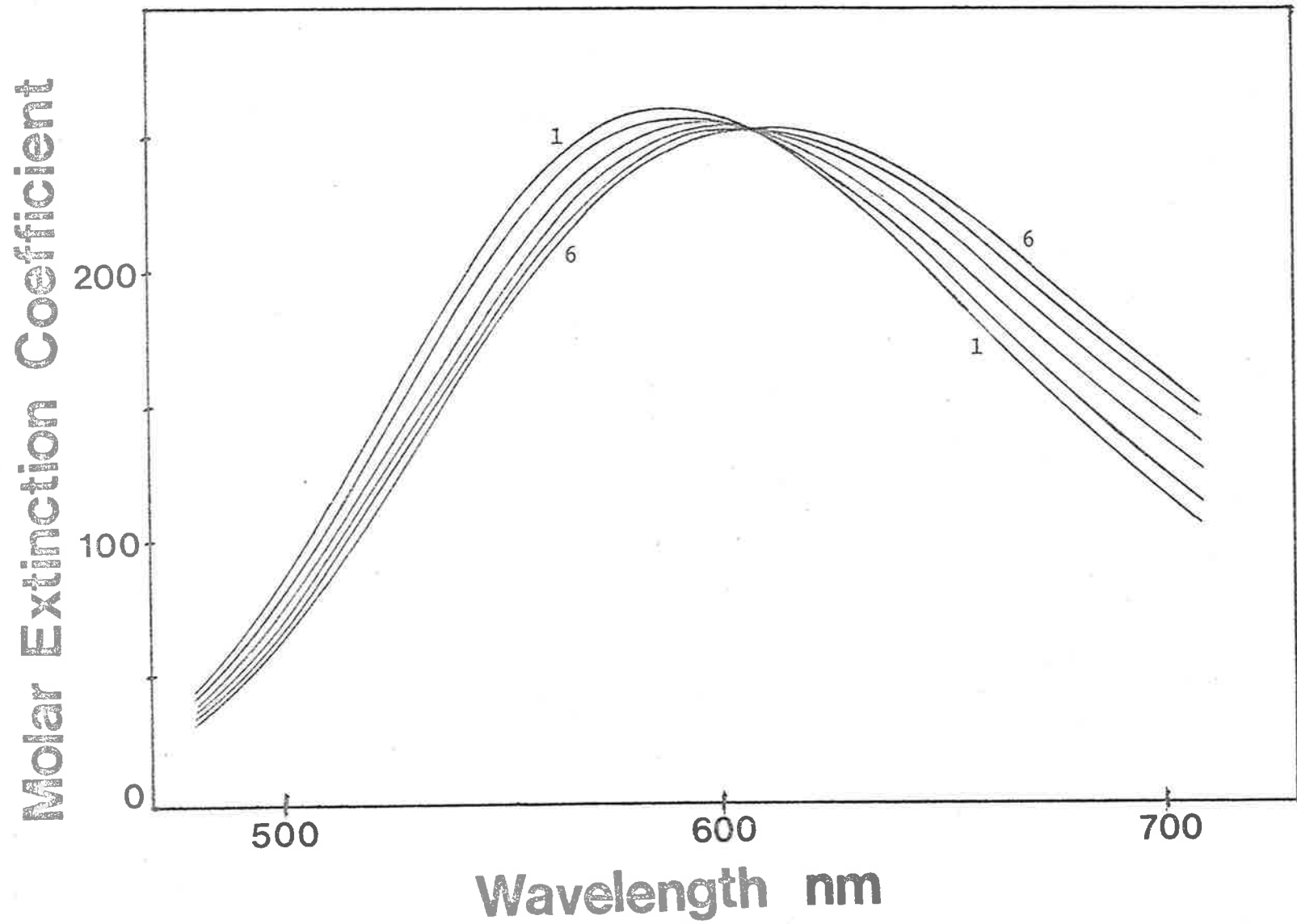


Figure 2.15

Table 2.6

K_{eq} , ΔH° and ΔS° values for the formation of $[\text{Cu}(\text{12aneN}_4)\text{N}_3]^+$, $[\text{Cu}(\text{12aneN}_4)\text{SCN}]^+$ and $[\text{Cu}(\text{12aneN}_4)\text{OCN}]^+$ complexes.

$10^4/T$ K	K_{eq}	ΔH° kJ mol ⁻¹	ΔS° J K ⁻¹ mol ⁻¹
1. <u>$[\text{Cu}(\text{12aneN}_4)]^{2+}/\text{N}_3^-$ system, $\lambda = 580$ nm.</u>			
34.65	7.37±0.02	8.8±3	48±10
33.56	8.93±0.8		
32.36	9.42±0.7		
2. <u>$[\text{Cu}(\text{12aneN}_4)]^{2+}/\text{SCN}^-$ system, $\lambda = 546$ nm.</u>			
34.65	11.9±0.8	-6±2	-1±9
33.56	10.3±0.5		
32.36	10.1±0.5		
3. <u>$[\text{Cu}(\text{12aneN}_4)]^{2+}/\text{OCN}^-$ system, $\lambda = 580$ nm.</u>			
34.65	12.6±0.1	-8±4	-7±16
33.56	12.8±0.3		
32.36	10.2±0.3		

N.B. The errors represent one standard deviation.

(b) $[\text{Cu}(\text{Me}_4\text{12aneN}_4)\text{X}]^+$ ($X = \text{N}_3^-$, SCN^- or OCN^-) formation

The equilibrium constants for the formation of $[\text{Cu}(\text{Me}_4\text{12aneN}_4)\text{X}]^+$ ($X = \text{N}_3^-$, SCN^- or OCN^-) complexes were determined under identical conditions as for the formation of $[\text{Cu}(\text{12aneN}_4)\text{X}]^+$ ($X = \text{N}_3^-$, SCN^- or OCN^-) system. The results are given in Table 2.7.

Table 2.7

K_{eq} , ΔH° and ΔS° values for the formation of $[\text{Cu}(\text{Me}_4\text{12aneN}_4)\text{X}]^+$ ($\text{X} = \text{N}_3^-$, SCN^- or OCN^-) complexes.

$10^4/T \text{ K}$	K_{eq}	ΔH° kJ mol^{-1}	ΔS° $\text{J K}^{-1} \text{ mol}^{-1}$
1. <u>$[\text{Cu}(\text{Me}_4\text{12aneN}_4)]^{2+}/\text{N}_3^-$ system, $\lambda = 580 \text{ nm}$.</u>			
34.65	18.3 ± 0.4	-2.9 ± 2	14 ± 7
33.56	18.6 ± 0.2		
32.36	16.9 ± 0.3		
2. <u>$[\text{Cu}(\text{Me}_4\text{12aneN}_4)]^{2+}/\text{SCN}^-$ system, $\lambda = 700 \text{ nm}$.</u>			
34.65	56.2 ± 0.2		
33.56	46.9 ± 0.1	-6.3 ± 4	11 ± 14
32.36	47.1 ± 0.8		
3. <u>$[\text{Cu}(\text{Me}_4\text{12aneN}_4)]^{2+}/\text{OCN}^-$ system, $\lambda = 720 \text{ nm}$.</u>			
34.65	20.4 ± 0.4		
33.56	18.3 ± 0.2	-6.5 ± 0.8	2.6 ± 3
32.36	17.0 ± 0.5		

N.B. The errors represent one standard deviation.

(c) $[\text{Ni}(\text{12aneN}_4)\text{N}_3]^+$ and $[\text{Ni}(\text{13aneN}_4)\text{SCN}]^+$ formation:-

The equilibrium constants for the formation of $[\text{Ni}(\text{12aneN}_4)\text{N}_3]^+$ and $[\text{Ni}(\text{13aneN}_4)\text{SCN}]^+$ complexes could not be determined because of slow precipitation occurring on continual addition of the ligand. The formation of the $[\text{Ni}(\text{13aneN}_4)\text{N}_3]^+$ complex could not be used for an equilibrium constant determination because of the slow reaction rate as mentioned in section 2.5.4.

2.5.6 Solid State Magnetic Moments by the Gouy Method (see Chapter 7):-

The $[\text{Ni}(\text{12aneN}_4)](\text{ClO}_4)_2$, $[\text{Ni}(\text{Me}_4\text{12aneN}_4)](\text{ClO}_4)_2$ and $[\text{Ni}(\text{Me}_4\text{14aneN}_4)](\text{ClO}_4)_2$ complexes were found to be diamagnetic. The magnetic moments of $[\text{Ni}(\text{Me}_4\text{12aneN}_4)\text{NCS}]\text{NCS}$, $[\text{Ni}(\text{Me}_4\text{12aneN}_4)\text{N}_3]\text{ClO}_4$, $[\text{Ni}(\text{Me}_4\text{12aneN}_4)(\text{dmf})](\text{ClO}_4)_2$ and $[\text{Ni}(\text{Me}_4\text{14aneN}_4)(\text{dmf})](\text{ClO}_4)_2$ were found to be 3.17, 3.22, 2.98 and 3.24 B.M., respectively. Usually the magnetic moments of five co-ordinate high spin nickel(II) complexes range from 3.2 to 3.4 B.M.⁴¹.

2.6.1 Isomeric Properties of $[\text{Ni}(\text{Me}_4\text{12aneN}_4)]^{2+}$ Complexes:-

The $[\text{Ni}(\text{Me}_4\text{12aneN}_4)](\text{ClO}_4)_2$ complex (pink colour) prepared in ordinary ethanol ($\approx 99\%$) rapidly decomposes in water and after refluxing this solution for several hours a new complex is formed with a brick red colour. This can be understood in terms of an intramolecular isomerisation through bond rupture of metal-ligand bond to form a thermodynamically stable complex in water. The complex was found to be insoluble in nitromethane. The colours of the complexes prepared in a ethanol water mixture, dry ethanol using triethylorthoformate and dry dmf are brick red, light brick red and green, respectively. The green complex when dissolved in nitromethane and in water gives yellow and reddish solution (probably due to the dissociation of co-ordinated dmf), respectively. The magnetic moment measurements of the above three complexes in nitromethane using the Gouy method (see Chapter 7) indicate that they are diamagnetic. The complex prepared in dry ethanol using triethylorthoformate decomposes partially in water giving a light reddish colour implying that the complex obtained is a mixture of different isomers. The solid complex prepared in a ethanol water mixture has the stereochemistry where all four methyl groups lie on the same side of the macrocyclic plane as shown from X-ray structural data (see Chapter 3). The uv/visible spectral data given in Table 2.8 show that the complexes prepared in a ethanol water mixture and in dmf produce similar spectra in different solvents used. Whereas, the complex prepared in dry ethanol using triethylorthoformate is characterised by a significantly different spectrum. The spectra

were recorded immediately after making the solutions. The aqueous solutions of both complexes (ethanol water and dmf preparation) were heated to 313.2 K for about eight days and the spectra obtained were similar to those recorded immediately after making up the initial solutions.

Table 2.8

Uv/visible Spectral Data for $[\text{Ni}(\text{Me}_4\text{12aneN}_4)](\text{ClO}_4)_2$ Complexes at 298.2K.

Complex	solvent	$\lambda_{\text{max}}/\text{nm}$ ($\epsilon/\text{mol}^{-1} \text{ dm}^3 \text{ cm}^{-1}$)
1. $[\text{Ni}(\text{Me}_4\text{12aneN}_4)](\text{ClO}_4)_2$ (ethanol water preparation)	H ₂ O	398 (69.3), 474 (98.9), 622 (22.7)
	dmf	396 (67.2),
	(0.5 mol dm ⁻³ NaClO ₄)	490 (52.0), 620 (27.9),
	CH ₃ NO ₂	455 (189)
2. $[\text{Ni}(\text{Me}_4\text{12aneN}_4)(\text{dmf})](\text{ClO}_4)_2 \text{ H}_2\text{O}$ (dmf preparation)	H ₂ O	398 (73.7), 474 (101), 622 (23.7)
	dmf	396 (68.7), 490 (51.2),
	(0.5 mol dm ⁻³ NaClO ₄)	620 (27.7)
	CH ₃ NO ₂	455 (190)
3. $\text{Ni}(\text{Me}_4\text{12aneN}_4)(\text{ClO}_4)_2$ (ethanol preparation using triethylortho- formate)	dmf	396 (47.2), 490 (24.7),
	(0.5 mol dm ⁻³ NaClO ₄)	620 (21.4)
	CH ₃ NO ₂	455 (168)

2.6.2 Isomeric Properties of $[\text{Ni}(\text{Me}_4\text{14aneN}_4)]^{2+}$ Complexes:-

The red $[\text{Ni}(\text{Me}_4\text{14aneN}_4)](\text{ClO}_4)_2$ complex (prepared in a ethanol water mixture) when dissolved in dmf (with $0.5 \text{ mol dm}^{-3} \text{ NaClO}_4$) gives a reddish solution which slowly turns green at a rate with a half life of 29.3 minutes at 307.0K using $3.81 \times 10^{-3} \text{ mol dm}^{-3}$ complex. The red complex prepared in dry ethanol using triethylorthoformate also gives a reddish solution in dmf ($0.5 \text{ mol dm}^{-3} \text{ NaClO}_4$) which turns green with a half life of 23.3 and 22.2 minutes (307.0K) using 3.79×10^{-3} and $8.70 \times 10^{-3} \text{ mol dm}^{-3}$ complexes, respectively. The green complex prepared in dmf gives a red solution in water and in nitromethane (probably due to the dissociation of co-ordinated dmf). The magnetic moment measurements of the three complexes in nitromethane indicate that they are diamagnetic. All of these complexes exhibit spin equilibria in different solvents (see Chapters 4 and 6) and they possess different percentages of low-spin species in a particular solvent at the same temperature. When equi-molar volume of $[\text{Ni}(\text{dmf})_6](\text{ClO}_4)_2$ and $\text{Me}_4\text{14aneN}_4$ solutions (dmf, $0.5 \text{ mol dm}^{-3} \text{ NaClO}_4$) are mixed together, a reddish solution is obtained and this reddish solution slowly turns green with a half life of 23.7 minutes at 307K (discussed in detail in section 2.6.3). The uv/visible spectral data given in Table 2.9 show that the spectra of the complexes produced in the four different preparations are different. The spectra of the complexes in water and in nitromethane were recorded immediately after making the solutions. However, those in dmf were recorded after the attainment of equilibrium, characterised by the red to green transformation. The aqueous solution of the complexes (ethanol water preparation, ethanol preparation using triethylorthoformate and dmf preparation) were heated to 305K for 64 hours and the spectral data given in Table 2.9 show that the spectra of the complexes prepared in ethanol using triethylorthoformate and in dmf became similar but different from those run immediately after the preparation of each solution.

Table 2.9

Uv/visible Spectral Data for $[\text{Ni}(\text{Me}_4\text{14aneN}_4)]^{2+}$ Complexes at 305.0K

Complex	Solvent	$\lambda_{\text{max}}/\text{nm}$ ($\epsilon/\text{mol}^{-1} \text{ dm}^3 \text{ cm}^{-1}$)
1. $[\text{Ni}(\text{Me}_4\text{14aneN}_4)](\text{ClO}_4)_2$ (ethanol water preparation)	H ₂ O	392 (80.5), 512 (86.4), 652 (22.5),
	H ₂ O (after 64 hours heating)	392 (85.5), 512 (85.8), 652 (23.2)
	dmf (0.5 mol dm ⁻³ NaClO ₄)	395 (123), 506 (30.0), 656 (35.9)
	CH ₃ NO ₂	514 (205)
2. $[\text{Ni}(\text{Me}_4\text{14aneN}_4)](\text{ClO}_4)_2$ (ethanol preparation using triethylorthoformate)	H ₂ O	392 (69.5), 512 (96.0), 652 (19.8)
	H ₂ O (after 64 hours heating)	392 (91.2), 512 (82.1), 652 (24.9)
	dmf (0.5 mol dm ⁻³ NaClO ₄)	400 (119), 514 (21.7), 660 (36.2)
	CH ₃ NO ₂	514 (176)

Table 2.9 (cont.)

Complex	Solvent	λ_{\max}/nm ($\epsilon/\text{mol}^{-1} \text{ dm}^3 \text{ cm}^{-1}$)
3. $[\text{Ni}(\text{Me}_4\text{14aneN}_4)(\text{dmf})](\text{ClO}_4)_2$ (dmf preparation)	H_2O	392 (95.2), 512 (74.4), 652 (26.5)
	H_2O	392 (90.5), 512 (82.0), 652 (24.8)
	(after 64 hours heating)	
	dmf	400 (142), 514 (26.0), 660 (43.4)
	(0.5 mol dm^{-3} NaClO_4)	
	CH_3NO_2	512 (165)
4. Complex obtained in solution by mixing $[\text{Ni}(\text{dmf})_6](\text{ClO}_4)_2$ and $\text{Me}_4\text{14aneN}_4$ (1:1 molar ratio)	dmf	400 (74.6), 490 (27.2), 658 (25.1)
	(0.5 mol dm^{-3} NaClO_4)	

2.6.3 Red to Green Colour Change of a Mixture of $[\text{Ni}(\text{dmf})_6](\text{ClO}_4)_2$ and $\text{Me}_4\text{14aneN}_4$ in dmf:-

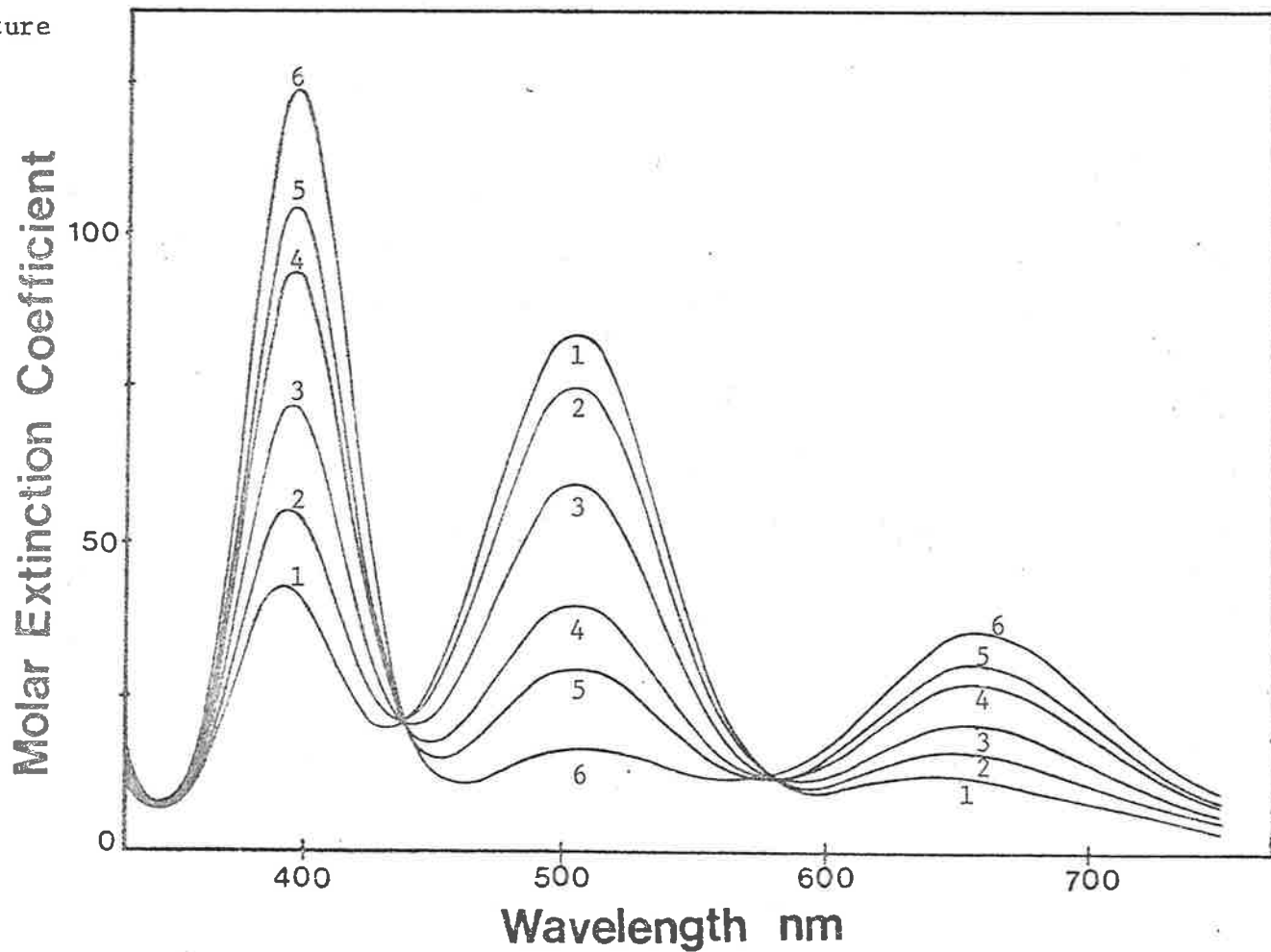
When equal volume of $[\text{Ni}(\text{dmf})_6](\text{ClO}_4)_2$ ($2.97 \times 10^{-3} \text{ mol dm}^{-3}$) and $\text{Me}_4\text{14aneN}_4$ ($2.93 \times 10^{-3} \text{ mol dm}^{-3}$) solutions (dmf, $0.5 \text{ mol dm}^{-3} \text{ NaClO}_4$) are mixed together, a red solution is formed rapidly which slowly turns green. This slow reaction was followed using a uv/visible spectrophotometer. The first metal-ligand bond is expected to form rapidly if substitution on $[\text{Ni}(\text{dmf})_6]^{2+}$ is characterised by a rate determining step involving the dissociation of dmf. The substitution of one water molecule of $[\text{Ni}(\text{OH}_2)_6]^{2+}$ by an amine nitrogen renders the remaining five more labile⁴² (also see Chapter 4). By analogy, one could postulate that the substitution of one dmf molecule of $[\text{Ni}(\text{dmf})_6]^{2+}$ by an amine nitrogen will also render the remaining five more labile and hence the remaining metal-ligand bond formation is expected to be very rapid. Consequently, the slow red to green interconversion may be attributed to isomerisation (co-ordination of dmf is expected to be fast). In principle four such isomers may arise (also see Chapter 1):-

- i) four methyl groups on the same side of the ring
- ii) three methyl groups one the same side
- iii) two methyl groups on either side (cis)
- iv) two methyl groups on either side (trans)

The available data cannot be used to distinguish between these possibilities. The $[\text{Ni}(\text{Me}_4\text{14aneN}_4)](\text{ClO}_4)_2$ complex may exist as one of the two square planar isomers (boat, R.S.R.S. and chair, R.S.S.R.) discussed in the literature^{33, 34}. The kinetic data (consistent with a first order rate equation) for this slow interconversion along with ΔS^\ddagger and ΔH^\ddagger (see Chapter 4, equation 4.9) are given in Table 2.10. Figure 2.16 shows the spectra recorded at the time intervals 0, 13, 38, 88, 133 minutes (from (1-5)) at 298.0K while spectrum (6) is the equilibrium spectrum. The slow process was also studied with excess metal ion and ligand concentrations. Figure 2.17

Figure 2.16

Time dependent uv/visible spectra of a mixture of equal volume of $2.97 \times 10^{-3} \text{ mol dm}^{-3}$ $[\text{Ni}(\text{dmf})_6](\text{ClO}_4)_2$ and $2.93 \times 10^{-3} \text{ mol dm}^{-3}$ $\text{Me}_4\text{14aneN}_4$ at 298.0 K in dmf (ionic strength adjusted to 0.5 with NaClO_4). Time = 0, 13, 38, 88 and 133 minutes for the spectra from 1 to 5 and spectrum (6) is the equilibrium spectrum.



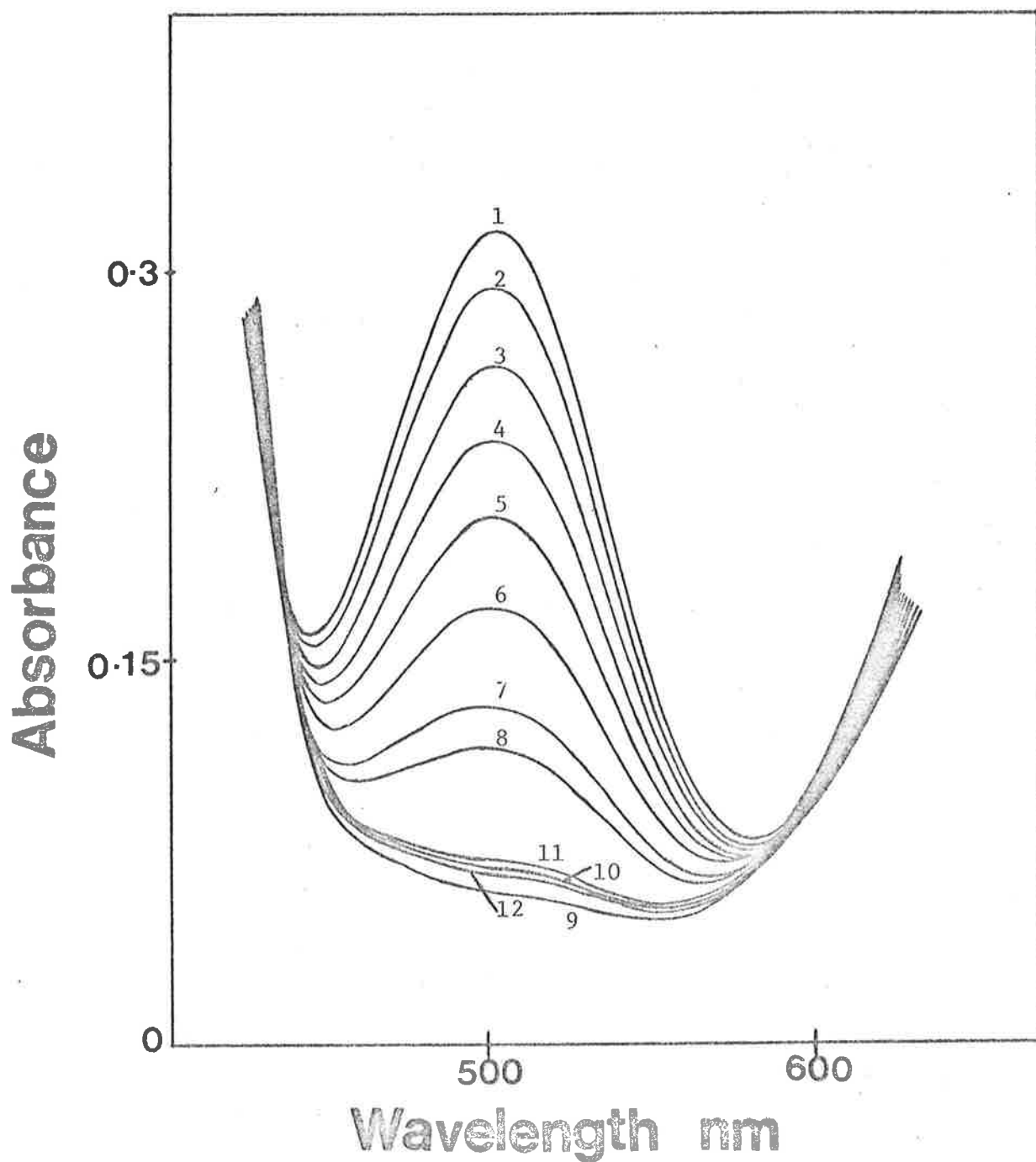


Figure 2.17

Time dependent uv/visible spectra of a mixture containing $19.5 \times 10^{-3} \text{ mol dm}^{-3}$ $[\text{Ni}(\text{dmf})_6](\text{ClO}_4)_2$ and $1.95 \times 10^{-3} \text{ mol dm}^{-3}$ $\text{Me}_4\text{14aneN}_4$ at 298.0 K in dmf (ionic strength adjusted to 0.5 with NaClO_4 and cell path = 2 cm).

Time = 0, 20, 35, 50, 70, 95, 120, 125, 130, 135, 145 and 170 minutes for the spectra from 1 to 12 respectively.

Table 2.10

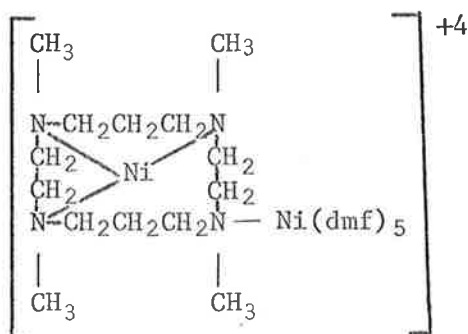
Kinetic data for the slow process (red \rightarrow green) observed after mixing equi-molar volume of $[\text{Ni}(\text{dmf})_6](\text{ClO}_4)_2$ and $\text{Me}_4\text{14aneN}_4$ (ionic strength 0.5)

$\frac{1}{T} \times 10^4$	$k_{\text{obs}} \times 10^5 \text{ s}^{-1}$	
34.55	8.80 \pm 0.09	$\Delta S^\ddagger = (-89 \pm 2) \text{ J K}^{-1} \text{ mol}^{-1}$
33.55	20.4 \pm 0.10	
32.53	48.7 \pm 0.16	$\Delta H^\ddagger = (68 \pm 0.5) \text{ kJ mol}^{-1}$

N.B. The errors represent one standard deviation

shows the spectra recorded at the time intervals 0, 20, 35, 50, 70, 95, 120, 125, 130, 135, 145 and 170 minutes at 298.0K in presence of excess metal ion. The effect of excess metal ion and excess ligand on the slow interconversion processes at a fixed wavelength are also shown in Figures 2.18 and 2.19, respectively. It is difficult to understand this unusual effect, but a possible explanation is as follows. During isomeric interconversion to achieve thermodynamic equilibrium, inversion of the nitrogen atoms occurs following the rupture of the metal-ligand bond, thereby allowing the possible formation of a temporary species. In the case of excess metal ion, the possible molecular formula of the species could be

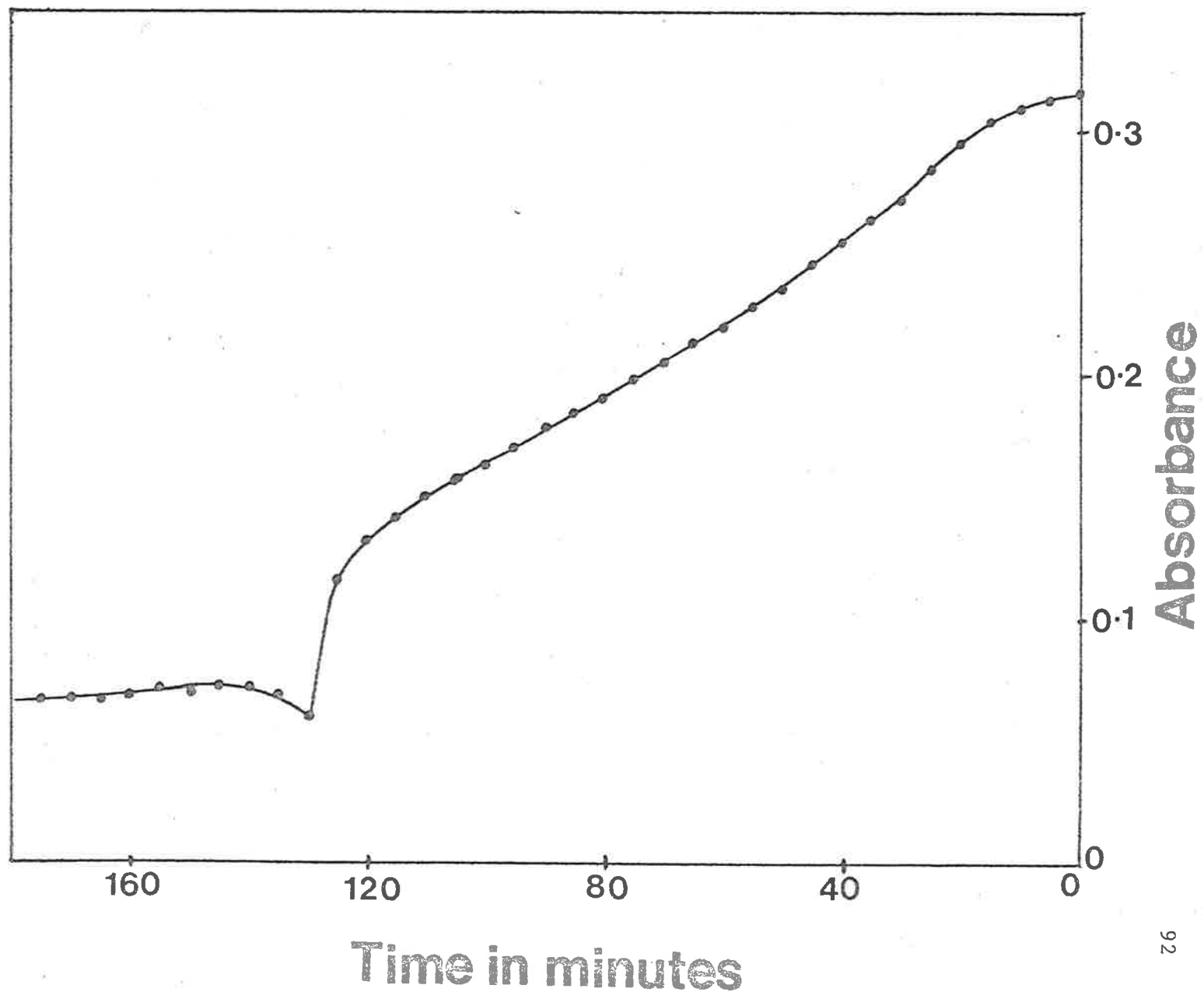
$[\text{Ni}_2(\text{Me}_4\text{14aneN}_4)(\text{dmf})_5]^{+4}$ as shown below



While in the case of excess ligand, the molecular formula of the temporary species could be $[\text{Ni}(\text{Me}_4\text{14aneN}_4)_2]^{2+}$ as shown below

Figure 2.18

Time dependent absorbance change
($\lambda = 504 \text{ nm}$ and cell path = 2 cm)
of a mixture containing 19.5×10^{-3}
 mol dm^{-3} $[\text{Ni}(\text{dmf})_6](\text{ClO}_4)_2$ and
 $1.95 \times 10^{-3} \text{ mol dm}^{-3}$ $\text{Me}_4\text{14aneN}_4$
at 298.0 K in dmf (ionic strength
adjusted to 0.5 with NaClO_4).



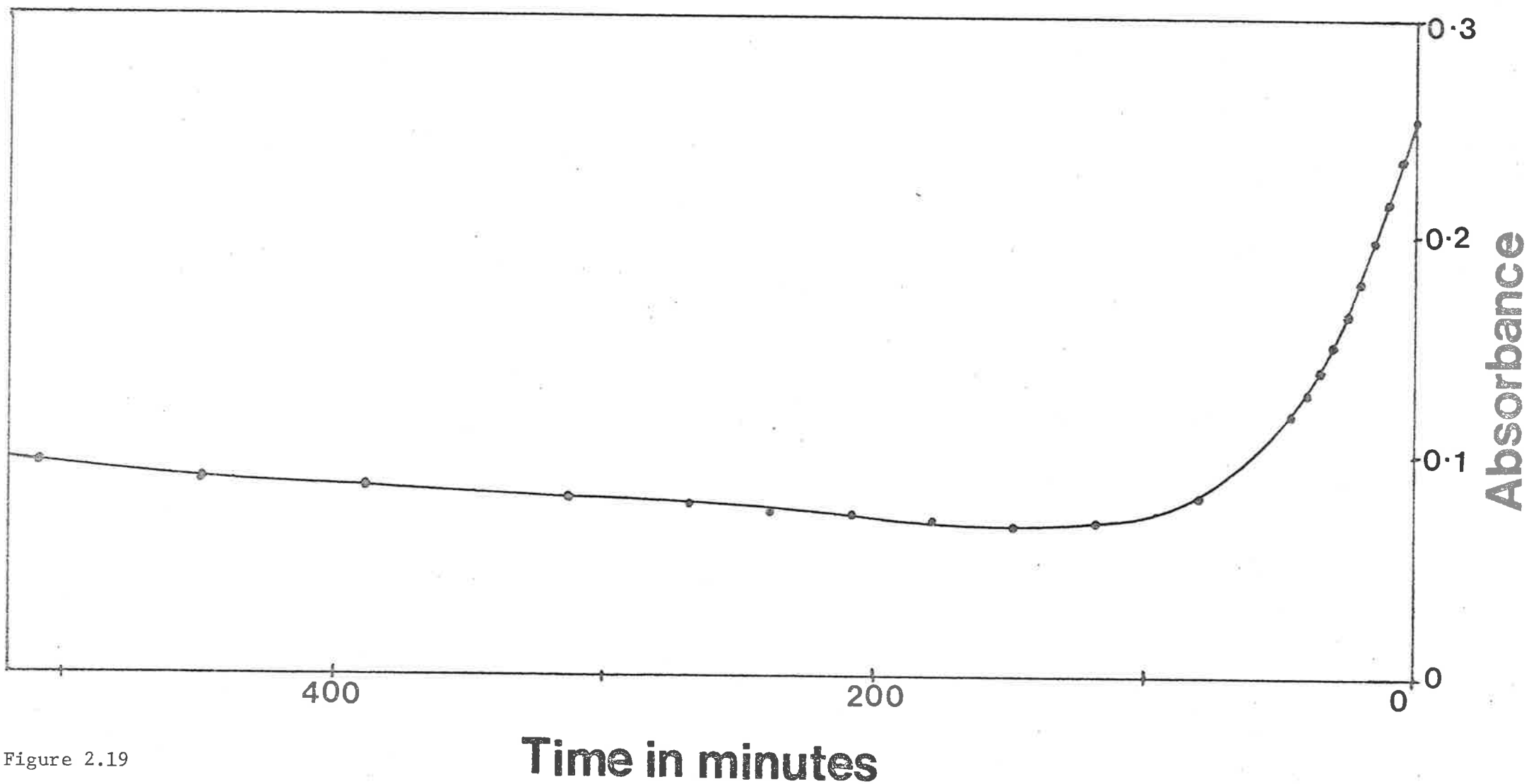
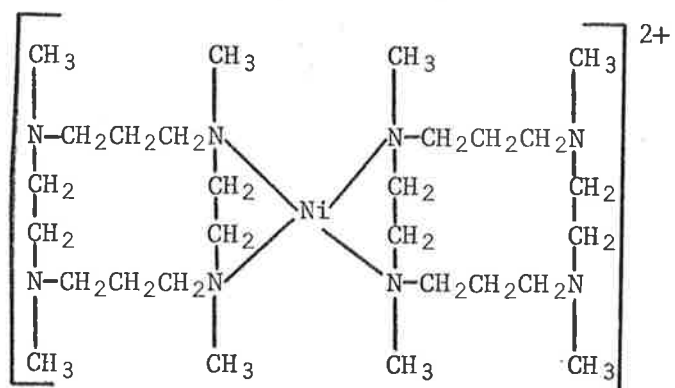


Figure 2.19

Time dependent absorbance change ($\lambda = 506 \text{ nm}$ and cell path = 2 cm) of a mixture containing $1.85 \times 10^{-3} \text{ mol dm}^{-3}$ $[\text{Ni}(\text{dmf})_6](\text{ClO}_4)_2$ and $1.95 \times 10^{-3} \text{ mol dm}^{-3}$ $\text{Me}_4\text{14aneN}_4$ at 307.4 K in dmf (ionic strength adjusted to 0.5 with NaClO_4).



References for Chapter Two

1. B.G. Doddridge, private communication.
2. L.Y. Martin, C.R. Sperati and D.H. Busch, J.A.C.S., 99, 2968 (1977).
3. J.E. Richman and T.J. Atkins, J.A.C.S., 96, 2268 (1974).
4. G.H. Searle, private communication.
5. M. Angley, private communication.
6. E.K. Barefield and F. Wagner, Inorg. Chem., 12, 2435 (1973).
7. Mass spectrum were run by P.C. Zeleny.
8. H. Wenker, J.A.C.S., 57, 2328 (1935).
9. P.A. Leighton, W.A. Perkins and M.L. Renquist, J.A.C.S., 69, 1540 (1947).
10. W.S. Gump and E.J. Nikawitz, J.A.C.S., 72, 1309 (1950).
11. G.R. Hansen and T.E. Burg, J. Heterocyclic Chem., 5, 305 (1968).
12. S.J. Brois, Journal of Organic Chemistry, 27, 3532 (1962).
13. E.K. Barefield, Inorg. Chem., 11, 2273 (1972).
14. S.F. Lincoln, private communication.
15. M. Ciampolini and N. Nardi, Inorg. Chem., 5, 41 (1966).
16. G.A. Kalligeros and E.L. Blinn, Inorg. Chem., 11, 1145 (1972).
17. P.W.N.M. Van Leeuwen and W.L. Groeneveld, Inorg. Nuclear Letters, 3, 145 (1967).
18. R.J. West, Ph.D. thesis, 1973, University of Adelaide.
19. D.H. Williams and I. Fleming, "Spectroscopic Methods in Organic Chemistry", 2nd edition, McGraw-Hill, New York (1966).
20. K. Nakamoto, "Infra-red and Raman Spectra of Inorganic and Co-ordination Compounds", 3rd edition, Wiley, New York (1978).
21. B.J. Hathaway and A.E. Underhill, J. Chem. Soc., 3091 (1961).
22. C.N. Banwell, "Fundamental of Molecular Spectroscopy", 2nd Edition, McGraw-Hill Book Company (U.K.) Ltd., (1972).
23. M.R. Rosenthal, J. Chem. Ed., 50, 331 (1973).

24. A.I. Vogel, "A Text Book of Quantitative Inorganic Analysis", 3rd Edition, Longmans, London (1961).
25. ^{13}C n.m.r. spectra were run by B.G. Doddridge on a Bruker WP80 spectrometer.
26. R.M. Lynden-Bell and R.K. Harris, "Nuclear Magnetic Resonance Spectroscopy", Thomas Nelson and Sons Ltd., London (1969).
27. H.A. Szymanski and R.E. Yelin, "N.M.R. Band Handbook", 1F1/Plenum Data Corporation, New York (1968).
28. R.L. Pecsok and L.D. Shields, "Modern Methods of Chemical Analysis", John Wiley and Sons Ltd., New York (1968).
29. P.R. Collins, Ph.D. thesis, 1979, University of Adelaide.
30. S.G. Zipp, A.P. Zipp and S.K. Madan in "Co-ord. Chem. Rev." edited by A.B.P. Lever, vol. 14, 29 (1974).
31. R. Buxtorf and T.A. Kaden, *Helv. Chim. Acta.*, 57, 1035 (1974).
32. N. Herron and P. Moore, *Inorg. Chim. Acta*, 36, 89 (1979).
33. F. Wagner and E.K. Barefield, *Inorg. Chem.*, 15, 408 (1976).
34. E.K. Barefield and F. Wagner, *Inorg. Chem.*, 12, 2435 (1973).
35. M.J. D'Aniello, M.T. Mocella, F. Wagner, E.K. Barefield and I.C. Paul, *J.A.C.S.*, 97, 192 (1975).
36. F. Wagner, M.T. Mocella, M.J. D'Aniello, A.H.J. Wang and E.K. Barefield, *J.A.C.S.*, 96, 2625 (1974).
37. R.I. Haines and A. McAuley, *Inorg. Chem.*, 19, 719 (1980).
38. C.K. Poon and Andrew W.M. TO, *Inorg. Chem.*, 18, 1277 (1979).
39. J.P. Hunt, and H.W. Dodgen, Department of Chemistry, Washington State University.
40. H.A. Benesi and J.H. Hildebrand, *J.A.C.S.*, 71, 2703 (1949).
41. L. Sacconi in "Transition Metal Chemistry", edited by R.L. Carlin, Edward Arnold Ltd., London, vol. 4, 220 (1968).
42. A.G. Desai, H.W. Dodgen and J.P. Hunt, *J.A.C.S.*, 92, 798 (1970).

CHAPTER THREE

Molecular Structure

Contents.

3.1. Introduction.

3.2. The Molecular Crystal Structure of $[\text{Ni}(\text{Me}_4\text{12aneN}_4)_3]\text{ClO}_4$ 3.3. The Molecular Crystal Structure of $[\text{Ni}(\text{Me}_4\text{12aneN}_4)](\text{ClO}_4)_2$

3.4. Discussion.

CHAPTER THREE

Molecular Structure3.1. Introduction:-

The interest in the structures of synthetic macrocyclic compounds and their cation complexes has been generated by their ability to surround or enclose several different cations. It is possible to investigate some of the factors which determine the type of co-ordination which occurs after obtaining the information from structural studies of macrocyclic molecules and their complexes. These factors are cation size, type and charge; ligand size, donor atom type, and substituent; and solvent type. The $\text{Me}_4\text{12aneN}_4$ ligand was prepared for the first time in this study. The $[\text{Ni}(\text{Me}_4\text{12aneN}_4)](\text{ClO}_4)_2$ complex (ethanol water preparation) showed interesting temperature dependent uv/visible spectral changes (see Chapter 4) at high LiClO_4 concentration which, together with the question of the conformation of the co-ordinated ligand, suggested the need for an X-ray analysis of the molecular crystal structure of the $[\text{Ni}(\text{Me}_4\text{12aneN}_4)_3]\text{ClO}_4$ and $[\text{Ni}(\text{Me}_4\text{12aneN}_4)](\text{ClO}_4)_2$ (ethanol water preparation) complexes. Molecular crystal structure studies of different macrocyclic molecules and their complexes are presented in the literature.^{1,2}

3.2. The Molecular Crystal Structure of $[\text{Ni}(\text{Me}_4\text{12aneN}_4)_3]\text{ClO}_4$:-³

Crystals of $[\text{Ni}(\text{Me}_4\text{12aneN}_4)_3]\text{ClO}_4$ were examined by precession film techniques and showed the crystal system to be orthorhombic. Lattice parameters were determined by least squares fit to 25 independent reflexions on a 4 circle CAD4 - Enraf Nonius diffractometer using Cu-K α radiation ($\lambda = 1.5418\text{\AA}$). $[\text{Ni}(\text{Me}_4\text{12aneN}_4)_3]\text{ClO}_4$, mol. wt = 428.2, orthorhombic space group $Pcab$; $a = 13.734(2)$,

$b = 14.071(1)$, $c = 19.870(2)\text{\AA}$; $v = 3840.21\text{\AA}^3$; $z = 8$, $d_m = 1.511$
 g.cm^{-3} , $d_c = 1.481 \text{ g.cm}^{-3}$, $F(000) = 1211e$, $\mu(\text{Cu} - K\alpha) = 33.7$.

Profile analysis of a representative reflexion indicated that the conditions for measurements of the integrated intensities would be optimized by $\omega - n(2\theta)$ scans, where $n = \frac{1}{2}$. The intensities were collected in the range $2.0^\circ \leq \theta \leq 70^\circ$. The ω -scan angle and the horizontal counter aperture were $(0.55 + 0.15 \tan\theta)^\circ$ and $(1.0 + 0.5 \tan\theta)$ mm, respectively. Each reflexion was scanned in 96 steps. The peak count P was recorded over the central 64 steps, with 16 steps at each end to measure the backgrounds B_1 and B_2 . The intensity I was calculated as $I = \nu[P - 2(B_1 + B_2)]$ with the standard deviation $\sigma(I) = \{\nu[P + 4(B_1 + B_2)]\}^{\frac{1}{2}}$, where ν is a factor to account for differences in scan speeds. Two reference reflexions were measured every 100 minutes of X-ray exposure time. No decomposition or movement of the crystal was detected. Lorentz and polarisation corrections were applied to all 4081 reflexions with the program SUSCAD.⁴ Of the 4081 reflexions, 1032 were rejected as being systematically absent or having zero or negative F_{obs} , giving 3049 unique reflexions.

For the purposes of structure analysis the unit cell and space group were transformed by $(010/100/00\bar{1})$ to give $a = 14.071(1)$, $b = 13.734(2)$, $c = 19.870(2)$ and space group $Pbca$. A schematic diagram of $[\text{Ni}(\text{Me}_4\text{12aneN}_4)\text{N}_3]^+$ is shown in Figure 3.1 and structural parameters in Tables 3.1 - 3.4. The nickel (II) atom was located by Patterson techniques.⁵ Subsequent difference fouriers gave the co-ordinated nitrogen atoms of the $\text{Me}_4\text{12aneN}_4$ ligand and the azide. The carbon atoms of the $\text{Me}_4\text{12aneN}_4$ ring showed a high degree of disorder and were not located with any degree of certainty. The chlorine atom of the perchlorate was located, the linked oxygen atoms were disordered.

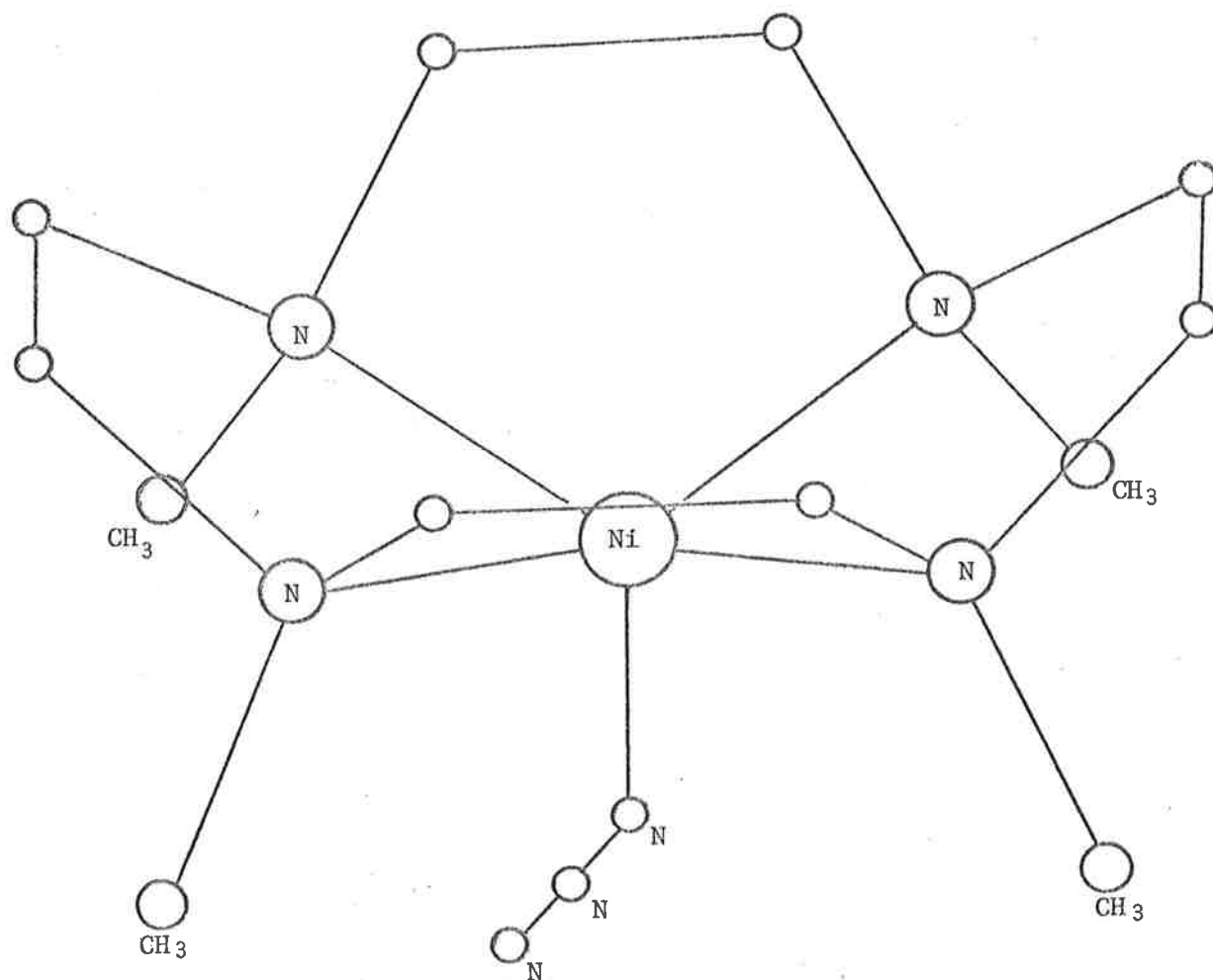


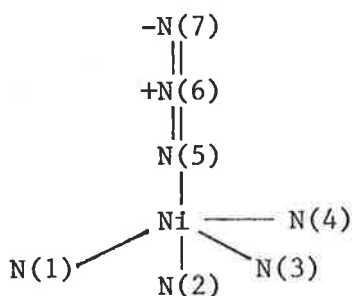
Figure 3.1

Schematic diagram (not to scale, drawn for visual aid) of $[\text{Ni}(\text{Me}_4,12\text{aneN}_4)\text{N}_3]^+$ where all four methyl groups and one azide are on the same side of the macrocyclic plane.



At this stage the $R = 29\%$ for 2527 reflexions having $F_{obs} > 5\sigma(F_{obs})$.

TABLE 3.1
Least Squares Plane through N(1),N(2),N(3),N(4)



Equation of the least squares plane is given by

$$0.9033x + 0.4069y - 0.1351z = 0.4346$$

Atom	Deviation from Plane (\AA)
Ni	0.602
N(1)	-0.1160
N(2)	0.1039
N(3)	-0.0906
N(4)	0.1028

TABLE 3.2
Atomic Co-ordinates

Atom	x	y	z
Ni	0.1074	0.2416	0.6210
N(1)	0.0100	0.3484	0.6493
N(2)	0.0408	0.2578	0.5255
N(3)	0.1232	0.0700	0.5966
N(4)	0.1056	0.2068	0.7251
N(5)	0.2256	0.3030	0.5974
N(6)	0.2996	0.2856	0.6152
N(7)	0.3810	0.2830	0.6343
Cl	0.2338	0.5517	0.8646

TABLE 3.3

Bond Lengths (Å)					
Ni - N(1)	2.084,	Ni - N(2)	2.128,	Ni - N(3)	2.416,
Ni - N(4)	2.123,	Ni - N(5)	1.922,	N(5) - N(6)	1.125,
N(6) - N(7)	1.195				

TABLE 3.4

Bond Angles (°)					
N(1) - Ni - N(2)	83.0	N(1) - Ni - N(3)	143.2		
N(1) - Ni - N(4)	83.6	N(1) - Ni - N(5)	109.0		
N(2) - Ni - N(3)	87.9	N(2) - Ni - N(4)	152.5		
N(2) - Ni - N(5)	96.8	N(3) - Ni - N(4)	88.7		
N(3) - Ni - N(5)	107.4	N(4) - Ni - N(5)	110.3		
Ni - N(5) - N(6)	129.1	N(5) - N(6) - N(7)	169.3		

3.3 The Molecular Crystal Structure of $[\text{Ni}(\text{Me}_4\text{12aneN}_4)](\text{ClO}_4)_2 \cdot 2\text{H}_2\text{O}$

$\text{C}_{12}\text{H}_{28}\text{N}_4\text{Ni}$, $(\text{ClO}_4)_2$, $2\text{H}_2\text{O}$, mol. wt. = 521.6, orthorhombic; space group $Pnma$ or $Pna2_1$; $a = 15.695(2)$, $b = 9.007(4)$, $c = 16.675(2)\text{Å}$; $v = 2357.19\text{Å}^3$; $z = 4$, $d_m = 1.501 \text{ g.cm}^{-3}$, $d_c = 1.47 \text{ g.cm}^{-3}$; $F(000) = 572e$; $\mu(\text{Mo} - K\alpha) = 5.28 \text{ cm}^{-1}$.

Intensity data were collected using an Enraf-Nonius CAD4 diffractometer in the ω - 2θ scan mode. The intensities were collected in the range $1.50 \leq \theta \leq 25^\circ$ using monochromated Mo-radiation ($\lambda = 0.71073\text{Å}$). The ω -scan angle and the horizontal counter aperture were $(0.85 + 0.35 \tan\theta)^\circ$ and $(2.1 + \tan\theta)\text{mm}$, respectively. Two standard reflexions were measured every 3600 secs of exposure time and indicated no decomposition or movement of the crystal. Lorentz and polarisation corrections were applied to give 2479 reflexions. 346 reflexions were rejected as being systematically absent or having zero or negative F_{obs} , giving 2133 unique reflexions. Details of intensity measurements and their related standard deviations are indicated in section 3.2.

The nickel atom was located by Pattersons methods.⁵ Subsequent difference fourier revealed the remaining non-hydrogen atoms. Refinement of the structure in space group $Pna2_1$ was unsuccessful as the R -factor reached a minimum of 21% (isotropic). However refinement in space group $Prma$ gave a better agreement $R = 15.2\%$ (isotropic). Further anisotropic refinement gave a final $R = 8.34\%$, for 1554 reflexions. The oxygen atoms of the perchlorates and the water molecules were highly disordered. All hydrogen atom positions were calculated with $C-H = 0.96\text{\AA}$. Figures 3.2 and 3.3 show the crystal structure of the $[\text{Ni}(\text{Me}_4\text{12aneN}_4)]^{2+}$ complex. Atomic co-ordinates are given in Table 3.5, whereas bond lengths and valence angles are given in Tables 3.6 and 3.7, respectively.

TABLE 3.5
Atomic Co-ordinates for $[\text{Ni}(\text{Me}_4\text{12aneN}_4)]^{2+}$ and the
Chlorine Atoms of the Perchlorates

The co-ordinates of all oxygen atoms have not been included since they are highly disordered.

Atom	x	y	z
Ni	0.2330(1)	$\frac{1}{4}$	0.1280(1)†
N(1)	0.1625(5)	0.0984(9)	0.1765(5)
N(2)	0.3198(5)	0.0993(8)	0.1091(5)
C(1)	0.2255(9)	-0.0157(16)	0.2027(10)
H(1)	0.2015	-0.1119	0.1895
H(2)	0.2327	-0.0079	0.2603
C(2)	0.3032(9)	-0.0112(16)	0.1697(9)
H(3)	0.3436	0.0060	0.2127
H(4)	0.3144	-0.1071	0.1453
C(3)	0.1270(10)	0.1666(14)	0.2495(8)
H(5)	0.0859	0.2423	0.2348
H(6)	0.1730	0.2116	0.2799
H(7)	0.0993	0.0915	0.2820
C(4)	0.4028(6)	0.1755(12)	0.1278(9)
C(5)	0.0949(7)	0.0321(15)	0.1294(8)
H(8)	0.1197	-0.0123	0.0818
H(9)	0.0540	0.1075	0.1137
H(10)	0.0664	-0.0439	0.1606
C(6)	0.3234(8)	0.4689(15)	0.0277(7)
Cl(1)	0.4618(2)	$\frac{1}{4}$	0.8495(2)†
Cl(2)	0.3535(3)	$\frac{1}{4}$	0.4154(2)†

† occupancy = 0.5

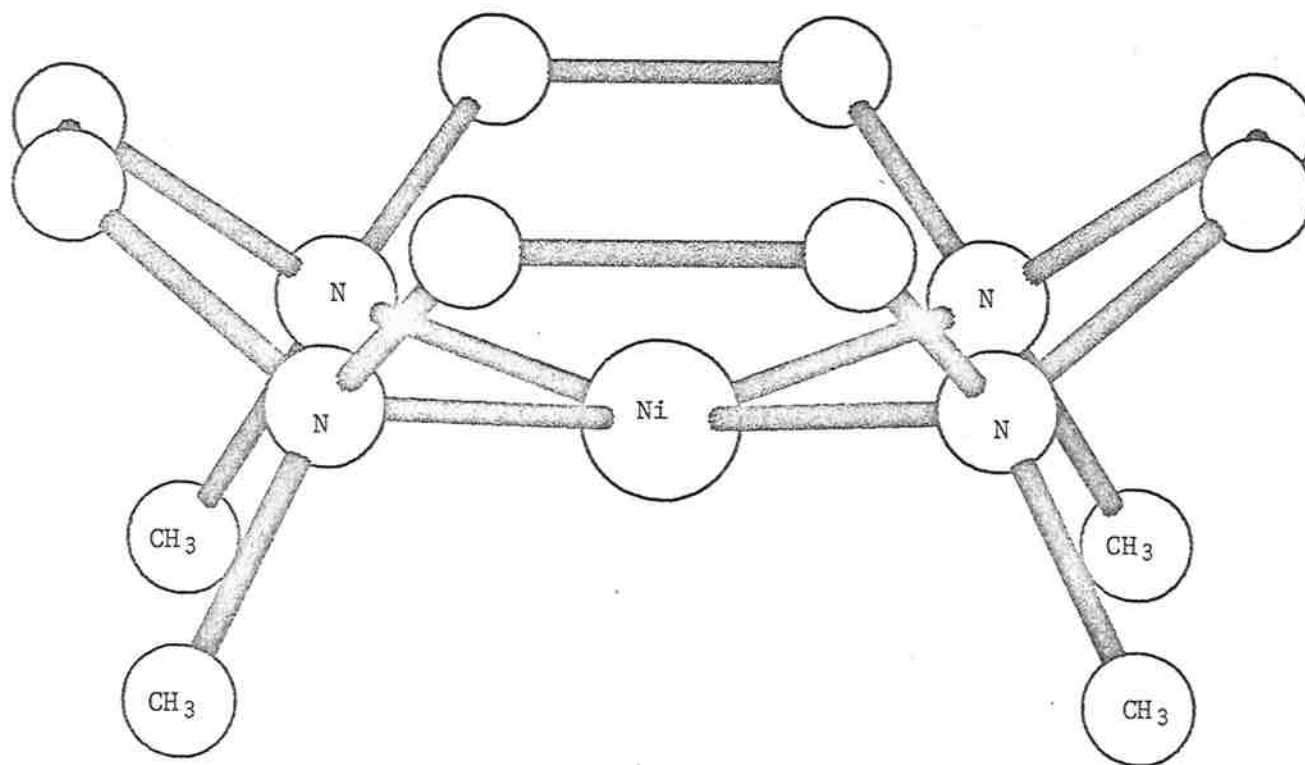


Figure 3.2

Pluto plot of the $[\text{Ni}(\text{Me}_{4,12}\text{aneN}_4)]^{2+}$ complex showing all four methyl groups on the same side of the macrocyclic plane.

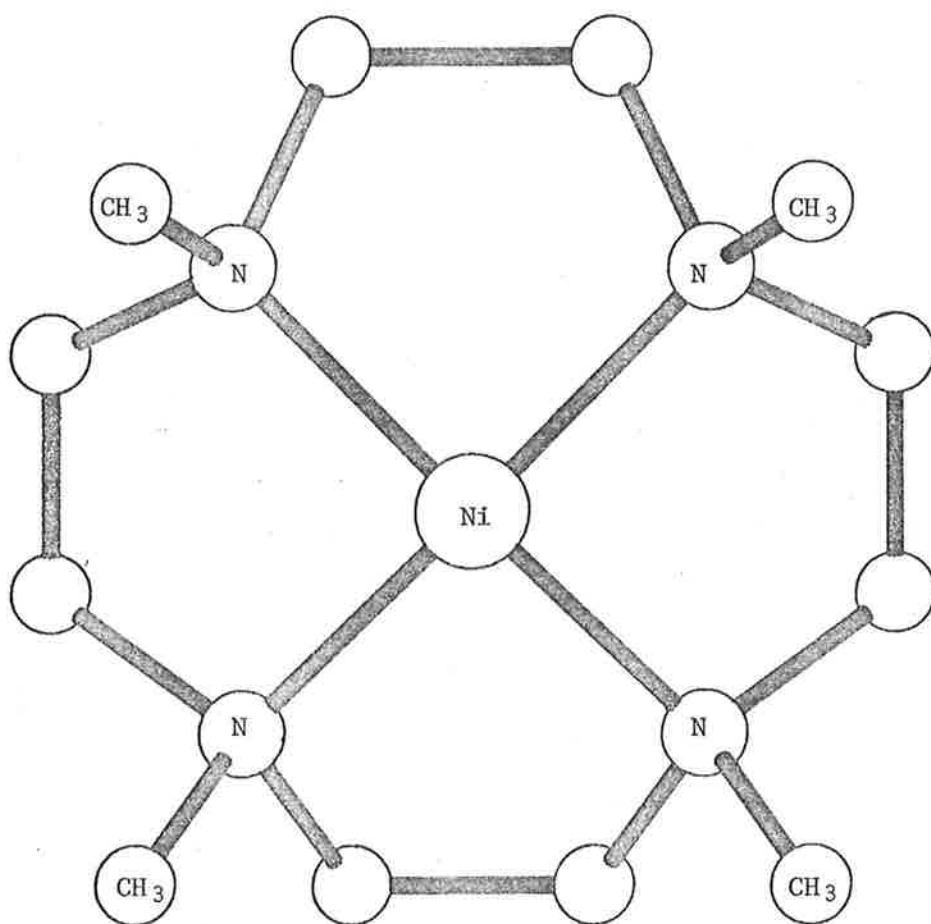


Figure 3.3

Pluto plot of the $[\text{Ni}(\text{Me}_4\text{12aneN}_4)]^{2+}$ complex viewed perpendicular to the plane of the four nitrogen atoms.

TABLE 3.6
Bond Lengths (Å)

Ni - N(1)	1.937(8)	Ni - N(2)	1.945(7)
N(1) - C(3)	1.47(2)	N(1) - C(1)	1.49(2)
N(1) - C(5)	1.45(1)	C(1) - C(2)	1.34(2)
C(2) - N(2)	1.44(2)	N(2) - C(4)	1.51(1)
N(2) - C(6)	1.49(1)	C(3) - C(3)*	1.50(3)
C(4) - C(4)*	1.34(2)		

* symmetry position : x, $\frac{1}{2}$ - y, z

TABLE 3.7
Valence Angles (°)

N(1) - Ni - N(2) = 88.6 (5)	Ni - N(1) - C(1) = 103.2 (7)
Ni - N(1) - C(3) = 105.7 (7)	C(1) - N(1) - C(3) = 107.2 (1.0)
Ni - N(1) - C(5) = 119.0 (7)	C(1) - N(1) - C(5) = 111.1 (9)
C(3) - N(1) - C(5) = 110.0 (9)	Ni - N(2) - C(2) = 104.0 (7)
Ni - N(2) - C(4) = 104.6 (6)	C(2) - N(2) - C(4) = 109.0 (9)
N(1) - C(1) - C(2) = 117.6 (1.3)	C(1) - C(2) - N(2) = 118.3 (1.3)

3.4 Discussion:-

The square-pyramidal cation, $[\text{Ni}(\text{Me}_4\text{14aneN}_4)\text{N}_3]^+$,⁶ has the azide ion co-ordinated on the same side of the macrocycle as the four methyl substituents, with nickel (II) ion 33 pm from the N_4 plane. A recent crystal structure determination on $[\text{Ni}(\text{Me}_4\text{14aneN}_4)\text{N}_3]\text{ClO}_4$ (see Chapter 2, Figure 2.13) showed that the nitrogen donors are co-planar and all methyl substituents are on the same side of the co-ordination plane.⁷ The macrocycle conformation present in the $[\text{Ni}(\text{Me}_4\text{12aneN}_4)](\text{ClO}_4)_2$ complex (ethanol water preparation and diamagnetic in the solid state) is similar to that found for the $[\text{Ni}(\text{Me}_4\text{14aneN}_4)\text{N}_3]\text{ClO}_4$ complex. The fact that the $[\text{Ni}(\text{Me}_4\text{12aneN}_4)](\text{ClO}_4)_2$ complex (ethanol water preparation) tends to be five co-ordinate in the solid state if a co-ordinating anion is present is well established by the magnetic moment measurement (see Chapter 2), uv/visible

spectrum (see Chapter 2) and molecular structure. This fact was also established for metal complexes with $\text{Me}_4\text{14aneN}_4$.⁶ The molecular crystal structure of $[\text{Ni}(\text{Me}_4\text{12aneN}_4)\text{NCS}]\text{NCS}$ could not be studied because of shattering of the crystal. However, it would be interesting to obtain informations from molecular crystal structure on the macrocycle conformation in the $[\text{Ni}(\text{Me}_4\text{12aneN}_4)\text{dmf}](\text{ClO}_4)_2$ (dmf preparation) complex.

REFERENCES FOR CHAPTER THREE

1. "Synthetic Multidentate Macrocyclic Compounds", edited by R. M. Izatt and J. J. Christensen, Academic Press, Inc., New York, (1978).
2. "Co-ordination Chemistry of Macrocyclic Compounds", edited by G. A. Melson, Plenum Press, New York, (1979).
3. Structural parameters were obtained from J. R. Rodgers and M. R. Snow, Department of Physical and Inorganic Chemistry, University of Adelaide, Australia.
4. SUSCAD CAD4-data processing program, University of Sydney, Australia.
5. G. H. Stout and L. H. Jensen, "X-ray Structure Determination", Macmillan Publ. Co., New York (1968).
6. E. K. Barefield and F. Wagner, Inorg. Chem., 12, 2435 (1973).
7. M. J. D'Aniello, M. T. Mocella, F. Wagner, E. K. Barefield and I. C. Paul, J.A.C.S., 97, 192, (1975).

CHAPTER FOUR

High-spin - Low-spin Equilibria of Nickel (II)
Systems in Aqueous Solution

Contents.

- 4.1 Introduction
- 4.2.1. The $[\text{Ni}(\text{12aneN}_4)](\text{ClO}_4)_2$ System.
- 4.2.2. Magnetic Moment Measurements by the Gouy Method and the Evans' Method.
- 4.2.3. The Temperature and Ionic Strength Dependence of Equilibrium Constants.
- 4.2.4. The Temperature Jump Kinetic Study.
- 4.2.5. ^{17}O n.m.r. Water Exchange Kinetic Study.
- 4.3.1. The $[\text{Ni}(\text{Me}_4\text{12aneN}_4)](\text{ClO}_4)_2$ System.
- 4.3.2. Magnetic Moment Measurements by the Gouy Method.
- 4.3.3. The Temperature and Ionic Strength Dependence of Equilibrium Constants.
- 4.3.4. The Temperature Jump Kinetic Study.
- 4.4.1. The $[\text{Ni}(\text{tb12aneN}_4)\text{Cl}]\text{Cl}$ and $[\text{Ni}(\text{tb12aneN}_4)\text{NO}_3]\text{NO}_3$ Systems.
- 4.4.2. The Temperature Dependence of UV/Visible Spectral Change.
- 4.5.1. The $[\text{Ni}(\text{13aneN}_4)](\text{ClO}_4)_2$ System.
- 4.5.2. The Temperature and Ionic Strength Dependence of Equilibrium Constants.
- 4.5.3. The Temperature Jump Kinetic Study.
- 4.6.1. The $[\text{Ni}(\text{Me}_4\text{14aneN}_4)](\text{ClO}_4)_2$ System.
- 4.6.2. Magnetic Moment Measurements by the Gouy Method.
- 4.6.3. The Temperature and Ionic Strength Dependence of Equilibrium Constants.
- 4.6.4. The Temperature Jump Kinetic Study.
- 4.6.5. General Discussion.

CHAPTER FOUR

High-spin - Low-spin Equilibria of Nickel (II)
Systems in Aqueous Solution

4.1. Introduction.

Octahedral complexes of $d^4 - d^8$ transition metal ions (e.g. ions such as chromium (II) (d^4), iron (III) (d^5), iron (II) (d^6), cobalt (II) (d^7) and nickel (II) (d^8)) may occur in high-spin or low-spin states depending upon whether the ligand field splitting energy is smaller or greater than the interelectronic repulsion energy, according to one of the predictions of ligand field theory.¹ Systems in which both high and low-spin species co-exist in solution are often described as systems in spin-equilibrium. The co-ordination number may remain constant ²⁻⁸ (e.g. the [iron(II)(hydrotris (1-pyrazolyl) borate)₂] and [nickel (II) aminotroponimineates] systems) or may not remain constant (e.g. the [Ni(12aneN₄)]²⁺ system described here). In all of the nickel (II) systems reported here, the co-ordination number either changes from six to four or five to four. The spin-equilibrium may exist for complexes for which the low-spin and the high-spin ground states do not differ greatly in energy (i.e. separated by only a few hundred reciprocal centimetres). Since the energies involved in changes in chemical bonding are in general much larger than this, the requirement is very restrictive and accounts for the fact that there are few cases of this type of equilibrium.

Figure 4.1 shows the approximate energy-level diagram¹ showing the splitting of the d orbitals for octahedral, square planar,

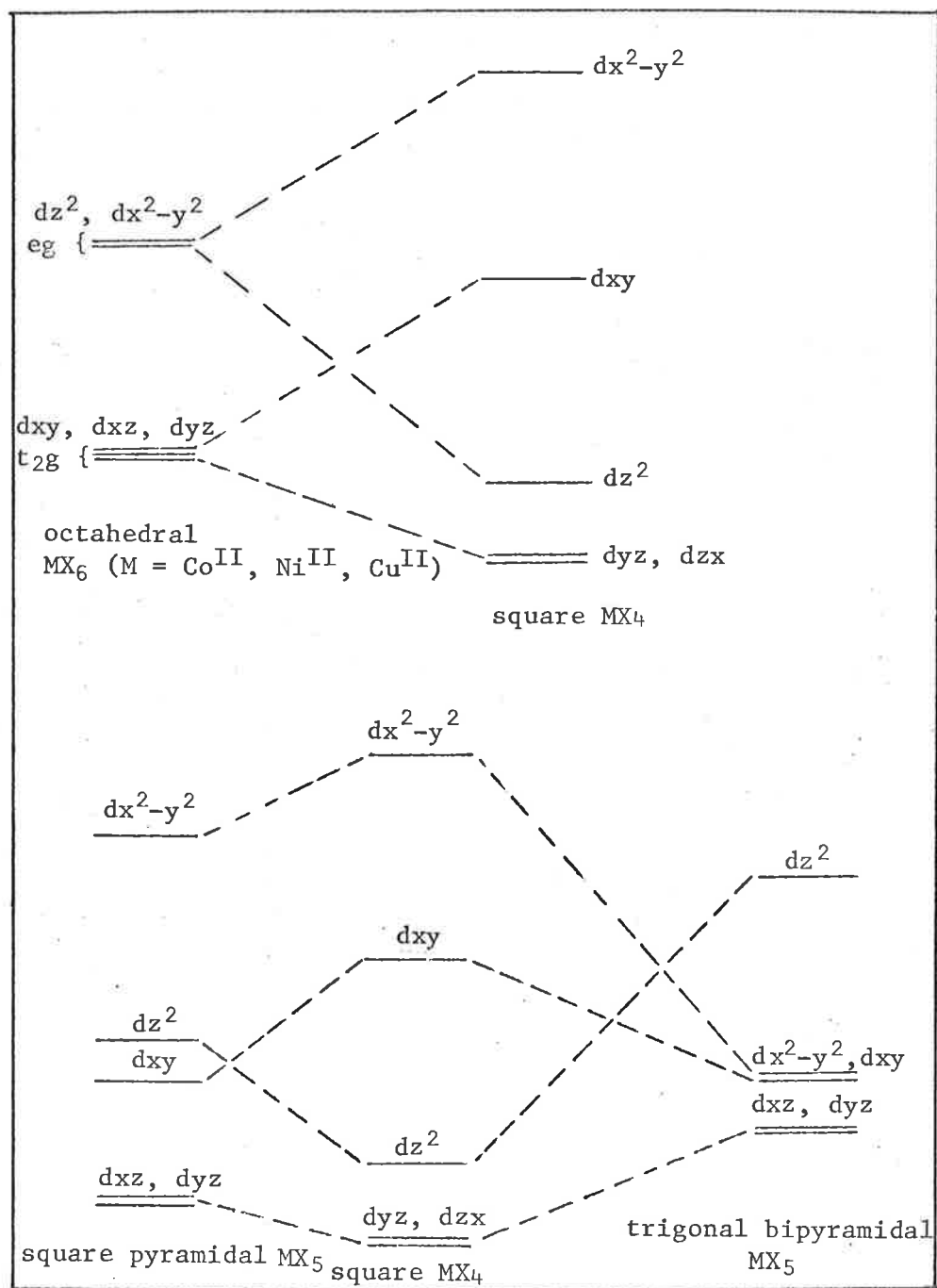


Figure 4.1

Approximate energy level diagram showing the splitting of the d orbitals for octahedral, square planar, square pyramidal and trigonal bipyramidal complexes of nickel(II).

square pyramidal and trigonal-bypyramidal complexes of nickel(II). It is in general possible for the energy of the d_z^2 orbital to drop below that of the d_{xy} orbital depending upon the distortion, as in the limiting case of a square planar complex. The geometry of the complex depends both upon the nature of the metal centre and the ligand. The spin-equilibria of the nickel (II) systems discussed here involve octahedral or square based pyramidal species (to a geometric first approximation, see Chapter 3) in the high-spin state and square planar species in the low-spin state. Firstly, a number of nickel (II) systems exhibit a temperature dependence of their uv/visible spectra and magnetic susceptibility consistent with a change in the position of the spin-equilibrium. Typical of such a system is:-

$$[\text{Ni}(\text{12aneN}_4)]^{2+} + 2\text{H}_2\text{O} \rightleftharpoons [\text{Ni}(\text{12aneN}_4)(\text{H}_2\text{O})_2]^{2+}$$

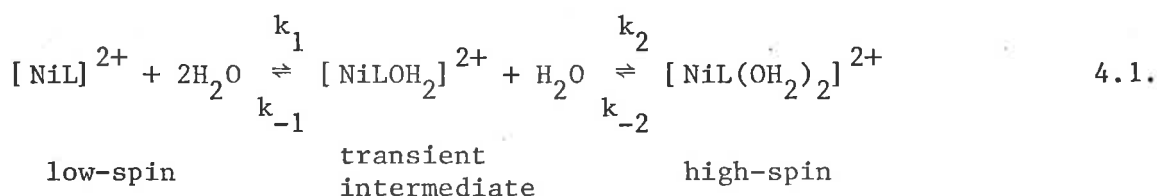
which is a system discussed in detail here. For nickel (II) systems, this type of equilibrium exists in both aqueous and non-aqueous solution,⁹⁻¹⁶ (e.g. the $[\text{Ni}(\text{14aneN}_4)]^{2+}$, $[\text{Ni}(\text{2,3,2-tet})]^{2+}$ systems) and has been shown to be sensitive to the nature of the ligand, the counter anion in the case of cationic complexes, temperature and also to pressure. The kinetics of square planar-octahedral equilibria of nickel (II) complexes have been studied using photochemical and temperature jump perturbations.^{9,15} (In the case of iron (II)^{8,17-20}, iron (III)^{5,6,8,21,22} and cobalt (II),⁷ the dynamics of spin-equilibria have been studied using Raman laser temperature jump and ultrasonic absorption techniques.)

In this study, a number of nickel (II) complexes with tetra-aza macrocyclic ligands have been prepared to observe the effects of ring size and steric hindrance on the dynamics of spin-equilibria. The magnetic moment (solid state and in solution), uv/visible spectroscopic, temperature jump, and ¹⁷O n.m.r. data for the

$[\text{Ni}(\text{12aneN}_4)]^{2+}$ system are first discussed. Discussion of similar data for the $[\text{Ni}(\text{Me}_4\text{12aneN}_4)]^{2+}$, $[\text{Ni}(\text{tb12aneN}_4)]^{2+}$, $[\text{Ni}(\text{13aneN}_4)]^{2+}$ and $[\text{Ni}(\text{Me}_4\text{14aneN}_4)]^{2+}$ systems then follows.

4.2.1. The $[\text{Ni}(\text{12aneN}_4)](\text{ClO}_4)_2$ System.

The low-spin square planar (singlet, diamagnetic, $^1\text{A}_{1g}$) and the high-spin octahedral (triplet, paramagnetic, $^3\text{A}_{2g}$) equilibrium (4.1) of nickel (II)



complexes with tetradentate polyamine ligands have been investigated extensively^{9, 15, 23-27} but the dynamics of sequential equilibria between (i) the four co-ordinate species and the transient five co-ordinate species (k_1/k_{-1}) and (ii) this intermediate and the six co-ordinate species (k_2/k_{-2}) have been separately characterised for the first time in this study. The ligand 12aneN_4 ('L' in equation 4.1) has been chosen to gain an insight into the factors controlling the lability of these equilibria and to determine which of them embraces the rate determining step for the spin state change. The 12aneN_4 ligand is the smallest tetra-aza macrocyclic ligand presenting a macrocyclic hole and is estimated to restrain the metal-nitrogen distance to 1.70\AA ²⁶ or 1.81\AA ²⁸. However in linear polyamine complexes, the observed low-spin and high-spin nickel (II) - nitrogen distances are $1.89 \pm 0.03\text{\AA}$ ⁰ and $2.1 \pm 0.05\text{\AA}$ ⁰ respectively^{25, 26, 28, 29}. Thus the coplanarity of nickel (II) and the four nitrogen atoms in low-spin $[\text{Ni}(\text{12aneN}_4)]^{2+}$ is more probable whereas the coplanarity in the high-spin state is improbable and indeed cis-stereochemistry is inferred for $[\text{Ni}(\text{12aneN}_4)(\text{H}_2\text{O})_2]^{2+}$ from spectroscopic data.²⁹ The existence of high-spin and low-spin states

in aqueous solution facilitates both temperature jump spectrophotometric and ^{17}O n.m.r. kinetic studies of the system under identical conditions; the stability of the complexes and the very slow dissociation of the 12aneN₄ ligand from the complex under strongly acidic or basic conditions (see Chapter 5) rules out the possibility of the interference of other reactions with the study of the square planar - octahedral interconversion.

4.2.2. Magnetic Moment Measurements by the Gouy Method and the Evans' Method:-

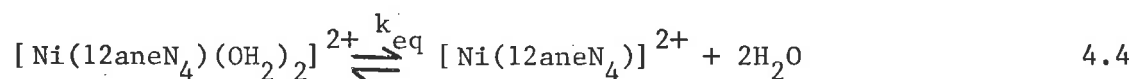
The ground electronic state of nickel (II) complexes is very sensitive to geometry and ligand field strength. The equilibrium between the high-spin and low-spin states can be studied by variable temperature magnetic moments measurement. In the solid state and in nitromethane solution [Ni(12aneN₄)](ClO₄)₂ was found to be diamagnetic using the Gouy method³⁰ and the Evans' method³¹ (see Chapter 7) respectively, implying that the same species exist in the solid state and in the nitromethane solution. The magnetic moment (μ_{eff}) of [Ni(12aneN₄)](ClO₄)₂ (0.101 mol dm⁻³) in aqueous solution at 274K was determined to be 2.90B.M. by the Evans' method which may be compared with the magnetic moments of the analogous dichloro (3.06), dibromo(3.16) and dinitro (3.15)²⁹ species in the solid state. The magnetic moment (μ_{obs}) of a solution of 4.06×10^{-2} mol dm⁻³ [Ni(12aneN₄)](ClO₄)₂ in aqueous 4.0 mol dm⁻³ LiClO₄ solution was determined by the Evans' method within the temperature range 288.40 - 362.9K. The equilibrium constant;

$$K_{\text{eq}} = \frac{[\text{Ni}(12\text{aneN}_4)^{2+}]}{[\text{Ni}(12\text{aneN}_4)(\text{OH}_2)_2^{2+}]} \quad 4.2$$

was calculated using the equation given below

$$K_{\text{eq}} = \frac{\mu_{\text{eff}}^2 - \mu_{\text{obs}}^2}{\mu_{\text{obs}}^2} \quad 4.3$$

assuming the square planar species to be diamagnetic in aqueous solution.³² The magnetic moment of the paramagnetic $[\text{Ni}(\text{12aneN}_4)(\text{OH}_2)_2]^{2+}$ species is μ_{eff} and μ_{obs} is the observed magnetic moment at a particular temperature. The enthalpy, ΔH° and entropy, ΔS° for the equilibrium (4.4) were determined by a linear



regression of the k_{eq} data according to the equation (4.5)

$$\Delta H^\circ - T\Delta S^\circ = -RT \ln k_{\text{eq}} \quad 4.5$$

The k_{eq} , ΔH° and ΔS° values are given in Table 4.1 and the plot of k_{eq} vs $\frac{1}{T}$ is shown in Figure 4.2. Both aqueous $4.0 \text{ mol dm}^{-3} \text{ LiClO}_4$ and aqueous $4.0 \text{ mol dm}^{-3} \text{ LiClO}_4$ with $[\text{Ni}(\text{12aneN}_4)](\text{ClO}_4)_2$ solutions were assumed to have the same volume expansion. The densities of aqueous $4.0 \text{ mol dm}^{-3} \text{ LiClO}_4$ solution were determined at different temperatures to make density corrections in evaluating the mass susceptibility of $[\text{Ni}(\text{12aneN}_4)](\text{ClO}_4)_2$. The concentration of $[\text{Ni}(\text{12aneN}_4)](\text{ClO}_4)_2$ at a particular temperature was calculated using the following equation

$$M_T = \frac{D_T}{D_{294.2}} \times M_{294.2} \quad 4.6$$

where $M_T = \text{mol dm}^{-3}$ at a particular temperature TK

$M_{294.2} = \text{mol dm}^{-3}$ at 294.2K

$D_T = \text{density at temperature TK}$

$D_{294.2} = \text{density at 294.2K}$

and the weight of $[\text{Ni}(\text{12aneN}_4)](\text{ClO}_4)_2$ in 1.0 cm^3 solution was calculated for each temperature.

Figure 4.2

The variation of K_{eq} with temperature and $[LiClO_4]$. The filled circles and squares represent spectrophotometric data obtained in a) 4.00, b) 3.00, c) 2.00, d) 0.00 (plotted as $5K_{eq}$) and e) 1.00 mol dm^{-3} aqueous $LiClO_4$ solution, and the solid lines represent least squares linear regression lines. The filled triangles represent data obtained from magnetic moment measurements in 4.00 mol dm^{-3} aqueous $LiClO_4$ solution. The open squares, circles and triangles represent data obtained from ^{17}O n.m.r. shift studies at 5.75, 11.5 and 13.2 MHz in 3.00 mol dm^{-3} aqueous $LiClO_4$ solution.

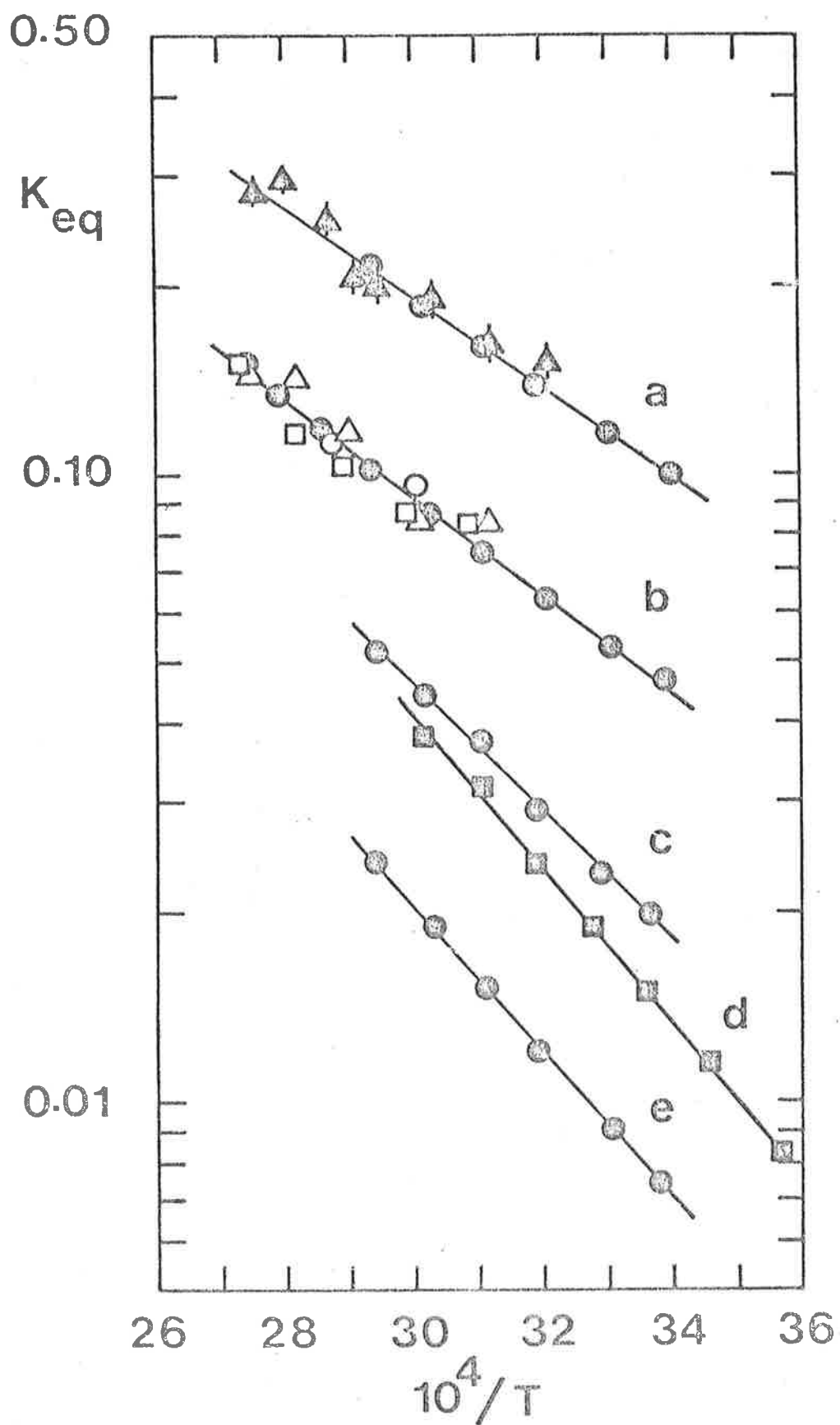


Figure 4.2

TABLE 4.1

K_{eq} , ΔH° and ΔS° Values from Magnetic Moment Measurements in Aqueous
4.0 mol dm⁻³ LiClO₄ for the [Ni(12aneN₄)(OH₂)₂]²⁺ System

$10^4/T$	K_{eq}^a
27.55	0.283 ± 0.01
28.00	0.294 ± 0.02
28.70	0.258 ± 0.02
29.10	0.209 ± 0.01
29.50	0.198 ± 0.01
30.35	0.192 ± 0.01
31.20	0.168 ± 0.01
32.20	0.157 ± 0.01
32.59	0.134 ± 0.01
33.60	0.110 ± 0.01
34.68	0.092 ± 0.004

(a) The errors represent one standard deviation

$${}^a\Delta H^\circ = (13.11 \pm 0.72) \text{ kJ mol}^{-1}$$

$${}^a\Delta S^\circ = (25.92 \pm 0.26) \text{ JK}^{-1} \text{ mol}^{-1}$$

4.2.3. The Temperature and Ionic Strength Dependence of Equilibrium Constants:-

The [Ni(12aneN₄)](ClO₄)₂ species exists in aqueous solution as a mixture of octahedral (high-spin, blue) and square planar (low-spin, yellow) species according to the equilibrium (4.4) given by equation 4.4. The visible spectrum of the aqueous [Ni(12aneN₄)]²⁺ system is markedly dependent upon temperature (Figure 4.3) and ionic strength. An increase of either the temperature or the supporting inert electrolyte concentration (e.g. LiClO₄) displaces the equilibrium (4.4) to the right. The electronic spectrum of aqueous [Ni(12aneN₄)(OH₂)₂]²⁺ is typical of a high-spin octahedral complex, probably cis octahedral. Qualitatively, at low temperature and low electrolyte concentration, this solution is

blue but addition of LiClO_4 (e.g. 4.0 mol dm^{-3}) causes the solution to become brown (yellowish) and more brown (yellowish) as the temperature increases. Quantitatively an increase of either temperature or ionic strength increases the intensity in the band at 443nm with simultaneous decrease in the bands at 357nm and 560nm as seen in Figure 4.3. The band at 443nm shows a progressive increase in intensity in the spectra at 293.7, 302.5, 313.2, 323.0, 332.3 and 344.0 K respectively. The two isosbestic points (365nm and 542nm, Figure 4.3) suggest the occurrence of two predominant species; low-spin $[\text{Ni}(\text{12aneN}_4)]^{2+}$ and high-spin $[\text{Ni}(\text{12aneN}_4)(\text{OH}_2)_2]^{2+}$, presumably in the cis-configuration.^{29, 33} The band at 443nm is typical of the yellow diamagnetic nickel (II) complex. The effect of temperature was studied in zero, 0.1, 1.0, 2.0 and 3.0 mol dm^{-3} aqueous LiClO_4 , and two isosbestic points were observed in each case as in the case of aqueous 4.0 mol dm^{-3} LiClO_4 solution. To determine the thermodynamics of the $[\text{Ni}(\text{12aneN}_4)]^{2+}/[\text{Ni}(\text{12aneN}_4)(\text{OH}_2)_2]^{2+}$ equilibrium at a fixed ionic strength, the molar extinction co-efficient (temperature independent, $71.0 \text{ mol}^{-1} \text{ dm}^3 \text{ cm}^{-1}$, 443nm) of $[\text{Ni}(\text{12aneN}_4)]^{2+}$ in dry nitromethane was determined from $3.49 \times 10^{-3} \text{ mol dm}^{-3}$ and $1.49 \times 10^{-2} \text{ mol dm}^{-3}$ $[\text{Ni}(\text{12aneN}_4)]^{2+}$ solutions and the species present in nitromethane solution was assumed to be identical to that of the low-spin species in aqueous solution. To determine the molar extinction co-efficient of the high spin species, an aqueous solution of $4.53 \times 10^{-3} \text{ mol dm}^{-3}$ $[\text{Ni}(\text{12aneN}_4)](\text{ClO}_4)_2$ was prepared and the spectra were recorded at different temperatures down to 280.15K (no 443nm band present at this temperature). The temperature-absorbance curve at 443nm (not shown) was extrapolated to 273.15K to obtain the molar extinction co-efficient ($1.43 \text{ mol}^{-1} \text{ dm}^3 \text{ cm}^{-1}$, 443nm) of the high spin (octahedral) species.

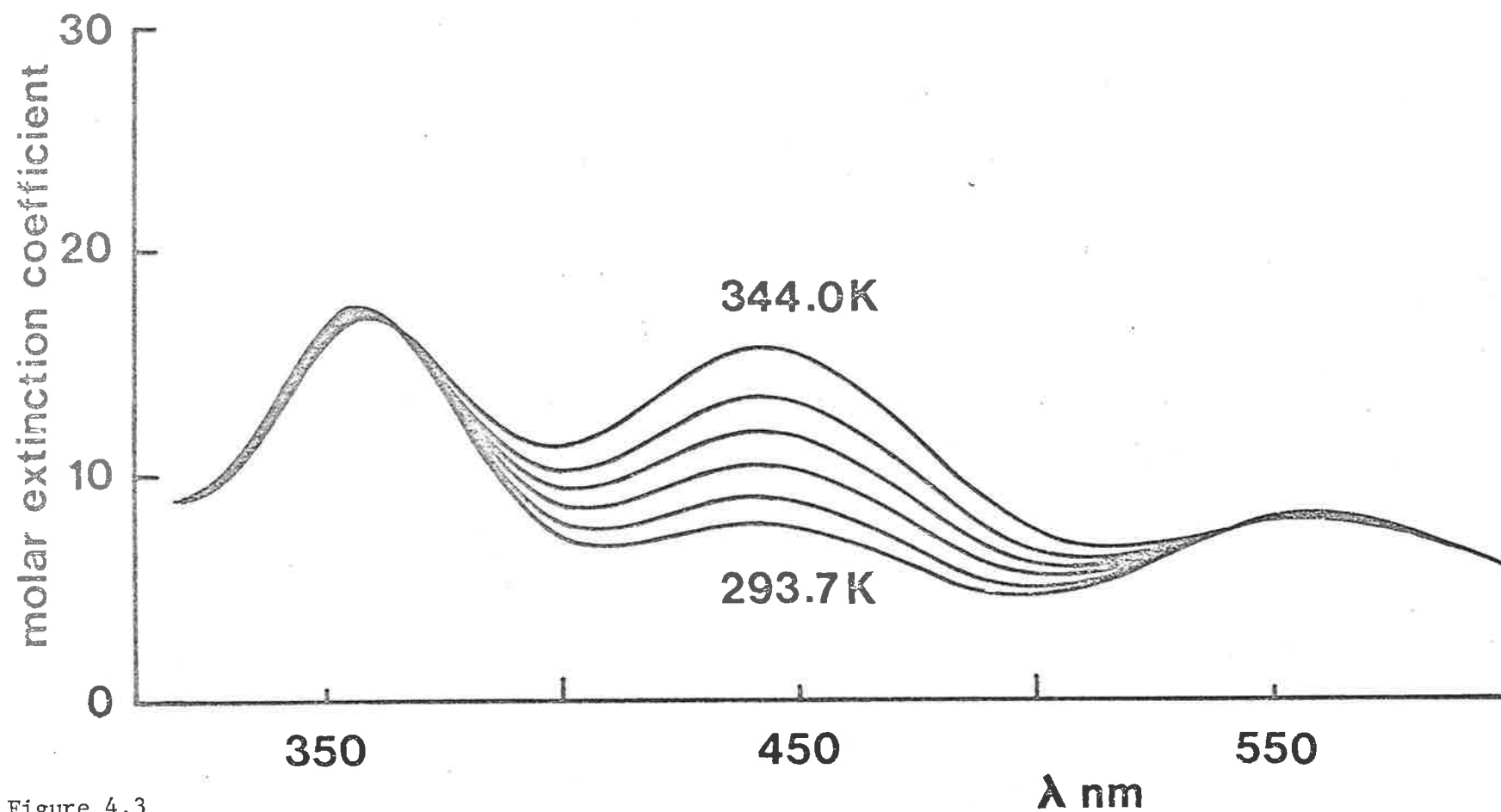


Figure 4.3

Temperature dependent uv/visible spectra of $4.67 \times 10^{-2} \text{ mol dm}^{-3}$ $[\text{Ni}(\text{12aneN}_4)](\text{ClO}_4)_2$ in aqueous 4.00 mol dm^{-3} LiClO_4 .

The band at 443 nm shows a progressive increase in intensity in the spectra recorded at 293.7, 302.5, 313.2, 323.0, 332.3 and 344.0 K respectively.

The equilibrium constant ($K_{eq} = C_{sp}/C_{oct}$) was calculated using the following two equations:-

$$C_{sp} = \frac{A_{tot} - \epsilon_{oct} C_{tot}}{\epsilon_{sp} - \epsilon_{oct}} \quad 4.7$$

$$C_{oct} = C_{tot} - C_{sp}$$

where C_{sp} = concentration of square planar species

C_{oct} = concentration of octahedral species

A_{tot} = total optical density of low-spin and high-spin species

C_{tot} = total concentration of low-spin and high-spin species

ϵ_{sp} = molar extinction co-efficient of square planar species

ϵ_{oct} = molar extinction co-efficient of octahedral species

The k_{eq} values at different temperatures are given in Table 4.2 and the plots of k_{eq} against $\frac{1}{T}$ are shown in Figure 4.2. The enthalpy, ΔH° and the entropy, ΔS° for the equilibrium (4.4) are determined by a least squares analysis of the K_{eq} data according to equation 4.5. These ΔH° and ΔS° values together with k_{eq} values at 298.2K for different $LiClO_4$ concentrations are given in Table 4.3.

The $[Ni(12aneN_4)](ClO_4)_2$ complex is slightly soluble in dmf (blue), triethylamine (yellow), nitrobenzene (yellow), pyridine (violet) and acetonitrile (violet) but insoluble in dichloromethane, tetrahydrofuran, chlorobenzene and tetrachloroethane. However, the present study of high-spin low-spin equilibrium is limited to aqueous medium only.

4.2.4. Temperature Jump Kinetic Study.

The temperature relaxation of the high-spin low-spin equilibrium at 443nm in aqueous 2.0, 3.0 and 4.0 mol dm⁻³ $LiClO_4$ was studied at different temperatures in the complex concentration range of 0.047 - 0.140 mol dm⁻³ and was characterised by a single

TABLE 4.2

K_{eq} Values at Different Temperatures and Ionic Strengths
for $Ni(12aneN_4)(OH_2)_2^{2+}$ System

$10^4/T$	$10^4 K_{eq}^a$	$10^4/T$	$10^4 K_{eq}^a$	$10^4/T$	$10^4 K_{eq}^a$
1. $[LiClO_4] = .0 \text{ mol dm}^{-3}$		3. $[LiClO_4] = 1.0 \text{ mol dm}^{-3}$		5. $[LiClO_4] = 3.0 \text{ mol dm}^{-3}$	
35.67	16.5 ± 1	33.81	74 ± 3	33.95	471 ± 19
34.57	23.0 ± 1	33.06	90.5 ± 5	33.07	529 ± 26
33.58	30.0 ± 2	31.92	120 ± 5	32.04	621 ± 34
32.78	37.5 ± 2	31.08	152 ± 7	31.10	751 ± 34
31.87	47.5 ± 2	30.28	189 ± 9	30.26	860 ± 40
31.03	63.5 ± 2	29.40	241 ± 13	29.36	1018 ± 56
30.17	78.0 ± 3			28.62	1183 ± 49
				27.92	1348 ± 63
				27.42	1512 ± 75
2. $[LiClO_4] = 0.1 \text{ mol dm}^{-3}$		4. $[LiClO_4] = 2.0 \text{ mol dm}^{-3}$		6. $[LiClO_4] = 4.0 \text{ mol dm}^{-3}$	
33.72	30.5 ± 2	33.63	197 ± 10	34.04	991 ± 55
32.93	40.0 ± 2	32.90	229 ± 12	33.05	1199 ± 51
31.92	54.5 ± 3	31.91	289 ± 12	31.92	1456 ± 68
30.87	67.5 ± 3	31.03	373 ± 17	30.95	1746 ± 87
30.13	88.0 ± 3	30.17	444 ± 21	30.10	2064 ± 93
29.34	114 ± 6	29.44	518 ± 28	29.07	2533 ± 106

^a The errors represent estimated error.

TABLE 4.3
 K_{eq} (298.2K), ΔH° and ΔS° Values for $[\text{Ni}(\text{12aneN}_4)]^{2+}$ System

$[\text{LiClO}_4]$ mol dm^{-3}	$10^4 K_{eq}^a$ (298.2K)	$b_{\Delta H^\circ}$ kJ mol^{-1}	$b_{\Delta S^\circ}$ $\text{JK}^{-1} \text{mol}^{-1}$
0	30.0 ± 2	23.6 ± 0.3	30.8 ± 1.1
0.10	33.0 ± 2	24.2 ± 0.8	33.7 ± 2.7
1.0	79.0 ± 4	22.1 ± 0.2	34.0 ± 0.7
2.0	200 ± 10	19.6 ± 0.5	33.3 ± 1.5
3.0	490 ± 20	15.0 ± 0.3	25.1 ± 0.9
4.0	1070 ± 50	15.5 ± 0.2	33.7 ± 0.6

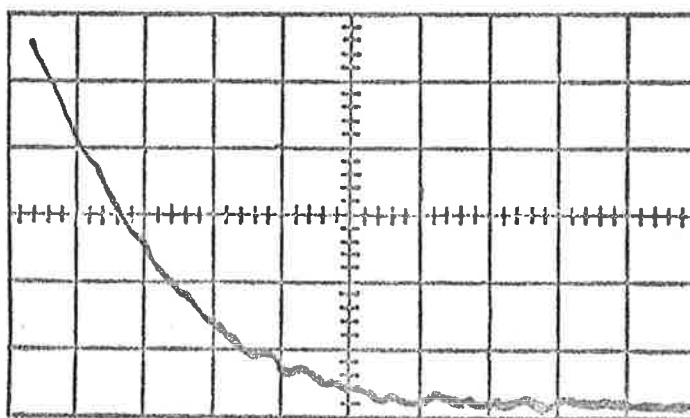
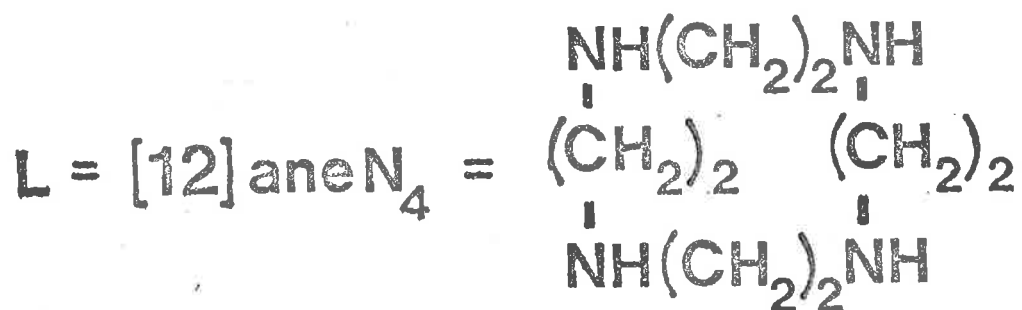
The errors represent (a) estimated error
 (b) one standard deviation

concentration independent relaxation (τ). Since the relaxation time for the spin-equilibrium in $1.0 \text{ mol dm}^{-3} \text{ LiClO}_4$ solution is similar to the heating time of the temperature jump apparatus at 285.5K (the lowest practical temperature), it was not possible to study the $[\text{Ni}(\text{12aneN}_4)](\text{ClO}_4)_2$ system in $1.0 \text{ mol dm}^{-3} \text{ LiClO}_4$ or evaluate accurate relaxation times. In aqueous $3.0 \text{ mol dm}^{-3} \text{ LiClO}_4$ solution at 298.8K, the relaxation time was found to be $(3.32 \pm 0.15) \times 10^{-6} \text{ s}$ and $(3.30 \pm 0.20) \times 10^{-6} \text{ s}$ using $0.070 \text{ mol dm}^{-3}$ and $0.140 \text{ mol dm}^{-3} [\text{Ni}(\text{12aneN}_4)](\text{ClO}_4)_2$ respectively, thus showing the concentration independence of relaxation time. Figure 4.4 shows a typical photograph for an aqueous $3.0 \text{ mol dm}^{-3} \text{ LiClO}_4$ solution at 298.8K. The relaxation time, is related to the rate constant, k_1 , of equation 4.1 by the equation 4.8

$$\frac{1}{\tau} = k_1 [\text{H}_2\text{O}] (1 + K_{eq}) \quad 4.8$$

The above equation 4.8, may be derived as follows:-

Since the concentration of water in any particular perturbation

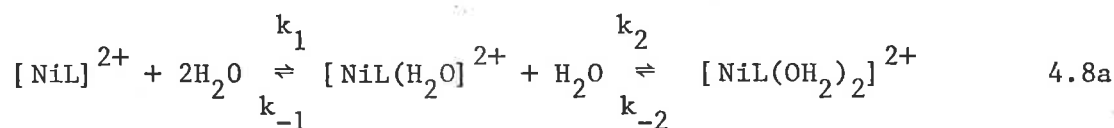


T-Jump 443 nm 20mv/cm
 2.0 μs/cm 298.8 K
 aq. LiClO₄ 3.00 mol dm⁻³

Figure 4.4

Typical temperature jump photograph for an aqueous solution of
 [Ni(12aneN₄)](ClO₄)₂ in 3.00 mol dm⁻³ LiClO₄ at 298.8 K.

experiment may be regarded as constant, the equation may be written as



(where L = ligand)

$$\text{Let } k'_1 = k_1[\text{H}_2\text{O}], \quad k'_2 = k_2[\text{H}_2\text{O}]$$

Hence the rate of disappearance of $[\text{NiL}]^{2+}$ may be written as

$$-\frac{d[\text{NiL}^{2+}]}{dt} = k'_1 [\text{NiL}^{2+}] - k_{-1} [\text{NiL}(\text{H}_2\text{O})^{2+}]$$

Expressing concentrations as an equilibrium plus a small perturbation

$$-\frac{d([\text{NiL}^{2+}] + \Delta[\text{NiL}^{2+}])}{dt} = k'_1([\text{NiL}^{2+}] + \Delta[\text{NiL}^{2+}]) - k_{-1}([\text{NiL}(\text{OH}_2)^{2+}] + \Delta[\text{NiL}(\text{OH}_2)^{2+}])$$

but at equilibrium $k'_1[\text{NiL}^{2+}] = k_{-1}[\text{NiL}(\text{OH}_2)^{2+}]$ and $[\text{NiL}^{2+}]$ is constant, hence

$$-\frac{d\Delta[\text{NiL}^{2+}]}{dt} = k'_1\Delta[\text{NiL}^{2+}] - k_{-1}\Delta[\text{NiL}(\text{OH}_2)^{2+}]$$

from ^{17}O n.m.r. data the second step in the equation 4.8a is in rapid equilibrium, hence at all times

$$k'_2 [\text{NiL}(\text{OH}_2)^{2+}] = k_{-2} [\text{NiL}(\text{OH}_2)_2^{2+}]$$

$$\text{Hence } k'_2 \Delta[\text{NiL}(\text{OH}_2)^{2+}] = k_{-2} \Delta[\text{NiL}(\text{OH}_2)_2^{2+}]$$

Additionally there must be conservation of $[\text{NiL}]^{2+}$,

$$\text{Hence } [\text{NiL}^{2+}] + [\text{NiL}(\text{OH}_2)^{2+}] + [\text{NiL}(\text{OH}_2)_2^{2+}] = [\text{NiL}^{2+}]_{\text{Total}}$$

$$\text{thus } \Delta[\text{NiL}^{2+}] + \Delta[\text{NiL}(\text{OH}_2)^{2+}] + \Delta[\text{NiL}(\text{OH}_2)_2^{2+}] = 0$$

But from equilibrium measurements $[\text{NiL}(\text{OH}_2)^{2+}]$ is small and during

perturbation $[\text{NiL}(\text{OH}_2)^{2+}]$ is believed to be invariant in the steady state, hence $\Delta[\text{NiL}(\text{OH}_2)^{2+}] = 0$

$$\text{Thus } \Delta[\text{NiL}^{2+}] = -\Delta[\text{NiL}(\text{OH}_2)_2^{2+}]$$

$$\text{and } k'_2 \Delta[\text{NiL}(\text{OH}_2)^{2+}] = k_{-2} \Delta[\text{NiL}(\text{OH}_2)_2^{2+}] = -k_{-2} \Delta[\text{NiL}^{2+}]$$

$$\therefore \Delta[\text{NiL}(\text{OH}_2)^{2+}] = -\frac{k_{-2}}{k'_2} \Delta[\text{NiL}^{2+}]$$

$$-\frac{d\Delta[\text{NiL}^{2+}]}{dt} = k'_1 \Delta[\text{NiL}^{2+}] + \frac{k_{-1}k_{-2}}{k'_2} \Delta[\text{NiL}^{2+}]$$

$$\text{Hence } \frac{1}{\tau} = k'_1 + \frac{k_{-1}k_{-2}}{k'_2}$$

$$\therefore \frac{1}{\tau} = k_1[\text{H}_2\text{O}] + \frac{k_{-1}k_{-2}}{k_2[\text{H}_2\text{O}]} = k_1[\text{H}_2\text{O}] (1 + K_{\text{eq}})$$

$$\text{where } K_{\text{eq}} = \frac{k_{-1}k_{-2}}{k_1k_2[\text{H}_2\text{O}]^2} = \frac{[\text{NiL}]}{[\text{NiL}(\text{H}_2\text{O})_2]}$$

Using the K_{eq} data from Table 4.2 and determining the densities of different concentration of LiClO_4 solution at different temperatures to obtain the concentration of water, the k_1 values obtained are given in Table 4.4. The kinetic parameters ΔH^\ddagger and ΔS^\ddagger are obtained by least squares analysis using the equation 4.9.

$$k_1 = \frac{k_B T}{h} e^{-\Delta H^\ddagger/RT} e^{\Delta S^\ddagger/R} \quad 4.9$$

where h = Planck's constant

k_B = Boltzmann's constant

R = $8.314 \text{ JK}^{-1} \text{ mol}^{-1}$

k_1 = forward rate constant

T = absolute temperature

The relaxation time, τ , H^\ddagger , S^\ddagger and $k_1(298.2\text{K})$ values are given in Table 4.5. The concentration of water determined for this study was found to be 50.9, 48.6 and 46.1 mol dm^{-3} in 2.0, 3.0 and 4.0 mol dm^{-3} LiClO_4 , respectively.

TABLE 4.4

Temperature jump Kinetic Data for the
 $[\text{Ni}(\text{12aneN}_4)]^{2+} / [\text{Ni}(\text{12aneN}_4)(\text{OH}_2)_2]^{2+}$ System

TK	a $10^4 K_{\text{eq}}$	b $k_1 \times 10^{-3}$ $\text{mol}^{-1} \text{dm}^3 \text{S}^{-1}$
$[\text{LiClO}_4] = 2.0 \text{ mol dm}^{-3}$		
286.05	143 ± 6	4.42 ± 0.11
291.45	167 ± 8	5.67 ± 0.12
296.35	190 ± 10	8.82 ± 0.21
$[\text{LiClO}_4] = 3.0 \text{ mol dm}^{-3}$		
287.20	387 ± 16	2.84 ± 0.05
293.35	441 ± 20	4.34 ± 0.11
298.75	493 ± 27	5.94 ± 0.13
$[\text{LiClO}_4] = 4.0 \text{ mol dm}^{-3}$		
305.75	1232 ± 58	6.86 ± 0.25
310.55	1340 ± 56	8.47 ± 0.13
315.95	1469 ± 66	9.27 ± 0.21

The errors represent

a estimated error

b one standard deviation

The k_{eq} value for a particular temperature are obtained by a least squares analysis of the K_{eq} data according to equation 4.5.

TABLE 4.5

Temperature jump Kinetic Data for the

 $[\text{Ni}(\text{12aneN}_4)]^{2+} / [\text{Ni}(\text{12aneN}_4)(\text{OH}_2)_2]^{2+}$ System

$[\text{LiClO}_4]$ mol dm^{-3}	$10^6 \tau$ s	$10^{-3} k_1$ (298.2K) $\text{mol}^{-1} \text{dm}^3 \text{s}^{-1}$	ΔH^\ddagger kJ mol^{-1}	ΔS^\ddagger $\text{JK}^{-1} \text{mol}^{-1}$
2.0	4.4 ± 0.2 (286.1K)	9.5 ± 0.5	44.5 ± 9.3	-19.4 ± 32
	3.4 ± 0.2 (291.5K)			
	2.2 ± 0.1 (296.4K)			
3.0	7.0 ± 0.3 (287.2K)	5.8 ± 0.3	43.1 ± 1.7	-28.15 ± 5.9
	4.5 ± 0.2 (293.4K)			
	3.3 ± 0.2 (298.8K)			
4.0	2.8 ± 0.1 (305.8K)	5.6 ± 0.3	20.9 ± 6.1	-103.0 ± 20
	2.3 ± 0.1 (310.6K)			
	2.0 ± 0.1 (316.0K)			

N.B. The errors represent one standard deviation

4.2.5 ^{17}O n.m.r. Water Exchange Kinetic Study:-³⁴

Fundamental to the understanding of reactions occurring at metal centres in aqueous solution is a knowledge of the water exchange process. Such knowledge is essential to the present study and accordingly the dynamics of water exchange in the $[\text{Ni}(\text{12aneN}_4)]^{2+}$ system are now considered. Initially a 0.0498 molal aqueous solution of $[\text{Ni}(\text{12aneN}_4)](\text{ClO}_4)_2$ using pure water as reference was studied for shift and line broadening measurements of the water resonance (H_2^{17}O) at 11.5 MHz within the temperature range 273.2 - 363.2K. Later on, 0.0498 molal $[\text{Ni}(\text{12aneN}_4)](\text{ClO}_4)_2$ in aqueous 3.0 mol dm^{-3} LiClO_4 solution using aqueous 3.0 mol dm^{-3} LiClO_4 as reference was studied for extensive measurements at 5.748, 11.493 and 13.199 MHz over the temperature range 253.2 - 363.2K. These data are plotted in

Figure 4.5. A decrease in shift with an increase of temperature indicates a parallel increase of the concentration of the low-spin species $[\text{Ni}(\text{12aneN}_4)]^{2+}$. The magnitude of the high temperature shift indicated the paramagnetic species contained two rapidly exchanging water molecules i.e. $[\text{Ni}(\text{12aneN}_4)(\text{OH}_2)_2]^{2+}$ as is discussed later. Equations 4.10 and 4.11 were used to calculate T_{2p}^* and Q respectively using shift and broadening measurement data.

$$\frac{1}{T_{2p}^*} = \frac{1}{T_{2p}} - \frac{1}{T_{2o}} = \frac{2\pi\Delta W \cdot 55.5}{m} \quad 4.10$$

$$Q = T \cdot \frac{\Delta f}{f_o} \cdot \frac{55.5}{m} \quad 4.11$$

where ΔW = increase in half width (in Hz) at half maximum amplitude of the water resonance of $[\text{Ni}(\text{12aneN}_4)](\text{ClO}_4)_2$ solution relative to that of the reference.

m = Molal concentration of $[\text{Ni}(\text{12aneN}_4)](\text{ClO}_4)_2$

T = absolute temperature

Δf = shift

f_o = spectrometer frequency

If the magnetic moment of $[\text{Ni}(\text{12aneN}_4)(\text{OH}_2)_2]^{2+}$ (paramagnetic) obeys Curie's law¹ and a single species is present in solution, Q should become independent of temperature and thus reach a limiting value Q_{lim}^o in the n.m.r. fast exchange limit (for example $Q_{lim}^o = 24$ for $[\text{Ni}(\text{OH}_2)_6]^{2+}$ solutions which exhibit this behaviour³⁵). The actual Q_{lim} value is given by the equation 4.12.

$$Q_{lim} = \chi_p Q_{lim}^o \quad 4.12$$

where χ_p = mol fraction of $[\text{Ni}(\text{12aneN}_4)](\text{OH}_2)_2^{2+}$ species (paramagnetic) present assuming the diamagnetic $[\text{Ni}(\text{12aneN}_4)]^{2+}$ species neither shifts nor broadens the water resonance.

Figure 4.5

Oxygen-17 n.m.r. data obtained in 3.00 mol dm^{-3} at 5.75, 11.5 and 13.2 MHz are shown as squares, circles and triangles respectively, and that obtained in absence of LiClO_4 at 11.5 MHz are shown as inverted triangles. The upper and lower sets of solid curves are respectively the simultaneous non-linear least squares best fits of the line broadening, T_{2p}^* , and shift, Q , data obtained in 3.00 mol dm^{-3} aqueous LiClO_4 solution to equations 4.14 and 4.15.

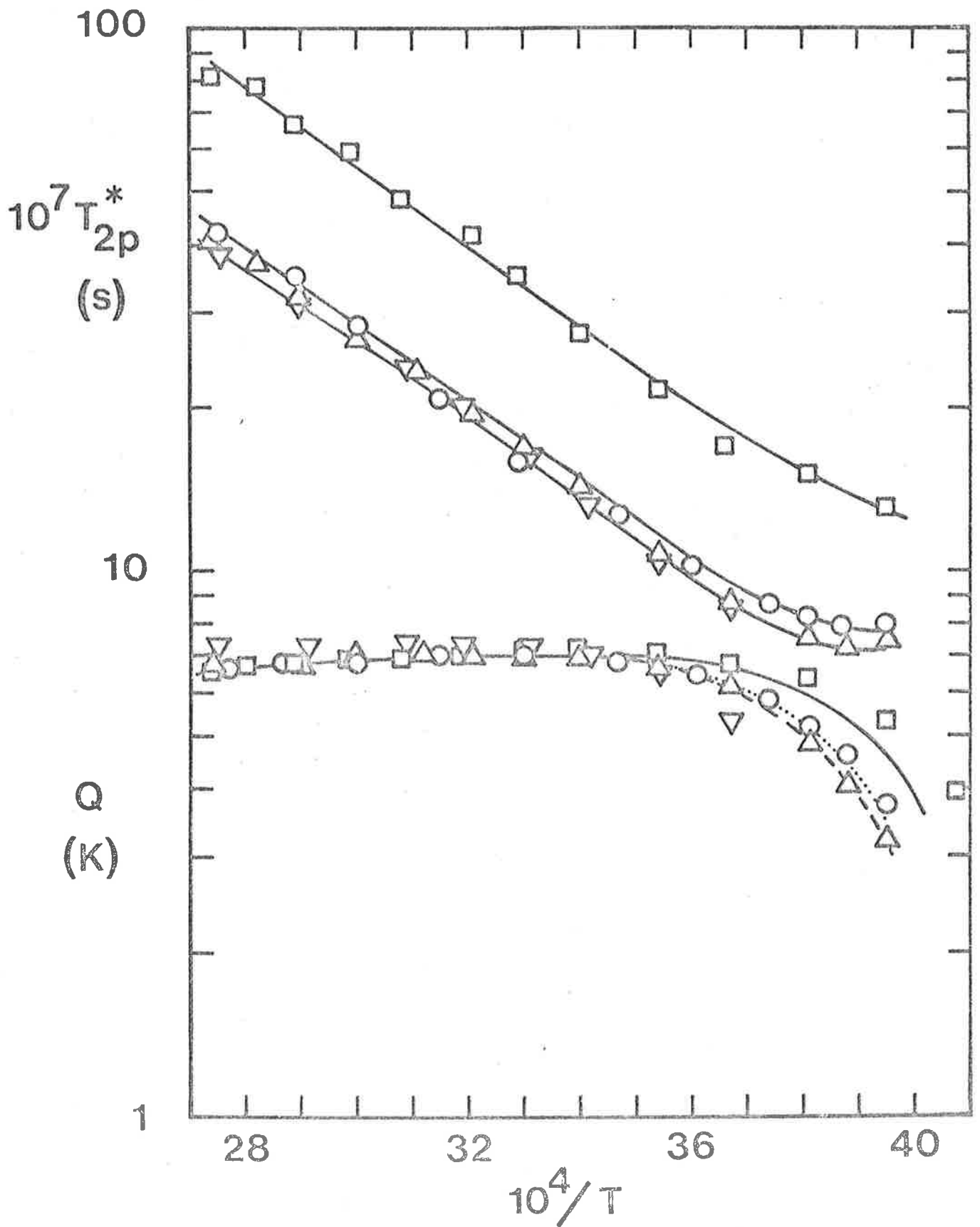


Figure 4.5

Equations 4.1 and 4.12 give

$$K_{eq} = \frac{Q_{lim}^{\circ} - Q_{lim}}{Q_{lim}} = \frac{\text{diamagnetic}}{\text{paramagnetic}} \quad 4.13$$

knowing Q_{lim}° , K_{eq} may be obtained from 4.13 using the high temperature shift measurements. It is not possible to get precise value of Q_{lim}° from the n.m.r. data alone but K_{eq} calculated with $Q_{lim}^{\circ} = 7.5$ for the aqueous $3.0 \text{ mol dm}^{-3} \text{ LiClO}_4$ solution is in excellent agreement with the spectrophotometrically determined K_{eq} values (Figure 4.2 and Table 4.2) and is also consistent with the maximum value of $Q_{lim} = 7.38$ obtained for aqueous $[\text{Ni}(\text{12aneN}_4)](\text{ClO}_4)_2$ solutions (no added LiClO_4) in which the spectrophotometric data shows the diamagnetic species fraction to be very small. The spectrophotometrically determined K_{eq} , H° and S° obtained in aqueous $3.0 \text{ mol dm}^{-3} \text{ LiClO}_4$ and $Q_{lim}^{\circ} = 7.5$ were used in the fitting of the T_{2p}^* and Q data to the Swift and Connick equations³⁶ 4.14 and 4.15

$$\frac{1}{T_{2p}^*} = \chi_p \cdot \frac{n}{\tau_M} \frac{\left[\frac{1}{T_{2M}^2} + \frac{1}{T_{2M}\tau_M} + \Delta\omega_M^2 \right]}{\left[\left(\frac{1}{T_{2M}} + \frac{1}{\tau_M} \right)^2 + \Delta\omega_M^2 \right]} \quad 4.14$$

$$Q = \chi_p \left\{ \frac{n(T\Delta\omega_M / \omega_o)}{\tau_M^2 \left[\left(\frac{1}{T_{2M}} + \frac{1}{\tau_m} \right)^2 + \Delta\omega_M^2 \right]} + Q_o \right\} \quad 4.15$$

using the Dye and Nicely³⁷ non-linear least squares program.

In equation 4.14 and 4.15,

n = number of co-ordinated water molecules of the complex which is set equal to two on the basis of A/h as is discussed later.

T_{2M} = ^{17}O transverse relaxation time of co-ordinated water in the complex.

τ_M = mean lifetime of one co-ordinated water molecule in the complex.

$\Delta\omega_M$ = frequency shift (radians/sec) between the ^{17}O resonances of co-ordinated water in the complex and in the bulk solvent.

Q_o = portion of Q_{lim}^o arising from interactions outside the first co-ordination sphere.

The following relevant equations are also used in the various derivations:-

$$\chi_p = 1/(1 + K_{eq}) \quad 4.16$$

$$\tau_M = \frac{h}{k_B T} e^{-\Delta S^\ddagger/R} e^{-\Delta H^\ddagger/RT} \quad 4.17$$

$$\frac{nT\Delta\omega_M}{\omega_o} = Q_{lim}^o - Q_o \quad 4.18$$

$$T_{2M} = T_{2M}^o e^{E(X-X_o)/R} + \frac{T_{2M}'}{f_o^2} e^{E'(X-X_o)/R} \quad 4.19$$

$$(X = 10^3/T \text{ and } X_o = 10^3/298.2)$$

Equation 4.16 is derived from equilibrium (4.1) and equation 4.17 in which ΔH^\ddagger and ΔS^\ddagger are the enthalpy and entropy of activation for the exchange of a single water molecule in the first co-ordination sphere.

Equation 4.18 arises from considering the high temperature limit of equation 4.15. Equation 4.19, a phenomenological equation, is constructed to give a frequency and temperature dependence of T_{2M} as required by the data. Initial attempts to fit the data indicated that an equation for T_{2M} based on an impact or rotationally modulated zero field splitting³⁸ alone was not adequate. Equation 4.19 may be arrived at by considering a combination of rotationally modulated zero field splitting and an anisotropic 'g' tensor as sources of electron spin relaxation in the system but in the data treatment it is simply used as an empirical equation (the kinetic data are little affected in any case).

The parameters allowed to vary in the final fitting of the shift and line broadening data to equations 4.14 and 4.15 were ΔH^\ddagger , ΔS^\ddagger , T_{2M}^0 , T'_{2M} , E and E' . Since the shift data do not extend significantly into the water exchange controlled region (where τ_M is dominant in determining the magnitude of Q) where Q_0 becomes important, a value of 0.3 was assigned to Q_0 on the basis of previous observations on nickel (II).³⁵ The parameters with standard deviations derived from the data fitting appear in Table 4.6 and the best fit computed curves appear in Figure 4.5.

TABLE 4.6
Kinetic and ^{17}O n.m.r. Parameters for Water Exchange on Nickel (II) Species.

Species	$[\text{Ni}(\text{12aneN}_4)(\text{OH}_2)_2]^{2+}$	$[\text{Ni}(\text{OH}_2)_6]^{2+}$ a	$[\text{Ni}(\text{trien})(\text{OH}_2)_2]^{2+}$ b
τ_M (298.2K)s	$(4.76 \pm 0.39) \times 10^{-8}$	3.18×10^{-5}	1.75×10^{-6}
$k_{\text{H}_2\text{O}}$ (298.2K)s ⁻¹	$(2.10 \pm 0.17) \times 10^7$	3.14×10^4	5.7×10^5
ΔH^\ddagger kJ mol ⁻¹	32.7 ± 1.1	56.9	34.4
ΔS^\ddagger JK ⁻¹ mol ⁻¹	5.0 ± 4.6	32.1	-19.2
T_{2M}^0 S	$(2.56 \pm 0.08) \times 10^{-6}$		
E kJ mol ⁻¹	-9.04 ± 0.54	-	-
T'_{2M} S kHz ²	119 ± 6	-	-
E' kJ mol ⁻¹	-14.2 ± 1.4	-	-
A/h MHz	23.2	22.2	22.5

a Data from reference 35

b Data from reference 39

N.B. The errors represent one standard deviation.

The value of the scalar coupling constant (A/h) was calculated from equation 4.18 and $\Delta\omega_M = \frac{S(S+1)}{3k_B T} \left(\frac{A}{h}\right) h \omega_S$ where S is the

summed unpaired electron spin, k_B is Boltzmann's constant and ω_S is the electronic Larmor precession frequency. The value of A/h calculated in this way is close to that observed^{35,39} (Table 4.6) for $[\text{Ni}(\text{OH}_2)_6]^{2+}$ and $[\text{Ni}(\text{trien})(\text{OH}_2)_2]^{2+}$ systems. The value of A/h found and the assumption⁴⁰ that A/h per water is not significantly dependent upon the composition of the first co-ordination sphere suggest that two water molecules are co-ordinated per nickel (II) consistent with the stoichiometry $[\text{Ni}(\text{12aneN}_4)(\text{OH}_2)_2]^{2+}$. The Q and T_{2p}^* data for aqueous solution (no added LiClO_4) were not fitted but the proximity of these data to those for aqueous $3.0 \text{ mol dm}^{-3} \text{ LiClO}_4$ solution suggest that $\tau_{\text{H}_2\text{O}}$ is probably not markedly dependent upon electrolyte concentrations. The different τ values derived from the temperature jump data are $>10^2 \tau_M$, the lifetime of a water molecule in $[\text{Ni}(\text{12aneN}_4)(\text{OH}_2)_2]^{2+}$, derived from the ^{17}O n.m.r. data (Table 4.6) (τ characterises the equilibrium between $[\text{Ni}(\text{12aneN}_4)]^{2+}$ and $[\text{Ni}(\text{12aneN}_4)(\text{OH}_2)_2]^{2+}$ as shown in equation 4.1). Under these conditions τ is related^{9,41} to the rate constants of equation 4.1 through equation 4.20

$$\begin{aligned} 1/\tau &= k_1[\text{H}_2\text{O}](1 + k_{-1}k_{-2}/(k_1k_2[\text{H}_2\text{O}]^2)) & 4.20 \\ &= k_1[\text{H}_2\text{O}](1 + k_{\text{eq}}) \end{aligned}$$

In aqueous $3.0 \text{ mol dm}^{-3} \text{ LiClO}_4$ solution at 298.8K,

$$\begin{aligned} \frac{1}{\tau} &= k_1[\text{H}_2\text{O}]\left(1 + \frac{k_{-1}k_{-2}}{k_1k_2[\text{H}_2\text{O}]^2}\right) = 3.028 \times 10^5 \text{ s}^{-1} \\ \left(\frac{k_{-1}k_{-2}}{k_1k_2[\text{H}_2\text{O}]^2}\right) &= \frac{[\text{NiL}^{2+}]}{[\text{NiL}(\text{OH}_2)_2]^{2+}} = 0.0493 \end{aligned}$$

Hence $k_1 = (5.94 \pm 0.13)10^3 \text{ mol}^{-1} \text{ dm}^3 \text{ s}^{-1}$ and utilizing $k_{-2} = 2k_{\text{H}_2\text{O}}$ (Table 4.6) $k_{-1}/k_2 = 0.016 \text{ mol dm}^{-3}$. At 298.8K, $\tau = (3.30 \pm 0.07)10^{-6} \text{ s}$ (Temperature jump) and $\tau_{\text{H}_2\text{O}} = \frac{1}{k_{\text{H}_2\text{O}}} = 4.7 \times 10^{-8} \text{ s}$ (^{17}O n.m.r.) in aqueous $3.0 \text{ mol dm}^{-3} \text{ LiClO}_4$ solution.

A comparison of $k_{\text{H}_2\text{O}}$ and τ values confirms that the release of water from $[\text{Ni}(\text{12aneN}_4)(\text{OH}_2)_2]^{2+}$ is not the rate determining step in the high-spin low-spin equilibrium and that τ characterising the relatively slow equilibrium between four and five co-ordinate species in equation 4.1 is the rate determining step i.e. k_1/k_{-1} is slower than k_2/k_{-2} .

Both the ^{17}O n.m.r. and spectrophotometric data indicate that the five co-ordinate species, $[\text{Ni}(\text{12aneN}_4)(\text{OH}_2)]^{2+}$, is unlikely to exist at a concentration of more than a few percent of the total nickel (II) concentration which is the basis of discussions appearing at the end of this chapter.

4.3.1 The $[\text{Ni}(\text{Me}_4\text{12aneN}_4)](\text{ClO}_4)_2$ System:-

Substitution on the nitrogen atoms of polyamine ligands has been shown to have a major effect on the molecular geometry; the stoichiometry, and the electronic configuration of nickel (II) complexes.^{42, 43} Depending upon the type of organic groups on the donor atoms and the counter anions, square planar, octahedral and tetrahedral geometries have been observed for nickel (II) complexes. The $[\text{Ni}(\text{Me}_4\text{12aneN}_4)](\text{ClO}_4)_2$ complex has been prepared for the first time to study its solution characteristics and it is probable that, due to the methyl group substituted on the nitrogen atoms, steric hindrance around the nickel (II) allows only a five co-ordinate geometry for the aquo species, $[\text{Ni}(\text{Me}_4\text{12aneN}_4)(\text{OH}_2)]^{2+}$, formed in aqueous solution.

4.3.2 Magnetic Moment Measurements by the Gouy Method:-

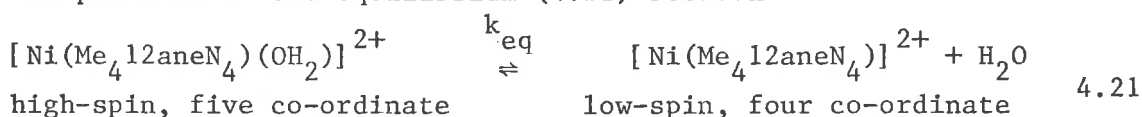
In both the solid state and the nitromethane solution $[\text{Ni}(\text{Me}_4\text{12aneN}_4)](\text{ClO}_4)_2$ was found to be diamagnetic using the Gouy method,³⁰ implying that the same species exists in the solid state

and in the nitromethane solution (i.e. $[\text{Ni}(\text{Me}_4\text{12aneN}_4)]^{2+}$).

4.3.3 The Temperature and Ionic Strength Dependence of Equilibrium Constants:-

The $[\text{Ni}(\text{Me}_4\text{12aneN}_4)](\text{ClO}_4)_2$ species dissolves in water to give a mixture of four co-ordinate and five co-ordinate species. The colour of the aqueous solution is yellow and its electronic spectrum is typical of a five co-ordinate high spin species⁴⁴ (Figure 4.6).

The position of the equilibrium (4.21) between



the high-spin and the low-spin species is markedly ionic strength and temperature (Figure 4.6) dependent. The high values of these two experimental variables favour the low-spin species. The band at 455nm shows a progressive increase in intensity in the spectra at 291.7, 303.8, 314.9, 324.4 and 340.1K respectively as seen in Figure 4.6. The isosbestic points (400nm and 578nm) observed in the spectra are consistent with two predominant species existing in solution:- low-spin $[\text{Ni}(\text{Me}_4\text{12aneN}_4)]^{2+}$ and high-spin $[\text{Ni}(\text{Me}_4\text{12aneN}_4)(\text{OH}_2)]^{2+}$ species. At 291.7K, 46.6% low-spin and 53.4% high-spin species co-exist at equilibrium and this changes to 57.0% low-spin and 43.0% high-spin species at 340.1K. The effect of ionic strength on the equilibrium (4.21) was also studied at different temperatures. As in aqueous solution, aqueous 0.25 and 0.50 mol dm⁻³ LiClO₄ solutions of $[\text{Ni}(\text{Me}_4\text{12aneN}_4)](\text{ClO}_4)_2$ have similar spectra which are typical of five co-ordinate species. In all these solutions, isosbestic points occur at the same wavelengths (400 and 578nm). In aqueous 1.0 mol dm⁻³ LiClO₄ solution the absorbance change with temperature is very small and isosbestic points occur at 392 and 526nm. It was observed that the band at 455nm decreases in amplitude with a simultaneous slight increase

Figure 4.6

Temperature dependent uv/visible spectra of $4.08 \times 10^{-3} \text{ mol dm}^{-3}$ $[\text{Ni}(\text{Me}_4\text{12aneN}_4)](\text{ClO}_4)_2$ (ethanol water preparation) in water. The band at 455 nm shows a progressive increase in intensity in the spectra recorded at 291.7, 303.8, 314.9, 324.4 and 340.1 K respectively.

Molar Extinction Coefficient

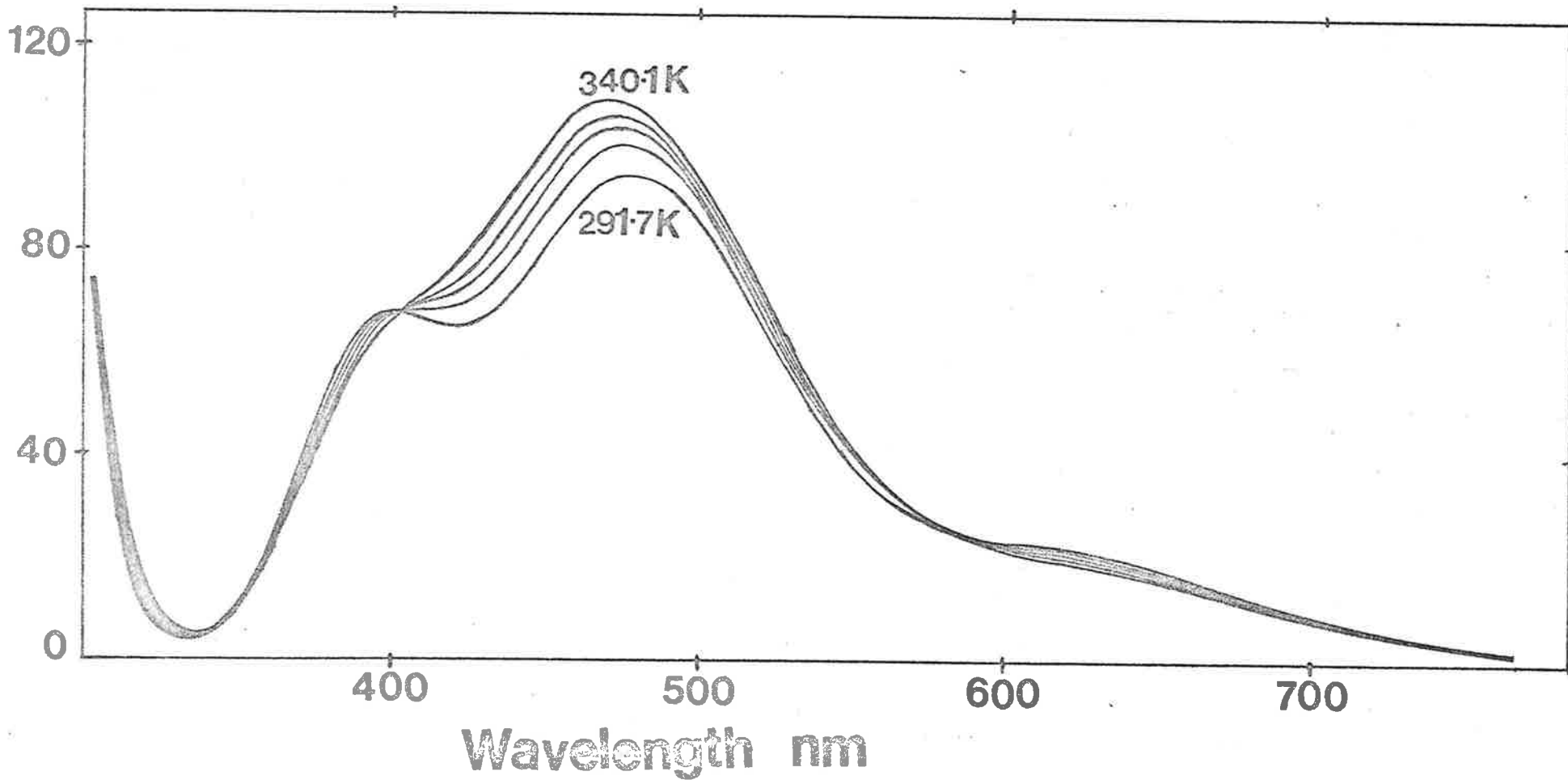


Figure 4.6

at 370 and 570nm as the temperature increases for aqueous 2.0, 3.0 and 4.0 mol dm⁻³ LiClO₄ solution (Figure 4.7). However, the two isosbestic points (426 and 512nm for 2.0 mol dm⁻³, 416 and 506nm for 3.0 mol dm⁻³, 416 and 502nm for 4.0 mol dm⁻³ LiClO₄ solution) indicate the existence of two predominant species in each solution. The different wavelengths of the isosbestic points observed in these solutions indicate, however, that the predominant species are not the same. Since high ionic strength favours the square planar species over the five co-ordinate species, a possible explanation of the spectra observed in 2.0 - 4.0 mol dm⁻³ LiClO₄ solution is that these spectra are predominantly due to square planar species and that the possible isomeric equilibrium between such species is ionic strength dependent. In principle, four such isomers may arise: (i) four methyl groups on the same side of the ring, (ii) three methyl groups on the same side, (iii) two methyl groups on either side (cis) and (iv) two methyl groups on either side (trans). The available data cannot be used to distinguish between these possibilities, but the structure of [Ni(Me₄12aneN₄)N₃] ClO₄ in which four methyl groups are on the same side of the ring (see Chapter 3) suggests that this is a probable stereochemistry for one of the square planar species in solution. (The [Ni(Me₄14aneN₄)](ClO₄)₂ complex may exist as one of the two square planar isomers (boat, R.S.R.S. and chair, R.S.S.R.) discussed in the literature.^{45,46}) The possibility of a variation in the position of the chair/boat conformational equilibrium for each N.CH₂.CH₂.N segment with ionic strength also exists. (A similar variation in the spectral temperature behaviour with variation in ionic strength is also observed with the [Ni(Me₄14aneN₄)](ClO₄)₂ system (Section 4.6.3)). The limiting spectrum of the pure square

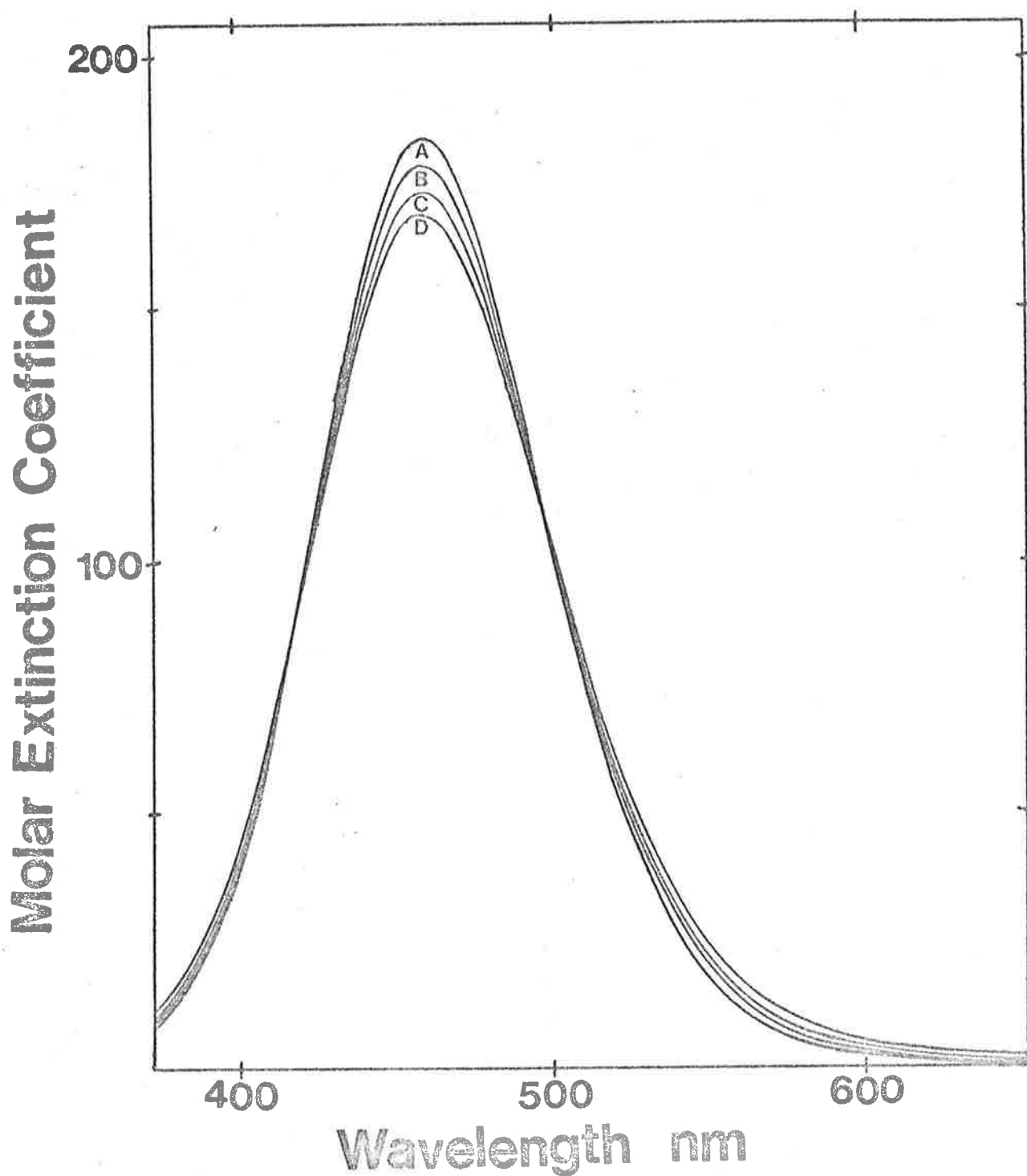


Figure 4.7

Temperature dependent uv/visible spectra of $4.12 \times 10^{-3} \text{ mol dm}^{-3}$

$[\text{Ni}(\text{Me}_4\text{12aneN}_4)](\text{ClO}_4)_2$ (ethanol water preparation) in aqueous 4.0 mol dm^{-3}

LiClO_4 solution. Temperatures are 290.5, 307.1 324.9 and 343.4 K for the spectra from A to D respectively.

planar species was recorded in dry nitromethane solution from which the molar extinction co-efficient was calculated to be $184.4 \text{ mol}^{-1} \text{ dm}^3 \text{ cm}^{-1}$ at 455nm. Using this extinction co-efficient for the square planar species, (and assuming that it is characteristic of the square planar species in aqueous solution) the equilibrium constants, $K_{\text{eq}}, \left(\frac{[\text{low spin}]}{[\text{high spin}]} \right)$ were calculated from the following equation¹⁴ at 455nm.

$$K_{\text{eq}} = \frac{\epsilon}{\epsilon_{\text{sq}} - \epsilon} \quad 4.22$$

where ϵ = experimental extinction co-efficient

ϵ_{sq} = extinction co-efficient of the square planar species

(assuming zero extinction co-efficient of the high spin species)

The K_{eq} values at different temperatures are given in Table 4.7.

The enthalpy, ΔH° and the entropy, ΔS° for the equilibrium (4.21) are determined by a least squares analysis of the K_{eq} data according to equation 4.5. The H° and S° values for different LiClO_4 concentrations are given in Table 4.8. No equilibrium calculation were carried out on the data from the 2.0, 3.0 and 4.0 mol dm^{-3} LiClO_4 solutions.

4.3.4 The Temperature Jump Kinetic Study:

The high-spin low-spin interconversion rate was studied by the temperature jump experiments at 455nm. A single relaxation process was observed in aqueous 0.25 and 0.50 mol dm^{-3} LiClO_4 solution. In aqueous 0.25 mol dm^{-3} LiClO_4 solution at 287.5K, the relaxation time was found to be $(4.60 \pm 0.27) \times 10^{-6} \text{ s}$ and $(5.70 \pm 0.34) \times 10^{-6} \text{ s}$ using 2.53×10^{-3} and $4.10 \times 10^{-3} \text{ mol dm}^{-3}$ $[\text{Ni}(\text{Me}_4\text{12aneN}_4)](\text{ClO}_4)_2$ solution respectively. This indicates that within experimental error the relaxation time is independent of complex concentration. As the ionic strength increases the relaxation time decreases as demonstrated

TABLE 4.7
 K_{eq} Values for the $[\text{Ni}(\text{Me}_4\text{12aneN}_4)](\text{ClO}_4)_2$ System

$\frac{1}{T} \times 10^4$	$a_{K_{eq}}$	$\frac{1}{T} \times 10^4$	$a_{K_{eq}}$
1. $[\text{LiClO}_4] = 0.0 \text{ mol dm}^{-3}$		3. $[\text{LiClO}_4] = 0.50 \text{ mol dm}^{-3}$	
34.28	0.85 ± 0.04	34.34	1.60 ± 0.09
32.91	1.0 ± 0.05	32.77	1.75 ± 0.08
31.75	1.1 ± 0.06	30.73	1.90 ± 0.09
30.82	1.2 ± 0.05	29.09	1.95 ± 0.08
29.40	1.3 ± 0.06		
2. $[\text{LiClO}_4] = 0.25 \text{ mol dm}^{-3}$			
34.34	1.25 ± 0.05		
32.89	1.4 ± 0.08		
31.45	1.5 ± 0.08		
30.37	1.6 ± 0.08		
29.16	1.7 ± 0.08		

TABLE 4.8
 ΔH° and ΔS° Value for $[\text{Ni}(\text{Me}_4\text{12aneN}_4)](\text{ClO}_4)_2$ System

$[\text{LiClO}_4]$ mol dm^{-3}	$b_{\Delta H^\circ}$ J mol^{-1}	$b_{\Delta S^\circ}$ $\text{JK}^{-1} \text{ mol}^{-1}$
0.0	7.17 ± 0.42	23.56 ± 1.33
0.25	4.71 ± 0.25	18.12 ± 0.81
0.50	3.29 ± 0.38	15.33 ± 1.20

The errors represent

a Estimated error

b One standard deviation.

by the determination of the relaxation time $((2.0 \pm 0.1) \times 10^{-6} \text{ s})$ in aqueous $0.50 \text{ mol dm}^{-3} \text{ LiClO}_4$ solution at 287.5K. However, two processes were observed in aqueous $2.0 \text{ mol dm}^{-3} \text{ LiClO}_4$ solution, the fast process is as fast as the heating time of the solution and the half life of the slower process was found to be roughly 75 μs . Because of the two processes and the small absorbance changes, the system was not studied to a great extent. However, no other relaxation was observed at a longer time scale.

4.4.1 The $[\text{Ni}(\text{tbl2aneN}_4)\text{Cl}]\text{Cl}$ and $[\text{Ni}(\text{tbl2aneN}_4)\text{NO}_3]\text{NO}_3$ Systems:-

Both $[\text{Ni}(\text{tbl2aneN}_4)\text{Cl}]\text{Cl}$ and $[\text{Ni}(\text{tbl2aneN}_4)(\text{NO}_3)](\text{NO}_3)$ complexes were prepared^{29,47} to study their solution characteristics. The solid state magnetic moment of $[\text{Ni}(\text{tbl2aneN}_4)\text{Cl}]\text{Cl}$, 3.7B.M.^{47,48} is too large for nickel (II) to exist in an octahedral configuration. It was concluded²⁹ that the large benzyl groups on the tbl2aneN_4 give rise to the five co-ordinate geometry of the $[\text{Ni}(\text{tbl2aneN}_4)(\text{OH}_2)]^{2+}$ species in aqueous solution.

4.4.2 The Temperature Dependence of UV/Visible Spectral Change:-

The $[\text{Ni}(\text{tbl2aneN}_4)\text{Cl}]\text{Cl}$ species is green while the $[\text{Ni}(\text{tbl2aneN}_4)\text{NO}_3]\text{NO}_3$ species is yellowish. Aqueous and nitromethane solution of both complexes are brown and yellow respectively. If a very small amount of inert electrolyte (LiClO_4 or NaClO_4) is added to the aqueous solution of these two complexes precipitation occurs immediately. The visible spectra of the two complexes are shown in Figure 4.8 and Figure 4.9. Qualitatively, an increase in temperature increases the intensity of the band at 476nm with a simultaneous decrease in amplitude of the bands at 400nm and 625nm (Figure 4.8 and Figure 4.9) in case of both complexes. A possible explanation for the temperature dependence of uv/visible

Molar Extinction Coefficient

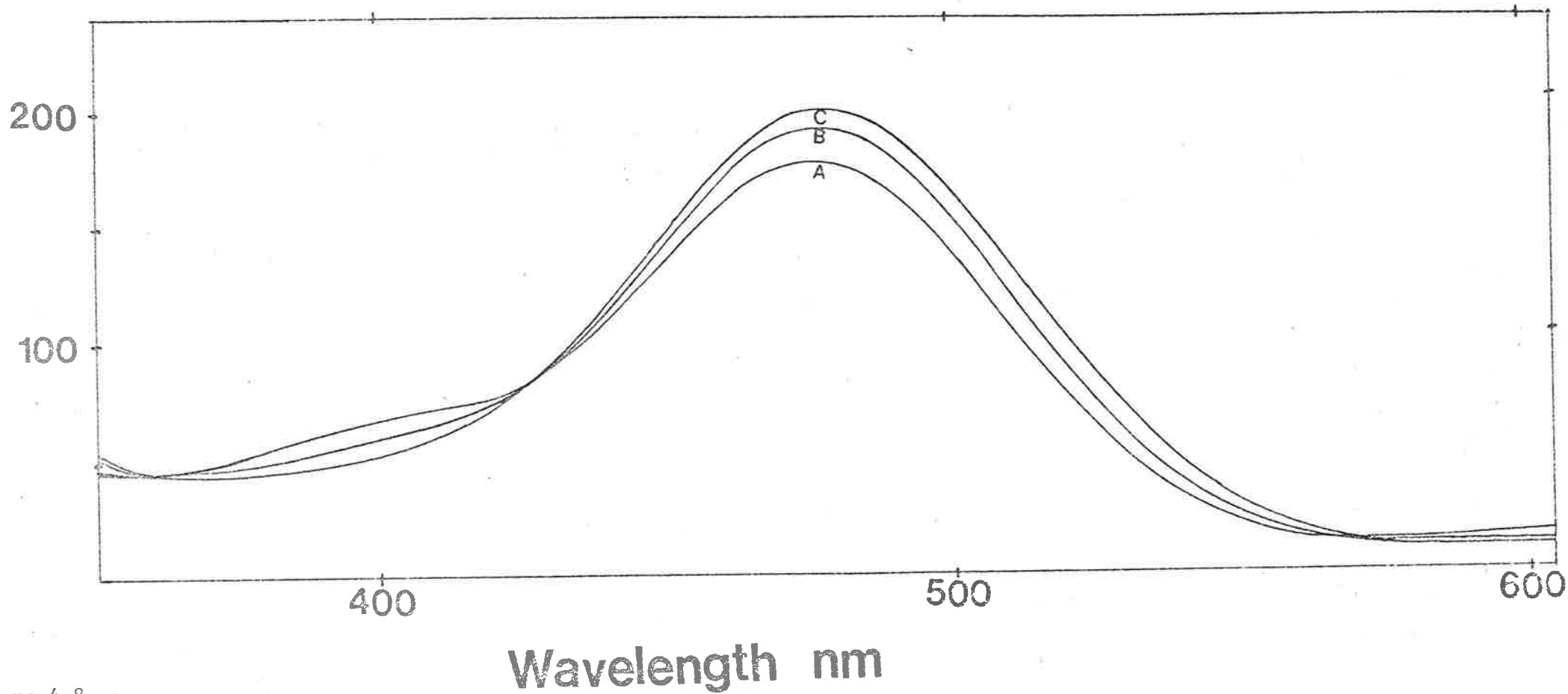


Figure 4.8

Temperature dependent uv/visible spectra of $9.82 \times 10^{-4} \text{ mol dm}^{-3}$ $[\text{Ni}(\text{tb}12\text{aneN}_4)\text{Cl}]\text{Cl}$ in water. Temperatures are 292.7, 312.3 and 340.1 K for the spectra from A to C respectively.

Figure 4.9

Temperature dependent uv/visible spectra of $1.15 \times 10^{-3} \text{ mol dm}^{-3}$ $[\text{Ni}(\text{tbi2aneN}_4)\text{NO}_3]\text{NO}_3$ in water. Temperatures are 294.0, 311.8 and 340.1 K for the spectra from A to C respectively.

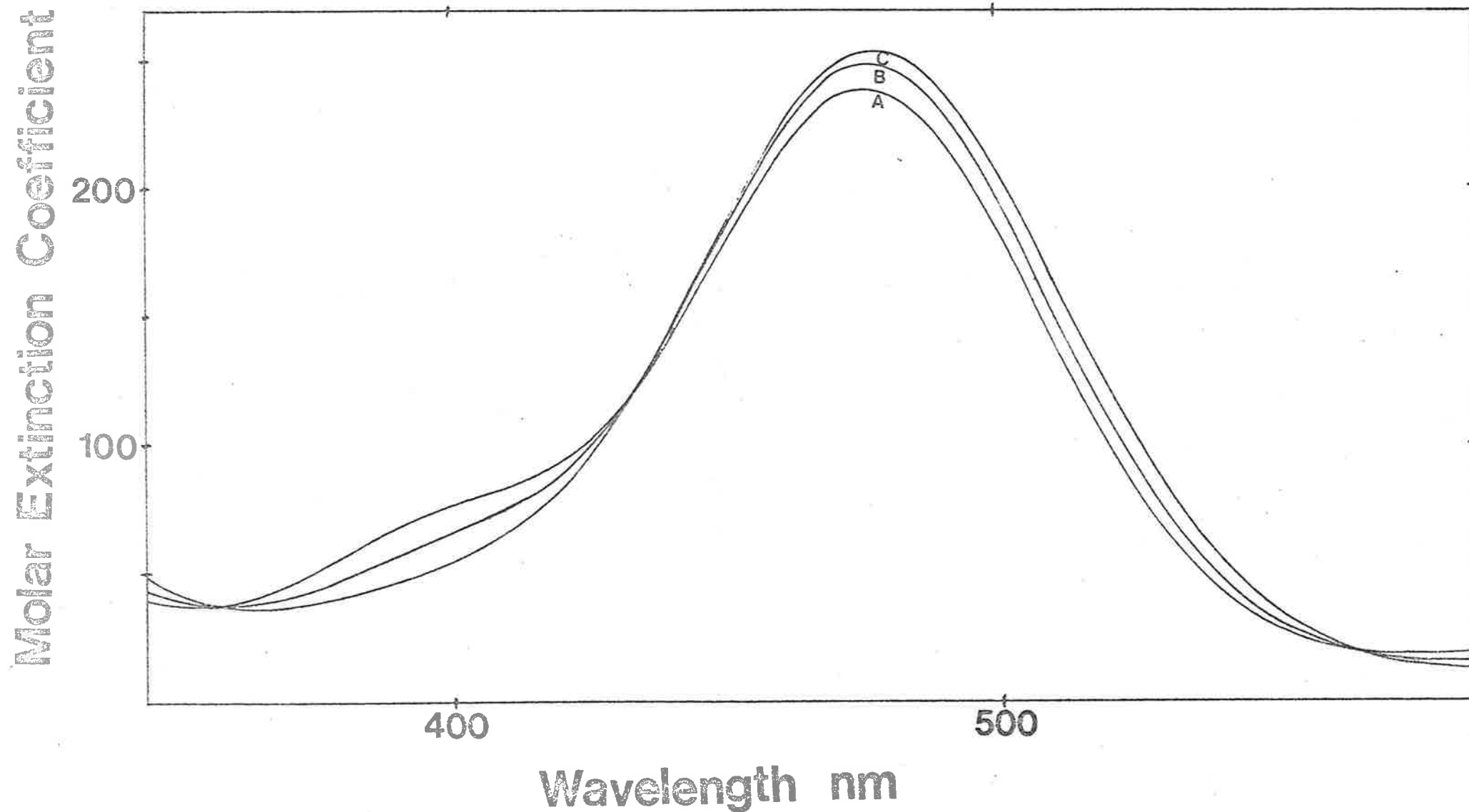


Figure 4.9

spectra may be that there exists either a spin-equilibrium or an equilibrium between the species $[\text{Ni}(\text{tbl2aneN}_4)\text{Cl}]^+$ (or $[\text{Ni}(\text{tbl2aneN}_4)\text{NO}_3]^+$) and $[\text{Ni}(\text{tbl2aneN}_4)(\text{OH}_2)]^{2+}$ which is temperature dependent in aqueous solution. The molar extinction co-efficients at 476 nm were found to be 200.1 and 254.0 $\text{mol}^{-1} \text{dm}^3 \text{cm}^{-1}$ for the dichloro and dinitro species respectively in aqueous solution at 340.1K. In nitromethane solution, the molar extinction co-efficients at a fixed temperature and at a particular wavelength are also different for the two complexes (two bands are observed in each case). The molar extinction co-efficients (at two bands) are 256.9 $\text{mol}^{-1} \text{dm}^3 \text{cm}^{-1}$ at 437 nm, 88.9 $\text{mol}^{-1} \text{dm}^3 \text{cm}^{-1}$ at 710 nm for the dichloro and 70.9 $\text{mol}^{-1} \text{dm}^3 \text{cm}^{-1}$ at 384 nm, 39.4 $\text{mol}^{-1} \text{dm}^3 \text{cm}^{-1}$ at 610 nm for the dinitro complexes in nitromethane solution at 293.2K. Solution magnetic moment measurements were not feasible because of the low solubility of the complexes in water. The temperature jump spectrophotometric study (discharge type) was not possible as the complexes precipitate out on addition of inert electrolyte in aqueous solution.

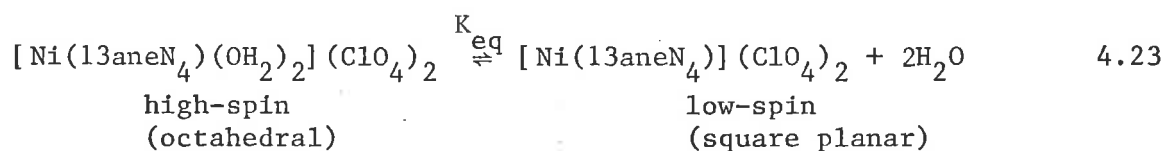
4.5.1 The $[\text{Ni}(\text{13aneN}_4)](\text{ClO}_4)_2$ System:-

The $[\text{Ni}(\text{13aneN}_4)](\text{ClO}_4)_2$ complex dissolves in water, nitromethane, nitroethane, nitrobenzene, pyridine, acetonitrile and formaldehyde giving yellow solution but is insoluble in CH_2Cl_2 , cyclohexane and chlorobenzene. In aqueous solution, the cis-stereochemistry of the high-spin $[\text{Ni}(\text{13aneN}_4)(\text{H}_2\text{O})_2]^{2+}$ species may be explained³³ in a similar way to the $[\text{Ni}(\text{12aneN}_4)(\text{H}_2\text{O})_2]^{2+}$ species. Since the macrocyclic hole of the 13aneN₄ ligand is slightly bigger than that of 12aneN₄ and the ionic radius of low-spin nickel (II) is slightly smaller than that of high-spin nickel (II), coplanarity of nickel (II) and four

nitrogen atoms in low-spin $[\text{Ni}(\text{13aneN}_4)]^{2+}$ is more probable.

4.5.2 The Temperature and Ionic Strength Dependence of Equilibrium Constants:-

The uv/visible spectrum of the $[\text{Ni}(\text{13aneN}_4)(\text{OH}_2)_2]^{2+}$ species is dependent upon temperature (Figure 4.10) and ionic strength as shown by the equilibrium 4.23



An increase of temperature or ionic strength increases the band intensity at 427nm but decreases at 345nm. Three isosbestic points (310, 370 and 535nm) are observed which are consistent with the existence of two predominant species, high-spin and low-spin species of the complex. A recent publication²⁵ reported the solution thermodynamic behaviour of this complex (in aqueous $0.1 \text{ mol dm}^{-3} \text{ NaClO}_4$) after completing the present study independently. The equilibrium constants, K_{eq} , enthalpy, ΔH° and entropy, ΔS° are calculated for the equilibrium (4.23) according to the equations 4.22 and 4.5. The molar extinction co-efficient at 450nm ($71.60 \text{ mol}^{-1} \text{ dm}^3 \text{ cm}^{-1}$) of the square planar species is obtained from the spectrum in nitromethane and the K_{eq} values are calculated at 450nm because the largest absorbance changes occur at this wavelength. The K_{eq} values together with associated ΔH° and ΔS° values are given in Table 4.9. In aqueous solution at 294.8K, there exists 71.2% low-spin and 28.8% high-spin species which changes to 82.1% and 17.9% respectively at 343.2K.

4.5.3 The Temperature Jump Kinetic Study:-

The $[\text{Ni}(\text{13aneN}_4)] (\text{ClO}_4)_2$ complex ($1.72 \times 10^{-2} \text{ mol dm}^{-3}$) in aqueous $2.0 \text{ mol dm}^{-3} \text{ LiClO}_4$ solution was studied by the temperature

Figure 4.10

Temperature dependent uv/visible spectra of $1.72 \times 10^{-2} \text{ mol dm}^{-3}$ $[\text{Ni}(\text{13aneN}_4)](\text{ClO}_4)_2$ in water. Temperatures are 294.8, 308.7, 325.1 and 343.2 K for the spectra from 1 to 4 respectively.

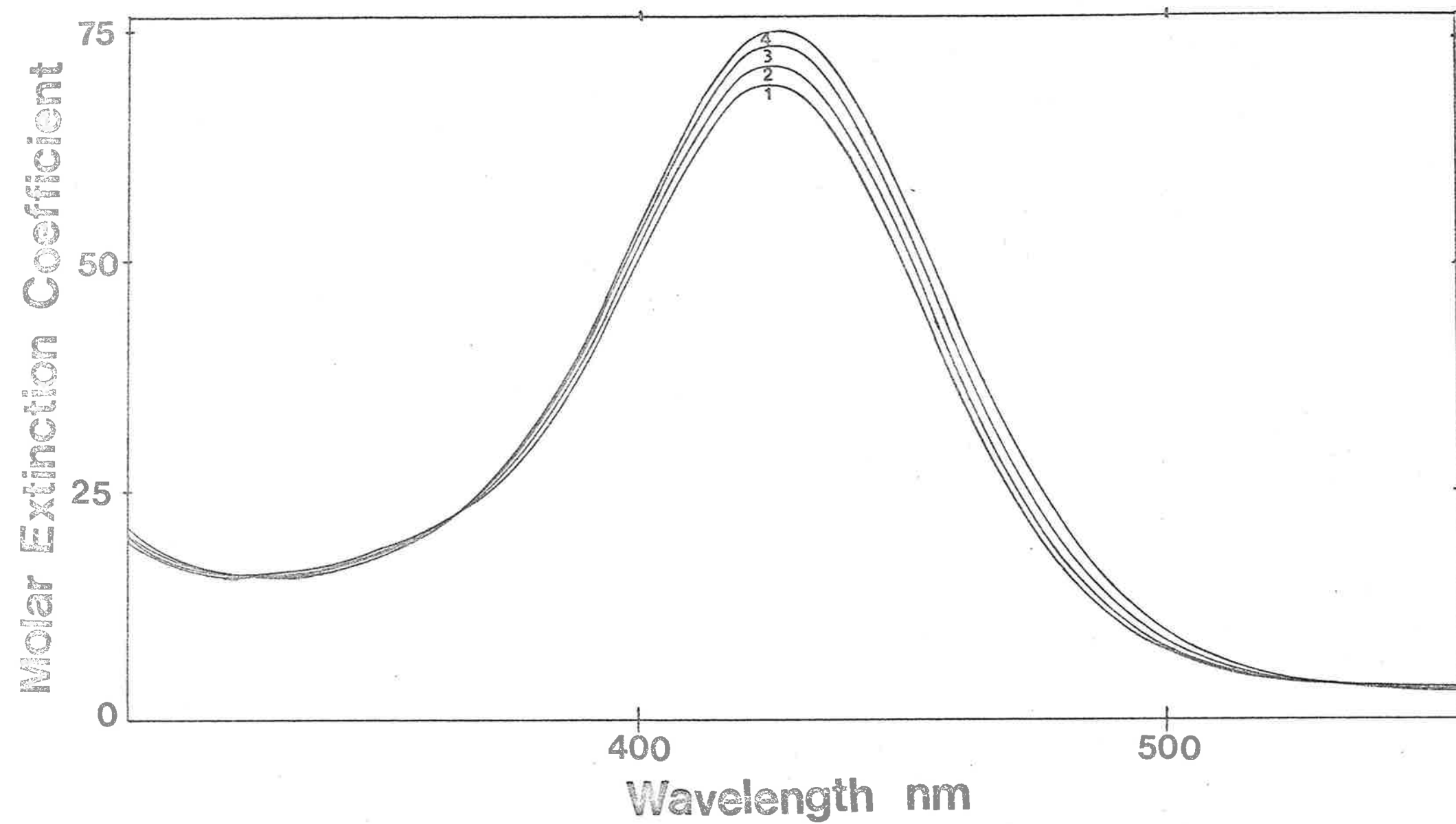


Figure 4.10

TABLE 4.9

K_{eq} , ΔH° and ΔS° Values for the $[Ni(13aneN_4)](ClO_4)_2$ System

$\frac{1}{T} \times 10^4$	${}^a K_{eq}$	b Activation Parameters
1. $[LiClO_4] = 0.0 \text{ mol dm}^{-3}$		
33.92	2.45 ± 0.10	$\Delta H^{\circ} = (10.75 \pm 0.06) \text{ kJ mol}^{-1}$
32.39	3.00 ± 0.15	
30.76	3.70 ± 0.20	$\Delta S^{\circ} = (43.97 \pm 0.12) \text{ JK}^{-1} \text{ mol}^{-1}$
29.14	4.60 ± 0.20	
2. $[LiClO_4] = 2.0 \text{ mol dm}^{-3}$		
33.78	4.55 ± 0.20	$\Delta H^{\circ} = (9.39 \pm 0.98) \text{ kJ mol}^{-1}$
32.72	5.10 ± 0.20	
30.70	6.05 ± 0.30	$\Delta S^{\circ} = (44.09 \pm 3.08) \text{ JK}^{-1} \text{ mol}^{-1}$
29.17	7.70 ± 0.45	
3. $[LiClO_4] = 4.0 \text{ mol dm}^{-3}$		
33.79	17.8 ± 0.80	$\Delta H^{\circ} = (34.65 \pm 10.5) \text{ kJ mol}^{-1}$
32.32	21.2 ± 1.0	
30.79	32.0 ± 1.5	$\Delta S^{\circ} = (138.8 \pm 33.0) \text{ JK}^{-1} \text{ mol}^{-1}$
29.12	133 ± 7.0	

The errors represent

a estimated error

b one standard deviation

jump technique at 286.5K and 450nm. In this system, a spectral change consistent with a shift in the square planar-octahedral equilibrium was observed and the approximate relaxation time (τ) is $0.4\mu\text{s}$ which is similar to the heating time of the solution. No other relaxation was observed at a longer time scale.

4.6.1 The $[Ni(Me_4 14aneN_4)](ClO_4)_2$ System:-

As with the $[Ni(Me_4 12aneN_4)](ClO_4)_2$ case, it is also assumed that due to the methyl groups substituted on the nitrogen atoms, the geometry of the $[Ni(Me_4 14aneN_4)](ClO_4)_2$ complex is five co-ordinate

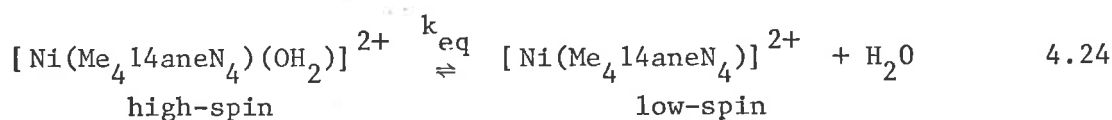
in aqueous solution (i.e. $[\text{Ni}(\text{Me}_4\text{14aneN}_4(\text{OH}_2))]^{2+}$). A recent publication¹⁰ reported the equilibrium studies of this complex in co-ordinating solvents including water (pure water and aqueous $0.2 \text{ mol dm}^{-3} \text{ NaClO}_4$ only) after completing the present study independently.

4.6.2 Magnetic Moment Measurements by the Gouy Method:-

In the solid state and in dry nitromethane solution $[\text{Ni}(\text{Me}_4\text{14aneN}_4)](\text{ClO}_4)_2$ was found to be diamagnetic using the Gouy method³⁰ indicating that the same species (four co-ordinate, square planar) exists in the solid state and in the nitromethane solution.

4.6.3 The Temperature and Ionic Strength Dependence of Equilibrium Constants:-

The equilibrium (4.24) between the high-spin (five co-ordinate, paramagnetic) and low-spin (four co-ordinate, diamagnetic) species has been studied as a function of



temperature and ionic strength. The visible spectrum of the complex in aqueous solution is consistent with the five co-ordinate species (Figure 4.11). With the increase in temperature or ionic strength, the intensity of the band at 514nm increases with simultaneous decrease at 390nm and 650nm as seen in Figure 4.11. The isosbestic points occur at 340, 434 and 596nm. The spectra of the $[\text{Ni}(\text{Me}_4\text{14aneN}_4)(\text{OH}_2)]^{2+}$ species in aqueous 0.5 mol dm^{-3} (isosbestic points at 340, 434, and 602nm) and 1.0 mol dm^{-3} (isosbestic points at 350, 434 and 606nm) LiClO_4 are similar to those in pure water. With aqueous $2.0 \text{ mol dm}^{-3} \text{ LiClO}_4$ solution and increasing temperature

Figure 4.11

Temperature dependent uv/visible spectra of $2.88 \times 10^{-3} \text{ mol dm}^{-3}$ $[\text{Ni}(\text{Me}_4\text{14aneN}_4)](\text{ClO}_4)_2$ (ethanol water preparation) in water. Temperatures are 293.2, 303.8, 313.9, 323.0, 331.1 and 340.1 K for the spectra from 1 to 6 respectively.

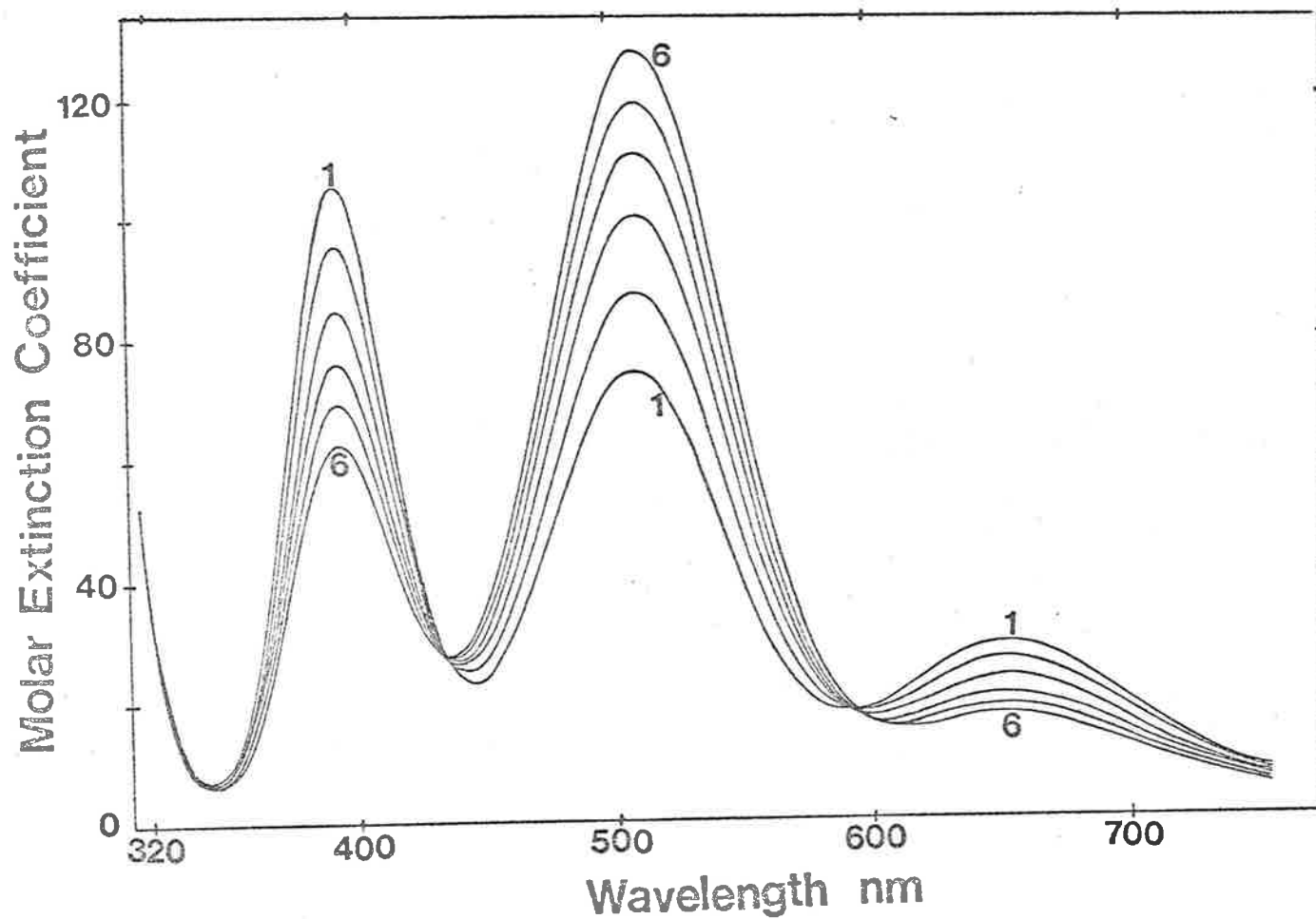


Figure 4.11

the band intensity at 514nm increases up to 307.4K and then starts to decrease. However, with 3.0 and 4.0 mol dm⁻³ LiClO₄ solutions, the band intensity decreases at 514nm as the temperature increases with simultaneous slight increases at 390 and 590nm (Figure 4.12). The two isosbestic points (370 and 532nm for 3.0 mol dm⁻³, 380 and 536nm for 4.0 mol dm⁻³ LiClO₄ solution) indicate the presence of two predominant species in each solution. However, the different wavelengths of the isosbestic points indicate that the predominant species are not the same. Since high ionic strength favours the square planar species over the five co-ordinate species, a possible explanation of the spectra observed in 3.0 - 4.0 mol dm⁻³ LiClO₄ solution is that these spectra are predominantly due to square planar species and that the possible isomeric equilibrium between such species is temperature and ionic strength dependent. In principle four such isomers may arise: (i) four methyl groups on the same side of the macrocyclic plane; (ii) three methyl groups on the same side; (iii) two methyl groups on either side (cis); (iv) two methyl groups on either side (trans). The available data cannot be used to distinguish between these possibilities. (The [Ni(Me₄14aneN₄)](ClO₄)₂ complex may exist as one of the two square planar isomers (boat, R.S.R.S. and chair, R.S.S.R.) discussed in the literature.^{45,46}). The molar extinction co-efficient at 514nm of the square planar species (i.e. [Ni(Me₄14aneN₄)]²⁺) calculated from the spectrum in nitromethane solution is 207.01 mol⁻¹ dm³ cm⁻¹. The equilibrium constants, K_{eq}, enthalpy, ΔH⁰ and entropy, ΔS⁰ are calculated using the equations 4.22 and 4.5. The K_{eq} values along with ΔH⁰ and ΔS⁰ values are given in Table 4.10. At 331.1K, 57% low-spin and 43% high-spin species exist in aqueous solution whereas at 330.7K, 70.7% low-spin and 29.3% high-spin

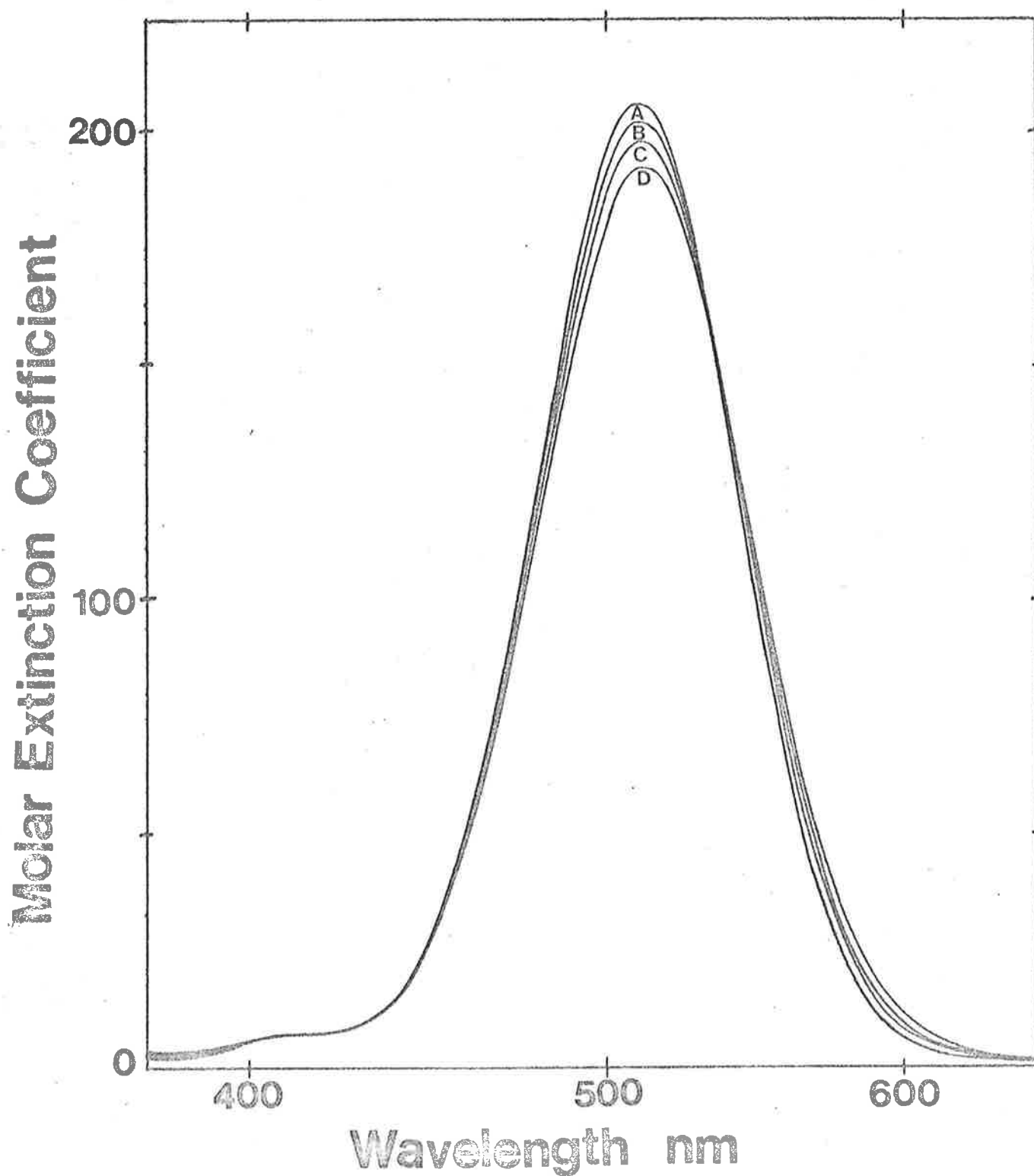


Figure 4.12

Temperature dependent uv/visible spectra of $4.03 \times 10^{-3} \text{ mol dm}^{-3}$ in $[\text{Ni}(\text{Me}_4\text{14aneN}_4)](\text{ClO}_4)_2$ (ethanol water preparation) in aqueous 4.00 mol dm^{-3} LiClO_4 solution.

Temperatures are 290.8, 308.6, 323.6 and 341.3K for the spectra from A to D respectively.

TABLE 4.10

K_{eq} , ΔH° and ΔS° Values for the $[\text{Ni}(\text{Me}_4\text{14aneN}_4)](\text{ClO}_4)_2$ System

$\frac{1}{T} \times 10^4$	${}^a K_{eq}$	b Activation Parameters
1. $[\text{LiClO}_4] = 0.0 \text{ mol dm}^{-3}$		
34.11	0.555 ± 0.05	$\Delta H^\circ = (18.51 \pm 0.09) \text{ kJ mol}^{-1}$
32.92	0.720 ± 0.05	
31.86	0.920 ± 0.05	$\Delta S^\circ = (58.26 \pm 0.29) \text{ JK}^{-1} \text{ mol}^{-1}$
30.96	1.15 ± 0.05	
30.20	1.35 ± 0.05	
29.40	1.60 ± 0.05	
2. $[\text{LiClO}_4] = 0.5 \text{ mol dm}^{-3}$		
33.87	1.45 ± 0.10	$\Delta H^\circ = (11.68 \pm 0.15) \text{ kJ mol}^{-1}$
32.55	1.75 ± 0.10	
31.40	2.05 ± 0.10	$\Delta S^\circ = (42.68 \pm 0.47) \text{ JK}^{-1} \text{ mol}^{-1}$
30.24	2.40 ± 0.10	
29.10	2.80 ± 0.15	
3. $[\text{LiClO}_4] = 1.0 \text{ mol dm}^{-3}$		
24.15	2.55 ± 0.15	$\Delta H^\circ = (8.29 \pm 0.29) \text{ kJ mol}^{-1}$
32.83	3.00 ± 0.15	
31.44	3.40 ± 0.15	$\Delta S^\circ = (36.2 \pm 0.93) \text{ JK}^{-1} \text{ mol}^{-1}$
30.28	3.75 ± 0.20	
29.13	4.25 ± 0.20	

The errors represent

a estimated error

b one standard deviation

species are in equilibrium in aqueous $0.5 \text{ mol dm}^{-3} \text{ LiClO}_4$ solution showing the effect of ionic strength.

4.6.4 The Temperature Jump Kinetic Study:-

The temperature jump kinetic experiments were performed with $5.0 \times 10^{-3} \text{ mol dm}^{-3} [\text{Ni}(\text{Me}_4\text{14aneN}_4)](\text{ClO}_4)_2$ concentration in

aqueous 0.5 and 1.5 mol dm⁻³ NaClO₄ at both 312nm and 390nm. The interconversion process is very fast, as fast as the heating time of the solution and therefore it was not possible to obtain any reliable kinetic data. A single relaxation was observed at 512nm with both 0.5 and 1.5 mol dm⁻³ NaClO₄ solution but at 390nm, two processes were observed with aqueous 0.5 mol dm⁻³ NaClO₄ solution, the slower process ($\tau \approx 7\mu\text{s}$) may be due to isomerisation. The square planar species of the complex (i.e. $[\text{Ni}(\text{Me}_4\text{14aneN}_4)]^{2+}$) may exist in different isomers depending upon the position of methyl groups and isomeric equilibrium between such species is temperature dependent. The equilibrium between two or more interconvertible isomers may give rise to the slower relaxation process. Hence the fast process probably characterises the spin-equilibrium.

4.7.1 General Discussion:-

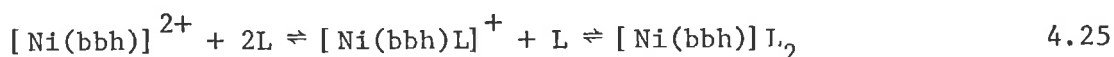
Both $[\text{Ni}(\text{12aneN}_4)(\text{H}_2\text{O})_2]^{2+}$ and $[\text{Ni}(\text{trien})(\text{H}_2\text{O})_2]^{2+}$ co-exist in solution with their square planar analogues and in consequence one mechanism for water exchange must be dissociation in nature (equation 4.1) (on the basis of ΔV^\ddagger measurements⁴⁹ it has been concluded that $[\text{Ni}(\text{OH}_2)_6]^{2+}$ undergoes water exchange through an I_d mechanism). The increased lability of $[\text{Ni}(\text{12aneN}_4)(\text{H}_2\text{O})_2]^{2+}$ over $[\text{Ni}(\text{H}_2\text{O})_6]^{2+}$ (Table 4.6) is consistent with the well established tendency of co-ordinated amine to labilise aquo ligands in octahedral nickel (II) systems.^{39, 40} The larger ΔH^\ddagger value for $[\text{Ni}(\text{OH}_2)_6]^{2+}$ is the major thermodynamic factor for the reduced lability of this species by comparison to the $[\text{Ni}(\text{12aneN}_4)(\text{OH}_2)_2]^{2+}$ species. The smaller ΔS^\ddagger value for $[\text{Ni}(\text{12aneN}_4)(\text{OH}_2)_2]^{2+}$ is the consequence of the greater lability of this species by comparison

to the $[\text{Ni}(\text{trien})(\text{OH}_2)_2]^{2+}$ species (significantly negative ΔS^\ddagger value). In principle, the $[\text{Ni}(\text{trien})(\text{OH}_2)_2]^{2+}$ species may exist as the α -cis and the β -cis isomers in which the aquo ligands are equivalent and non-equivalent, respectively and also as the trans isomer.^{23, 24} The cis configuration is preferred from spectroscopic data²⁴ and the observation of a single water exchange process in the ^{17}O studies (exchange rates differing by a factor of <3 are unlikely to be distinguished separately) suggests either one isomer predominates in solution or that the water exchange rates are very similar for various isomeric sites available in $[\text{Ni}(\text{trien})(\text{OH}_2)_2]^{2+}$. Because of this uncertainty it is difficult to explain the kinetic differences between the $[\text{Ni}(\text{12aneN}_4)(\text{OH}_2)_2]^{2+}$ and $[\text{Ni}(\text{trien})(\text{OH}_2)_2]^{2+}$ on the basis of detailed stereochemical arguments. The high-spin $[\text{Ni}(\text{12aneN}_4)(\text{OH}_2)_2]^{2+}$ in which the ligand restrains nickel (II) to be out of the plane of the four nitrogen atoms results in a relatively small stereochemical rearrangement to form a high-spin transition state or intermediate $[\text{Ni}(\text{12aneN}_4)(\text{OH}_2)]^{2+}$ in which nickel (II) is also out of the ligand N_4 plane. But in the case of $[\text{Ni}(\text{trien})(\text{OH}_2)_2]^{2+}$, the greater flexibility of the trien should permit a greater stereochemical rearrangement in the formation of the transition state such that this in conjunction with the concurrent solvent rearrangements is the origin of the ΔS^\ddagger difference between the two systems. The five co-ordinate high-spin species $[\text{Ni}(\text{tb12aneN}_4)\text{X}]^+$ (where X = Cl, Br or SCN) is reported²⁹ to have trigonal bipyramidal geometry but $[\text{Ni}(\text{12aneN}_4)(\text{OH}_2)]^{2+}$ could have either trigonal bipyramidal or square based pyramidal geometry because of the small energy differences⁵⁰ between the two geometries.

The rate determining equilibrium between the square planar to

octahedral interconversion is that between the high-spin $[\text{Ni}(\text{12aneN}_4)(\text{OH}_2)]^{2+}$ and low-spin $[\text{Ni}(\text{12aneN}_4)]^{2+}$ as was concluded from a comparison of the τ values derived from temperature jump data (Table 4.5) and $\tau_{\text{H}_2\text{O}}$ (Table 4.6) derived from ^{17}O n.m.r. studies. Two extreme mechanisms may be possible for the spin state change. In the first mechanism the spin change occurs in $[\text{Ni}(\text{12aneN}_4)(\text{OH}_2)]^{2+}$ prior to any stereochemical rearrangement and nickel (II) subsequently moves into the N_4 plane with the prior, synchronous or subsequent loss of the aquo ligand. The second mechanism differs only in that the spin change occurs subsequently to nickel (II) achieving co-planarity with the N_4 plane. The much shorter τ characterising the interconversion in the $[\text{Ni}(\text{13aneN}_4)(\text{OH}_2)_2]^{2+}$ system in which the larger macrocyclic hole (1.80 or 1.92 \AA^0)^{26, 29} should ease the high-spin nickel (II) movement into the N_4 plane suggests that the second mechanism may be operative. Data from linear tetramine systems⁹ also support this view to some extent. Square planar-octahedral interconversions in the $[\text{Ni}(\text{trien})(\text{OH}_2)_2]^{2+}$ and $[\text{Ni}(\text{2,3,2-tet})(\text{OH}_2)_2]^{2+}$ systems have been interpreted in terms of the equilibrium between high-spin $[\text{Ni}(\text{trien})(\text{OH}_2)]^{2+}$ and low-spin $[\text{Ni}(\text{trien})]^{2+}$ being rate determining in the overall square planar-octahedral interconversion.⁹ A re-examination of the data suggests that this may not be so since for the $[\text{Ni}(\text{trien})(\text{OH}_2)_2]^{2+}$ system the spectrophotometrically determined $\tau = 0.6\mu\text{s}$ (296.2K) whereas τ for the $[\text{Ni}(\text{trien})(\text{OH}_2)_2]^{2+} / [\text{Ni}(\text{trien})(\text{OH}_2)]^{2+}$ equilibrium will be $\approx 0.9\mu\text{s}$ ($1/\tau = 2/\tau_{\text{H}_2\text{O}} + k_2$, see equation 4.1 and Table 4.6). It is improbable that such similar τ values could be distinguished separately from the spectrophotometric data and thus in the $[\text{Ni}(\text{trien})(\text{OH}_2)_2]^{2+}$ system either the τ values characterising the sequential equilibrium in equation 4.1 are very similar or else

the octahedral-five co-ordinate equilibrium is rate determining.^{51, 52} It has been shown^{51, 52} from microwave temperature jump and ¹⁴N n.m.r. studies that the octahedral to five co-ordinate interconversion is the rate determining step in the overall octahedral to square planar interconversion in the system (4.25)



where L is a substituted pyridine and bbh is tetradentate biacetyl bis- α -hydroxybenzylidenehydrazone (2-)-N¹N^{1'}OO'.

The equilibrium shift towards the square planar species with increase in temperature and electrolyte concentration (Table 4.2 and 4.3) is consistent with such observations in related systems^{10, 13, 16, 25, 26, 53}. Fabbrizzi¹³ reported a similar equilibrium shift in aqueous 6.0 mol dm⁻³ NaClO₄ with no observed isosbestic points for the [Ni(12aneN₄(OH₂)₂)]²⁺ system. The present study appears to be the first in which the accompanying variation in ΔH° and ΔS° has been examined. In the [Ni(12aneN₄(OH₂)₂)]²⁺ system, as [LiClO₄] increases ΔH° decreases systematically whereas ΔS° exhibits a smaller and non-systematic variation. Ion pairing between the nickel (II) and ClO₄⁻ ($K_{1p} = 0.1$ calculated from the Fuoss equation⁵⁴) will occur to an increasing extent as [LiClO₄] increases and consequently the observed ΔH° and ΔS° values are composed of contributions from the ion-paired and non-ion-paired nickel (II) species. The perchlorate ion does not interact significantly (both in the solid and solution states) with the nickel (II) centre to perturb the low-spin state of [Ni(12aneN₄)]²⁺ which thereby rules out the probability that ClO₄⁻ significantly modifies the component of ΔH° which arises from the bonding between nickel (II) and the ligands in the first co-ordination sphere of

the ion-paired species. However, the ion pairing with ClO_4^- may modify the component of ΔH° provided significant solvation changes accompany changes in spin state and stereochemistry. In the $[\text{Ni}(\text{12aneN}_4)]^{2+} \text{ClO}_4^-$ ion pair, ClO_4^- is likely to be in a position perpendicular to the N_4 plane, thereby blocking access of a potential aquo ligand to this axial co-ordination site and also as a consequence of the net charge distribution difference between the ion pair and $[\text{Ni}(\text{12aneN}_4)]^{2+}$, causing a change in solvation. Mechanistically the first effect attributed to ion-pairing should reduce the magnitude of k_1 as is seen to be the trend (Table 4.5) as $[\text{LiClO}_4]$ increases from 2.0 - 4.0 mol dm⁻³. This trend is also accompanied by a decrease in ΔH^\ddagger and a tendency for ΔS^\ddagger to become more negative as $[\text{LiClO}_4]$ increases. However, a detailed mechanistic interpretation of these activation parameters is not warranted because of the accumulated errors in the k_1 data derived through equation 4.8.

In the $[\text{Ni}(\text{Me}_4\text{12aneN}_4)(\text{OH}_2)]^{2+}$ and the $[\text{Ni}(\text{Me}_4\text{14aneN}_4)(\text{OH}_2)]^{2+}$ systems, as $[\text{LiClO}_4]$ increases both ΔH° and ΔS° decrease systematically (see Table 4.8 and 4.10). The smaller ΔH° values may be ascribed due to the changes in the ionic radius of the nickel (II) in going from high-spin to low-spin states. On the other hand, the steric repulsions between the methyl portions of the ligand and the co-ordinated water molecule may give rise to smaller ΔS° values. The K_{eq} , ΔH° , ΔS° and % low-spin species in aqueous solution at 298.2K for all the systems are given in Table 4.11 for comparison. As the steric hindrance increases, the % low-spin species increases in the case of $[\text{Ni}(\text{12aneN}_4)(\text{OH}_2)_2]^{2+}$ system but there is no systematic trend in the percentage of low-spin species as the ring size increases. Moreover the steric hindrance does not increase the

TABLE 4.11

K_{eq} , ΔH° , ΔS° , and % Low-spin Species in Aqueous Solution 298.2K for all the Systems

System	$^a K_{eq}$	$^b \Delta H^\circ$ kJ mol ⁻¹	$^b \Delta S^\circ$ JK ⁻¹ mol ⁻¹	% Low-spin Species
1. [Ni(12aneN ₄)](ClO ₄) ₂	0.00305 ± 0.0002	23.6 ± 0.3	30.8 ± 1.1	0.30
2. [Ni(Me ₄ 12aneN ₄)](ClO ₄) ₂	0.945 ± 0.05	7.17 ± 0.42	23.6 ± 1.33	48.6
3. [Ni(13aneN ₄)](ClO ₄) ₂	2.60 ± 0.12	10.8 ± 0.06	44.0 ± 0.12	72.4
4. [Ni(14aneN ₄)](ClO ₄) ₂ ¹⁴	2.45 ± 0.12	22.60	83.7	71.0
5. [Ni(Me ₄ 14aneN ₄)](ClO ₄) ₂	0.630 ± 0.03	18.5 ± 0.09	58.3 ± 0.29	38.4
6. [Ni(13aneN ₄)](ClO ₄) ₂ ²⁵	6.89	31.4 ± 0.42	125 ± 2.1	87.3
7. [Ni(Me ₄ 14aneN ₄)](ClO ₄) ₂ ¹⁰	0.95	12.2 ± 1.6	41 ± 9	48.7

N.B. Data from reference 14 and 25 were in 0.1 mol dm⁻³ aqueous NaClO₄

Data from reference 10 were in 0.2 mol dm⁻³ aqueous NaClO₄

The errors represent

a estimated error

b one standard deviation

percentage of low-spin species in the case of $[\text{Ni}(\text{14aneN}_4)(\text{OH}_2)_n]^{2+}$ system. The low-spin species in the $[\text{Ni}(\text{15aneN}_4)(\text{OH}_2)_n]^{2+}$ system is about one percent²⁵ (room temperature and low ionic strength) and the high-spin species has trans-octahedral stereochemistry.³³ In these studies, LiClO_4 was used as supporting electrolyte. Different electrolytes may have different effects⁵³ on the equilibrium constants. It can be concluded from the temperature jump kinetic experiments, that the τ value characterising the high-spin low-spin interconversion becomes shorter and shorter as the ring size increases. The methyl group substitution on the nitrogen atoms of the ligand also resulted in a shorter τ values than the absence of such substitution group on the ligand. The two relaxations observed in both the $[\text{Ni}(\text{Me}_4\text{12aneN}_4)(\text{OH}_2)]^{2+}$ and $[\text{Ni}(\text{Me}_4\text{14aneN}_4)(\text{OH}_2)]^{2+}$ systems may be interpreted as a fast spin state change followed by a slower isomeric change. The square planar species of both complexes may exist in different isomers depending upon the position of methyl groups and isomeric equilibrium between such species is temperature and ionic strength dependent. The fast process characterises the spin-equilibrium and the slower process characterises the isomeric equilibrium between two interconvertible square planar isomers.

REFERENCES FOR CHAPTER FOUR

1. F. A. Cotton and G. Wilkinson, *Advanced Inorganic Chemistry*, 3rd Edition, Wiley Eastern Ltd., New Delhi (1978).
2. J. P. Jesson, S. Trofimenko and D. R. Eaton, *J.A.C.S.*, 89, 3158 (1967).
3. M. A. Hoselton, L. J. Wilson and R. S. Drago, *J.A.C.S.*, 97, 1722 (1975).
4. L. J. Wilson, D. Georges and M. A. Hoselton, *Inorg. Chem.*, 14, 2968 (1975).
5. M. F. Tweedle and L. J. Wilson, *J.A.C.S.*, 98, 4824 (1976).
6. E. V. Dose, K. M. M. Murphy and L. J. Wilson, *Inorg. Chem.*, 15, 2622 (1976).
7. M. G. Simmons and L. J. Wilson, *Inorg. Chem.*, 16, 126, (1977).
8. E. V. Dose, M. A. Hoselton, N. Sutin, M. F. Tweedle and L. J. Wilson, *J.A.C.S.*, 100, 1141 (1978).
9. K. J. Ivin, R. Jamison and J. J. McGarvey, *J.A.C.S.*, 94, 1763 (1972).
10. N. Herron and P. Moore, *Inorg. Chim. Acta.*, 36, 89 (1979).
11. S. V. Gerald, C. L. Watkins and H. F. Bowen, *Inorg. Chim. Acta.*, 35, 255 (1979).
12. L. Rusnak and R. B. Jordan, *Inorg. Chem.*, 10, 2199 (1971).
13. L. Fabbrizzi, *Inorg. Chem.*, 16, 2667 (1977).
14. A. Anichini, L. Fabbrizzi, P. Paoletti and R. M. Clay, *Inorg. Chim. Acta.*, 24, L21 (1977).
15. C. Creutz and N. Sutin, *J.A.C.S.*, 95, 7177 (1973).
16. L. Sabatini and L. Fabbrizzi, *Inorg. Chem.*, 18, 438 (1979).
17. J. K. Beattie, N. Sutin, D. H. Turner and G. W. Flynn, *J.A.C.S.*, 95, 2052 (1973).
18. M. A. Hoselton, R. S. Drago, L. J. Wilson and N. Sutin, *J.A.C.S.*, 98, 6967 (1976).
19. K. A. Reeder, E. V. Dose and L. J. Wilson, *Inorg. Chem.*, 17, 1071 (1978).
20. J. K. Beattie, R. A. Binstead and R. J. West, *J.A.C.S.*, 100, 3044 (1978).

21. R. H. Petty, E. V. Dose, M. F. Tweedle and L. J. Wilson, *Inorg. Chem.*, 17, 1064 (1978).
22. R. A. Binstead, J. K. Beattie, E. V. Dose, M. F. Tweedle and L. J. Wilson, *J.A.C.S.*, 100, 5609. (1978).
23. B. Bosnick, R. D. Gillard, E. D. McKenzie and G. A. Webb, *J. Chem. Soc. A.*, 1331 (1966).
24. R. G. Wilkins, R. Yelin, D. W. Margerum and D. C. Weatherburn, *J.A.C.S.*, 91, 4326 (1969).
25. L. Fabbrizzi, *J.C.S., Dalton*, 1857 (1979).
26. L. Fabbrizzi, M. Micheloni and P. Paoletti, *Inorg. Chem.*, 19, 535 (1980).
27. D. H. Busch, *Acc. Chem. Res.*, 11, 392 (1978).
28. L. Y. Martin, L. J. Dehayes, L. J. Zompa and D. H. Busch, *J.A.C.S.*, 96, 4046 (1974).
29. R. Smierciak, J. Passariello and E. L. Blinn, *Inorg. Chem.*, 16, 2646 (1977).
30. B. N. Figgis and J. Lewis in "Modern Co-ordination Chemistry", eds. J. Lewis and R. G. Wilkins, Interscience, New York (1960).
31. D. F. Evans, *J. Chem. Soc.*, 2003 (1959).
32. D. F. Evans and T. A. Evans, *J.C.S., Dalton*, 723 (1979).
33. L. Y. Martin, C. R. Sperati and D. H. Busch, *J.A.C.S.*, 99, 2968 (1977).
34. ¹⁷O water exchange kinetic data were obtained from J. P. Hunt and H. W. Dodgen, Department of Chemistry, Washington State University.
35. D. B. Bechtold, G. Liu, H. W. Dodgen and J. P. Hunt, *J. Phys. Chem.*, 82, 333 (1978).
36. T. J. Swift and R. E. Connick, *J. Chem. Phys.*, 37, 307 (1962); 41, 2553 (1964).
37. J. L. Dye and V. A. Nicely, *J. Chem. Ed.*, 48, 443 (1971).
38. M. Rubinstein, A. Baram and Z. Luz, *Mol. Phys.*, 20, 67 (1971).
39. D. P. Rablen, H. W. Dodgen and J. P. Hunt, *Inorg. Chem.*, 15, 931 (1976).
40. J. P. Hunt, *Co-ord. Chem. Rev.*, 7, 1 (1971).
41. R. D. Farina and J. H. Swinehart, *J.A.C.S.*, 91, 568 (1969).
42. L. Sacconi, "Transition metal chem.", 4, 244 (1968).

43. E. V. Uhlig, *Co-ord. Chem. Rev.*, 10, 227 (1973).
44. E. J. Billo, *Inorg. Chim. Acta.*, 37, L533 (1979).
45. F. Wagner and E. K. Barefield, *Inorg. Chem.*, 15, 408 (1976).
46. E. K. Barefield and F. Wagner, *Inorg. Chem.*, 12, 2435 (1973).
47. G. A. Kalligeros and E. L. Blinn, *Inorg. Chem.*, 11, 1145 (1972).
48. W. H. Plassman, R. G. Swisher and E. L. Blinn, *Inorg. Chem.*, 19, 1101 (1980).
49. Y. Ducommun, W. L. Earl and A. E. Merbach, *Inorg. Chem.*, 18, 2754 (1979).
50. D. L. Keppert, *Inorg. Chem.*, 12, 1938, 1942 (1973).
51. M. Cusumano, *J.C.S. Dalton*, 2133, 2137 (1976).
52. J. Sachinidis and M. W. Grant, *J.C.S. Chem. Comm.*, 157 (1978).
53. R. G. Swisher, J. P. Dayhuff, D. J. Stuehr and E. L. Blinn, *Inorg. Chem.*, 19, 1136 (1980).
54. R. M. Fuoss, *J.A.C.S.*, 80, 5059 (1958).

CHAPTER FIVE

Formation and Dissociation of Macrocyclic Complexes in Aqueous Solution

Contents.

5.1. Introduction

5.2. Determination of the Stoichiometry of $[\text{Ni}(\text{12aneN}_4)(\text{OH}_2)_2]^{2+}$ Formation.5.3. Formation Rate Constants of $[\text{Ni}(\text{12aneN}_4)(\text{OH}_2)_2]^{2+}$ 5.4. The Effect of Hydrogen Ion Concentration and Temperature on the rates of Dissociation of $[\text{Ni}(\text{12aneN}_4)](\text{ClO}_4)_2$, $[\text{Cu}(\text{12aneN}_4)](\text{ClO}_4)_2$ and $[\text{Cu}(\text{Me}_4\text{12aneN}_4)](\text{ClO}_4)_2$.5.5. The Effect of Ionic Strength on the Rates of Dissociation of $[\text{Ni}(\text{12aneN}_4)](\text{ClO}_4)_2$, $[\text{Cu}(\text{12aneN}_4)](\text{ClO}_4)_2$ and $[\text{Cu}(\text{Me}_4\text{12aneN}_4)](\text{ClO}_4)_2$.5.6. The Reaction of $[\text{Ni}(\text{12aneN}_4)(\text{OH}_2)_2]^{2+}$ with Sodium Hydroxide.

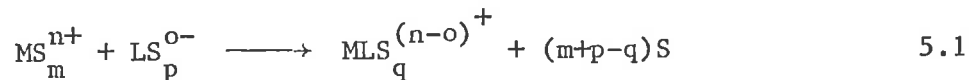
5.7. General Discussion.

CHAPTER FIVE

Formation and Dissociation of Macrocyclic Complexes in Aqueous Solution5.1 Introduction

The relationship between the structural features of ligands and the properties of their metal complexes is dramatically demonstrated in the case of tetra aza macrocycles. The formation of complexes of macrocyclic ligands with metal ions which are markedly more stable than that of comparable open chain ligands has been termed the macrocyclic effect¹ or multiple juxtapositional fixedness² in order to distinguish it from the well known chelate effect. For example, there is more than a 10^6 -fold³ difference in the stability constant of $[\text{Ni}(\text{14aneN}_4)]^{2+}$ compared with $[\text{Ni}(2,3,2\text{-tet})]^{2+}$.

Complex formation in solution may be described by equation 5.1



where 'M' is the metal ion, 'S' is the solvent and 'L' is the ligand. In the case of $[\text{Ni}(\text{14aneN}_4)]^{2+}$ formation⁴, the solvation of the macrocyclic ligand is less than that of the linear open chain analogue. Therefore, the solvation entropy change for the macrocyclic ligand complexation may be less than that expected for the open chain analogue. However, this entropy difference between the macrocycle and the linear ligand will be reduced somewhat because of the loss of rotational entropy by a linear ligand which does not occur in the case of a macrocycle. As far as formation enthalpy changes are concerned, the smaller desolvation that occurs in macrocyclic complexes leads to a more favourable enthalpy change for a macrocycle compared to a linear molecule.

As discussed in chapter 1, in the case of $[\text{Cu}(12\text{aneN}_4)]^{2+}$ formation⁴, although the ligand solvation is less than that of the linear open chain analogue, the macrocyclic effect is likely to be entropic in origin whereas the effect is probably of enthalpic origin in the case of $[\text{Ni}(14\text{aneN}_4)]^{2+}$ formation. This apparent contrast between the results with $[\text{Cu}(12\text{aneN}_4)]^{2+}$ and $[\text{Ni}(14\text{aneN}_4)]^{2+}$ is not fully explained by differences between the metal ions and rings. Space filling molecular models show that nickel (II) or copper (II) can fit neatly into the cavity of the larger 14aneN₄ ligand and this observation is confirmed by X-ray crystallographic studies⁵⁻⁷. However, molecular models demonstrate that the cavity of the smaller 12aneN₄ (see chapter 3) is too small to accommodate these cations. Thus, the question arises as to whether the studies of $[\text{Cu}(12\text{aneN}_4)]^{2+}$ and $[\text{Ni}(14\text{aneN}_4)]^{2+}$ formation measure the same "macrocyclic effect".

Solution properties such as thermodynamic and kinetic stabilities, redox behaviour and spin-state equilibria of tetra aza macrocyclic complexes are strongly dependent upon the size of the ligand cavity. For instance, in the formation of nickel (II) and copper (II) complexes with a series of 12 to 16-membered cyclic tetramines, the most exothermic reactions occur with the 14-membered ring⁸. A smaller or a larger ligand cavity gives rise to a substantial decrease (up to 60%) in the enthalpy of formation. The ring size, substituents at both the co-ordinating amino groups and the carbon atoms of the ring, and the electrostatic interactions between the incoming ligand and polarised solvent molecules in the first co-ordination sphere of the metal ion effect⁹ the rate of complexation, which for the protonated macrocycles is slower than that of the analogous open chain polyamines. In the formation of the nickel (II) complex with the 14aneN₄ ligand, Kaden¹⁰ reported that the mono and

diprotonated ligand species exhibited formation rate constants which were 30,000 times smaller than those observed for the corresponding species of the open chain polyamine trien¹¹. Kaden suggested that the kinetic effect of a more rigid cyclic structure 14aneN₄ in comparison with trien is a consequence of the rate limiting step which is the formation of the second co-ordination bond. The rates of complexation of different metal ions with macrocyclic ligands have been studied^{6,12-21}, the rates of formation and dissociation have also been reviewed^{22,23}.

Because of extreme kinetic inertness and the associated high formation constants, comparative studies of kinetic and thermodynamic stabilities of tetra aza macrocyclic complexes have proved difficult^{19,24,25}. Moreover, the study of the ring size effects on the kinetics of dissociation of tetra aza macrocyclic nickel complexes is complicated by stereochemical and spin-state changes²³. However, the dissociation of macrocyclic complexes has been studied to a limited extent^{19,26-28}. The present study appears to be the first of its kind since it includes the formation of $[\text{Ni}(\text{12aneN}_4)(\text{OH}_2)_2]^{2+}$, and the acid dissociation of $[\text{Ni}(\text{12aneN}_4)]^{2+}$, $[\text{Cu}(\text{12aneN}_4)]^{2+}$ and $[\text{Cu}(\text{Me}_4\text{12aneN}_4)]^{2+}$. The reaction of $[\text{Ni}(\text{12aneN}_4)]^{2+}$ with sodium hydroxide is also reported here.

5.2 Determination of stoichiometry of $[\text{Ni}(\text{12aneN}_4)(\text{OH}_2)_2]^{2+}$ formation:-

The possible interactions of $[\text{Ni}(\text{12aneN}_4)(\text{OH}_2)_2]^{2+}$ and $[\text{Ni}(\text{OH}_2)_6]^{2+}$ with the buffers ν collidine, lutidine, hepes and pipes, respectively, were investigated using uv/visible spectrophotometry. The uv/visible spectra of $[\text{Ni}(\text{OH}_2)_6]^{2+}$ and $[\text{Ni}(\text{12aneN}_4)(\text{OH}_2)_2]^{2+}$ were not apparently affected by the presence of pipes buffer. Solutions of 12aneN₄ (0.01842 mol dm⁻³) and $[\text{Ni}(\text{ClO}_4)_2] \cdot 6\text{H}_2\text{O}$ (0.02600 mol dm⁻³)

were prepared separately in aqueous $1.0 \text{ mol dm}^{-3} \text{ LiClO}_4$ containing 0.1 mol dm^{-3} pipes, the pH of both solutions was adjusted to 6.65. Job's method^{29,30} of continuous variations (see section 7.3) (using uv/visible spectrophotometry) was carried out at 298.2K. The pH was subsequently checked and found to be slightly less (0.10 - 0.30) than 6.65 indicating that the buffer cannot maintain the pH. Knowing the molar extinction co-efficients of $[\text{Ni}(\text{OH}_2)_6]^{2+}$ (0.25) and 12aneN_4 (0.067) at 560 nm, the absorbance difference, Y (A measured - A calculated) values at 560 nm were calculated for each spectrum. The Y values are plotted against the mol fraction of the ligand in Figure 5.1. The solid lines are calculated by least squares linear regression. The maximum occurs at 0.46 mol fraction of the ligand, indicating the predominance of one to one complex formation (ideally the mol fraction of the ligand should be 0.5). The discrepancy (8%) may be due to a slight change in pH and experimental errors.

5.3 Formation rate constants of $[\text{Ni}(12\text{aneN}_4)(\text{OH}_2)_2]^{2+}$:-

The rate of formation of $[\text{Ni}(12\text{aneN}_4)(\text{OH}_2)_2]^{2+}$ was studied using uv/visible spectrophotometry ($\lambda = 560 \text{ nm}$) at pH values 5.95, 6.35 and 6.60 in $1.0 \text{ mol dm}^{-3} \text{ LiClO}_4$ and 0.1 mol dm^{-3} pipes at 290.1K, with an excess concentration of $0.1002 \text{ mol dm}^{-3} [\text{Ni}(\text{OH}_2)_6]^{2+}$ and $0.01 \text{ mol dm}^{-3} 12\text{aneN}_4$. It was found that the reaction is highly pH dependent (Table 5.1). The rate of formation was also studied at pH 6.35 (290.1K, $1.0 \text{ mol dm}^{-3} \text{ LiClO}_4$ and 0.1 mol dm^{-3} pipes) with various metal ion concentrations again under pseudo 1st order conditions (Table 5.1). The observed rate constants (k_{obs}) are plotted against $[\text{Ni}(\text{OH}_2)_6]^{2+}$ in Figure 5.2. The solid line is the least squares linear regression. The negative intercept is probably due to experimental errors and the inability of the buffer to hold the

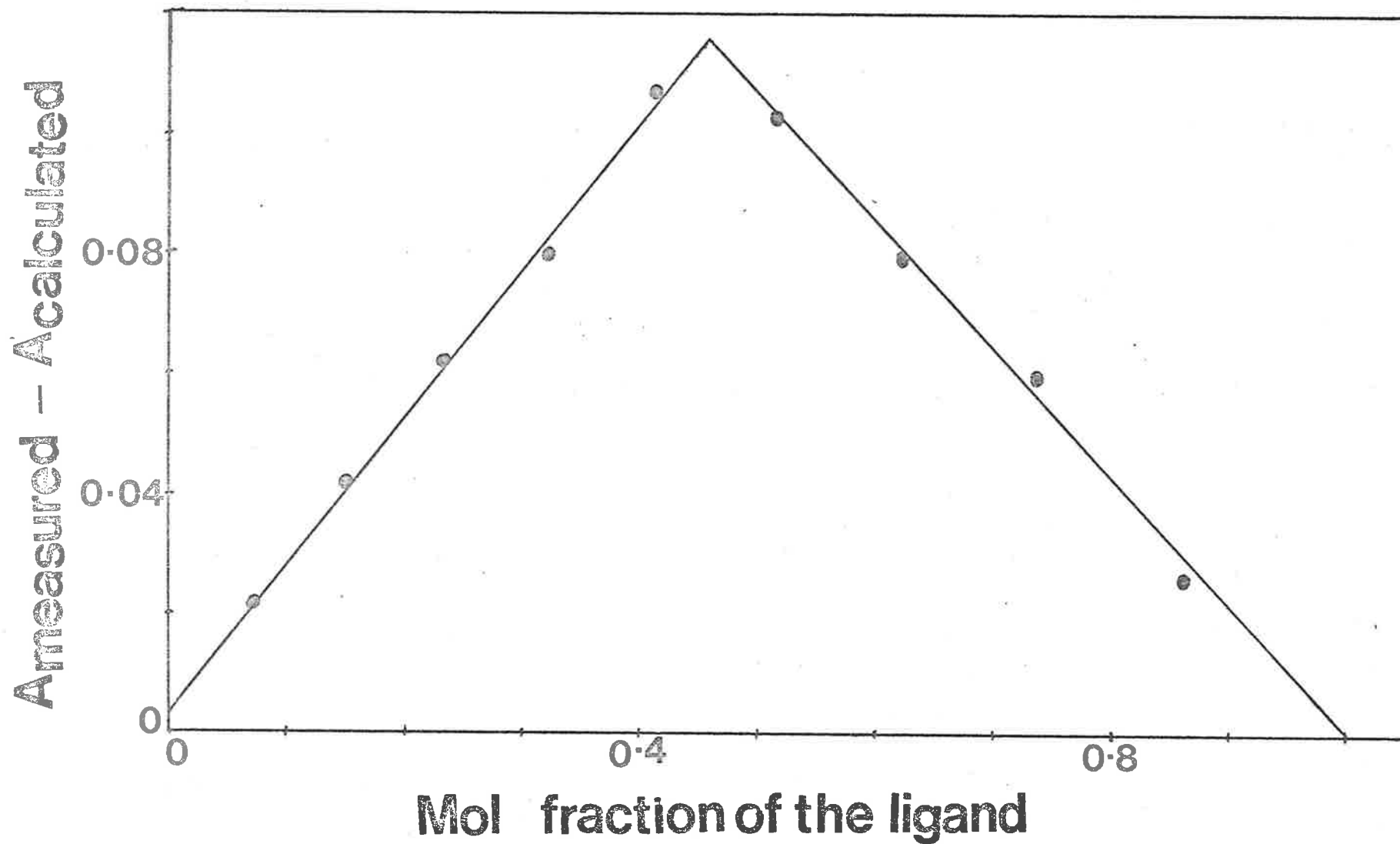


Figure 5.1 $A_{\text{measured}} - A_{\text{calculated}}$ ($\lambda = 560 \text{ nm}$ and cell path = 1 cm) vs mol fraction of 12aneN₄ for Job's method of continuous variation for the determination of stoichiometry of $[\text{Ni}(\text{12aneN}_4)(\text{OH}_2)_2]^{2+}$ formation in an aqueous medium at 298.2 K. Stock solutions of $2.60 \times 10^{-2} \text{ mol dm}^{-3}$ $[\text{Ni}(\text{OH}_2)_6]^{2+}$ and $1.84 \times 10^{-2} \text{ mol dm}^{-3}$ 12aneN₄ were prepared in aqueous 1 mol dm^{-3} LiClO₄ containing 0.1 mol dm^{-3} pipes (pH = 6.65).

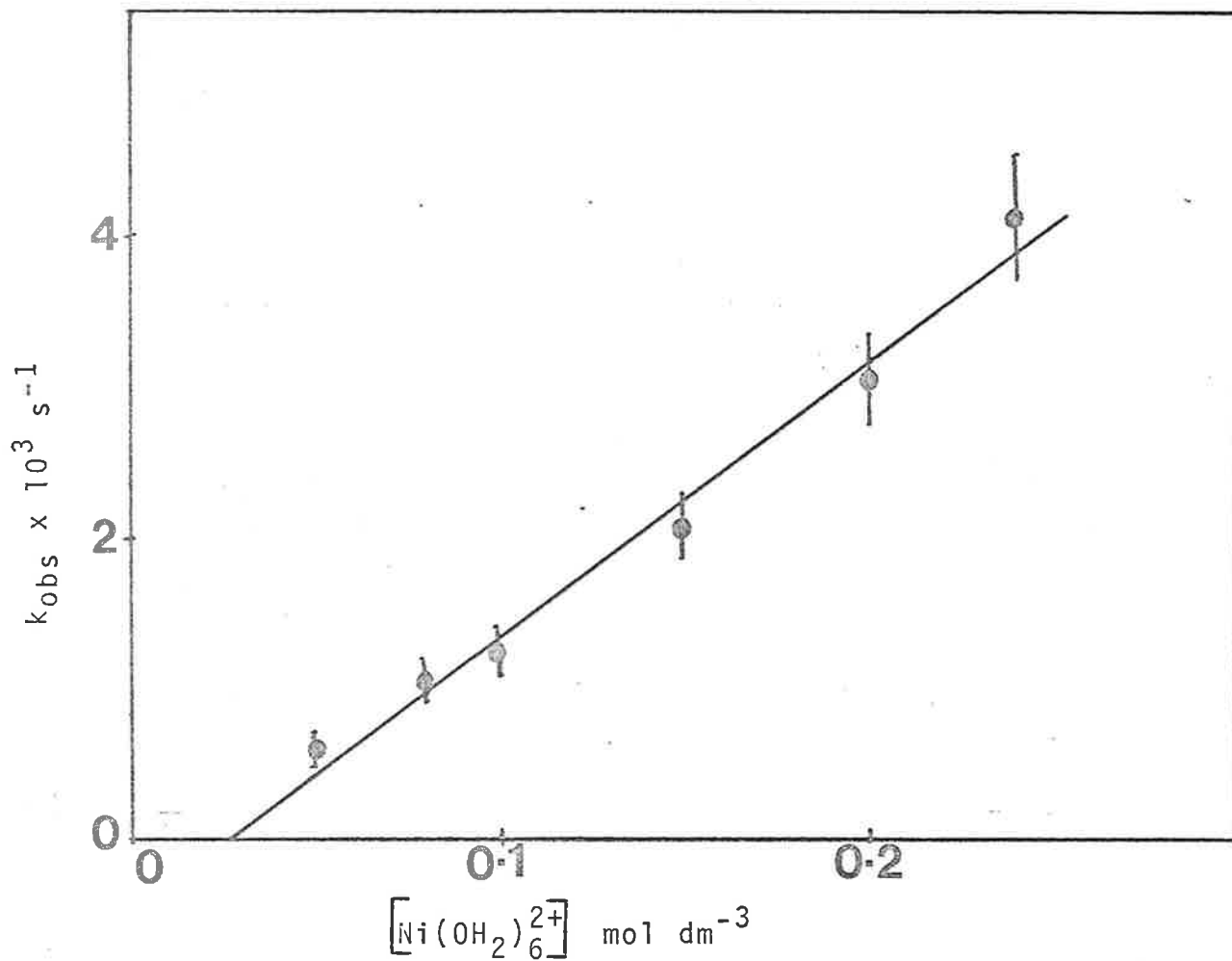


Figure 5.2

k_{obs} vs $[\text{Ni}(\text{OH}_2)_6^{2+}]$ for the formation of the $[\text{Ni}(\text{12aneN}_4)(\text{OH}_2)_2]^{2+}$ complex in water containing $1 \text{ mol dm}^{-3} \text{ LiClO}_4$ and 0.1 mol dm^{-3} pipes (pH = 6.35) at 290.1 K and $\lambda = 560 \text{ nm}$. $[\text{12aneN}_4] = 5.0 \times 10^{-3} \text{ mol dm}^{-3}$ for all reactions. The solid line is a least squares linear regression line.

Table 5.1

k_{obs} values for $[\text{Ni}(\text{12aneN}_4(\text{OH}_2)_2)^{2+}$ formation

pH = 6.35 ± 0.10

$k_{\text{obs}} \times 10^3 \text{s}^{-1}$	$[\text{Ni}(\text{OH}_2)_6^{2+}] \text{ mol dm}^{-3}$
0.59 ± 0.06	0.05
1.02 ± 0.10	0.08
1.24 ± 0.12	0.10
2.05 ± 0.19	0.15
3.03 ± 0.27	0.20
4.12 ± 0.41	0.24

$k_{\text{obs}} \times 10^3 \text{s}^{-1}$	pH	$[\text{Ni}(\text{OH}_2)_6^{2+}] \text{ mol dm}^{-3}$
0.75 ± 0.08	5.95 ± 0.1	
1.24 ± 0.12	6.35 ± 0.1	(in all experiments)
(2.61 ± 0.24)	6.60 ± 0.1	0.1002

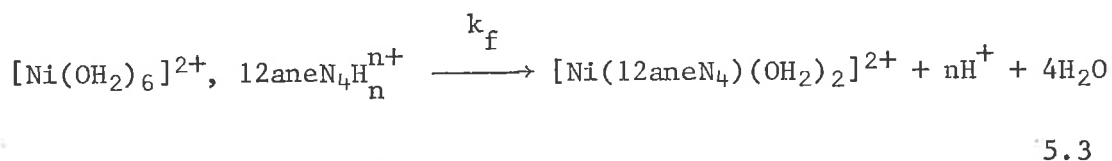
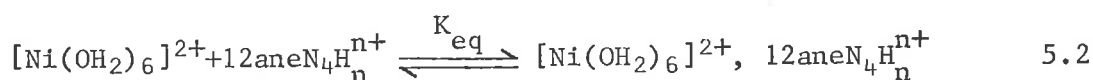
N.B. The errors represent estimated uncertainty

pH constant. At the end of the reaction pH was found to decrease by about 0.3 units. In the pH region studied, the ligand mainly exists as the diprotonated species with a small amount of monoprotonated and a negligible amount of unprotonated species (see chapter 2). The metal ion therefore probably reacts with ligand giving the product $[\text{Ni}(\text{12aneN}_4)(\text{OH}_2)_2]^{2+}$ and releasing protons. The observed rate of reaction is directly proportional to $[\text{Ni}(\text{OH}_2)_6^{2+}]$ and $[\text{12aneN}_4\text{H}_n^{n+}]$ as shown in equation 5.1a (Figure 5.2).

$$\frac{d[\text{Ni}(\text{12aneN}_4)(\text{OH}_2)_2]^{2+}}{dt} = k_{\text{obs}} [\text{Ni}(\text{OH}_2)_6^{2+}] [\text{12aneN}_4\text{H}_n^{n+}] \quad 5.1a$$

If the pH is increased, the rate of formation increases, suggesting that monoprotonated ligand is more reactive than the diprotonated species and unprotonated ligand is more reactive than monoprotonated species.

It is of interest to explore the possibility of the fitting of this complex formation data to the dissociative interchange model³¹, believed to apply to substitution on nickel (II).

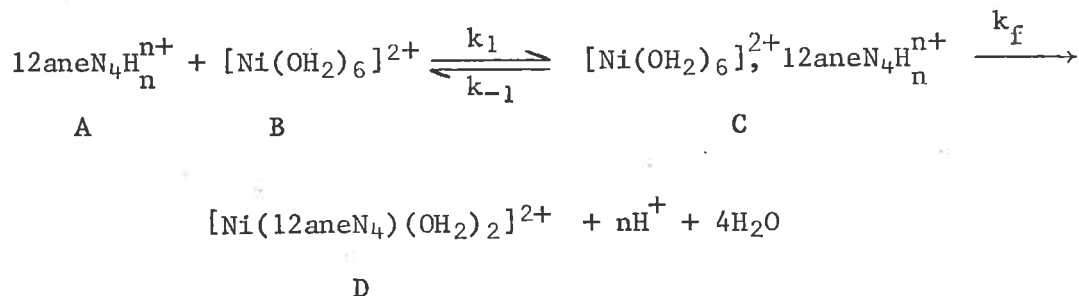


The ligand and the aquated metal ion are in rapid equilibrium with an outer sphere complex in which the incoming group occupies a position in the second co-ordination sphere. The collapse of this outer sphere complex to give the inner sphere complex is the rate determining step.

The observed rate constant, k_{obs} would be given by equation 5.4.

$$k_{\text{obs}} = k_f K_{\text{eq}} [\text{Ni}(\text{OH}_2)_6^{2+}] \quad 5.4$$

Equation 5.4 may be deduced in the following way³²⁻³⁴ considering 'B' in excess.



If the first step is fast compared with the second, then

$$K_{\text{eq}} = \frac{[\text{C}]}{[\text{A}][\text{B}]} = \frac{k_1}{k_{-1}}$$

and

$$k_1, k_{-1} \gg k_f$$

The rate of production of D must be equal to the rate of loss of (A + C).

$$\text{Rate} = \frac{d[\text{D}]}{dt} = \frac{-d([\text{A}]+[\text{C}])}{dt} = k_{\text{obs}}([\text{A}]+[\text{C}]) = k_f[\text{C}] = k_f K_{\text{eq}}[\text{A}][\text{B}]$$

$$\therefore k_{\text{obs}} = \frac{k_f K_{\text{eq}}[\text{A}][\text{B}]}{[\text{A}] + [\text{C}]} = \frac{k_f K_{\text{eq}}[\text{B}]}{1 + K_{\text{eq}}[\text{B}]} = \frac{k_f K_{\text{eq}}[\text{Ni}(\text{OH}_2)_6^{2+}]}{1 + K_{\text{eq}}[\text{Ni}(\text{OH}_2)_6^{2+}]}$$

$$\text{If } K_{\text{eq}}[\text{Ni}(\text{OH}_2)_6^{2+}] \gg 1, \quad \text{then } k_{\text{obs}} = k_f$$

$$\text{and if } 1 \gg K_{\text{eq}}[\text{Ni}(\text{OH}_2)_6^{2+}], \quad \text{then } k_{\text{obs}} = k_f K_{\text{eq}}[\text{Ni}(\text{OH}_2)_6^{2+}]$$

where $[\text{Ni}(\text{OH}_2)_6^{2+}]$ is the metal ion concentration which essentially

remains constant under pseudo 1st order conditions. k_{obs} is the observed pseudo 1st order rate constant for the reaction.

The value of $k_f K_{\text{eq}}$ was calculated to be $(18.2 \pm 1.2) \times 10^{-3} \text{ mol}^{-1} \text{ dm}^3 \text{ s}^{-1}$ from the slope of the plot of k_{obs} vs $[\text{Ni}(\text{OH}_2)_6^{2+}]$.

The value of K_{eq} may be approximately estimated in two ways:

(1) The rate constant of water exchange³⁵ on $[\text{Ni}(\text{OH}_2)_6]^{2+}$ at 298.2K was reported to be $16.2 \times 10^4 \text{ s}^{-1}$. Taking k_f as $16.2 \times 10^4 \text{ s}^{-1}$, the K_{eq} value is calculated to be $1.12 \times 10^{-7} \text{ mol}^{-1} \text{ dm}^3$. This value of K_{eq} implies that the concentration of outer sphere complex is very small indeed, such a concentration of complex could represent simply molecular collisions between the reactants. Obviously this K_{eq} value is in accord with $1 \gg K_{\text{eq}} [\text{Ni}(\text{OH}_2)_6^{2+}]$.

(2) The K_{eq} value may be estimated using equation 5.4a^{34,36}

$$K_{\text{eq}} = \frac{4\pi N a^3}{3000} \exp - \frac{U(a)}{kT} \quad 5.4a$$

($U(a)$ is the Debye Hückel interionic potential)

$$\text{where } U(a) = \frac{Z_1 Z_2 e^2}{a D} - \frac{Z_1 Z_2 e^2 k}{D(1+k/a)}$$

$$k^2 = \frac{8\pi N e^2 I}{1000 D k T}$$

N = Avogadro's number

a = centre to centre distance of closest approach of the solvated metal ion and the reacting site of the ligand.

k = Boltzmann's constant

e = charge of an electron in e.s.u. unit

D = bulk dielectric constant

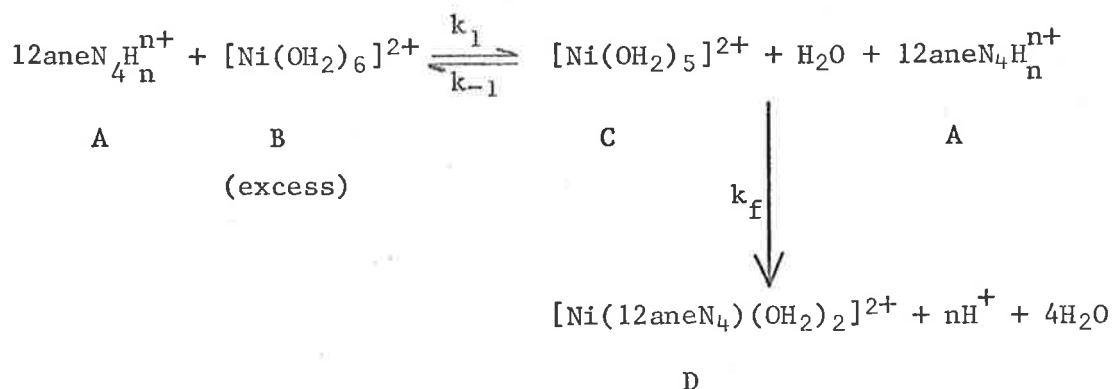
I = ionic strength

Z_1, Z_2 = charges of reactants

T = absolute temperature

Setting $a = 4A^\circ$ arbitrarily, the value of K_{eq} is calculated to be $0.16 \text{ mol}^{-1} \text{ dm}^3$ and k_f becomes 0.114 S^{-1} which is much slower than water exchange rate. However the K_{eq} values calculated by both methods are only approximate. As soon as one of the nitrogens co-ordinates to the metal ion after removal of a water molecule, desolvation of the metal ion becomes more labile³⁷ (chapter 4) and co-ordination of metal ion with other nitrogen atoms become favourable. Hence it is more probable that the first co-ordination bond between metal ion and ligand is the rate determining step.

The alternative mechanism to that so far discussed is the dissociative (D) mechanism³⁸ (see chapter 1) which could also give rise to the equation 5.4 as shown below (also discussed in chapter 6).



$$\text{rate} = \frac{d[\text{D}]}{dt} = k_f[\text{C}][\text{A}]$$

Under steady state conditions

$$\frac{d[\text{C}]}{dt} = k_1[\text{B}] - k_{-1}[\text{C}][\text{H}_2\text{O}] - k_f[\text{A}][\text{C}] = 0$$

$$\therefore [\text{C}] = \frac{k_1[\text{B}]}{k_{-1}[\text{H}_2\text{O}] + k_f[\text{A}]}$$

$$\therefore \text{rate} = \frac{d[\text{D}]}{dt} = \frac{k_f k_1[\text{A}][\text{B}]}{k_{-1}[\text{H}_2\text{O}] + k_f[\text{A}]}$$

Thus $\frac{d[D]}{dt}$ will exhibit a non-linear dependence upon [A] between the limits.

(i) $k_{-1}[H_2O] \gg k_f[A]$ when

$$\frac{d[D]}{dt} = - \frac{d[A]}{dt} \approx \frac{k_f k_1 [A][B]}{k_{-1}[H_2O]}$$

At a fixed excess concentration of B, an apparent first order plot will be obtained with

$$k_{obs} = \frac{k_f k_1 [B]}{k_{-1}[H_2O]}$$

(ii) $k_{-1}[H_2O] \ll k_f[A]$ when

$$\frac{d[D]}{dt} = - \frac{d[A]}{dt} \approx k_1[B]$$

At a fixed excess concentration of B, an apparent zero order plot would be obtained at this limit. Since experimentally in the system under discussion, a first order plot is obtained, if the reaction were dissociative limit (i) would apply. Accordingly the appropriate expression for k_{obs} , the pseudo first order rate constant, would be

$$k_{obs} = \frac{k_f k_1 [B]}{k_{-1}[H_2O]} = K k_f [B] \quad \left(\text{where } K = \frac{k_1}{k_{-1}[H_2O]} \right)$$

In form this expression is identical to equation 5.4. Thus one cannot distinguish between an I_d or D mechanism using the available data. Moreover, the possibility of an associative interchange mechanism, (1a)³⁸ cannot be ruled out because the rate law is identical to that for the dissociative interchange mechanism. In this mechanism an outer sphere association occurs between metal ion and the ligand, the

ligand moves inside the first co-ordination sphere thereby forming an intermediate of co-ordination number 7. However, this intermediate is quite unlikely to form because both the ligand and the metal ion are positively charged. Moreover, ligand substitution on nickel (II)^{39,40} with other ligands in other solvents appear to proceed through an I_d or D mechanism and it is not likely that an 'Ia' mechanism is operating in this system.

Because of the inability of the buffer to hold pH constant, further experiments in this system and systems using different metal ions and different ligands were not attempted.

5.4 The Effect of Hydrogen Ion Concentration and Temperature on the Rates of Dissociation of $[\text{Ni}(12\text{aneN}_4)](\text{ClO}_4)_2$, $[\text{Cu}(12\text{aneN}_4)](\text{ClO}_4)_2$ and $[\text{Cu}(\text{Me}_412\text{aneN}_4)](\text{ClO}_4)_2$:-

The dissociation of $[\text{Ni}(12\text{aneN}_4)](\text{ClO}_4)_2$, $[\text{Cu}(12\text{aneN}_4)](\text{ClO}_4)_2$ and $[\text{Cu}(\text{Me}_412\text{aneN}_4)](\text{ClO}_4)_2$ was studied at various acid concentrations as a function of temperature under pseudo 1st order conditions using uv/visible spectrophotometry.

Figure 5.3 shows the spectra of approximately 2.5×10^{-2} mol dm⁻³ $[\text{Ni}(12\text{aneN}_4)](\text{ClO}_4)_2$ in 0, 0.2, 0.4, 0.6, 0.8 and 1.0 mol dm⁻³ HClO₄ (ionic strength 1.0 adjusted by NaClO₄). The spectra were recorded immediately after mixing at 288.2K. The lower absorbances at higher acid concentrations indicate that some complex has been dissociated prior to the recording of the spectra. The absorbance band at 558.5 nm is shifted towards higher wavelengths as the acid concentration increases (Table 5.2). Figure 5.4 shows the spectra of $[\text{Ni}(12\text{aneN}_4)](\text{ClO}_4)_2$ recorded at increasing times after mixing in

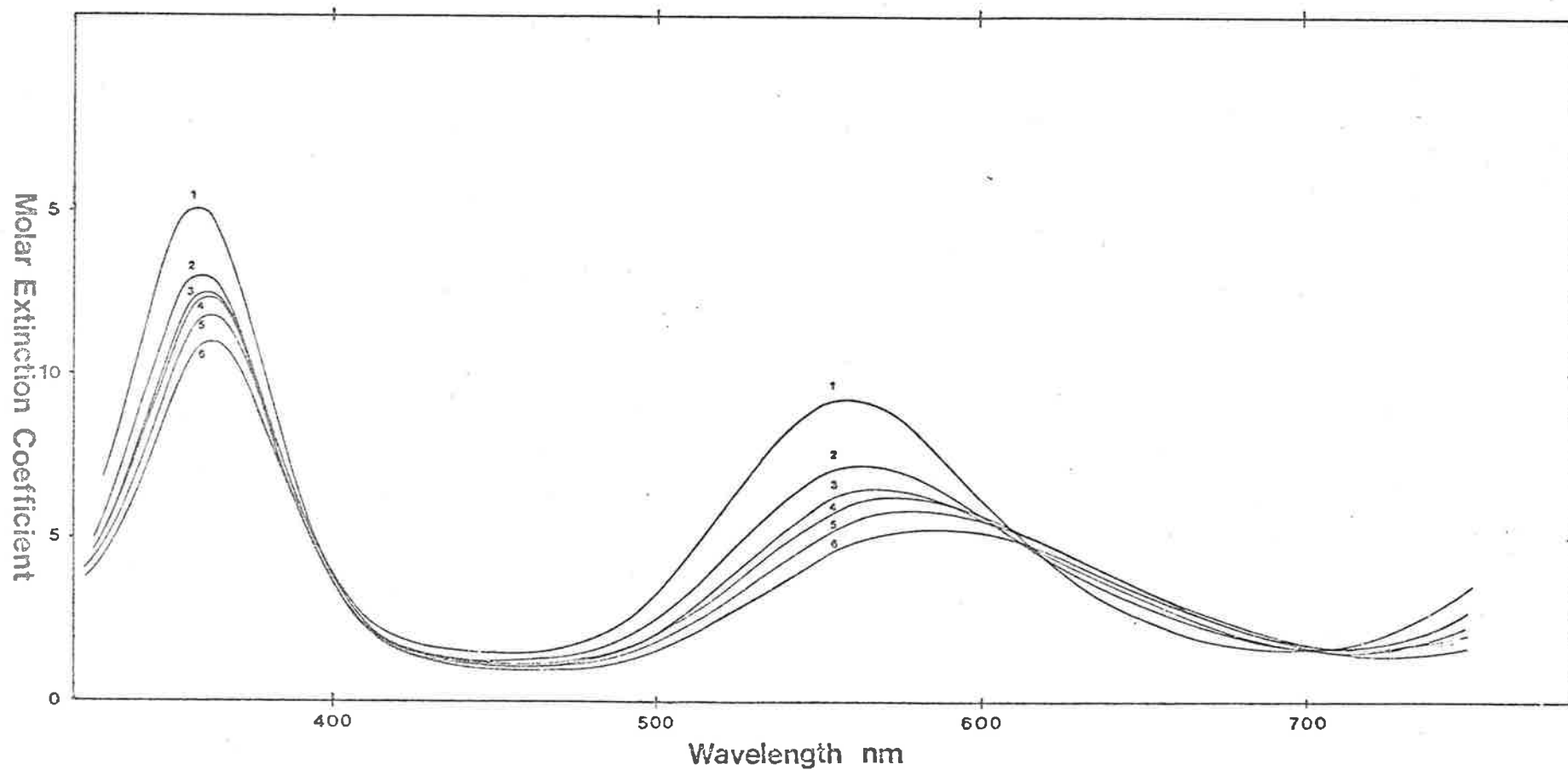


Figure 5.3 Uv/visible spectra of $2.50 \times 10^{-2} \text{ mol dm}^{-3} [\text{Ni}(12\text{aneN}_4)](\text{ClO}_4)_2$ in 0.0, 0.2, 0.4, 0.6, 0.8 and 1.0 $\text{mol dm}^{-3} \text{HClO}_4$ (from 1 to 6 respectively) at 288.2 K (ionic strength = 1.0). The spectra were recorded immediately after making the solutions.

Figure 5.4

Uv/visible spectra of $3.48 \times 10^{-2} \text{ mol dm}^{-3} [\text{Ni}(12\text{aneN}_4)](\text{ClO}_4)_2$ at increasing times after mixing in $1.0 \text{ mol dm}^{-3} \text{ HClO}_4$ (ionic strength = 1.0) at 312.1 K. Time intervals are 0, 12, 23, 34 and 45 minutes for the spectra from 1 to 5 respectively. Spectrum (6) is the equilibrium spectrum. Spectrum (7) was obtained by mixing $[\text{Ni}(\text{OH}_2)_6]^{2+}$ and 12aneN₄ in $1.0 \text{ mol dm}^{-3} \text{ HClO}_4$ (after heating at 312.1 K for about two hours) whereas spectrum (8) is the difference spectrum between (6) and (7). Spectrum (9) was obtained by adding the spectra of $[\text{Ni}(\text{OH}_2)_6]^{2+}$ and 12aneN₄ in $1.0 \text{ mol dm}^{-3} \text{ HClO}_4$ run separately (after heating at 312.1 K for about two hours) whereas spectrum (10) is the difference spectrum between spectra (9) and (6).

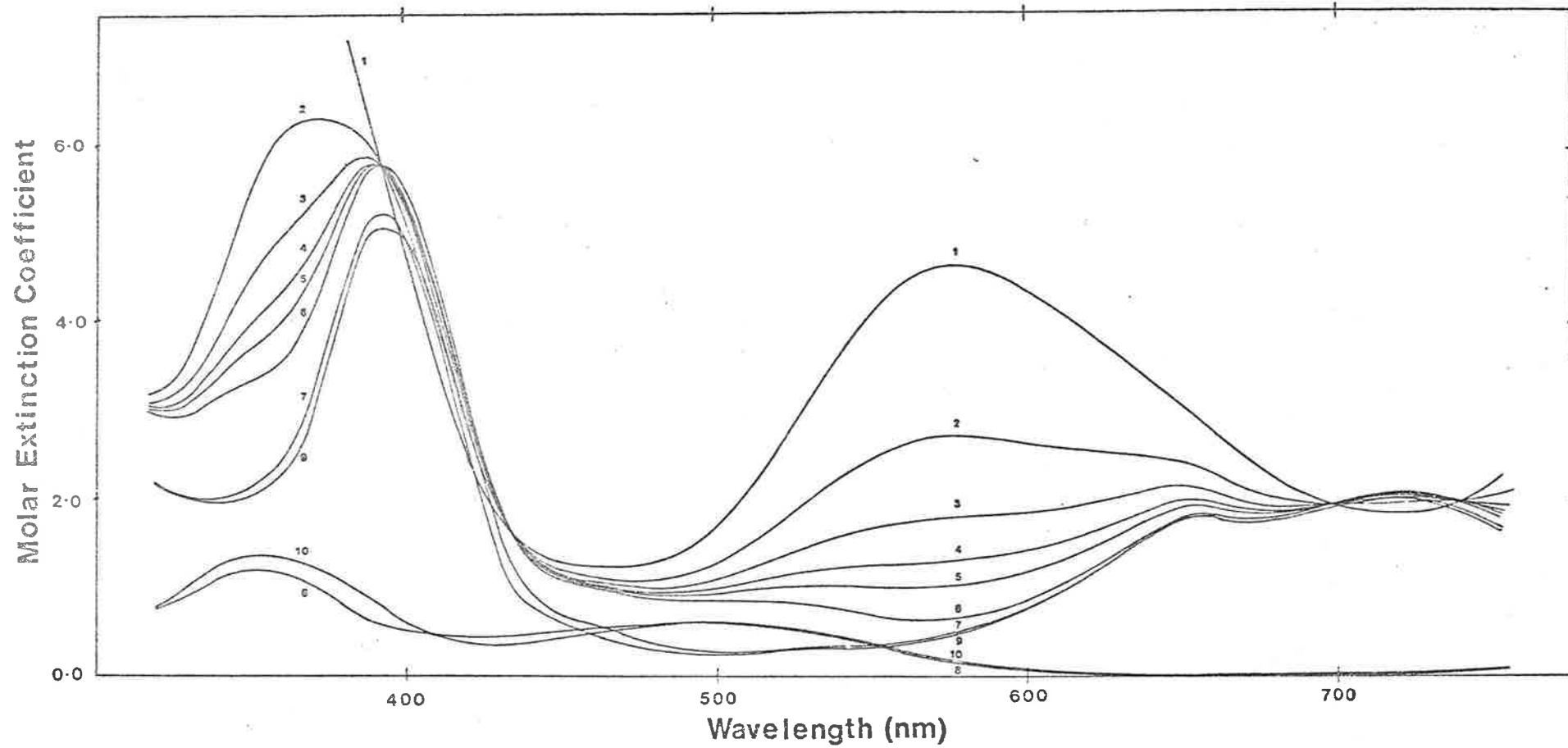


Figure 5.4

Table 5.2

Shifting of absorbance band for $[\text{Ni}(\text{12aneN}_4)](\text{ClO}_4)_2$

$[\text{HClO}_4]$ mol dm^{-3}	0.2	0.2	0.4	0.6	0.8	1.0
wavelength of absorbance band	558.5	563.0	570.5	574.0	578.5	583.5

$1.0 \text{ mol dm}^{-3} \text{ HClO}_4$ (ionic strength = 1.0) at 312.1K. The equilibrium spectrum (6) was obtained after eight half lives. Spectrum (7) was obtained by mixing $[\text{Ni}(\text{OH}_2)_6]^{2+}$ and 12aneN₄ in $1.0 \text{ mol dm}^{-3} \text{ HClO}_4$ (after heating at 312.1K for about two hours) whereas spectrum (8) is the difference spectrum between spectra (6) and (7). Spectrum (9) was obtained by adding the spectra of $[\text{Ni}(\text{OH}_2)_6]^{2+}$ and 12aneN₄ in $1.0 \text{ mol dm}^{-3} \text{ HClO}_4$ run separately (after heating at 312.1K for about two hours) and spectrum (10) is the difference spectrum between spectra (9) and (6). Theoretically for a simple dissociation reaction spectra (6), (7) and (9) should be identical, The difference between spectra 7 and 9 may be due to experimental errors. However, it appears that there is an additional species present in the equilibrium solution. The plot of observed rate constant (k_{obs}) against the acid concentration (at different temperatures and ionic strengths) is shown in Figure 5.5 and the k_{obs} values are given in Table 5.3. Since it was not possible to form the complex $[\text{Ni}(12\text{aneN}_4)(\text{OH}_2)_2]^{2+}$ at high temperature (333.2K) in $0.1 \text{ mol dm}^{-3} \text{ HClO}_4$ (ionic strength = 1.0) by reaction of $[\text{Ni}(\text{OH}_2)_6]^{2+}$ with 12aneN₄, it is thus assumed that the backward reaction does not occur apparently under the conditions used.

The rate of dissociation of $[\text{Cu}(12\text{aneN}_4)](\text{ClO}_4)_2$ with HClO_4 at low ionic strength is very slow and therefore it was studied at an ionic strength of 6.0 (adjusted by NaClO_4) under which conditions the rate is greater. The spectra of $[\text{Cu}(12\text{aneN}_4)](\text{ClO}_4)_2$ were recorded at 288.2K immediately after mixing with 0, 0.5 and $1.0 \text{ mol dm}^{-3} \text{ HClO}_4$ (ionic strength = 1.0) as well as 0, 1.0, 2.0 and $3.0 \text{ mol dm}^{-3} \text{ HClO}_4$ (ionic strength = 6.0), but the absorbance band did not shift at a fixed ionic strength probably because of the slow dissociation reaction.

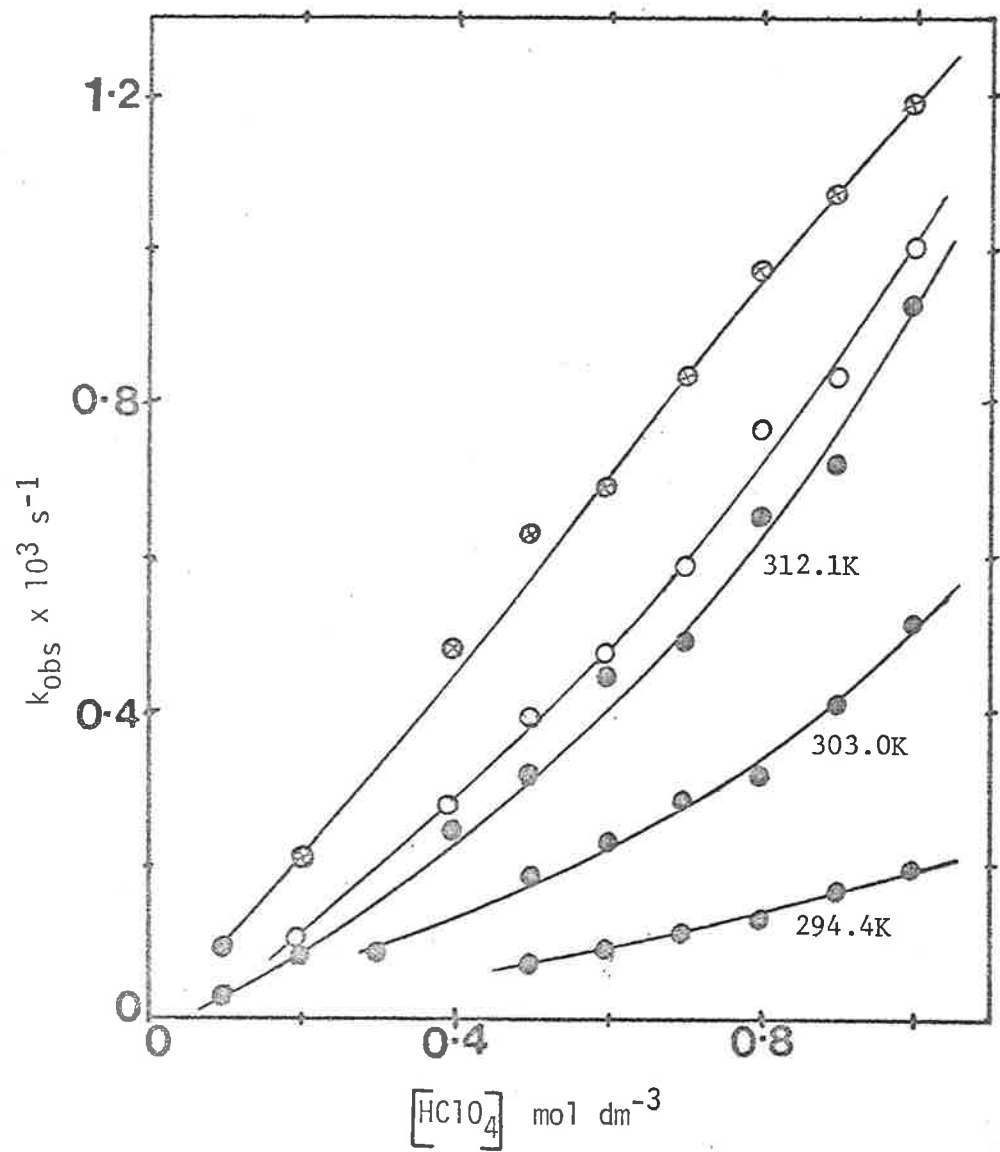


Figure 5.5

k_{obs} vs $[\text{HClO}_4]$ for the dissociation of the $[\text{Ni}(\text{12aneN}_4)](\text{ClO}_4)_2$ complex at different ionic strengths and temperatures ($\lambda = 558 \text{ nm}$). The filled circles represent kinetic data at 294.4, 303.0 and 312.1 K for ionic strength adjusted to 1.0 with NaClO_4 . The open circles represent kinetic data at 302.7 K for ionic strength 3.0 whereas the cross circles represent kinetic data at 297.4 K for ionic strength 6.0.

TABLE 5.3

 k_{obs} Values for $[\text{Ni}(\text{12aneN}_4)](\text{ClO}_4)_2$ Dissociation $\lambda = 558 \text{ nm}$

$[\text{HClO}_4]$ mol dm^{-3}	$k_{\text{obs}} \times 10^5 \text{ s}^{-1}$	$[\text{HClO}_4]$ mol dm^{-3}	$k_{\text{obs}} \times 10^5 \text{ s}^{-1}$
<u>Ionic Strength = 1.0</u>		<u>Ionic Strength = 3.0</u>	
(a) T = 294.4K		(a) T = 302.7K	
0.5	6.95 ± 0.03	0.2	10.3 ± 0.03
0.6	9.28 ± 0.05	0.4	27.8 ± 0.10
0.7	11.2 ± 0.04	0.5	39.3 ± 0.30
0.8	13.3 ± 0.09	0.6	46.9 ± 0.20
0.9	16.2 ± 0.10	0.7	58.6 ± 0.30
1.0	19.5 ± 0.10	0.8	76.1 ± 0.80
(b) T = 303.0K		0.9	83.4 ± 0.70
0.3	8.33 ± 0.06	1.0	100 ± 1.1
0.5	18.4 ± 0.17	<u>Ionic Strength = 6.0</u>	
0.6	22.8 ± 0.18	(a) T = 297.4K	
0.7	28.4 ± 0.15	0.1	9.08 ± 0.06
0.8	31.9 ± 0.09	0.2	20.7 ± 0.20
0.9	40.7 ± 0.25	0.4	48.0 ± 1.0
1.0	51.0 ± 0.67	0.5	62.7 ± 1.1
(c) T = 312.1K		0.6	68.5 ± 0.80
0.1	3.30 ± 0.04	0.7	82.9 ± 0.60
0.2	8.16 ± 0.08	0.8	97.4 ± 0.60
0.4	24.2 ± 0.10	0.9	107 ± 1.10
0.5	31.2 ± 0.40	1.0	119 ± 0.40
0.6	44.0 ± 0.28	(b) T = 303.0K	
0.7	49.0 ± 0.75	1.0	219 ± 4.6
0.8	65.0 ± 0.23	2.0	262 ± 8.6
0.9	72.0 ± 0.70		
1.0	92.8 ± 0.30		

N.B. The errors represent one standard deviation.

Figure 5.6 curves 1-7 shows the spectra obtained at times of 0, 11, 21, 31, 41, 51 and 64 minutes after mixing at 306.2K with $3.0 \text{ mol dm}^{-3} \text{ HClO}_4$ and ionic strength 6.0. The equilibrium spectrum (8) was run after at least eight half lives. The equilibrium spectrum was found to be similar to the spectrum of a mixture of $[\text{Cu}(\text{OH}_2)_6]^{2+}$ and 12aneN_4 under identical conditions, indicating that the reaction goes to completion and only two species $[\text{Cu}(\text{OH}_2)_6]^{2+}$ and $12\text{aneN}_4\text{H}_n^{n+}$ are present in the equilibrium solution. The rate of dissociation was studied at 303.0K and 313.0K at ionic strength 6.0 ($\lambda = 570\text{nm}$). At 303.0K, the reaction was also studied (ionic strength = 6.0) in presence of $0.01 \text{ mol dm}^{-3} 12\text{aneN}_4$. It was observed that the excess ligand does not have any effect on the rate of dissociation under these conditions. The plots of observed rate constants (k_{obs}) against the acid concentrations are shown in Figure 5.7 and the associated k_{obs} values are given in Table 5.4.

Because of its very slow dissociation in acid, the $[\text{Cu}(\text{Me}_412\text{aneN}_4)](\text{ClO}_4)_2$ system was studied at ionic strength 8.0 (adjusted by NaClO_4) and at high temperature to speed up the reaction. The reaction was followed at a fixed wavelength (600nm) using uv/visible spectrophotometry. The plots of observed rate constant (k_{obs}) against the acid concentrations are shown in Figure 5.8 and the associated k_{obs} values are given in Table 5.5.

The rates of dissociation are highly dependent upon acid concentration for all three complexes. A number of studies^{19, 22, 23}, involving transition metal complexes of macrocycles containing nitrogen donor atoms have shown the existence of an acid dependence pathway for dissociation. It is not possible at present to interpret the plots in Figure 5.5, 5.7 and 5.8 (curves are drawn by hand) quantitatively in terms of the degree of protonation of the complex. However, the results and observations for all three systems might

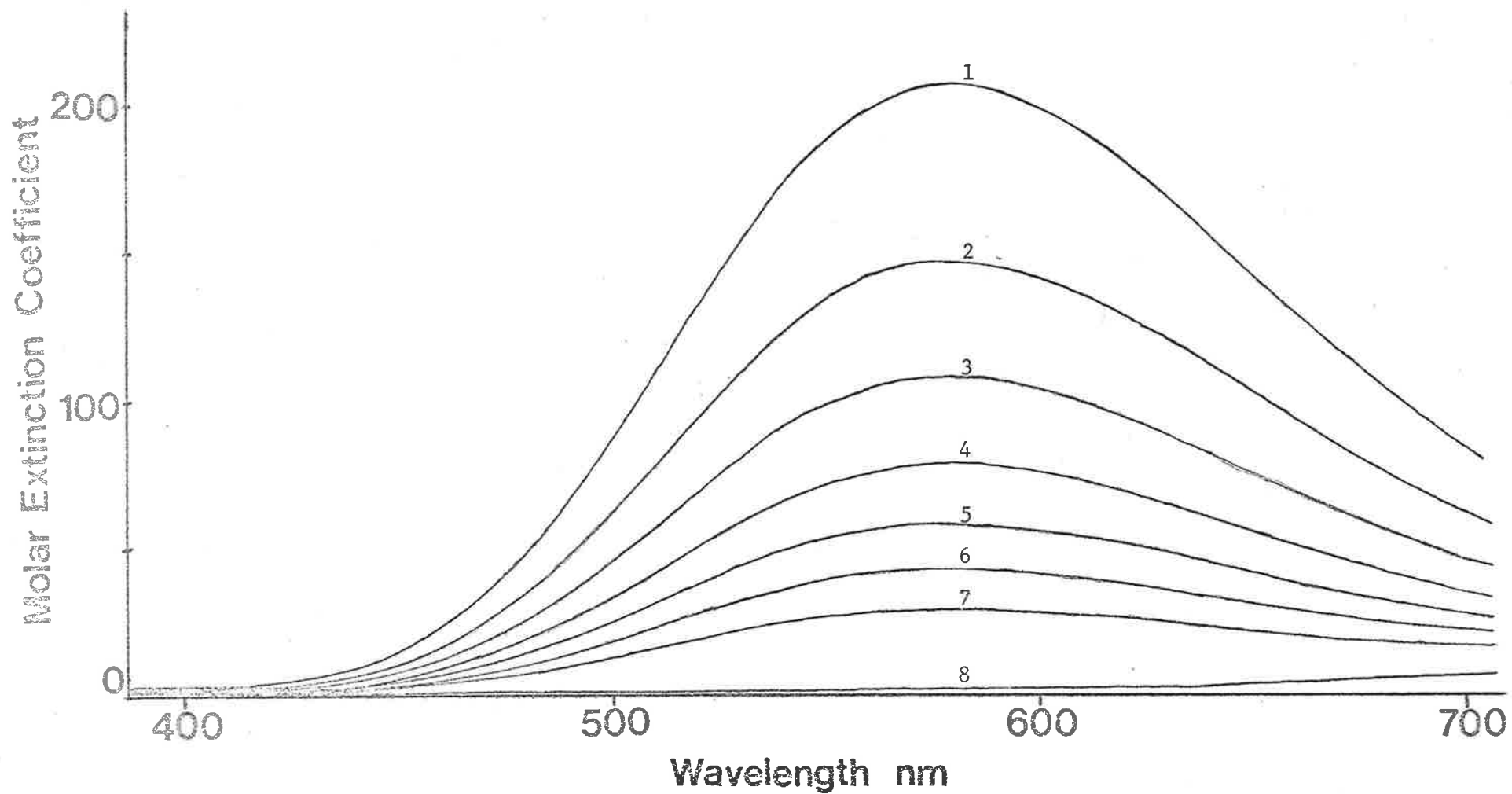


Figure 5.6 Uv/visible spectra of $1.70 \times 10^{-3} \text{ mol dm}^{-3} [\text{Cu}(12\text{aneN}_4)](\text{ClO}_4)_2$ at increasing times after mixing in $3.0 \text{ mol dm}^{-3} \text{ HClO}_4$ (ionic strength 6) at 306.2 K. Time intervals are 0, 11, 21, 31, 41, 51 and 64 minutes for the spectra from 1 to 7 respectively. Spectrum (8) is the equilibrium spectrum.

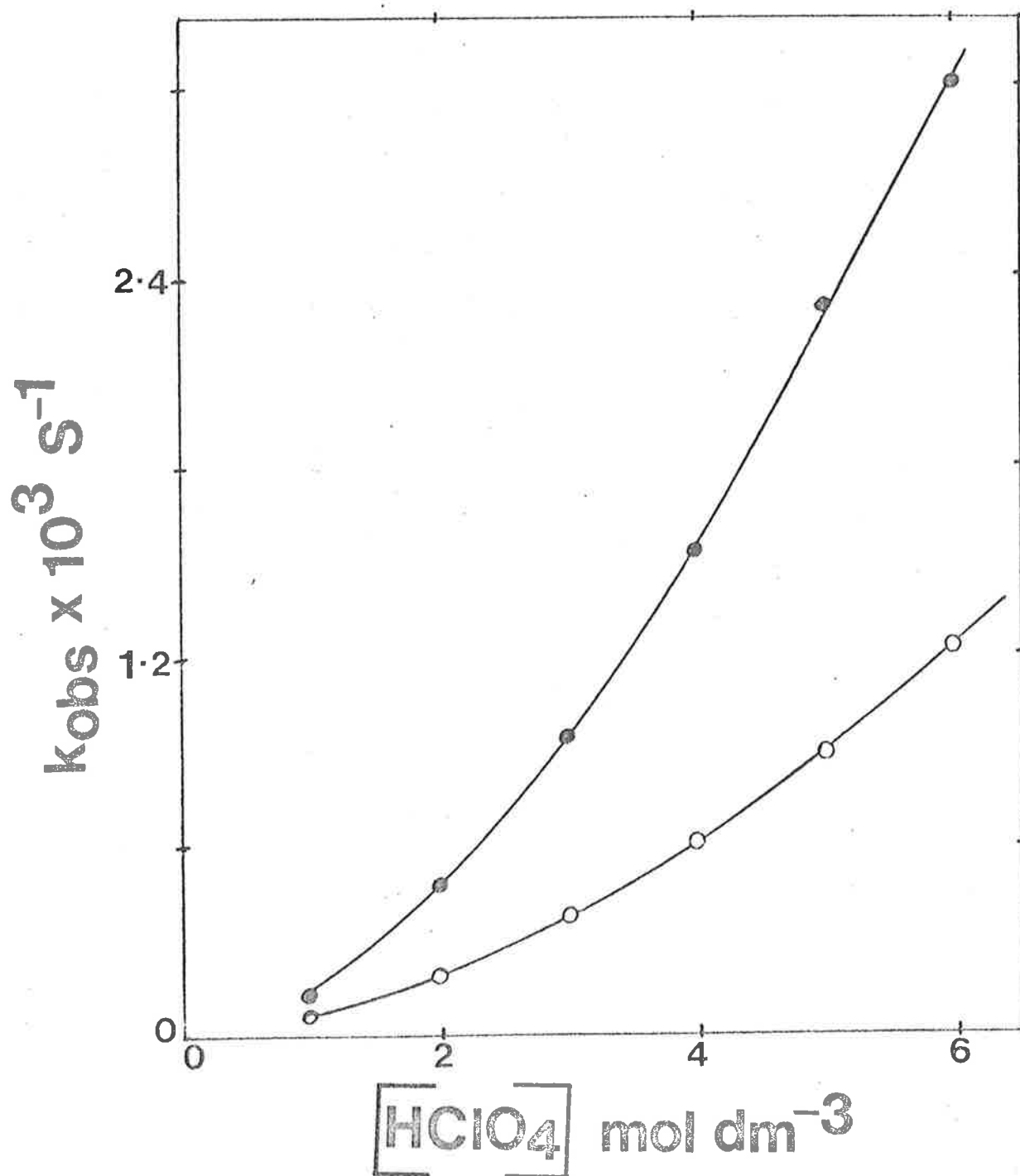


Figure 5.7 k_{obs} vs $[\text{HClO}_4]$ for the dissociation of the $[\text{Cu}(\text{12aneN}_4)](\text{ClO}_4)_2$ complex ($\lambda = 570 \text{ nm}$ and ionic strength = 6.0). The open circles and filled circles represent kinetic data at 303.0 and 313.0 K respectively.

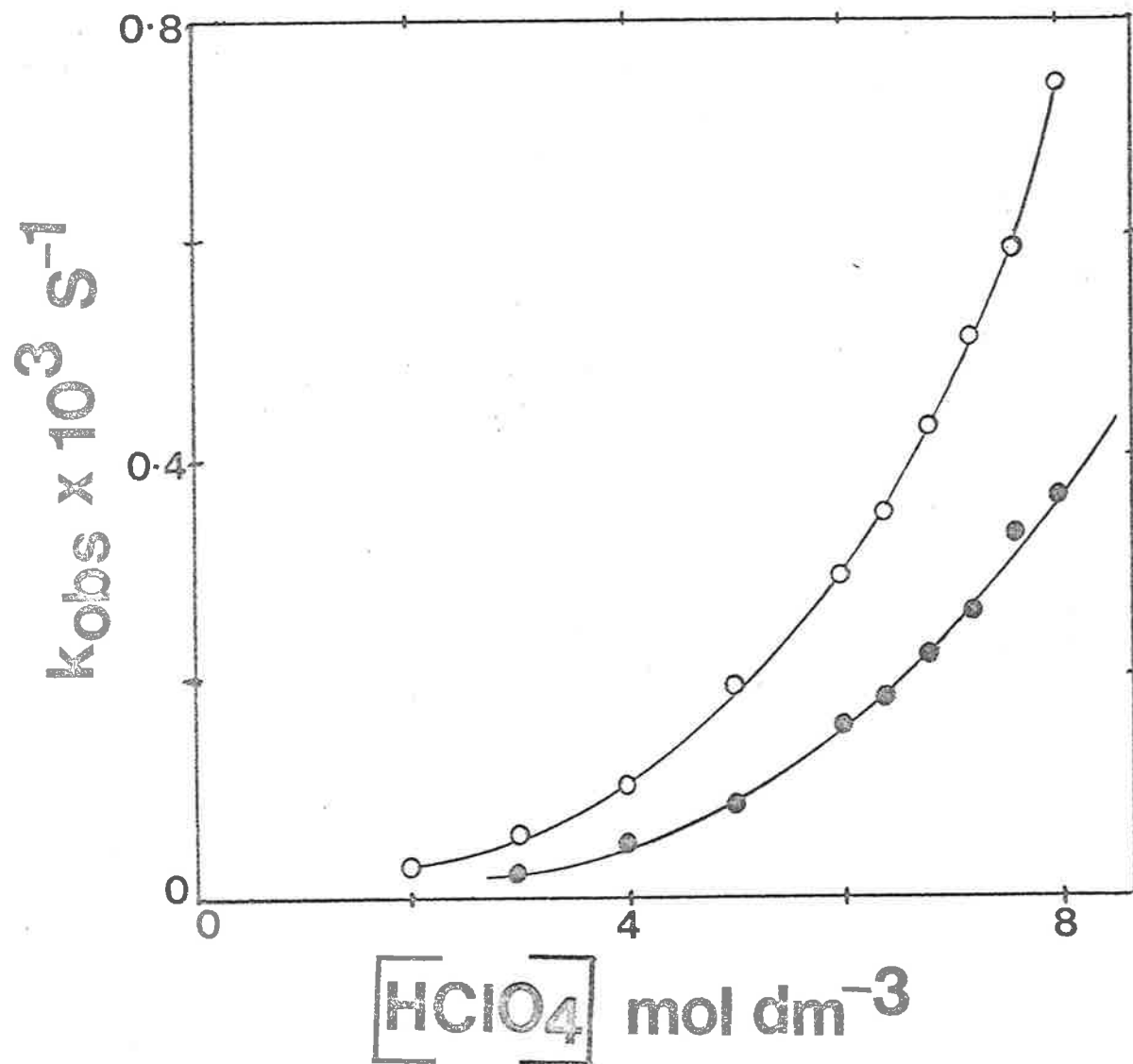


Figure 5.8 k_{obs} vs $[\text{HClO}_4]$ for the dissociation of the $[\text{Cu}(\text{Me}_4\text{12aneN}_4)](\text{ClO}_4)_2$ complex ($\lambda = 600 \text{ nm}$ and ionic strength = 8.0). The filled circles and the open circles represent kinetic data at 331.7 and 341.4 K respectively.

TABLE 5.4

k_{obs} Values for $[\text{Cu}(\text{12aneN}_4)](\text{ClO}_4)_2$ Dissociation.

$[\text{HClO}_4]$ mol dm^{-3}	$k_{\text{obs}} \times 10^5 \text{S}^{-1}$ at 303.0K	$k_{\text{obs}} \times 10^5 \text{S}^{-1}$ at 303.0K ($0.1 \text{ mol dm}^{-3} \text{12aneN}_4$ added)	$k_{\text{obs}} \times 10^5 \text{S}^{-1}$ at 313.0K
1	5.50 ± 0.01	6.49 ± 0.03	13.7 ± 0.04
2	18.5 ± 0.04	19.9 ± 0.04	46.8 ± 0.17
3	37.2 ± 0.12	36.7 ± 0.11	93.7 ± 0.44
4	60.6 ± 0.60	63.7 ± 0.14	152 ± 0.72
5	88.1 ± 0.29	91.7 ± 0.31	229 ± 1.6
6	123 ± 0.57		299 ± 2.2

N.B. The errors represent one standard deviation.

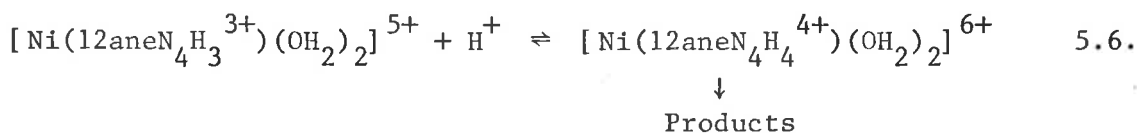
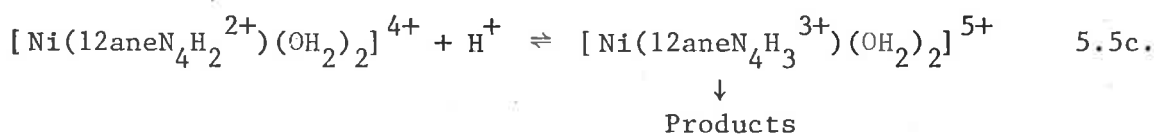
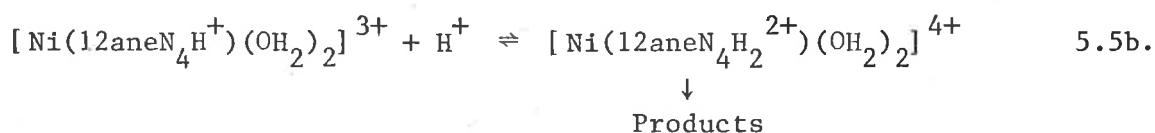
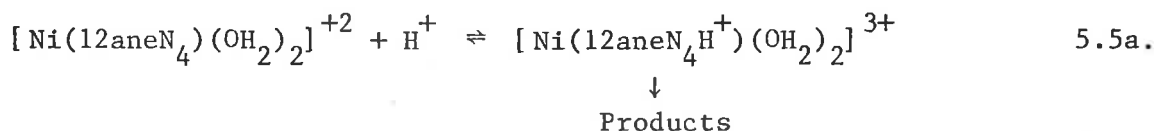
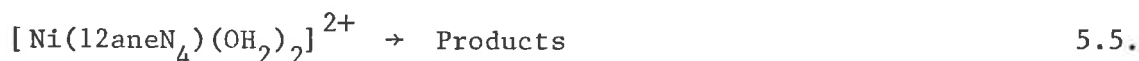
TABLE 5.5

k_{obs} Values for $[\text{Cu}(\text{Me}_4\text{12aneN}_4)](\text{ClO}_4)_2$ Dissociation

$[\text{HClO}_4]$ mol dm^{-3}	$k_{\text{obs}} \times 10^5 \text{S}^{-1}$ at 331.7K	$k_{\text{obs}} \times 10^5 \text{S}^{-1}$ at 341.4K
2		2.66 ± 0.01
3	2.63 ± 0.01	5.76 ± 0.05
4	4.82 ± 0.01	10.5 ± 0.08
5	8.36 ± 0.02	19.0 ± 0.11
6	15.3 ± 0.06	29.3 ± 0.31
6.4	18.5 ± 0.04	35.1 ± 0.24
6.8	22.0 ± 0.12	42.6 ± 0.25
7.2	25.7 ± 0.11	50.8 ± 0.21
7.6	33.0 ± 0.21	58.9 ± 0.25
8.0	36.4 ± 0.17	74.1 ± 0.43

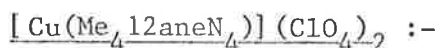
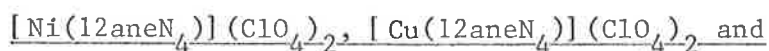
N.B. The errors represent one standard deviation.

possibly be rationalised by various protonation steps followed by dissociation of protonated species according to equations 5.5 to 5.6.



More than one protonated species may be formed in the course of the acid dissociation reaction and the proton transfer probably occurs directly to the nitrogen atoms of the ligand. Different protonated species will dissociate at different rates.

5.5 The Effect of Ionic Strength on the Rates of Dissociation of



The rates of dissociation of all the three complexes are highly dependent upon ionic strength as shown in Tables 5.6, 5.7 and 5.8. The curvature in Figure 5.5 decreases as the ionic strength increases for the $[\text{Ni}(\text{12aneN}_4)](\text{ClO}_4)_2$ system. The absorbance band of $[\text{Ni}(\text{12aneN}_4)](\text{ClO}_4)_2$ at 558.5nm (spectra recorded immediately after

TABLE 5.6

Ionic Strength Effect for $[\text{Ni}(\text{12aneN}_4)](\text{ClO}_4)_2$ Dissociation
with $1.0 \text{ mol dm}^{-3} \text{ HClO}_4$ (303.0K)

Ionic Strength	1	3	6
$k_{\text{obs}} \times 10^5 \text{ s}^{-1}$	51.0 ± 0.67	100 ± 1.1	219 ± 4.6

TABLE 5.7

Ionic Strength Effect for $[\text{Cu}(\text{12aneN}_4)](\text{ClO}_4)_2$ Dissociation
with $3.0 \text{ mol dm}^{-3} \text{ HClO}_4$ (303.0K).

Ionic Strength	3	6
$k_{\text{obs}} \times 10^5 \text{ s}^{-1}$	13.9 ± 0.04	37.2 ± 0.12

TABLE 5.8

Ionic Strength Effect for $[\text{Cu}(\text{Me}_4\text{12aneN}_4)](\text{ClO}_4)_2$ Dissociation (341.4K).

Ionic Strength	$6(6.0 \text{ mol dm}^{-3} \text{ HClO}_4)$	$8(6.0 \text{ mol dm}^{-3} \text{ HClO}_4$ and $2.0 \text{ mol dm}^{-3} \text{ NaClO}_4)$	$7.2(7.2 \text{ mol dm}^{-3} \text{ HClO}_4)$	$8(7.2 \text{ mol dm}^{-3} \text{ HClO}_4$ and $0.8 \text{ mol dm}^{-3} \text{ NaClO}_4)$
$k_{\text{obs}} \times 10^5 \text{ s}^{-1}$	6.66 ± 0.02	29.3 ± 0.31	27.0 ± 0.05	50.8 ± 0.21

TABLE 5.9

Ionic Strength Effect on the Shifting of Absorbance Band with
 $1.0 \text{ mol dm}^{-3} \text{ HClO}_4$ (288.2K) for $[\text{Ni}(\text{12aneN}_4)](\text{ClO}_4)_2$ Dissociation

Ionic Strength	1	2	3	4	5	6
Wavelength of Absorbance Band	579,0	589.5	597.5	603.5	508.5	611.6

N.B. The errors represent one standard deviation.

mixing) is observed to shift towards the higher wavelength as the ionic strength increases when the acid concentration is constant (Table 5.9). In the case of the $[\text{Cu}(\text{12aneN}_4)](\text{ClO}_4)_2$ system, the absorbance band for ionic strength 1.0 ($1.0 \text{ mol dm}^{-3} \text{ HClO}_4$) occurs at 585nm whereas for ionic strength 6.0 ($1.0 \text{ mol dm}^{-3} \text{ HClO}_4$ and $5.0 \text{ mol dm}^{-3} \text{ NaClO}_4$), it appears at 575nm showing a shift towards the lower wavelength as the ionic strength increases (spectra recorded immediately after mixing at 288.2K).

The effect of ionic strength at a constant acid concentration is to increase the rate of dissociation for all the three complexes. The higher ionic strength results in the reduction of charge-charge repulsion between charged complex and acid, therefore the association constant for the hydrogen ion with the complex will be greater. This will produce a higher concentration of highly protonated species for which the rate of dissociation is markedly enhanced.

5.6 The Reaction of $[\text{Ni}(\text{12aneN}_4)(\text{OH}_2)]^{2+}$ with Sodium Hydroxide:-

On addition of NaOH to a purple aqueous solution of $[\text{Ni}(\text{12aneN}_4)(\text{OH}_2)_2]^{2+}$, the solution becomes blue and the original purple colour reappears on addition of acid (HClO_4). Similarly, a blue solution of $[\text{Cu}(\text{12aneN}_4)(\text{OH}_2)_2]^{2+}$ changes to light blue on addition of NaOH and the original colour reappears on addition of acid. The colour change in this system is too fast to be studied by the stopped flow technique. (Colour changes from yellow to yellowish green and yellow to yellowish blue are also observed on addition of NaOH to aqueous solutions of $[\text{Ni}(\text{13aneN}_4)](\text{ClO}_4)_2$ and $[\text{Ni}(\text{14aneN}_4)](\text{ClO}_4)_2$, respectively.) The $[\text{Ni}(\text{12aneN}_4)]^{2+}$ system was studied at 0.125, 0.25 and 0.5 mol dm^{-3} NaOH (ionic strength = 2.0 adjusted with NaClO_4) at 560nm by stopped flow technique under

pseudo 1st order conditions. The k_{obs} value was found (Table 5.10) to be independent of the concentrations of sodium hydroxide. The

TABLE 5.10

k_{obs} Values for Reaction of $[\text{Ni}(\text{12aneN}_4)(\text{OH}_2)_2]^{2+}$ with NaOH

[NaOH] mol dm ⁻³	k_{obs} S ⁻¹ 308.2K	k_{obs} S ⁻¹ 313.2K	k_{obs} S ⁻¹ 318.5K
0.125	(0.313 ± 0.04)		(1.25 ± 0.13)
0.25	(0.338 ± 0.03)	(0.414 ± 0.04)	(1.18 ± 0.13)
0.50	(0.316 ± 0.04)	(0.425 ± 0.03)	(1.16 ± 0.11)
N.B. The errors represent one standard deviation			

kinetic parameters ΔH^\ddagger and ΔS^\ddagger are obtained from least squares analysis using equation 5.7 (see equation 4.9, Chapter 4)

$$k_{\text{obs}} = \frac{k_B T}{h} e^{-\Delta H^\ddagger / RT} e^{\Delta S^\ddagger / R} \quad 5.7$$

for the system. The ΔH^\ddagger and ΔS^\ddagger values are found to be (101 ± 35) kJ mol⁻¹ and (73 ± 30) JK⁻¹ mol⁻¹ respectively (one standard deviation error). Both bands at 357nm and 558.5nm in the uv/visible spectrum of $[\text{Ni}(\text{12aneN}_4)(\text{OH}_2)_2]^{2+}$ (ionic strength = 1.0) are shifted slightly towards the higher wavelength in 0.5 mol dm⁻³ NaOH (ionic strength = 1.0). The water exchange rate constant on $[\text{Ni}(\text{12aneN}_4)(\text{OH}_2)_2]^{2+}$ is very fast and therefore substitution by hydroxide ion is expected to be fast. The purple to blue interconversion of $[\text{Ni}(\text{12aneN}_4)(\text{OH}_2)_2]^{2+}$ with NaOH may possibly be accounted for by an isomerisation in which inversion of nitrogen atoms are required to attain thermodynamic equilibrium. In principle four such isomers may arise: i) four hydrogens on the same side of the ring; ii) three hydrogens on the same side;

iii) two hydrogens on either side (cis); iv) two hydrogens on either side (trans). The available data cannot be used to distinguish between these possibilities. As the pH increases the absorbance of $[\text{Ni}(\text{12aneN}_4(\text{OH}_2)_2)]^{2+}$ in water also increases at all wavelengths and markedly increases at 350nm, therefore strong base may deprotonate the complex, and this proton transfer reaction is expected to be very fast.

5.7 General Discussion.

The kinetics of formation of transition metal complex with 12 - 16 membered tetra aza macrocycles have been studied²¹ by others using pH stat and stopped flow techniques. The results have been analysed as bimolecular reactions between the metal ions and various protonated species of the ligands. The rate of complexation for a given protonated species of the ligand follows the order Copper (II) > zinc (II) > cobalt (II) > nickel (II) which parallel the sequence of their water exchange rates and the macrocycles react less rapidly than the analogous open chain amines. A study of the complexation of $[\text{Cu}(\text{12aneN}_4)]^{2+}$ by a polarographic method using acetate buffer was reported^{14, 41} in which complicated mechanisms were proposed explaining the pH dependence of the rate constant. The observed rate constants of $[\text{Ni}(\text{12aneN}_4)]^{2+}$ formation complexation were found to be $(0.75 \pm 0.02) \times 10^{-3} \text{ s}^{-1}$ and $(2.61 \pm 0.13) \times 10^{-3} \text{ s}^{-1}$ at pH 5.95 and 6.60 respectively in this study. It was found (see Chapter 2) that 12aneN₄ accepts two protons when titrated with 1.0 mol dm⁻³ HClO₄ (ionic strength 1.0) and therefore mono and diprotonated 12aneN₄ are expected to be present within the pH range studied. The two protons are forced much closer together in the 12aneN₄ structure than in the more flexible analogous open chain amine 2,2,2-tet. Therefore the complexation

of $[\text{Ni}(\text{12aneN}_4)]^{2+}$ is slower than that of the open chain amine. As the pH increases, the k_{obs} value increases showing that the mono-protonated species is more reactive than the diprotonated species. The pH dependence of k_{obs} is consistent with similar systems.^{9, 12-14, 19, 21, 41, 42,}

A qualitative experiment showed that the rate of dissociation of $[\text{Ni}(\text{Me}_4\text{12aneN}_4)](\text{ClO}_4)_2$ is slower than that of $[\text{Ni}(\text{12aneN}_4)](\text{ClO}_4)_2$ with HClO_4 under identical conditions showing the effect of steric hindrance. The $[\text{Ni}(\text{13aneN}_4)](\text{ClO}_4)_2$ complex also dissociates very slowly with HClO_4 but with HCl , the dissociation becomes faster showing that the chloride ion influences the rate of dissociation. The k_{obs} values for the rate of dissociation of $[\text{Ni}(\text{13aneN}_4)](\text{ClO}_4)_2$ with 0.3, 1.0, 2.0 and 5.0 mol dm^{-3} HCl at 341.3K (430nm, ionic strength 5.0 adjusted by NaCl) are obtained in this study (under pseudo 1st order conditions) as $(38.4 \pm 0.5) \times 10^{-5} \text{s}^{-1}$, $(58.8 \pm 0.5) \times 10^{-5} \text{s}^{-1}$, $(66.4 \pm 0.8) \times 10^{-5} \text{s}^{-1}$ and $(83.3 \pm 2.6) \times 10^{-5} \text{s}^{-1}$, respectively. On anticipating a complicated mechanism, further studies were not carried out with HCl dissociation of $[\text{Ni}(\text{13aneN}_4)](\text{ClO}_4)_2$. The data from Table 5.11 shows that the rate of dissociation of $[\text{Ni}(\text{12aneN}_4)](\text{ClO}_4)_2$ is faster than that of $[\text{Cu}(\text{12aneN}_4)](\text{ClO}_4)_2$ which in turn is faster than that of $[\text{Cu}(\text{Me}_4\text{12aneN}_4)](\text{ClO}_4)_2$. From these observations, it appears that the dissociation of the 12-membered complex is faster than that of the 13-membered complex and the steric crowding on the nitrogen atoms dramatically decrease the rate of dissociation. These results are also consistent with similar observations.^{19, 23, 27}

Raycheba and Margerum⁴³ reported the acid dissociation of nickel (II) tetraglycinamide and concluded that as many as three protons can assist in the acid dissociation. The rate of dissociation was found to be highly dependent on pH. The plot

TABLE 5.11
Half Lives for $[\text{Ni}(\text{12aneN}_4)](\text{ClO}_4)_2$, $[\text{Cu}(\text{12aneN}_4)](\text{ClO}_4)_2$
and $[\text{Cu}(\text{Me}_4\text{12aneN}_4)](\text{ClO}_4)_2$ Dissociation.

	$[\text{Ni}(\text{12aneN}_4)]^{2+}$ System	$[\text{Cu}(\text{12aneN}_4)]^{2+}$ System	$[\text{Cu}(\text{Me}_4\text{12aneN}_4)]^{2+}$ System
Half Lives	9.65 minutes at 297.4K (1.0 mol dm ⁻³ HClO ₄ and ionic strength 6.0)	210.0 minutes at 303.0K (1.0 mol dm ⁻³ HClO ₄ and ionic strength 6.0) 12.3 minutes at 313.0K (3.0 mol dm ⁻³ HClO ₄ and ionic strength 6.0)	439.3 minutes at 331.7K (3.0 mol dm ⁻³ HClO ₄ and ionic strength 8.0)

of k_{obs} for nickel (II) tetra-glycinamide dissociation against acid concentration is similar to the plots in Figures 5.5, 5.7 and 5.8 for $[\text{Ni}(\text{12aneN}_4)](\text{ClO}_4)_2$, $[\text{Cu}(\text{12aneN}_4)](\text{ClO}_4)_2$ and $[\text{Cu}(\text{Me}_4\text{12aneN}_4)](\text{ClO}_4)_2$ dissociation. As with the case of nickel (II) tetraglycinamide system, the protonation step for these systems (reported here) are expected to be fast, equilibrium constant becoming smaller as the higher protonated species are formed. Different protonated species will dissociate at different rates and the higher protonated species will dissociate faster than that of lower protonated species, thereby increasing the overall observed rate constant with increasing acid concentration.

Margerum and co-workers⁴⁴ observed that the blue-to-red interconversion of Cu(5,5,7,12,12,14-hexamethyl-1,4,8,11-tetra-azacyclotetradecane is base catalysed. The blue isomer is converted into the red isomer very slowly in slightly basic solution. The rate of interconversion increases as the pH increase up to pH 12 after which the rate becomes nearly constant. It was concluded from crystal structure determination of blue and red

isomers that two of the nitrogen atoms must invert for the blue-to-red reaction. They proposed that blue-to-red interconversion occurs via monohydroxy species (blue) and co-ordinated hydroxide is much more reactive than free hydroxide. The pH dependence of the kinetic data and the fact that halide ions inhibit the interconversion reaction by blocking hydroxide ion from a co-ordination site support this proposal.

Poon and Tobe⁴⁵ observed that the cis-to-trans isomerisation of $\text{cis-}[\text{Co}(\text{14aneN}_4)\text{Cl}_2]^+$ is accompanied by the exchange of two of the four amine protons, the most likely way of inverting co-ordinated nitrogen atoms. They proposed from their studies of the kinetics of the exchange of the amine protons of $\text{trans-}[\text{Co}(\text{14aneN}_4)(\text{OH}_2)_2]^{3+}$ and $\text{trans-}[\text{Co}(\text{14aneN}_4)(\text{OH})(\text{OH}_2)]^{2+}$ as a function of pH that the facile hydrogen exchange and isomerisation of these hydroxoquo complexes is a consequence of an intramolecular proton transfer from nitrogen to oxygen thereby allowing the otherwise unfavoured exchange with inversion of configuration to take place. They also found chloride ion inhibition in the isomerisation studies.

The reaction of $[\text{Ni}(\text{12aneN}_4)(\text{OH}_2)_2]^{2+}$ with NaOH seems very similar with these two systems^{44,45} discussed above but with the limited data obtained, it is probable that an isomerisation reaction takes place and this is probably a consequence of inversion of nitrogen atoms because any proton transfer reaction is expected to be very fast.

REFERENCES FOR CHAPTER FIVE.

1. D. K. Cabbiness and D. W. Margerum, J.A.C.S., 91, 6540 (1969).
2. D. H. Busch, K. Farmery, V. Goedken, V. Katovic, A. C. Melnyk, C. R. Sperati and N. Tokel, Advanced Chem. Ser., No. 100, 44 (1971).
3. F. P. Hinz and D. W. Margerum, J.A.C.S., 96, 4993 (1974).
4. J. D. Lamb, Reed M. Izatt, J. J. Christensen and D. J. Eatough in "Co-ordination Chemistry of Macrocyclic Compounds", edited by G. A. Melson, Plenum Press, New York (1979).
5. C. Nave and M. R. Truter, J.C.S., Dalton, 2351 (1974).
6. B. Bosnich, M. L. Tobe and G. A. Webb, Inorg. Chem., 4, 1109 (1965).
7. N. F. Curtis, D. A. Swann and T. N. Waters, J.C.S., Dalton, 1408 (1973).
8. L. Fabbrizzi, Inorg. Chim. Acta., 40, X45 (1980).
9. P. S. Grunow and T. A. Kaden, Helv. Chim. Acta., 61, 2291 (1978).
10. T. A. Kaden, Helv. Chim. Acta., 53, 617 (1970).
11. D. W. Margerum, D. B. Rorabacher and J. F. Clarke, Inorg. Chem., 2, 667 (1963).
12. R. W. Hay and C. R. Clarke, J.C.S., Dalton, 1148 (1977).
13. M. Kodama, J.C.S., Chem. Comm., 891 (1975).
14. M. Kodama, J.C.S., Chem. Comm., 326 (1975).
15. D. K. Cabbiness and D. W. Margerum, J.A.C.S., 92, 2151 (1970).
16. A. Ekstrom, L. Findoy, L. Hyacinth, R. Smith, H. Goodwin, M. M. McPartlin and P. Tasker, J.C.S., Dalton, 1027 (1979).
17. M. Kodama and E. Kimura, J.C.S., Dalton, 2269 (1977).
18. B. F. Liang and C. S. Chung, J.C.S., Dalton, 1349 (1980).
19. L. Hertli and T. A. Kaden, Helv. Chim. Acta., 57, 1328 (1974).
20. L. Diaddario, L. Zimmes, T. Jones, L. Sokol, R. Cruz, E. Yee, L. Ochrymowycz and D. Rorabacher, J.A.C.S., 101, 3511 (1979).
21. A. P. Leugger, L. Hertli and T. A. Kaden, Helv. Chim. Acta., 61, 2296 (1978).

22. G. W. Liesegang and E. M. Eyring in "Synthetic Multidentate Macrocyclic Compounds" edited by R. M. Izatt and J. J. Christensen, Academic Press, New York (1978).
23. D. H. Busch, *Acc. Chem. Res.*, 11, 392 (1978).
24. A. Anichini, L. Fabbrizzi, P. Paoletti and R. M. Clay, *Inorg. Chim. Acta.*, 22, L25 (1977).
25. A. Die and R. Gori, *Inorg. Chim. Acta.*, 14, 157 (1974).
26. L. F. L. and R. J. S., *J.A.C.S.*, 101, 4014 (1979).
27. A. Ekstrom, L. F. Lindoy and R. J. Smith, *Inorg. Chem.*, 19, 724 (1980).
28. D. P. Rillema, J. F. Endicott and J. R. Barber, *J.A.C.S.*, 95, 6988 (1973).
29. D. M. Adams and J. B. Raynor, "Advanced Practical Inorganic Chemistry", John Wiley, London (1965).
30. P. Job, *Ann. Chim., Paris*, 9, 113 (1928).
31. M. Eigen, "Proceedings of the VIIth International Conference on Co-ordination Chemistry", Butterworths, London, 97 (1962); C. H. Langford and H. B. Gray, "Ligand Substitution Processes", W. A. Benjamin, Inc., New York (1966).
32. F. M. Beringer and E. M. Gindler, *J.A.C.S.*, 77, 3200 (1955).
33. R. Gorassi, A. Haim and W. Wilmarth, *Inorg. Chem.*, 6, 237 (1967).
34. R. G. Wilkins, "The Study of Kinetics and Mechanisms of Reactions of Transition Metal Complexes", Boston, Allyn and Bacon (1976).
35. N. Sutin in "The Kinetics of Inorganic Reactions in Solution", *Ann. Rev. Phy. Chem.* edited by H. Eyring, Vol. 17 (1966).
36. R. M. Fuoss, *J.A.C.S.*, 80, 5059 (1958).
37. A.G. Desai, H.W. Dodgen and J.P. Hunt, *J.A.C.S.*, 92, 798 (1970).
38. C. H. Langford and H. B. Gray, "Ligand Substitution Processes", W. A. Benjamin, Inc., New York (1966).
39. P. K. Chattopadhyay and B. Kratochvil, *Can. J. Chem.*, 55, 3449 (1977).
40. R. G. Wilkins, *Acc. Chem. Res.*, 3, 408 (1970).
41. M. Kodama and E. Kimura, *J.C.S., Dalton*, 116 (1976).
42. R. Buxtorf and T. A. Kaden, *Helv. Chim. Acta.*, 57, 1035 (1974).

43. J. M. T. Raycheba and D. W. Margerum, *Inorg. Chem.*, 19, 497 (1980).
44. B. F. Liang, D. W. Margerum and C. S. Chung, *Inorg. Chem.*, 18, 2001 (1979).
45. C. K. Poon and M. L. Tobe, *Inorg. Chem.*, 7, 2398 (1968);
C. K. Poon, *Co-ordination Chem. Rev.*, 10, 1 (1973).

CHAPTER SIX

Non-aqueous Chemistry

Contents.

6.1. Introduction

6.2. Determination of the Stoichiometry of the Metal-macrocylic
Complexes in dmf.

6.3. Rate Measurements on the Formation of

6.3.1. $[\text{Ni}(\text{Me}_4\text{14aneN}_4)]^{2+}$ Complex.6.3.2. $[\text{Ni}(\text{Me}_4\text{12aneN}_4)]^{2+}$ Complex.6.3.3. $[\text{Cu}(\text{Me}_4\text{12aneN}_4)]^{2+}$ Complex.6.3.4. $[\text{Cu}(\text{Me}_4\text{14aneN}_4)]^{2+}$ Complex.6.3.5. $[\text{Co}(\text{Me}_4\text{14aneN}_4)]^{2+}$ Complex6.4. The Temperature Dependence of the Spin-equilibria of
Nickel (II) Complexes.

6.5. General Discussion.

CHAPTER SIX

Non-Aqueous Chemistry6.1. Introduction.

Macrocyclic ligands form more stable complexes¹⁻³ with metal ions than do their open chain analogues. This enhanced stability, the macrocyclic effect, is one of the main reasons for wide spread attention to these ligands. The ability to discriminate among closely related metal ions based on the relative fit of the ligand cavity size to the metal ion radius (ring size effect)^{1, 3-6} is another reason for interest in macrocyclic ligands. The kinetics of formation of metal complexes with macrocyclic ligands containing nitrogen⁷⁻¹⁵ or the polyether crown type¹⁶⁻¹⁸ or sulphur¹⁹ donors have recently been reported. Although most of these investigations have been carried out in aqueous media, several studies involving other solvents¹⁸⁻²⁰ have also been reported. In this chapter results from the study of the rate of formation of nickel (II), copper (II) and cobalt (II) complexes with Me₄12aneN₄ and Me₄14aneN₄ in dmf are reported for the first time. Spin-equilibria measurements of nickel (II) complexes with 12aneN₄, Me₄12aneN₄ and Me₄14aneN₄ in dmf and acetonitrile are also reported here. All of the latter equilibria were found to be reversible with temperature. Systematic thermodynamic studies of metal macrocyclic complexes, i.e. [Ni(14aneN₄)](ClO₄)₂, in a variety of solvents have been previously reported.²¹⁻²³ It should be mentioned here that different nickel (II) complexes prepared in a variety of solvents (see Chapter 2) possess different properties and their spin-equilibria measurements are also

included in this chapter.

Dmf is an important aprotic solvent frequently used as a reaction medium for inorganic and organic reactions because of its ability to solvate both metal ions and non-polar organic compounds. The rate of complex formation with macrocyclic ligands is dramatically increased in dmf compared with water and the kinetics can be studied using the stopped flow technique. The stoichiometry of complex formation in dmf was measured using Job's method of continuous variation.

6.2. Determination of the Stoichiometry of the Metal Macrocyclic Complexes in dmf Solution.

Solutions of metal salt $[M(\text{dmf})_6](\text{ClO}_4)_2$ ($M = \text{metal}$) and ligand were prepared in dmf (ionic strength adjusted to 0.5 with NaClO_4). Different solution mixtures were prepared with varying amounts of ligand and metal ion for Job's method of continuous variation (see Chapter 7) and the uv/visible spectra were recorded at 298.2K. Figure 6.1, for example, shows the plot of Y ($A_{\text{measured}} - A_{\text{calculated}}$) at 396nm against mol fraction of the ligand $\left(\frac{[\text{ligand}]}{[\text{ligand}] + [\text{metal salt}]}\right)$ for $[\text{Ni}(\text{Me}_4\text{12aneN}_4)]^{2+}$ formation. The solid lines are least squares linear regression lines. The maximum occurs at 0.53 mol fraction of the ligand showing the formation of a one to one complex within experimental error. Similar experiments were performed for other complexes and the results are given in Table 6.1 and Figures 6.1 to 6.7. Within experimental error, one to one complexes were formed in all cases except for the $[\text{Cu}(\text{tb12aneN}_4)_2]^{2+}$ system where one metal ion appears to combine with two ligand molecules.

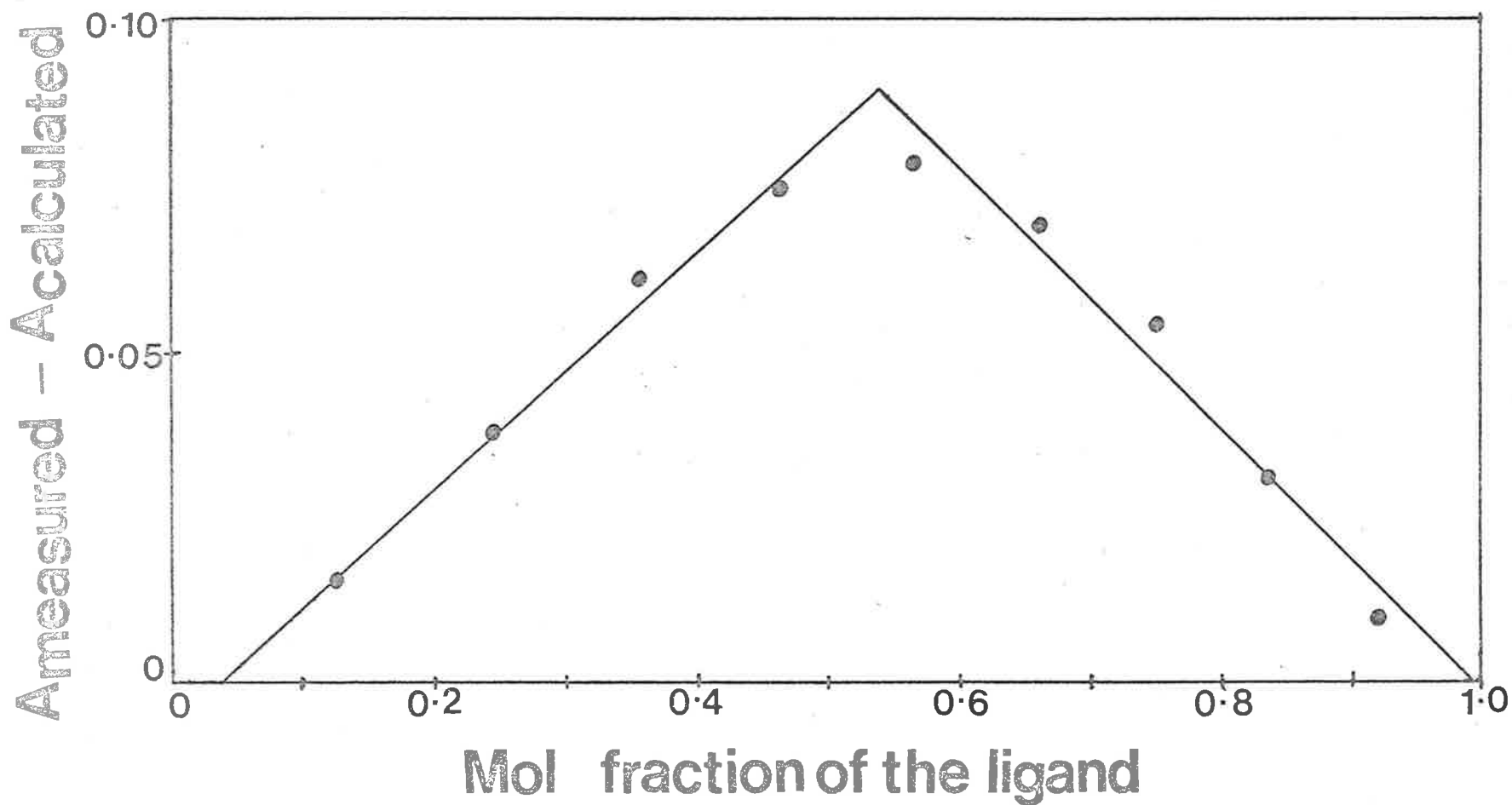


Figure 6.1 $A_{\text{measured}} - A_{\text{calculated}}$ ($\lambda = 396 \text{ nm}$ and cell path = 2 cm) vs mol fraction of $\text{Me}_4\text{12aneN}_4$ for Job's method of continuous variation for the determination of stoichiometry of $[\text{Ni}(\text{Me}_4\text{12aneN}_4)]^{2+}$ formation in dmf at 298.2 K. Stock solutions of $2.99 \times 10^{-3} \text{ mol dm}^{-3} [\text{Ni}(\text{dmf})_6](\text{ClO}_4)_2$ and $3.89 \times 10^{-3} \text{ mol dm}^{-3} \text{Me}_4\text{12aneN}_4$ were used (ionic strength adjusted to 0.5 with NaClO_4).

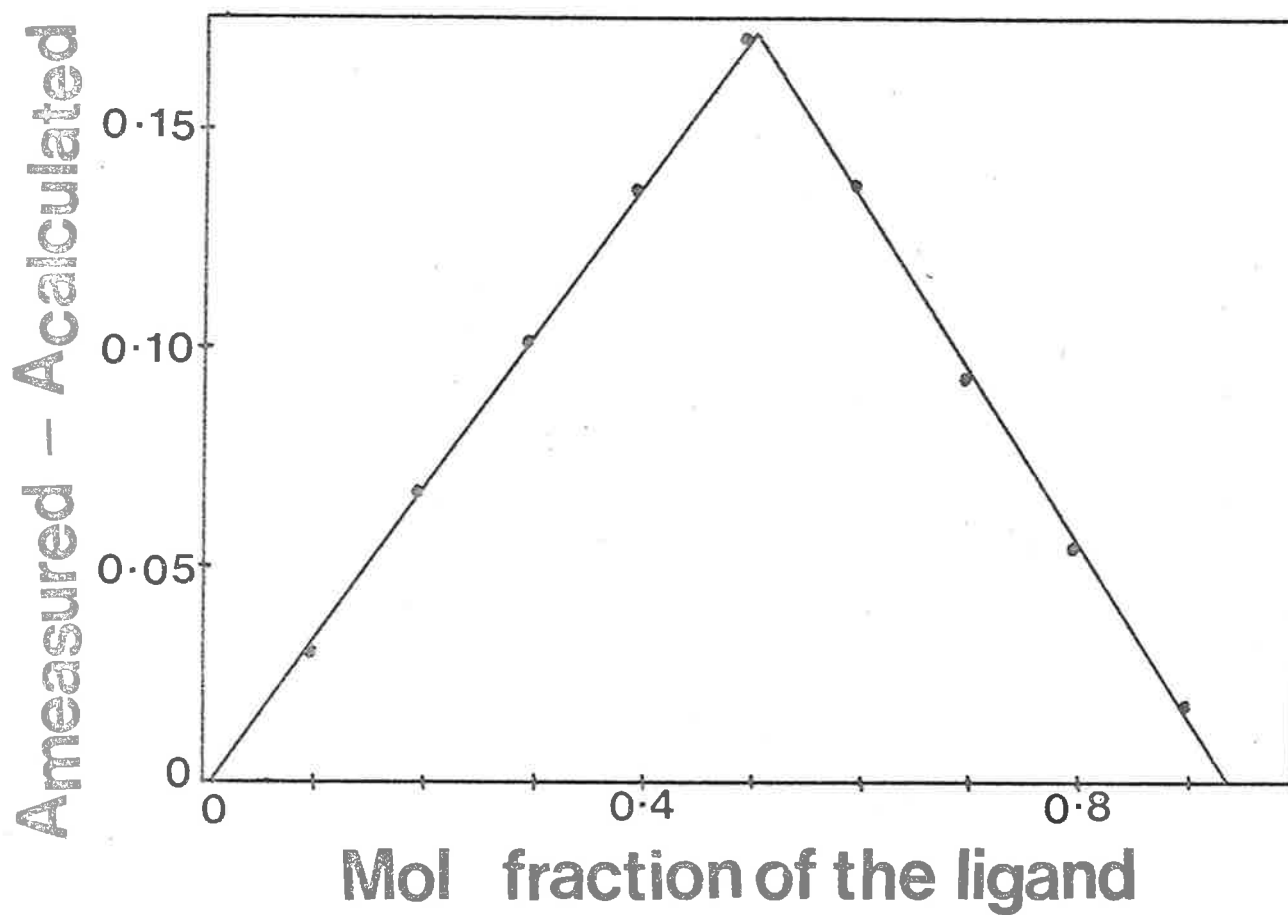


Figure 6.2 $A_{\text{measured}} - A_{\text{calculated}}$ ($\lambda = 398 \text{ nm}$ and cell path = 1 cm) vs mol fraction of $\text{Me}_4\text{14aneN}_4$ for Job's method of continuous variation for the determination of stoichiometry of $[\text{Ni}(\text{Me}_4\text{14aneN}_4)]^{2+}$ formation in dmf at 298.2 K. Stock solutions of $2.97 \times 10^{-3} \text{ mol dm}^{-3} [\text{Ni}(\text{dmf})_6](\text{ClO}_4)_2$ and $2.93 \times 10^{-3} \text{ mol dm}^{-3} \text{Me}_4\text{14aneN}_4$ were used (ionic strength adjusted to 0.5 with NaClO_4)

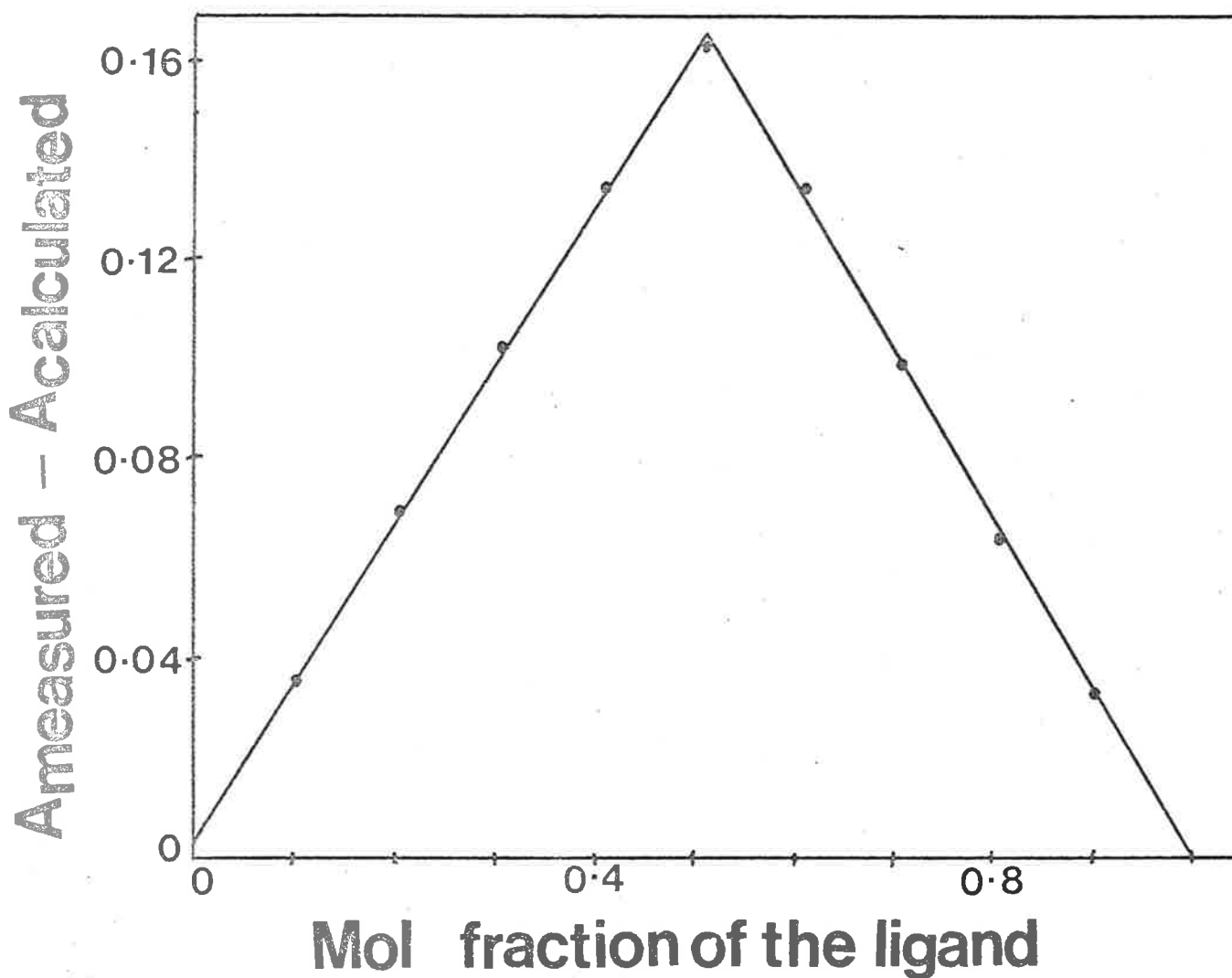


Figure 6.3

$A_{\text{measured}} - A_{\text{calculated}}$
 $(\lambda = 602 \text{ nm and cell path} = 2 \text{ cm})$ vs mol fraction if
 12aneN₄ for Job's method
 of continuous variation for
 the determination of
 stoichiometry of
 $[\text{Cu}(\text{12aneN}_4)]^{2+}$ formation
 in dmf at 298.2 K. Stock
 solutions of 4.89×10^{-4}
 $\text{mol dm}^{-3} [\text{Cu}(\text{dmf})_6](\text{ClO}_4)_2$
 and $5.16 \times 10^{-4} \text{ mol dm}^{-3}$
 12aneN₄ were used (ionic
 strength adjusted to 0.5
 with NaClO₄).

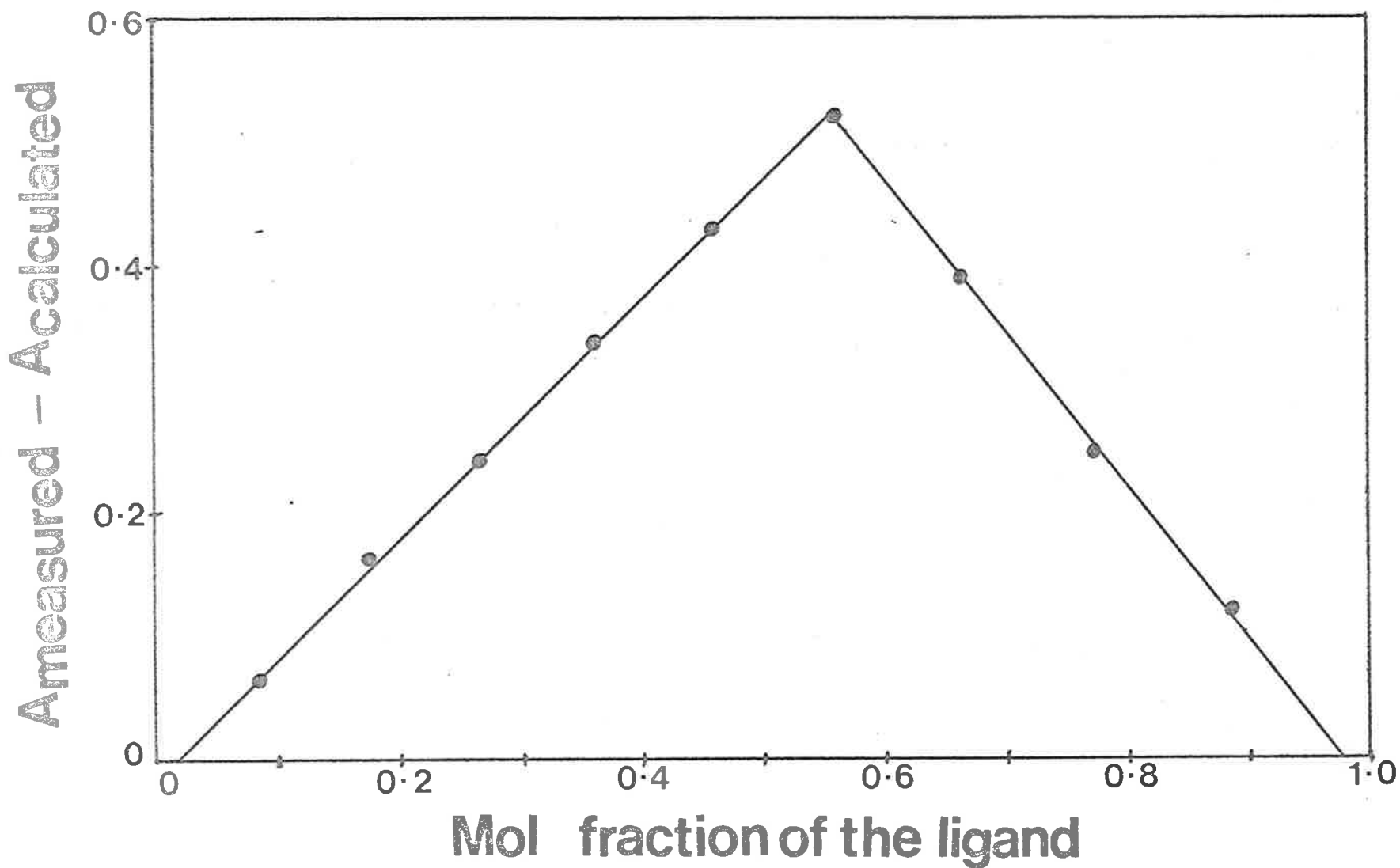


Figure 6.4 $A_{\text{measured}} - A_{\text{calculated}}$ ($\lambda = 610 \text{ nm}$ and cell path = 1 cm) vs mol fraction of $\text{Me}_4\text{12aneN}_4$ for Job's method of continuous variation for the determination of stoichiometry of $[\text{Cu}(\text{Me}_4\text{12aneN}_4)]^{2+}$ formation in dmf at 298.2 K. Stock solutions of $2.45 \times 10^{-3} \text{ mol dm}^{-3}$ $[\text{Cu}(\text{dmf})_6](\text{ClO}_4)_2$ and $2.10 \times 10^{-3} \text{ mol dm}^{-3}$ $\text{Me}_4\text{12aneN}_4$ were used (ionic strength adjusted to 0.5 with NaClO_4).

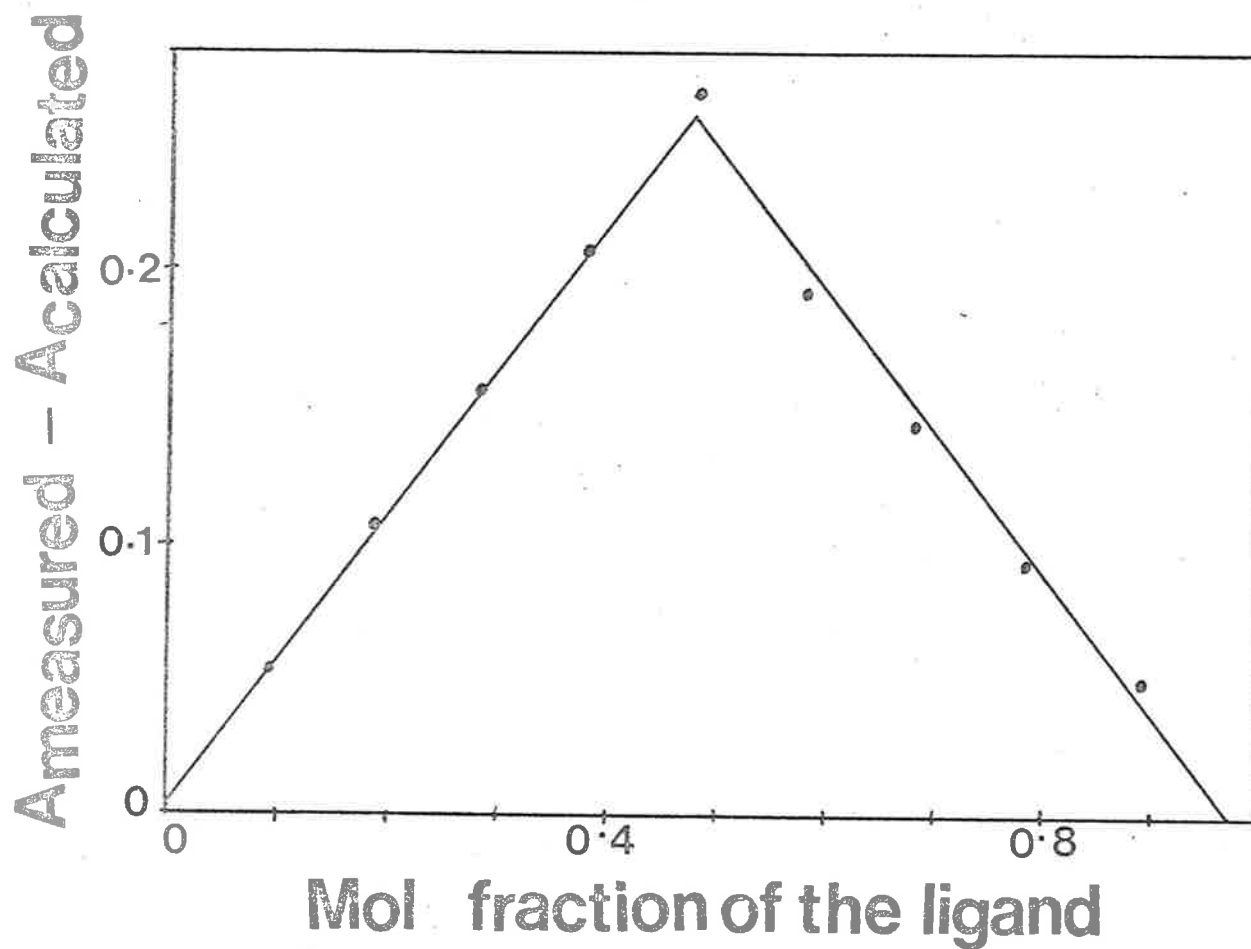


Figure 6.5 $A_{\text{measured}} - A_{\text{calculated}}$ ($\lambda = 620 \text{ nm}$ and cell path = 1 cm) vs mol fraction of $\text{Me}_4\text{14aneN}_4$ for Job's method of continuous variation for the determination stoichiometry of $[\text{Cu}(\text{Me}_4\text{14aneN}_4)]^{2+}$ formation in dmf at 298.2 K. Stock solutions of $2.25 \times 10^{-3} \text{ mol dm}^{-3}$ $[\text{Cu}(\text{dmf})_6](\text{ClO}_4)_2$ and $2.10 \times 10^{-3} \text{ mol dm}^{-3}$ $\text{Me}_4\text{14aneN}_4$ were used (ionic strength adjusted to 0.5 with NaClO_4).

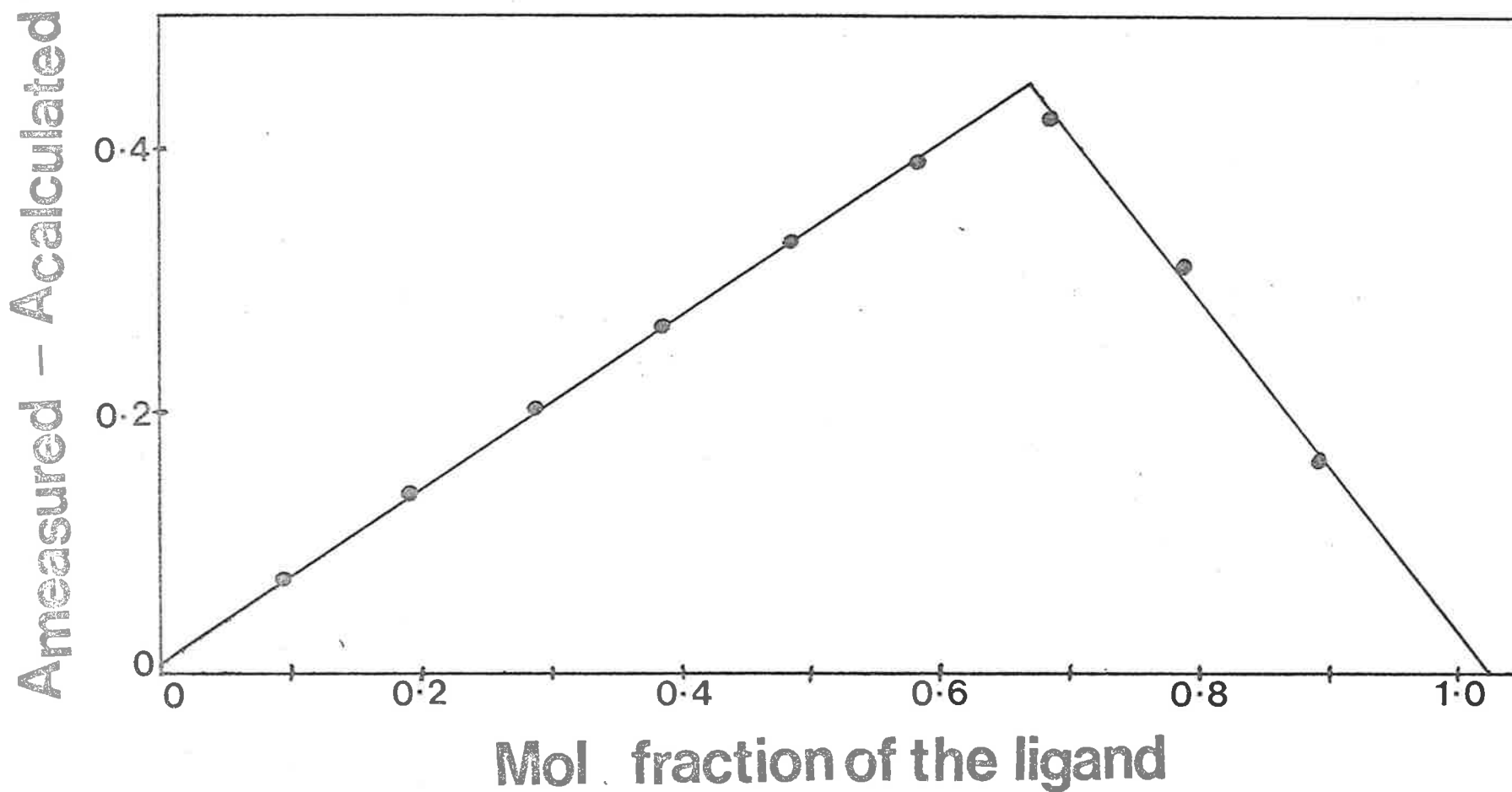


Figure 6.6 $A_{\text{measured}} - A_{\text{calculated}}$ ($\lambda = 310$ nm and cell path = 1 cm) vs mol fraction of tbl2aneN_4 for Job's method of continuous variation for the determination of stoichiometry of $[\text{Cu}(\text{tbl2aneN}_4)_2]^{2+}$ formation in dmf at 298.2 K. Stock solutions of 1.55×10^{-4} mol dm^{-3} $[\text{Cu}(\text{dmf})_6](\text{ClO}_4)_2$ and 1.46×10^{-4} mol dm^{-3} tbl2aneN_4 were used (ionic strength adjusted to 0.5 with NaClO_4).

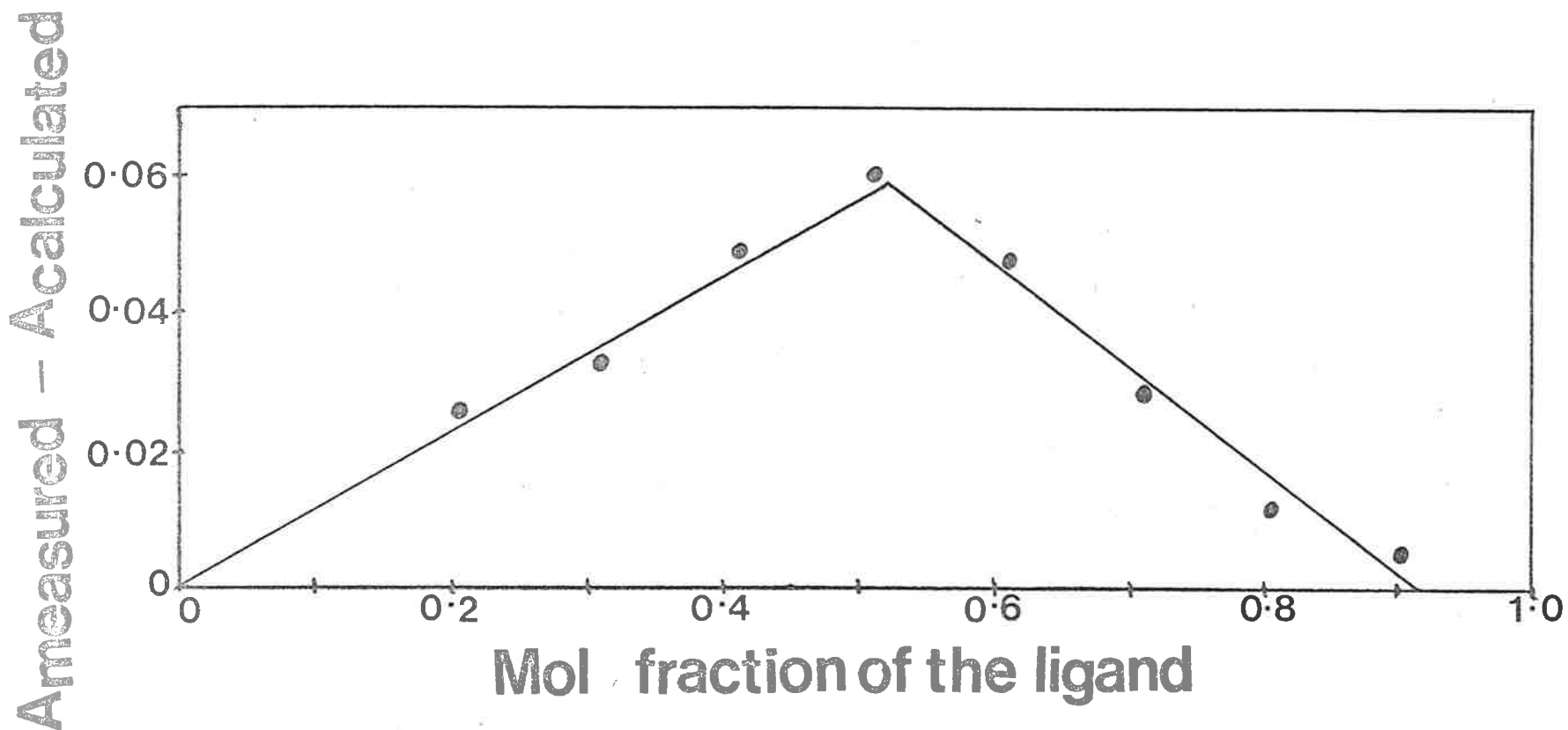


Figure 6.7 $A_{\text{measured}} - A_{\text{calculated}}$ ($\lambda = 470 \text{ nm}$ and cell path = 2 cm) vs mol fraction of $\text{Me}_4\text{14aneN}_4$ for Job's method of continuous variation for the determination of stoichiometry of $[\text{Co}(\text{Me}_4\text{14aneN}_4)]^{2+}$ formation in dmf at 298.2 K. Stock solutions of $2.48 \times 10^{-3} \text{ mol dm}^{-3}$ $[\text{Co}(\text{dmf})_6](\text{ClO}_4)_2$ and $2.61 \times 10^{-3} \text{ mol dm}^{-3}$ $\text{Me}_4\text{14aneN}_4$ were used (ionic strength adjusted to 0.5 with NaClO_4).

TABLE 6.1.

Data for Job's Method of Continuous Variation^a

Complex	[Metal Salt] $\times 10^4$ mol dm ⁻³	[Ligand] $\times 10^4$ mol dm ⁻³	Wavelength in nm of Measurement	Mol Fraction of the Ligand at which Maximum Occurs
1. [Ni(Me ₄ 12aneN ₄)] ²⁺	29.9	38.9	396	0.53 ^a
2. [Ni(Me ₄ 14aneN ₄)] ²⁺	29.7	29.3	398	0.50
3. [Cu(12aneN ₄)] ²⁺	4.89	5.16	602	0.51
4. [Cu(Me ₄ 12aneN ₄)] ²⁺	24.5	21.0	610	0.55
5. [Cu(Me ₄ 14aneN ₄)] ²⁺	22.5	21.0	620	0.48
6. [Cu(tb 12aneN ₄) ₂] ²⁺	1.55	1.46	310	0.67
7. [Co(Me ₄ 14aneN ₄)] ²⁺	24.8	26.2	470	0.52

a See Figures 6.1 to 6.7, respectively.

6.3. Rate Measurement on the Formation of:6.3.1. [Ni(Me₄14aneN₄)]²⁺ Complex.

When a solution of Me₄14aneN₄ is added to a solution of [Ni(dmf)₆](ClO₄)₂, the resulting mixture rapidly turns red and then very slowly turns green (see Chapter 2). The fast process was studied using the stopped flow technique at 298.2K at different wavelengths under pseudo 1st order conditions keeping ligand concentration constant (1.0×10^{-3} mol dm⁻³). Figure 6.8 shows the plot of k_{obs} (510nm) against [Ni(dmf)₆(ClO₄)₂] and the data are given in Table 6.2. The solid line in Figure 6.8 is a least squares linear regression line passing through the origin. The rate of complex formation between Me₄14aneN₄ and nickel (II) is proportional to [Ni(dmf)₆(ClO₄)₂] and [Me₄14aneN₄] as shown in equation 6.1

Figure 6.8

k_{obs} vs $[\text{Ni}(\text{dmf})_6^{2+}]$ for formation of $[\text{Ni}(\text{Me}_4\text{14aneN}_4)]^{2+}$ in dmf at 298.2 K and $\lambda = 510$ nm. $[\text{Me}_4\text{14aneN}_4] = 1 \times 10^{-3}$ mol dm $^{-3}$ for all reactions (ionic strength = 0.5). The solid line is a least squares linear regression line.

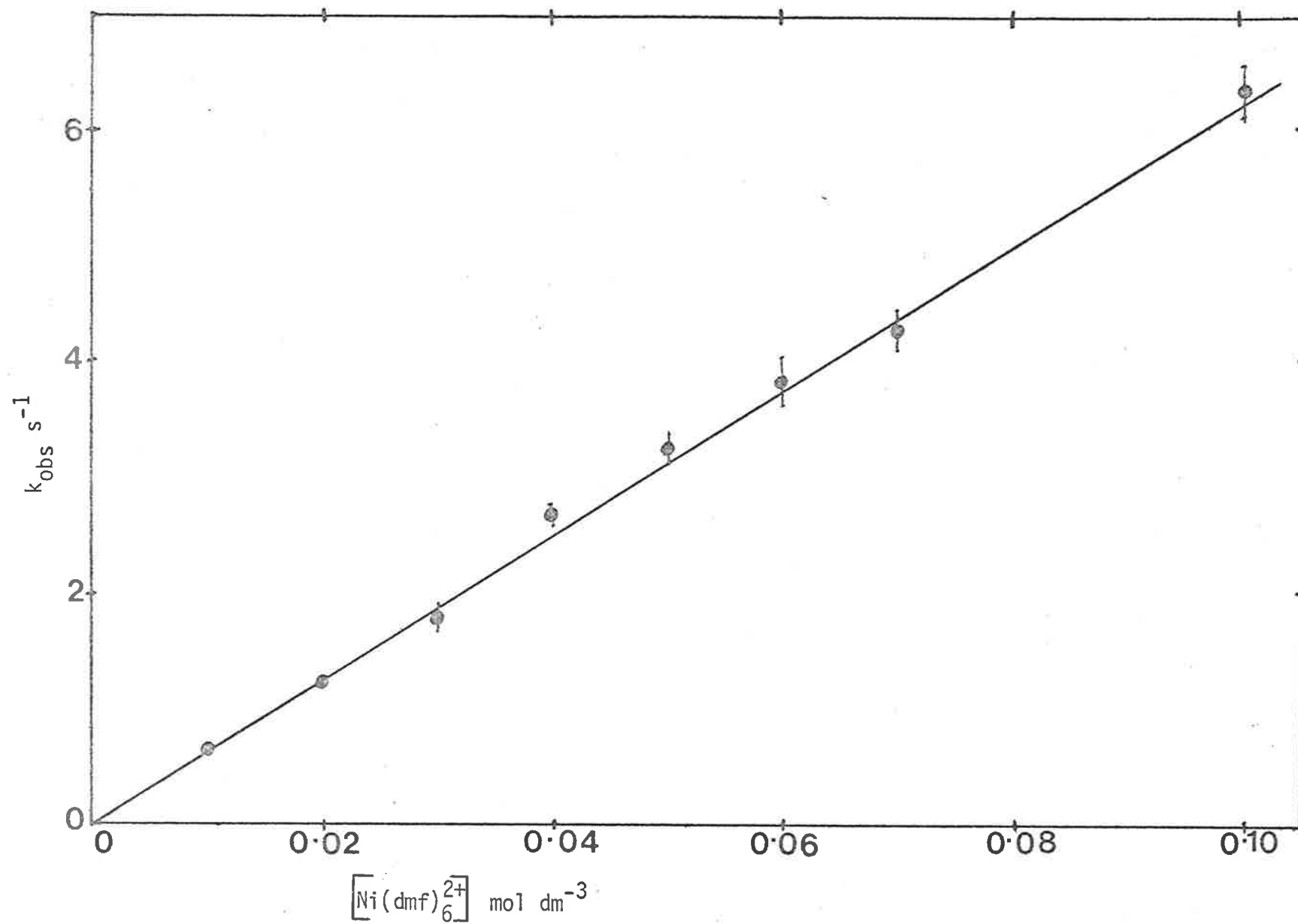


Figure 6.8

TABLE 6.2.

Kinetic Data for $[\text{Ni}(\text{Me}_4\text{14aneN}_4)]^{2+}$ System

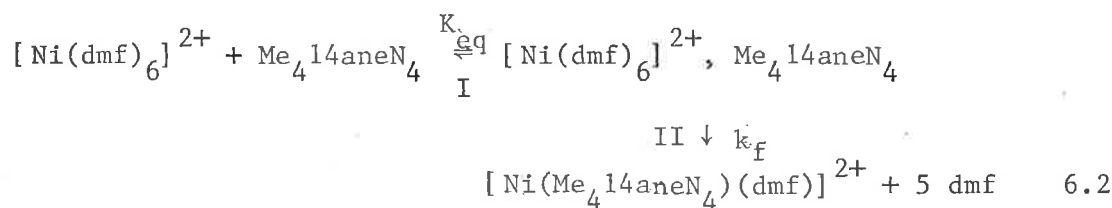
$[\text{Ni}(\text{dmf})_6(\text{ClO}_4)_2]$ mol dm^{-3}	$k_{\text{obs}} \text{ s}^{-1}$ $\lambda = 510\text{nm}$	$k_{\text{obs}} \text{ s}^{-1}$ $\lambda = 400\text{nm}$	$k_{\text{obs}} \text{ s}^{-1}$ $\lambda = 435\text{nm}$	$k_{\text{obs}} \text{ s}^{-1}$ $\lambda = 660\text{nm}$ (with filter)	$k_{\text{obs}} \text{ s}^{-1}$ $\lambda = 660\text{nm}$ (without filter)
0.01	0.64 ± 0.01	0.57 ± 0.02	0.53 ± 0.02	0.66 ± 0.02	0.55 ± 0.03
0.02	1.26 ± 0.04	-	-	-	-
0.03	1.8 ± 0.1	-	-	-	-
0.04	2.66 ± 0.06	-	-	-	-
0.05	3.2 ± 0.1	-	-	-	-
0.06	3.8 ± 0.2	-	-	-	-
0.07	4.2 ± 0.1	-	-	-	-
0.10	6.4 ± 0.2	-	-	-	-

N.B. The errors represent one standard deviation

$$\frac{d[\text{Ni}(\text{Me}_4\text{14aneN}_4)(\text{dmf})^{2+}]}{dt} = k[\text{Ni}(\text{dmf})_6(\text{ClO}_4)_2^{2+}][\text{Me}_4\text{14aneN}_4] \quad 6.1$$

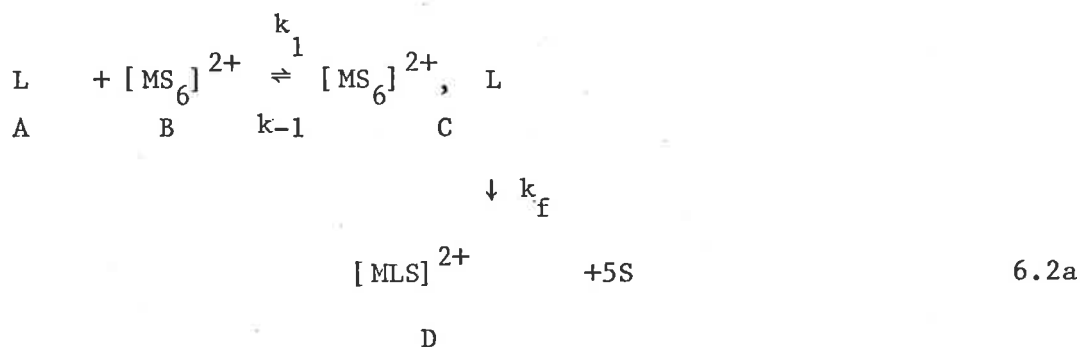
(here ligand exists as an uncharged species)

Firstly, the possibility of a dissociative interchange mechanism, $I_d^{24,25}$ (also see Chapter 1) will be explored here. For an I_d mechanism, the pathways for the reaction between nickel (II) and $\text{Me}_4\text{14aneN}_4$ can be represented by equation 6.2



in which the rate determining step for the formation of the inner sphere complex (step II) is preceded by the rapid formation of an outer sphere complex (step I). The rate equation 6.3 may be

deduced in the following way²⁶ considering 'B' in excess.



(where L = macrocyclic ligand, M = metal ion and S = solvent molecule)

If the first step is fast compared with the second, then

$K_{eq} = \frac{[\text{C}]}{[\text{A}][\text{B}]} = \frac{k_1}{k_{-1}}$ and $k_1, k_{-1} \gg k_f$. The rate of appearance of D must be equal to the rate of disappearance of (A + C).

$$\text{rate} = \frac{d[\text{D}]}{dt} = \frac{-d([\text{A}] + [\text{C}])}{dt} = k_{\text{obs}}([\text{A}] + [\text{C}]) = k_f[\text{C}]$$

$$\therefore k_{\text{obs}} = \frac{k_f[\text{C}]}{[\text{A}] + [\text{C}]} = \frac{k_f K_{eq} [\text{A}][\text{B}]}{[\text{A}] + K_{eq} [\text{A}][\text{B}]}$$

$$\text{or } k_{\text{obs}} = \frac{k_f K_{eq} [\text{B}]}{1 + K_{eq} [\text{B}]} = \frac{k_f K_{eq} [\text{MS}_6^{2+}]}{1 + K_{eq} [\text{MS}_6^{2+}]}$$

If $K_{eq} [\text{MS}_6^{2+}] \gg 1$, then $k_{\text{obs}} = k_f$

and if $1 \gg K_{eq} [\text{MS}_6^{2+}]$, then

$$k_{\text{obs}} = k_f K_{eq} [\text{MS}_6^{2+}] \qquad 6.3$$

where $[\text{MS}_6^{2+}]$ is the metal ion concentration which essentially remains constant under pseudo 1st order conditions. k_{obs} is the overall observed rate constant for the reaction.

From the plot of k_{obs} vs $[\text{Ni}(\text{dmf})_6^{2+}]$, the value of $k_f K_{eq}$ was found to be $(63 \pm 2) \text{ mol}^{-1} \text{ dm}^3 \text{ s}^{-1}$ in the case of the ligand $\text{Me}_4\text{14aneN}_4$. The K_{eq} value may be roughly estimated in two ways:-

(a) The rate constant for dmf exchange on $[\text{Ni}(\text{dmf})_6]^{2+}$ at 298.2K was reported²⁷ to be $6 \times 3.8 \times 10^3 \text{ s}^{-1}$ and this exchange rate

constant is very fast compared with the observed rates constants $0.64 - 6.4 \text{ S}^{-1}$ of the $[\text{Ni}(\text{Me}_4\text{aneN}_4)]^{2+}$ system. The K_{eq} value was calculated to be $2.77 \times 10^{-3} \text{ mol}^{-1} \text{ dm}^3$ by equating dmf exchange rate constant to k_f and this value is consistent with the assumption $1 \gg K_{\text{eq}} [\text{Ni}(\text{dmf})_6^{2+}]$.

(b) The K_{eq} value may be approximately obtained using equation 6.4²⁶

$$K_{\text{eq}} = \frac{4\pi N a^3}{3000} \exp - \frac{U(a)}{kT} \quad 6.4.$$

(U(a) = Debye-Hückel interionic potential)

$$U(a) = \frac{Z_1 Z_2 e^2}{aD} - \frac{Z_1 Z_2 e^2 k}{D(1+ka)}$$

$$k^2 = \frac{8\pi N e^2 I}{1000 D k T}$$

N = Avogadro's number.

a = centre to centre distance of closest approach of the solvated metal ion and the reacting site of the ligand.

k = Boltzmann's constant

e = charge of an electron in e.s.u. unit

D = bulk dielectric constant

I = ionic strength

Z_1, Z_2 = charges of reactants, T = absolute temperatures

The K_{eq} value was calculated to be $0.16 \text{ mol}^{-1} \text{ dm}^3$ setting

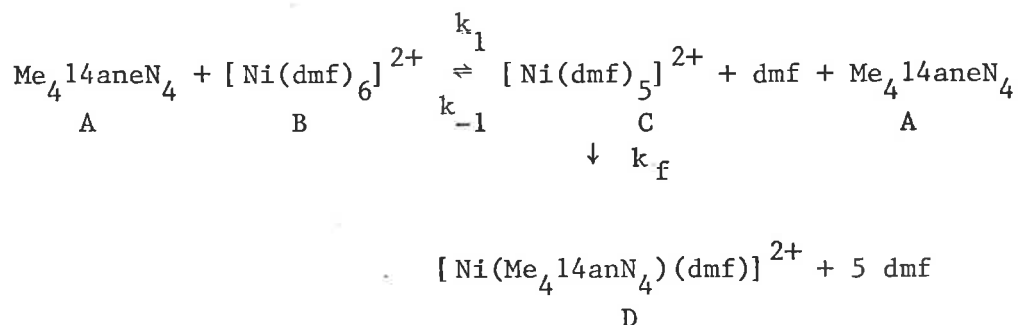
$a = 4\text{Å}^0$ arbitrarily and this is consistent with $1 \gg K_{\text{eq}} [\text{Ni}(\text{dmf})_6^{2+}]$.

Using this K_{eq} value, k_f becomes $3.95 \times 10^2 \text{ S}^{-1}$ which is slower than the dmf exchange rate constant on $[\text{Ni}(\text{dmf})_6]^{2+}$ and in the I_d mechanism,²⁸

k_f is expected to be less than the dmf exchange rate constant because the ligand is in competition with solvent molecules when it comes to entering the co-ordination shell. However, the K_{eq} values estimated from both methods are only approximate because the calculations use

indirect methods.

An alternative mechanism to the one so far discussed is the dissociative (D) mechanism²⁵ which could also give rise to the equation 6.3 as shown below considering 'B' in excess.



$$\text{rate} = \frac{d[\text{D}]}{dt} = k_f [\text{A}][\text{C}]$$

Under steady state conditions

$$\frac{d[\text{C}]}{dt} = k_1[\text{B}] - k_{-1}[\text{C}][\text{dmf}] - k_f[\text{A}][\text{C}] = 0$$

$$\therefore [\text{C}] = \frac{k_1[\text{B}]}{k_{-1}[\text{dmf}] + k_f[\text{A}]}$$

$$\therefore \text{rate} = \frac{d[\text{D}]}{dt} = \frac{k_f k_1 [\text{A}][\text{B}]}{k_{-1}[\text{dmf}] + k_f[\text{A}]}$$

Thus $\frac{d[\text{D}]}{dt}$ will exhibit a non-linear dependence upon [A] between the limits

i) $k_{-1}[\text{dmf}] \gg k_f[\text{A}]$ when

$$\frac{d[\text{D}]}{dt} = -\frac{d[\text{A}]}{dt} \approx \frac{k_f k_1 [\text{A}][\text{B}]}{k_{-1}[\text{dmf}]}$$

At a fixed excess concentration of B, an apparent first order plot will be obtained with

$$k_{\text{obs}} = \frac{k_f k_1 [\text{B}]}{k_{-1}[\text{dmf}]}$$

ii) $k_{-1}[\text{dmf}] \ll k_f[\text{A}]$ when

$$\frac{d[\text{D}]}{dt} = -\frac{d[\text{A}]}{dt} \approx k_1[\text{B}]$$

At a fixed excess concentration of B, an apparent zero order plot would be obtained at this limit. Since experimentally in the system under discussion, a first order plot is obtained, if the reaction were dissociative limit (i) would apply. Accordingly the appropriate expression for k_{obs} , the pseudo first order rate constant, would be

$$k_{\text{obs}} = \frac{k_f k_1 [B]}{k_{-1} [\text{dmf}]} = K k_f [B] \quad (\text{where } K = \frac{k_1}{k_{-1} [\text{dmf}]})$$

In form this expression is identical to equation 6.3. Thus using the available data, one cannot distinguish between a D or an I_d mechanism. However, the main features of formation for many labile complexes of nickel (II) in water,^{29, 30} methanol³¹ and ethanol³² are consistent with an I_d mechanism and it was observed that the rates of formation of the complexes are controlled by the rates of exchange of solvent molecules between the inner sphere of the nickel ion and the bulk solvent. The possibility of an associative interchange mechanism²⁵ (I_a) cannot be ruled out but the formation of an increased co-ordination number between a charged metal ion and an uncharged ligand seems to be improbable. Moreover, ligand substitution on nickel (II)^{33, 34} by other ligands in other solvents appear to proceed through an I_d or a D mechanism. Therefore it is quite unlikely that an I_a mechanism is operating in this system.

6.3.2. $[\text{Ni}(\text{Me}_4\text{12aneN}_4)]^{2+}$ Complex:-

The rate of formation of $[\text{Ni}(\text{Me}_4\text{12aneN}_4)]^{2+}$ from $[\text{Ni}(\text{dmf})_6]^{2+}$ (ClO_4)₂ and $\text{Me}_4\text{12aneN}_4$ was studied under pseudo 1st order conditions at 298.2K. The ligand concentration was kept constant (2.0×10^{-3} mol dm⁻³) and the rate was studied as a function of excess $[\text{Ni}(\text{dmf})_6]^{2+}$. Two processes (Figure 6.9) were observed with

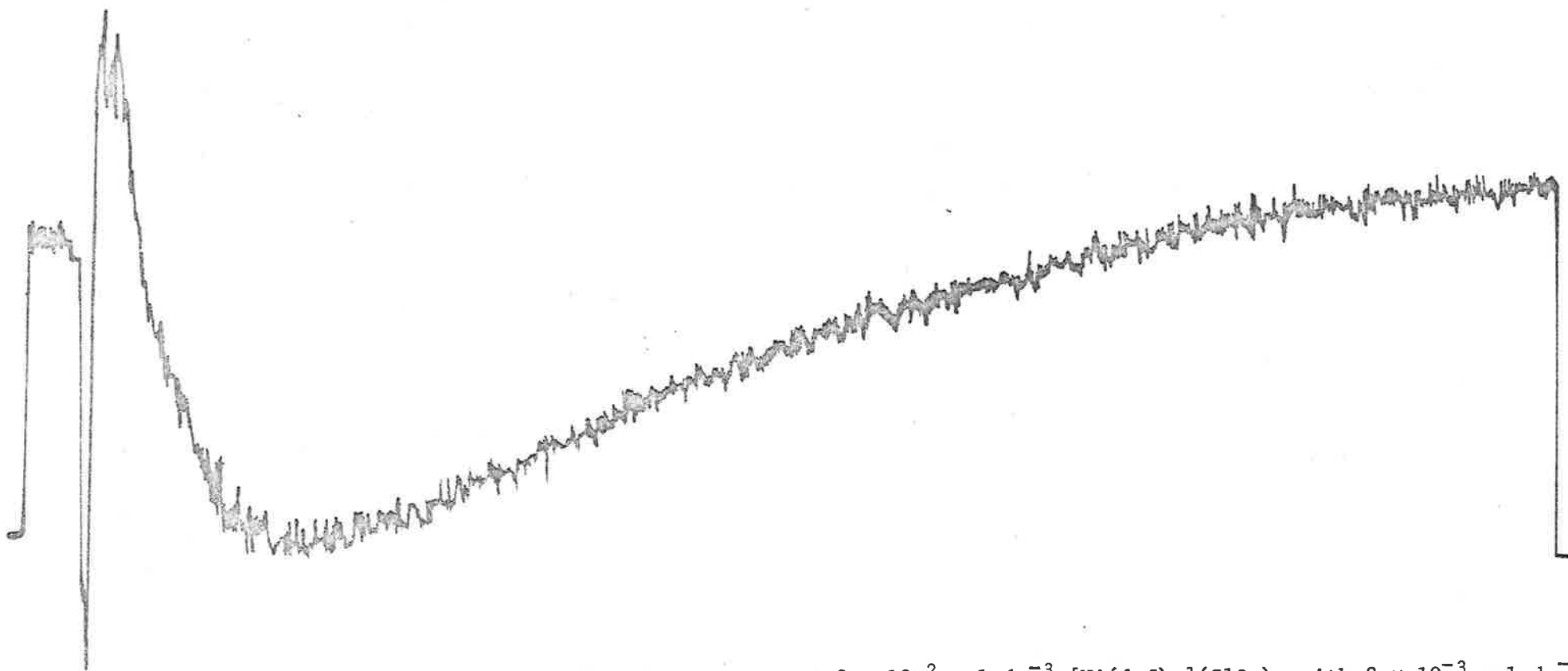


Figure 6.9 Two kinetic processes for the reaction of $2 \times 10^{-2} \text{ mol dm}^{-3}$ $[\text{Ni}(\text{dmf})_6](\text{ClO}_4)_2$ with $2 \times 10^{-3} \text{ mol dm}^{-3}$ $\text{Me}_4\text{12aneN}_4$ in dmf at 298.2 K and $\lambda = 600 \text{ nm}$ (ionic strength = 0.5). 80 ms/cm, 4 mv/cm, $V_\alpha = -1.8 \text{ mv}$ and back off = 2.0 volts. The trace was obtained in a shorter time scale to observe both process simulataneously.

the stopped flow instrument and a very slow process ($t_{1/2} \approx 1$ hour at 298 K) was observed using uv/visible spectrophotometry in excess metal ion concentration. The more rapid first process was studied at 600nm while the second slower process was studied at both 600nm and 400nm. The approximate observed rate constants for the first process varied non-systematically from 17 ± 3 to $30 \pm 2 \text{ s}^{-1}$ over the metal concentration range of 0.02 to 1.0 mol dm^{-3} . Because of two processes occurring within a very short time, it is not clear whether the first process depends upon the concentration of metal ion or not. If it is not dependent upon metal ion concentration, then it is probably preceded by a very fast process which is too fast to be studied using the stopped flow technique. The first metal-ligand bond is expected to form rapidly if substitution on $[\text{Ni}(\text{dmf})_6]^{2+}$ is characterised by a rate determining step involving the dissociation of dmf. The substitution of one water molecule of $[\text{Ni}(\text{OH}_2)_6]^{2+}$ by an amine nitrogen renders the remaining five more labile³⁵ (also see Chapter 4). By analogy, one could postulate that the substitution of one dmf molecule of $[\text{Ni}(\text{dmf})_6]^{2+}$ by an amine nitrogen will also render the remaining five more labile and hence the remaining metal-ligand bond formation is expected to be very rapid. Consequently the slower processes observed in this system may probably be attributed to isomerisation which is a consequence of inversion of the nitrogen atoms of the ligand^{36, 37} (see Chapter 1). The ligand in the non-co-ordinated state exists as a number of stereochemical isomers in equilibrium with each other. On co-ordination of the ligand, this equilibrium is changed and the attainment of a new equilibrium corresponds to the slower processes mentioned above (i.e. the attainment of thermodynamic equilibrium between different isomers

of nickel (II) complexes give rise to the slower processes). The kinetic data for the second process are given in Table 6.3 and the plot of the observed rate constants (k_{obs}) against metal ion concentrations is shown in Figure 6.10.

TABLE 6.3
Kinetic Data for $[\text{Ni}(\text{Me}_4\text{12aneN}_4)]^{2+}$ System

$[\text{Ni}(\text{dmf})_6(\text{ClO}_4)_2]$ mol dm^{-3}	$k_{\text{obs}} \text{ s}^{-1}$ 2nd Process $\lambda = 600\text{nm}$	$k_{\text{obs}} \text{ s}^{-1}$ 2nd Process $\lambda = 400\text{nm}$
0.02	1.55 ± 0.02	1.66 ± 0.2
0.03	1.65 ± 0.1	1.70 ± 0.1
0.04	1.56 ± 0.11	1.78 ± 0.3
0.05	1.72 ± 0.2	1.78 ± 0.2
0.06	1.70 ± 0.2	1.82 ± 0.2
0.07	1.60 ± 0.2	-
0.10	1.57 ± 0.2	-

N.B. The errors represent one standard deviation

The rate constant for dmf exchange on $[\text{Ni}(\text{dmf})_6]^{2+}$,²⁷ ($6 \times 3.8 \times 10^3 \text{ s}^{-1}$ at 298.2K) is very fast compared with the observed rate constant $17 \pm 3 - 30 \pm 2 \text{ s}^{-1}$ of the first process. It has been observed²⁸ in aqueous solution that in the I_d mechanism the rate constant for the second step in equation 6.2a can be less than the solvent exchange rate constant since even though the ligand forms an outer sphere complex, it is still in competition with solvent molecules when it comes to entering the co-ordination shell. In an I_a mechanism this rate constant can be greater, since the ligand in the outer co-ordination sphere has some influence on the rate at which the co-ordinated solvent leaves. In the D mechanism, the rate constant for the formation of intermediate with reduced co-ordination

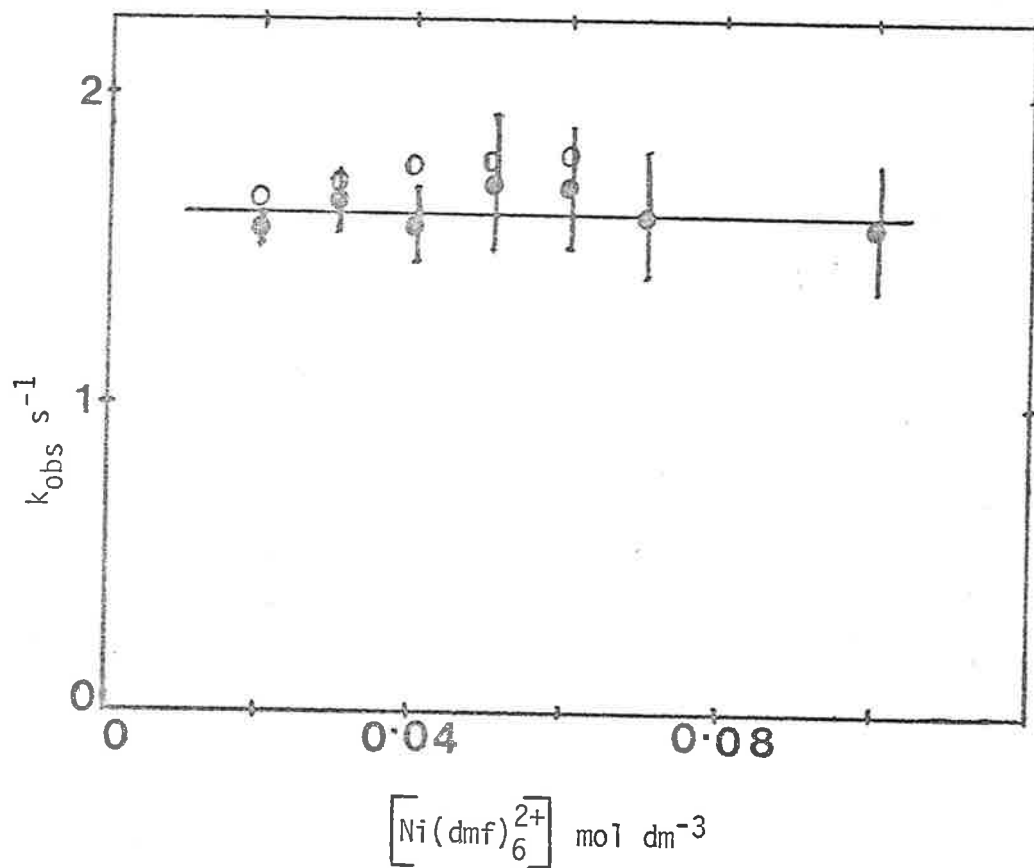


Figure 6.10

k_{obs} vs $[\text{Ni}(\text{dmf})_6]^{2+}$ for the second process of $[\text{Ni}(\text{Me}_4\text{12aneN}_4)]^{2+}$ formation in dmf at 298.2 K, $\lambda = 600 \text{ nm}$ (filled circles) and $\lambda = 400 \text{ nm}$ (open circles). $[\text{Me}_4\text{12aneN}_4] = 2 \times 10^{-3} \text{ mol dm}^{-3}$ for all reactions (ionic strength = 0.5). The solid line is a least squares linear regression line for datum points at $\lambda = 600 \text{ nm}$.

number must be equal to the solvent exchange rate constant.

The present system is very similar to the $[\text{Ni}(\text{Me}_4\text{14aneN}_4)]^{2+}$ system discussed in the previous section and therefore the same mechanism may be operating in this case.

6.3.3. $[\text{Cu}(\text{Me}_4\text{12aneN}_4)]^{2+}$ Complex:-

The kinetics of formation of $[\text{Cu}(\text{Me}_4\text{12aneN}_4)]^{2+}$ keeping ligand concentration constant ($5.0 \times 10^{-4} \text{ mol dm}^{-3}$) were studied under pseudo 1st order conditions at 298.2K with excess metal ion. Two processes were observed using the stopped flow technique as shown in Figure 6.11. Because the two processes occur within such a short time scale, the k_{obs} values obtained for the first process varied approximately from 6 ± 0.2 to $30 \pm 2 \text{ S}^{-1}$ over the concentration range of 0.01 to 0.1 mol dm^{-3} and these k_{obs} values were found to increase with the increase of metal ion concentration. For the second process the kinetic data are given in Table 6.4 and the plot of k_{obs} vs $[\text{Cu}(\text{dmf})_6(\text{ClO}_4)_2]$ is shown in Figure 6.12. For the reasons discussed in Section 6.3.2., the second process may be due to isomerisation. The dmf exchange rate constant on $[\text{Cu}(\text{dmf})_6]^{2+}$ should be greater than that on $[\text{Ni}(\text{dmf})_6]^{2+}$ and $[\text{Co}(\text{dmf})_6]^{2+}$, and may be tentatively estimated as $6 \times 1 \times 10^8 \text{ S}^{-1}$ (at 298.2K) which is very fast compared with the observed rate constants obtained for the first process and the same mechanism as discussed in Section 6.3.1. may be expected to be operating.

6.3.4. $[\text{Cu}(\text{Me}_4\text{14aneN}_4)]^{2+}$ Complex:-

One process was observed using the stopped flow technique for the $[\text{Cu}(\text{Me}_4\text{14aneN}_4)]^{2+}$ system under pseudo 1st order conditions (excess metal ion) at 288.2 and 298.2K and no slower process was detected using a uv/visible spectrophotometer. The kinetic data

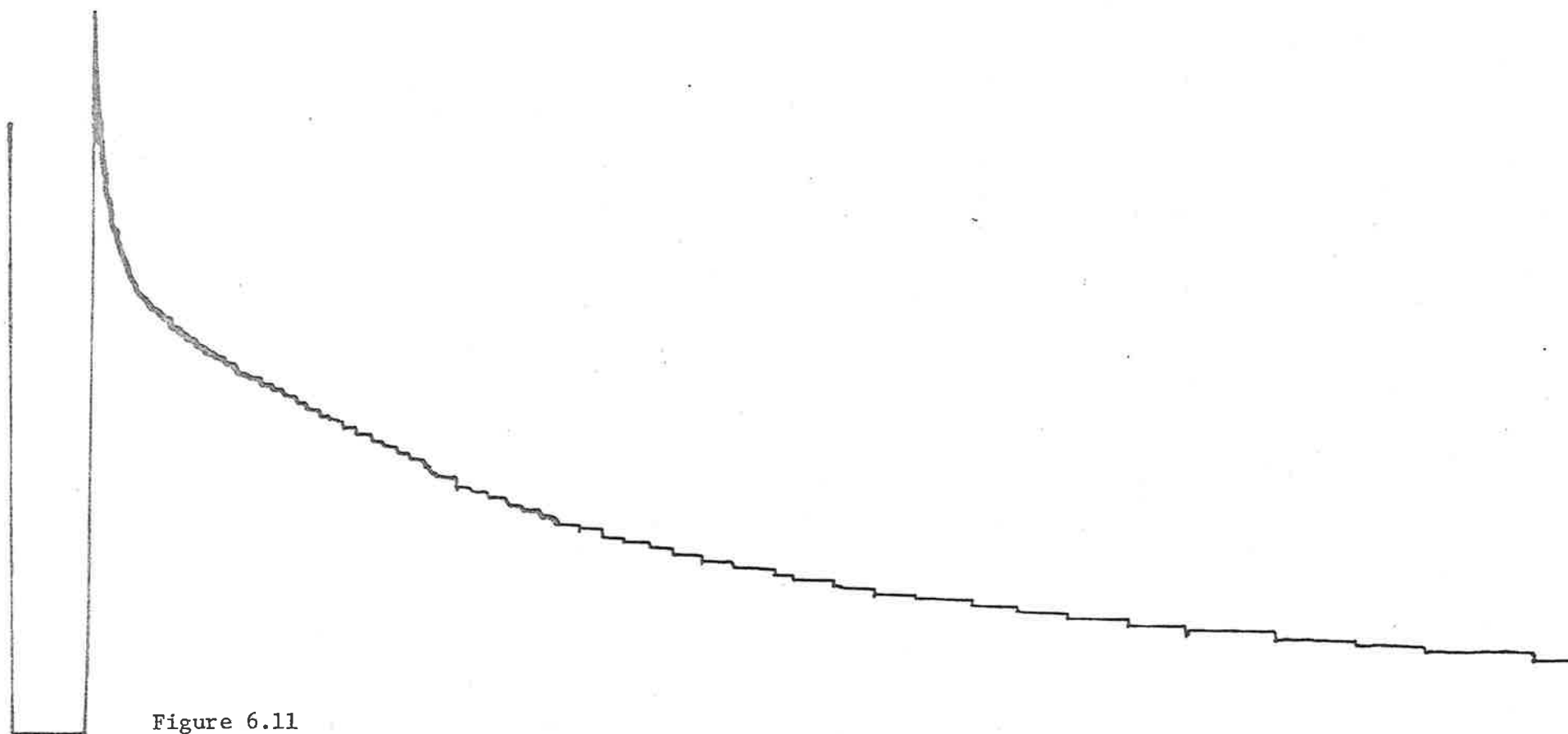


Figure 6.11

Two kinetic processes for the reaction of $1 \times 10^{-2} \text{ mol dm}^{-3} [\text{Cu}(\text{dmf})_6](\text{ClO}_4)_2$ with $5 \times 10^{-4} \text{ mol dm}^{-3} \text{Me}_4\text{12aneN}_4$ in dmf at 298.2 K and $\lambda = 610 \text{ nm}$ (ionic strength = 0.5). 400 ms/cm, 200 mv/cm, $V_\alpha = -0.28 \text{ volt}$ and back off = -2.0 volts. The trace was obtained in a suitable time scale to observe both processes simultaneously.

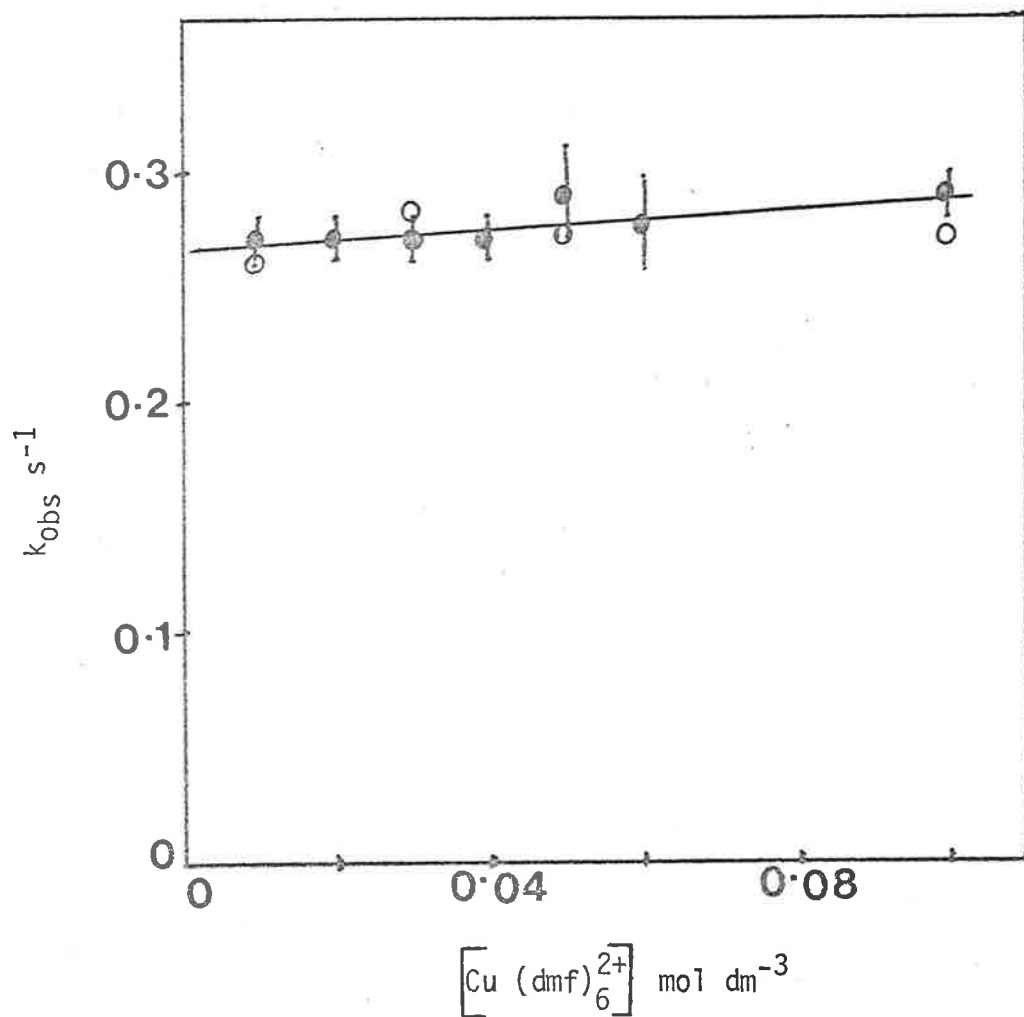


Figure 6.12

k_{obs} vs $[\text{Cu}(\text{dmf})_6^{2+}]$ for the second process of $[\text{Cu}(\text{Me}_4\text{12aneN}_4)]^{2+}$ formation in dmf at 298.2 K, $\lambda = 610$ nm (filled circles) and $\lambda = 525$ nm (open circles). $[\text{Me}_4\text{12aneN}_4] = 5 \times 10^{-4} \text{ mol dm}^{-3}$ for all reactions (ionic strength = 0.5). The solid line is a least squares linear regression line for datum points at $\lambda = 610$ nm.

TABLE 6.4
Kinetic Data for the $[\text{Cu}(\text{Me}_4\text{12aneN}_4)]^{2+}$ System

$[\text{Cu}(\text{dmf})_6(\text{ClO}_4)_2]$ mol dm^{-3}	$k_{\text{obs}} \text{ s}^{-1}$ 2nd Process $\lambda = 610\text{nm}$	$k_{\text{obs}} \text{ s}^{-1}$ 2nd Process $\lambda = 525\text{nm}$
0.01	0.27 ± 0.01	0.26 ± 0.01
0.02	0.27 ± 0.01	0.27 ± 0.03
0.03	0.27 ± 0.01	0.28 ± 0.03
0.04	0.27 ± 0.01	0.27 ± 0.04
0.05	0.29 ± 0.02	0.27 ± 0.03
0.06	0.27 ± 0.02	0.27 ± 0.01
0.10	0.29 ± 0.01	0.27 ± 0.02

N.B. The errors represent one standard deviation

are given in Table 6.5 and the plot of k_{obs} vs $[\text{Cu}(\text{dmf})_6(\text{ClO}_4)_2]$ is shown in Figure 6.13. The parameters ΔS^\ddagger and ΔH^\ddagger (see Chapter 4, equation 4.9) for the process were calculated to be $-69.8\text{JK}^{-1}\text{mol}^{-1}$ and 45.8kJ mol^{-1} , respectively. As with the $[\text{Ni}(\text{Me}_4\text{12aneN}_4)]^{2+}$ system discussed in section 6.3.2., this process is attributed to isomerisation, and the first bond formation between the ligand and the metal ion is assumed to be too fast to be studied using the stopped flow technique.

TABLE 6.5
Kinetic Data for the $[\text{Cu}(\text{Me}_4\text{14aneN}_4)]^{2+}$ System

$[\text{Cu}(\text{dmf})_6(\text{ClO}_4)_2]$ mol dm^{-3}	$k_{\text{obs}} \text{ s}^{-1}$ $\lambda = 610\text{nm}$ 298.2K	$k_{\text{obs}} \text{ s}^{-1}$ $\lambda = 610\text{nm}$ 288.2K	$k_{\text{obs}} \text{ s}^{-1}$ $= 525\text{nm}$ 288.2K
0.01	13.8 ± 0.5	6.9 ± 0.2	7.1 ± 0.3
0.02	13.3 ± 0.9	6.8 ± 0.5	6.8 ± 0.1
0.03	13.6 ± 0.4	6.9 ± 0.4	-
0.04	13.1 ± 0.7	-	-
0.05	13.8 ± 0.8	-	-
0.06	13.5 ± 1.0	-	-
0.07	13.4 ± 1.0	-	-
0.10	13.6 ± 0.3	-	-

N.B. The errors represent one standard deviation

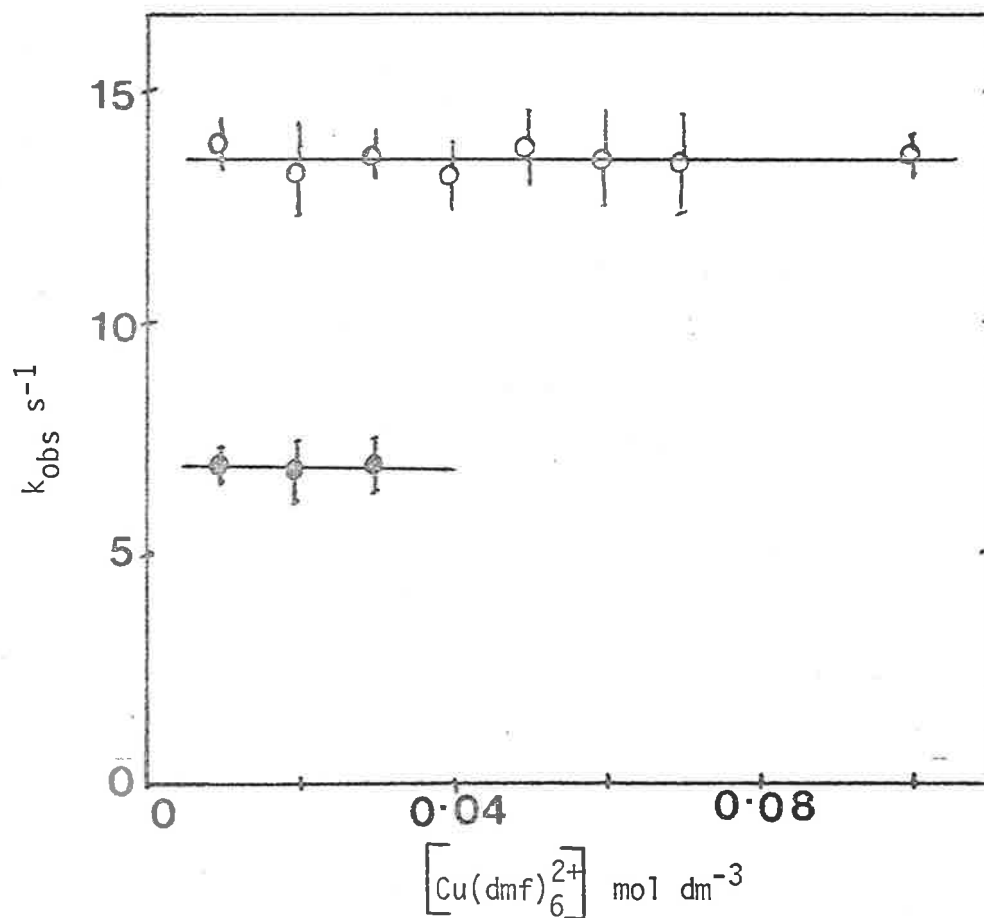


Figure 6.13

k_{obs} vs $[\text{Cu(dmf)}_6^{2+}]$ for formation of $[\text{Cu}(\text{Me}_4\text{14aneN}_4)]^{2+}$ in dmf at 288.2 K (filled circles), 298.2 K (open circles) and $\lambda = 610 \text{ nm}$. $[\text{Me}_4\text{14aneN}_4] = 1 \times 10^{-3} \text{ mol dm}^{-3}$ for all reactions (ionic strength = 0.5). The solid lines are least squares linear regression lines.

6.3.5. [Co(Me₄14aneN₄)²⁺ Complex:-

Two processes (Figure 6.14) were observed using the stopped flow technique under pseudo 1st order conditions (excess metal ion) at 298.2K. The observed rate constants for the first process varied un-systematically between 14 ± 1 and $19 \pm 2 \text{ S}^{-1}$ over the concentration range of $0.01 - 0.07 \text{ mol dm}^{-3}$ and this k_{obs} value is very slow compared with dmf exchange rate constant ($6 \times 3.9 \times 10^5 \text{ S}^{-1}$ at 298.2K) on $[\text{Co}(\text{dmf})_6]^{2+}$.²⁷ The approximate half life for the second process (small absorbance change prevented satisfactory study) is 0.5 S with 0.01 mol dm^{-3} and 0.05 mol dm^{-3} $[\text{Co}(\text{dmf})_6](\text{ClO}_4)_2$. As with other systems, it is expected that complex formation should be followed by isomerisation to attain thermodynamic equilibrium between different isomers.

6.4. The Temperature Dependence of the Spin-equilibria of Nickel (II) Complexes in dmf Solution:-

A solution of $[\text{Ni}(\text{12aneN}_4)](\text{ClO}_4)_2$ in dmf is purple in colour and the uv/visible spectrum is dependent upon the temperature, probably indicating the presence of an equilibrium between diamagnetic square planar (low-spin) and paramagnetic (high-spin) solvated species. The intensity of the band at 421nm increases with a simultaneous decrease at both 560nm and 358nm. The molar extinction co-efficient of the low-spin form (ϵ_{sq}) at 421nm is $59.2 \text{ mol}^{-1} \text{ dm}^3 \text{ cm}^{-1}$ in CH_3NO_2 thus the equilibrium constants could be calculated using the equation, $\text{Keq} = \frac{\epsilon}{\epsilon_{\text{sq}} - \epsilon}$ (see Chapter 4, equation 4.22). Spin-equilibria were studied for other nickel (II) complexes in different solvents. The Keq values are given in Table 6.6 and associated ΔS° and ΔH° values (see Chapter 4, equation 4.5) are given in Table 6.7. Figure 6.15 shows the spectra

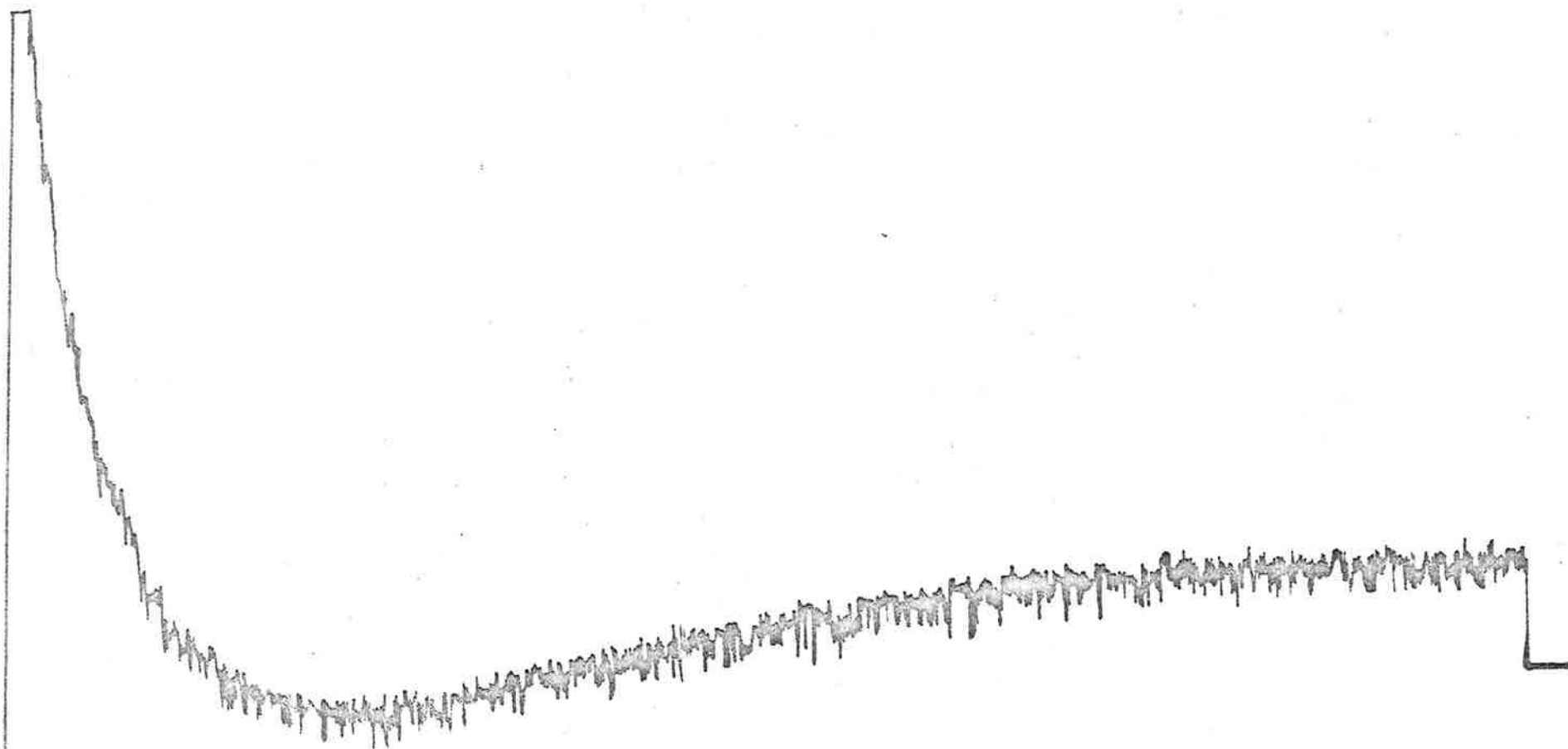


Figure 6.14

Two kinetic processes for the reaction of $1 \times 10^{-2} \text{ mol dm}^{-3}$ $[\text{Co}(\text{dmf})_6](\text{ClO}_4)_2$ with $1 \times 10^{-3} \text{ mol dm}^{-3}$ $\text{Me}_4\text{14aneN}_4$ in dmf at 298.2 K and $\lambda = 470 \text{ nm}$ (ionic strength = 0.5). 80 ms/cm, 8 mv/cm, $V_\infty = -74 \text{ mv}$ and back off = -2.0 volts. The trace was obtained in a suitable time scale to observe both processes simultaneously.

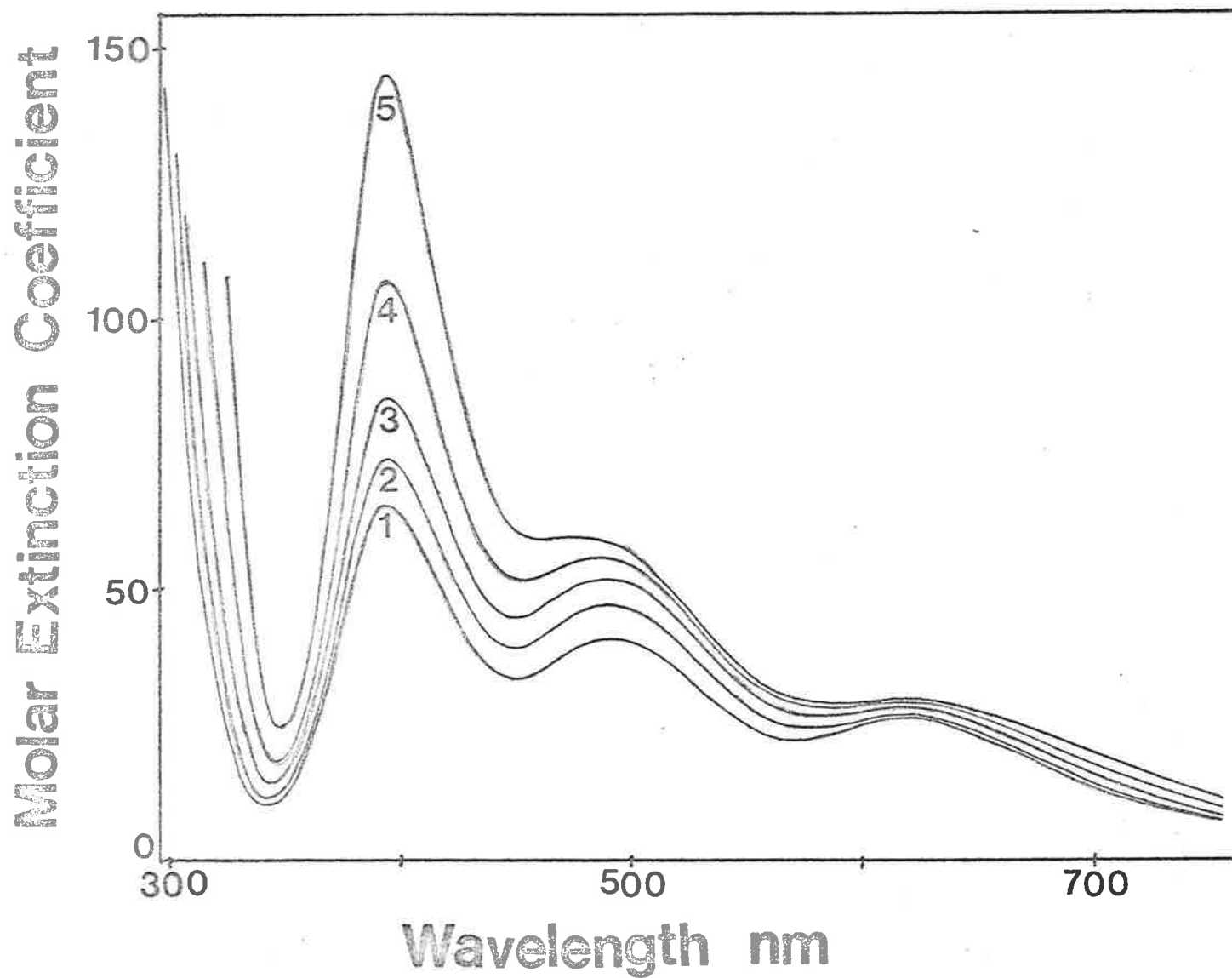


Figure 6.15
Temperature dependent uv/visible spectra of $2.90 \times 10^{-3} \text{ mol dm}^{-3}$ $[\text{Ni}(\text{Me}_4\text{12aneN}_4)](\text{ClO}_4)_2$ (ethanol water preparation) in dmf. Temperatures are 290.7, 304.7, 318.2, 330.2 and 341.2 K for the spectra from 1 to 5 respectively.

TABLE 6.6
Keq Values for Different Nickel (II) Systems

Complex	Solvent	$\frac{1}{T} \times 10^4$	Keq
1. $[\text{Ni}(\text{12aneN}_4)](\text{ClO}_4)_2$	dmf	34.48	0.049 ± 0.002
		33.33	0.051 ± 0.003
		31.84	0.053 ± 0.003
		30.70	0.056 ± 0.003
		29.92	0.057 ± 0.003
2. $[\text{Ni}(\text{Me}_4\text{12aneN}_4)](\text{ClO}_4)_2$ (ethanol water preparation)	CH_3CN	34.38	0.389 ± 0.02
		33.05	0.405 ± 0.02
		30.91	0.427 ± 0.02
		29.35	0.430 ± 0.02
	dmf	34.40	0.229 ± 0.01
		32.82	0.279 ± 0.02
		31.42	0.331 ± 0.02
		30.28	0.392 ± 0.02
		29.31	0.478 ± 0.03
3. $[\text{Ni}(\text{Me}_4\text{14aneN}_4)](\text{ClO}_4)_2$ (ethanol water preparation)	CH_3CN	33.95	0.089 ± 0.004
		32.82	0.107 ± 0.006
		31.87	0.129 ± 0.01
		31.02	0.148 ± 0.01
		30.09	0.169 ± 0.01
	dmf	32.52	0.099 ± 0.005
		31.53	0.108 ± 0.01
		30.64	0.117 ± 0.01
		29.95	0.123 ± 0.01
		29.07	0.137 ± 0.01
	dmf (with 0.5 mol dm^{-3} NaClO_4)	33.80	0.134 ± 0.01
		32.53	0.167 ± 0.01
		31.57	0.185 ± 0.01
		30.70	0.212 ± 0.01
29.98		0.242 ± 0.01	
29.24		0.270 ± 0.02	
4. $[\text{Ni}(\text{Me}_4\text{14aneN}_4)](\text{ClO}_4)_2$ (ethanol preparation using triethylorthoformate)	dmf (with 0.5 mol dm^{-3} NaClO_4)	33.54	0.123 ± 0.01
		32.57	0.141 ± 0.01
		31.57	0.164 ± 0.01
		30.67	0.188 ± 0.01
		29.85	0.213 ± 0.01
		29.18	0.242 ± 0.02
5. $[\text{Ni}(\text{Me}_4\text{14aneN}_4)\text{dmf}](\text{ClO}_4)_2$ (dmf preparation)	dmf (with 0.5 mol dm^{-3} NaClO_4)	33.98	0.160 ± 0.01
		32.61	0.188 ± 0.01
		31.69	0.216 ± 0.01
		30.69	0.252 ± 0.01
		29.98	0.285 ± 0.02
		29.16	0.330 ± 0.02

continued

TABLE 6.6 *continued*

Complex	Solvent	$\frac{1}{T} \times 10^4$	Keq
6. Mixture of [Ni(dmf) ₆](ClO ₄) ₂ and Me ₄ 14aneN ₄	dmf	34.55	0.216 ± 0.01
	(with	31.93	0.359 ± 0.02
	0.5 mol dm ⁻³	30.76	0.453 ± 0.03
	NaClO ₄)	29.45	0.618 ± 0.04

N.B. The errors represent estimated errors.

TABLE 6.7

 ΔS° , ΔH° and % Low-spin Values for Different Nickel (II) Systems

Complex	Solvent	ΔS° JK ⁻¹ mol ⁻¹	ΔH° kJ mol ⁻¹	% Low-spin at 298.2K ^a
1. [Ni(12aneN ₄)](ClO ₄) ₂	dmf	-14.9 ± 0.3	2.97 ± 0.07	4.8
	H ₂ O	30.8 ± 1.1	23.6 ± 0.3	0.3
	aqueous ₃ 1.0 mol dm ⁻³ LiClO ₄	34.0 ± 0.7	22.1 ± 0.2	0.8
2. [Ni(Me ₄ 12aneN ₄)](ClO ₄) ₂ (ethanol water preparation)	CH ₃ CN	- 1.90 ± 0.98	1.71 ± 0.31	28.5
	dmf	28.0 ± 2.2	11.8 ± 0.7	20.2
	H ₂ O	23.6 ± 1.3	7.17 ± 0.42	49.4
	aqueous ₃ 0.25 mol dm ⁻³ LiClO ₄	18.1 ± 0.8	4.71 ± 0.25	57.0
3. [Ni(Me ₄ 14aneN ₄)](ClO ₄) ₂ (ethanol water preparation)	CH ₃ CN	27.8 ± 1.4	14.1 ± 0.45	8.7
	dmf	5.63 ± 1.1	7.66 ± 0.35	8.2
	dmf (with 0.5 mol dm ⁻³ NaClO ₄)	25.9 ± 1.2	12.6 ± 0.4	12.3
	H ₂ O	7.01 ± 0.04	18.5 ± 0.1	38.7
	aqueous ₃ 0.5 mol dm ⁻³ LiClO ₄	42.7 ± 0.5	11.7 ± 0.2	60.4

continued

TABLE 6.7 *continued*

Complex	Solvent	ΔS° JK ⁻¹ mol ⁻¹	ΔH° kJ mol ⁻¹	% Low-spin at 298.2K ^a
4. [Ni(Me ₄ 14aneN ₄)](ClO ₄) ₂ (ethanol preparation using triethylorthoformate)	dmf (with 0.5 mol dm ⁻³ NaClO ₄)	25.3 ± 0.8	12.8 ± 0.26	10.9
5. [Ni(Me ₄ 14aneN ₄)(dmf)](ClO ₄) ₂ (dmf preparation)	dmf (with 0.5 mol dm ⁻³ NaClO ₄)	27.2 ± 1.6	12.6 ± 0.5	14.3
6. Mixture of [Ni(dmf) ₆](ClO ₄) ₂ and Me ₄ 14aneN ₄	dmf (with 0.5 mol dm ⁻³ NaClO ₄)	45.7 ± 1.7	16.9 ± 0.54	20.8
7. [Ni(14aneN ₄)](ClO ₄) ₂	CH ₃ CN	79.2	29.0	10.2
	dmf	91.2	35.4	3.55
	DMSO	52.7	17.5	32.0
	H ₂ O	53.6	13.9	69.9
	aqueous 1.0 mol dm ⁻³ NaClO ₄	46.9	11.5	72.5

N.B. (1) Data for water and aqueous LiClO₄ solution were taken from Chapter 4.

(2) Data for the [Ni(14aneN₄)](ClO₄)₂ system was taken from reference 21.

(3) The errors represent one standard deviation.

a The errors (estimated) are ±5%.

of $2.90 \times 10^{-3} \text{ mol dm}^{-3}$ $[\text{Ni}(\text{Me}_4\text{12aneN}_4)](\text{ClO}_4)_2$ (ethanol water preparation) in dmf at various temperatures. There is no isobestic point, showing that the extinction co-efficient of the low-spin and solvated species are different at all different wavelengths examined. Temperature dependent spectra of $3.11 \times 10^{-3} \text{ mol dm}^{-3}$ $[\text{Ni}(\text{Me}_4\text{14aneN}_4)](\text{ClO}_4)_2$ (ethanol preparation using triethyl orthoformate) and $3.29 \times 10^{-3} \text{ mol dm}^{-3}$ $[\text{Ni}(\text{Me}_4\text{14aneN}_4)(\text{dmf})](\text{ClO}_4)_2$ (dmf preparation) in dmf (ionic strength 0.5) are shown in Figures 6.16 and 6.17, respectively. Table 6.8 shows further information on the spin equilibrium studies. The complexes $[\text{Ni}(\text{12aneN}_4)](\text{ClO}_4)_2$, $[\text{Ni}(\text{Me}_4\text{12aneN}_4)](\text{ClO}_4)_2$ and $[\text{Ni}(\text{Me}_4\text{14aneN}_4)](\text{ClO}_4)_2$ were found to be diamagnetic in nitromethane solution and in the solid state using the Gouy method. The $[\text{Ni}(\text{Me}_4\text{14aneN}_4)(\text{dmf})](\text{ClO}_4)_2$ complex was also found to be diamagnetic in dmf by the same method. In Figure 6.17, the spectrum (1) does not pass through the isobestic point due to experimental error or a species is present other than the two predominant species (four co-ordinate and five co-ordinate species). The molar extinction co-efficient of $[\text{Ni}(\text{Me}_4\text{14aneN}_4)(\text{dmf})](\text{ClO}_4)_2$ at 514 nm in nitromethane is used for the mixture of $[\text{Ni}(\text{dmf})_6](\text{ClO}_4)_2$ and $\text{Me}_4\text{14aneN}_4$ as the molar extinction co-efficient of the low-spin form (ϵ_{sq}) to obtain K_{eq} values. In this system, equal volume of $2.97 \times 10^{-3} \text{ mol dm}^{-3}$ $[\text{Ni}(\text{dmf})_6](\text{ClO}_4)_2$ and $2.93 \times 10^{-3} \text{ mol dm}^{-3}$ $\text{Me}_4\text{14aneN}_4$ in dmf containing 0.5 mol dm^{-3} NaClO_4 were mixed together and the spin-equilibrium was studied as a function of temperature after the attainment of final formation equilibrium.

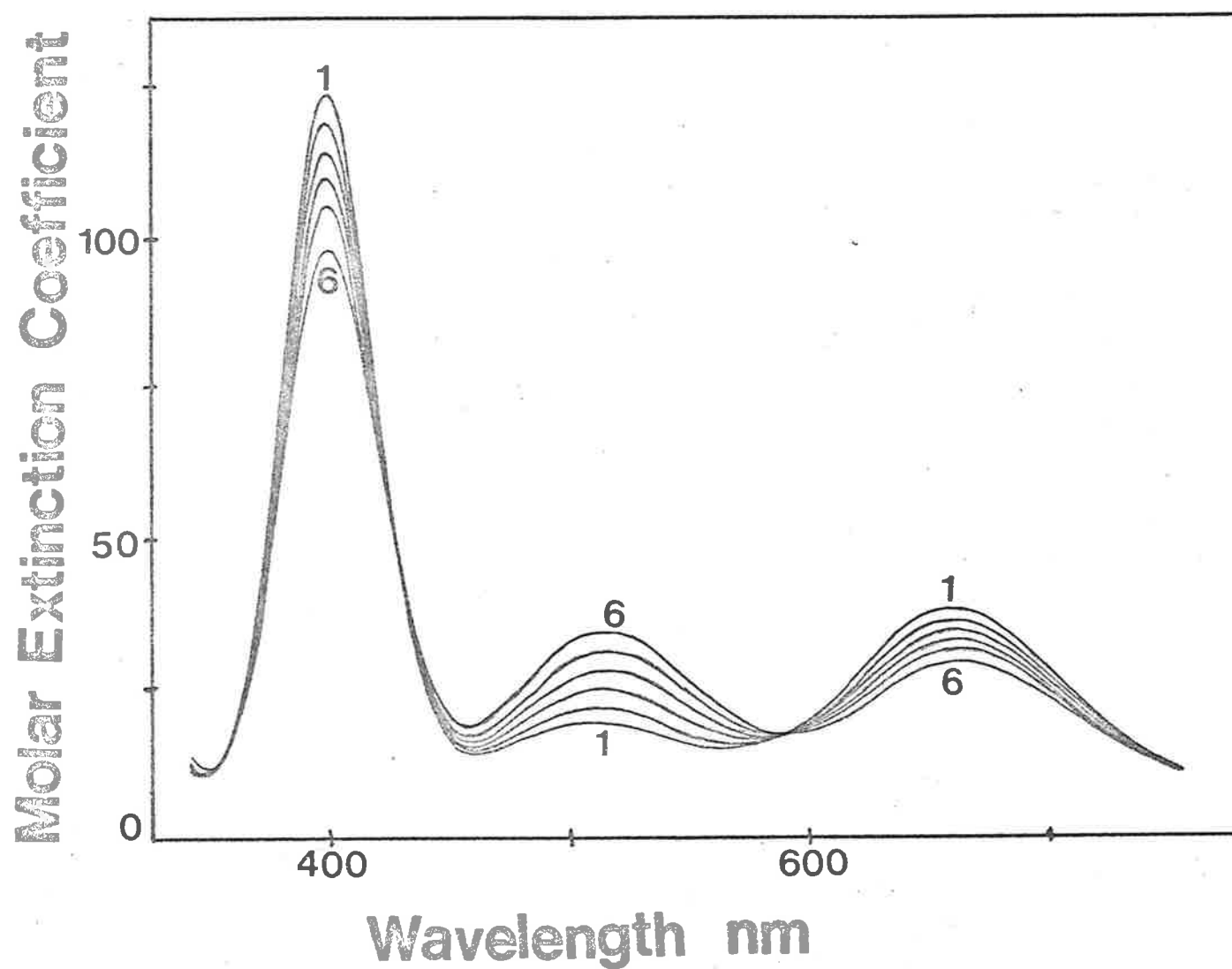


Figure 6.16 Temperature dependent uv/visible spectra of $3.11 \times 10^{-3} \text{ mol dm}^{-3}$ $[\text{Ni}(\text{Me}_4.14\text{aneN}_4)](\text{ClO}_4)_2$ (ethanol preparation using triethylorthoformate) in dmf (ionic strength = 0.5). Temperatures are 298.2, 307.1, 316.7, 326.1, 335.0 and 342.8 K for the spectra from 1 to 6 respectively.

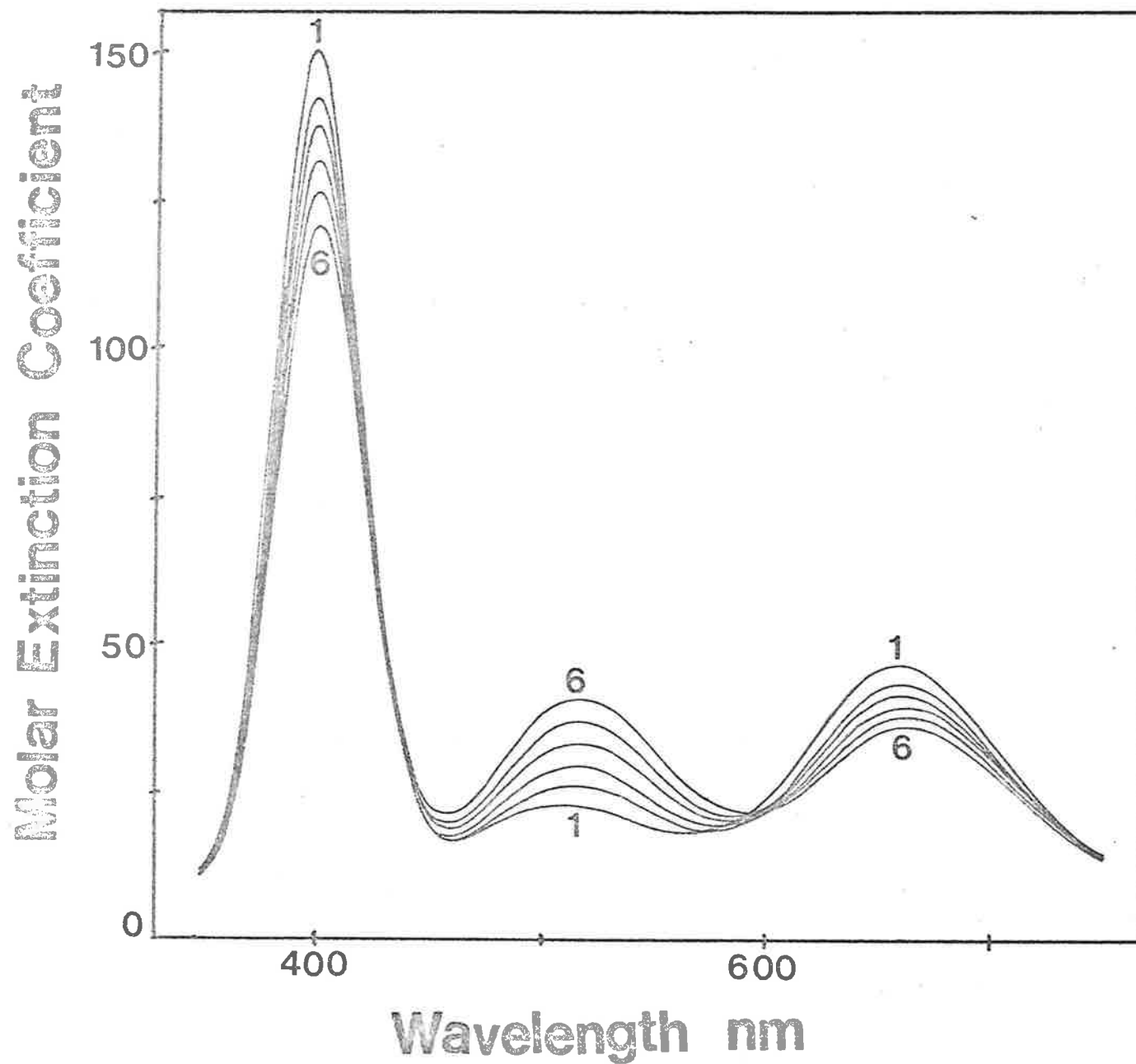


Figure 6.17

Temperature dependent uv/visible spectra of $3.29 \times 10^{-3} \text{ mol dm}^{-3}$ $[\text{Ni}(\text{Me}_4\text{14aneN}_4)\text{dmf}](\text{ClO}_4)_2(\text{dmf}$ preparation) in dmf (ionic strength = 0.5). Temperatures are 294.3, 306.7, 315.5, 325.8, 333.6 and 343.0K for the spectra from 1 to 6 respectively.

TABLE 6.8

Some Data for Spin-equilibrium Studies

Complex	Wavelength at which molar extinction co-efficient is calculated	Molar extinction co-efficient ₁ (mol ⁻¹ dm ³ cm ⁻¹ in nitromethane)	Solvent for equilibrium study	Wavelength at which isosbestic points occur	Colour after attainment of equilibrium
1. [Ni(12aneN ₄)](ClO ₄) ₂	421	59.2	dmf	365, 482, 585	Purple
2. [Ni(Me ₄ 12aneN ₄)](ClO ₄) ₂ (ethanol water preparation)	455	184.4	CH ₃ CN dmf	354 x	Purple Greenish red
3. [Ni(Me ₄ 14aneN ₄)](ClO ₄) ₂ (ethanol water preparation)	514	207.0	CH ₃ CN dmf dmf (with 0.5 mol dm ⁻³ NaClO ₄)	384, 584 442, 576 422, 600	Blue Green Green
4. [Ni(Me ₄ 14aneN ₄)](ClO ₄) ₂ (ethanol preparation using triethylorthoformate)	514	175.8	dmf (with 0.5 mol dm ⁻³ NaClO ₄)	427, 591	Green
5. [Ni(Me ₄ 14aneN ₄)(dmf)](ClO ₄) ₂ (dmf preparation)	514	165.4	dmf (with 0.5 mol dm ⁻³ NaClO ₄)	429, 599	Green
6. Mixture of [Ni(dmfd) ₆](ClO ₄) ₂ and Me ₄ 14aneN ₄	514	assumed to be 165.4	dmf (with 0.5 mol dm ⁻³ NaClO ₄)	422, 600	Green

6.5. General Discussion.

The rates of complexation of macrocyclic ligands with different metal ions have been investigated ^{7, 8, 13, 20, 38-44} but only a few studies have been reported in non-aqueous solvents. ¹⁸⁻²⁰ There appears to be no previous study in dmf. The complex formation in all the systems reported here appears to involve the usual I_d or D mechanism and the additional slow processes may be attributed to isomerisation for achievement of thermodynamic equilibrium as discussed earlier. L. F. Lindoy and co-workers ²⁰ studied the kinetics of complexation of $NiCl_2$ in methanol with two O_2N_2 -donor macrocyclic ligands using the stopped flow technique. They observed an initial fast process followed by a slower step and the fast process depends upon the concentration of both the ligand and the metal ion while the slower process is independent of ligand concentration at a constant nickel (II) concentration. L. Hertli and T. A. Kaden ¹³ studied the formation of copper (II), nickel (II), cobalt (II) and zinc (II) complexes with $Me_4\text{14ane}N_4$ in an aqueous medium. They have conjectured that the slow process could be a conformational change of the ligand. This change may occur in a rapid pre-equilibrium before the complexation step or an intermediate with one or more nitrogen atoms already co-ordinated to metal ion. ¹²

It has been demonstrated for other macrocyclic systems ^{10-15, 19, 45} that the rate determining step in the formation kinetics is not controlled by the dissociation of the first co-ordinated solvent molecule. Rorabacher and co-workers ^{19, 45} studied the formation of copper (II) complexes and they proposed that second bond formation is the rate determining step because of the steric constraints associated with macrocyclic ligands compared with polydentate ligands. However, the results reported here are in dmf and can

be best explained by an I_d or D mechanism. One of the main reasons for fast complexation in dmf compared with water is that the protonation of the ligand does not arise at all in dmf. The approximately estimated K_{eq} value (298.2K) for $[\text{Ni}(\text{Me}_4\text{14aneN}_4)(\text{dmf})]^{2+}$ formation in dmf is $2.8 \times 10^{-3} \text{ mol}^{-1} \text{ dm}^3$ whereas this value becomes equal to $1.1 \times 10^{-7} \text{ mol}^{-1} \text{ dm}^3$ (290.1K) for $[\text{Ni}(\text{12aneN}_4)(\text{OH}_2)_2]^{2+}$ formation (Chapter 5) in water. This large difference in K_{eq} value cannot be expected due to different temperature and ligand. It is more logical to conclude that the concentration of the outer sphere complex formed from a charged nickel (II) and a neutral ligand is expected to be higher than that formed between two charged reactants of same sign.

The following important factors influence the rate of substitution at nickel (II) especially in dipolar aprotic solvents such as CH_3CN , $\text{HCO N}(\text{CH}_3)_2$ and $(\text{CH}_3)_2\text{SO}^{33, 46}$ with ligands other than macrocyclic ligands:-

- a. a solvent dependent steric requirement demonstrated by multi-dentate ligands during chelation.
- b. a solvent dependent rotational barrier to the proper orientation in space of co-ordinating ligand atoms during chelation.
- c. stabilization of metal-ligand outer sphere complexes by π orbital or electrostatic interactions between the incoming ligand and polarised solvent molecules in the first co-ordination of the metal ion. Hence a study of ligand substitution reaction at nickel (II) in dipolar aprotic solvents such as $\text{HCO N}(\text{CH}_3)_2$, CH_3CN and $(\text{CH}_3)_2\text{SO}$ with macrocyclic ligands of varying ring size and steric properties could aid in identifying several specific rate-determining effects.

The percentages of low-spin form of different complexes of

nickel (II) in different solvents at 298.2K are given in Table 6.7 together with the associated ΔS° and ΔH° values. From Table 6.7, it appears that the order of stability (low-spin formation) for solvents employed is $\text{dmf} > \text{aqueous } 1.0 \text{ mol dm}^{-3} \text{ LiClO}_4 > \text{H}_2\text{O}$ for $[\text{Ni}(\text{12aneN}_4)]^{2+}$ system, $\text{aqueous } 0.25 \text{ mol dm}^{-3} \text{ LiClO}_4 > \text{H}_2\text{O} > \text{CH}_3\text{CN} > \text{dmf}$ for $[\text{Ni}(\text{Me}_4\text{12aneN}_4)]^{2+}$ system and $\text{aqueous } 0.5 \text{ mol dm}^{-3} \text{ NaClO}_4 > \text{H}_2\text{O} > \text{dmf}$ ($0.5 \text{ mol dm}^{-3} \text{ NaClO}_4$) $> \text{CH}_3\text{CN} > \text{dmf}$ for $[\text{Ni}(\text{Me}_4\text{14aneN}_4)]^{2+}$ system. In dmf ($0.5 \text{ mol dm}^{-3} \text{ NaClO}_4$), the order of stability for different complexes of $[\text{Ni}(\text{Me}_4\text{14aneN}_4)]^{2+}$ is found to be $A > B > C > D$ where

A = complex obtained by mixture of $[\text{Ni}(\text{dmf})_6](\text{ClO}_4)_2$ and $\text{Me}_4\text{14aneN}_4$

B = complex prepared in dmf

C = complex prepared in ethanol water mixture.

D = complex prepared in ethanol using triethylorthoformate.

The order of stability in different solvents for the

$[\text{Ni}(\text{14aneN}_4)](\text{ClO}_4)_2$ system was reported²¹ to be aqueous

$0.1 \text{ mol dm}^{-3} \text{ NaClO}_4 > \text{H}_2\text{O} > \text{DMSO} > \text{CH}_3\text{CN} > \text{dmf}$. The stability order

may be different for solvents of different donor properties. For

different nickel (II) complexes, the order of stability is found to be

$[\text{Ni}(\text{Me}_4\text{12aneN}_4)]^{2+} > [\text{Ni}(\text{Me}_4\text{14aneN}_4)]^{2+} > [\text{Ni}(\text{12aneN}_4)]^{2+} >$

$[\text{Ni}(\text{14aneN}_4)]^{2+}$ in dmf ,

$[\text{Ni}(\text{14aneN}_4)]^{2+} > [\text{Ni}(\text{Me}_4\text{12aneN}_4)]^{2+} > [\text{Ni}(\text{Me}_4\text{14aneN}_4)]^{2+} >$

$[\text{Ni}(\text{12aneN}_4)]^{2+}$ in H_2O and

$[\text{Ni}(\text{Me}_4\text{12aneN}_4)]^{2+} > [\text{Ni}(\text{14aneN}_4)]^{2+} > [\text{Ni}(\text{Me}_4\text{14aneN}_4)]^{2+}$ in

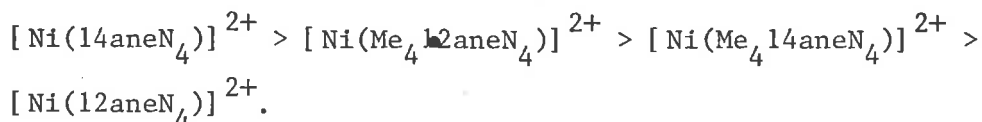
CH_3CN . The stability orders are given for low-spin formation and

therefore these orders will be reversed for solvent adduct (high spin)

formation in different solvents. Both ΔH° and ΔS° values are

highest for mixture of $[\text{Ni}(\text{dmf})_6](\text{ClO}_4)_2$ and $\text{Me}_4\text{14aneN}_4$ in

dmf but ΔH° value is lowest for $[\text{Ni}(\text{Me}_4\text{12aneN}_4)]^{2+}$ system in CH_3CN and ΔS° value is highest for $[\text{Ni}(\text{12aneN}_4)]^{2+}$ system in dmf. In dmf, both ΔH° and ΔS° values follow the order



Herron and Moore⁴⁷ studied the rates of acetonitrile exchange with two isomers of $[\text{Ni}(\text{Me}_4\text{14aneN}_4)](\text{ClO}_4)_2$ (see Chapter 1, section 1.2) by ^{13}C n.m.r. line broadening experiments. They claimed that $[\text{Ni}(\text{R.S.R.S.} - \text{Me}_4\text{14aneN}_4)](\text{ClO}_4)_2$ and $[\text{Ni}(\text{R.S.S.R.} - \text{Me}_4\text{14aneN}_4)](\text{ClO}_4)_2$ are completely converted into the respective five and six co-ordinate complexes in acetonitrile. The present study contradicts with this and showed that the $[\text{Ni}(\text{Me}_4\text{14aneN}_4)](\text{ClO}_4)_2$ (ethanol water preparation, four methyl groups are expected to be on the same side of the macrocyclic plane) complex exists in acetonitrile as a mixture of 8.7% low spin (four co-ordinate) and 91.3% high spin (five co-ordinate) species at 298.2K. The formation of low spin species is favoured by an increase in temperature.

It would be expected that the entropy changes may be attributed to the reduction of spin-multiplicity (negative entropy) and the release of co-ordinated solvent molecules (positive entropy) whereas solvating power, steric effect and solvent lODq might be contributing factors to the ΔH° values. However, the ΔH° and ΔS° values are not systematic indicating the probability that a number of compensating factors may be at work and therefore qualitative analysis of these values would be futile.

REFERENCES FOR CHAPTER SIX

1. H. K. Frensdorft, J.A.C.S., 93, 600 (1971).
2. D. K. Cabbiness and D. W. Margerum, J.A.C.S., 91, 6540 (1969).
3. D. H. Busch, K. Farmery, V. Goedken, V. Katovic, A. C. Melnyk, C. R. Sperati and N. Tokel, Advanced Chem. Ser. No. 100, 44 (1971).
4. L. Y. Martin, L. J. Dehayes, L. J. Zompa and D. H. Busch, J.A.C.S., 96, 4046 (1974).
5. D. D. Watkins, D. P. Riley, A. J. Stone and D. H. Busch, Inorg. Chem., 15, 387 (1976).
6. Y. Hung, L. Y. Martin, S. C. Jackels, A. M. Tait and D. H. Busch, J.A.C.S., 99, 4029 (1977).
7. D. K. Cabbiness and D. W. Margerum, J.A.C.S., 92, 2151 (1970).
8. R. W. Hay and C. R. Clarke, J.C.S. Dalton, 1148 (1978).
9. J. Weaver and P. Hambright, Inorg. Chem., 8, 167 (1969).
10. R. Buxtorf, W. Steinmann and T. A. Kaden, Chimia, 28, 15 (1974).
11. T. A. Kaden, Chimia, 30, 207 (1976).
12. T. A. Kaden, Helv. Chim. Acta., 53, 617 (1970), 54, 2307 (1971).
13. L. Hertli and T. A. Kaden, Helv. Chim. Acta., 57, 1328 (1974).
14. R. Buxtorf and T. A. Kaden, Helv. Chim. Acta., 57, 1035 (1974).
15. W. Steinmann and T. A. Kaden, Helv. Chim. Acta., 58, 1358 (1975).
16. G. W. Liesegang, M. M. Farrow, F. A. Vazquez, N. Purdie and E. M. Eyring, J.A.C.S., 99, 3240 (1977).
17. V. M. Loyola, R. G. Wilkins and R. Pizer, J.A.C.S., 97, 7382 (1975).
18. E. Schhori, J. Jagur-Grodzinski and M. Shpores, J.A.C.S., 95, 3842 (1973).
19. T. E. Jones, L. L. Zimmer, L. L. Diaddario, D. B. Rorabacher and L. A. Ochrymowycz, J.A.C.S., 97, 7163 (1975).
20. A. Ekstrom, L. F. Lindoy, H. C. Lip, R. J. Smith, H. J. Goodwin, M. McPartlin and P. A. Tasker, J.C.S., Dalton, 1027 (1979).
21. G. S. Vigee, C. L. Watkins and H. F. Bowen, Inorg. Chim. Acta., 35, 255 (1979).

22. A. Anichini, L. Fabbrizzi, P. Paoletti and R. M. Clay, *Inorg. Chim. Acta.*, 24, L21 (1977).
23. L. Rusnak and R. B. Jordan, *Inorg. Chem.*, 10, 2199 (1971).
24. M. Eigen, "Proceedings of the VIIth International Conference on Co-ordination Chemistry", Butterworths, London, p.97, (1962).
25. C. H. Langford and H. B. Gray, "Ligand Substitution Processes", W. A. Benjamin, Inc., New York (1966).
26. R. G. Wilkins, "The Study of Kinetics and Mechanisms of Transition Metal Complexes", Boston, Allyn and Bacon (1976).
27. N. A. Matwiyoff, *Inorg. Chem.*, 5, 788 (1966).
28. M. L. Tobe, "Inorganic Reaction Mechanisms", The Camelton Press Ltd., London, 91 (1972).
29. M. Eigen and R. G. Wilkins, *Adv. Chem. Ser.*, 49, 55 (1965).
30. R. G. Wilkins, *Acc. Chem., Res.*, 3, 408 (1970).
31. R. G. Pearson and P. Ellegen, *Inorg. Chem.*, 6, 1379 (1967).
32. M. L. Sanduja and W. M. Smith, *Can. J. Chem.*, 50, 3861 (1972).
33. P. K. Chattopadhyay and B. Kratochvil, *Can. J. Chem.*, 55, 3449 (1977).
34. R. G. Wilkins, *Acc. Chem. Res.*, 3, 408 (1970).
35. A.G. Desai, H.W. Dodgen and J.P. Hunt, *J.A.C.S.*, 92, 798 (1970).
36. B. Bosnich, C. K. Poon and M. L. Tobe, *Inorg. Chem.*, 4, 1102 (1965).
37. L. G. Warner and D. H. Busch, *J.A.C.S.*, 91, 4092 (1969).
38. M. Kodama, *J.C.S., Chem. Comm.*, 891 (1975).
39. M. Kodama, *J.C.S., Chem. Comm.*, 326 (1975).
40. M. Kodama and E. Kimura, *J.C.S., Dalton*, 2269 (1977).
41. B. F. Liang and C. S. Chung, *J.C.S., Dalton*, 1349 (1980).
42. L. Diaddario, L. Zimmer, T. Jones, L. Sokol, R. Cruz, E. Yee, L. Ochrymowycz and D. Rorabacher, *J.A.C.S.*, 101, 3511 (1979).
43. B. Bosnich, M. L. Tobe and G. A. Webb, *Inorg. Chem.*, 4, 1109 (1965).
44. A. P. Leugger, L. Hertli and T. A. Kaden, *Helv. Chim. Acta.*, 61, 2296 (1978).
45. C. T. Lin, D. B. Rorabacher, G. R. Cayley and D. W. Margerum, *Inorg. Chem.*, 14, 919 (1975).

46. P. K. Chattopadhyah and J. F. Coetzee, *Anal. Chem.*, 46, 2014 (1974). *Inorg. Chem.*, 12, 113 (1973).
47. N. Herron and P. Moore, *J.C.S., Dalton*, 441 (1979).

CHAPTER SEVEN

Experimental Techniques

Contents.

- 7.1 Spectrophotometric measurements and pH determinations.
- 7.2 Magnetic moment measurements:-
 - (a) The Gouy method
 - (b) The Evans' method.
- 7.3 Job's method of continuous variation.
- 7.4 Oxygen-17 n.m.r. measurements.
- 7.5 The temperature jump method:-
 - (a) The relation between relaxation time and rate constants.
 - (b) The magnitude of the displacement of equilibrium concentrations.
 - (c) Experimental considerations.
 - (d) Analysis of the Photographs.
- 7.6 The stopped flow method:-
 - (a) Principle of the stopped flow method.
 - (b) The stopped flow apparatus.
 - (c) Analysis of stopped flow traces.
 - (d) Estimation of the rate constant for the 1st order process.
 - (e) Estimation of the apparatus dead time.
 - (f) Second variety of stopped flow apparatus.

CHAPTER SEVEN

Experimental Techniques7.1 Spectrophotometric Measurements and pH Determinations:

Ultra-violet and visible spectra were recorded on a Zeiss DMR10 spectrophotometer with therostated cell holders. The temperature of the circulating water was controlled to ± 0.2 . A platinum resistance thermometer was used to determine the temperature of the cell contents. A pH M64 digital-readout Radiometer pH meter was used to adjust the pH of solutions. Phosphate, pH, and potassium hydrogen pthalate, pH, buffers were used to standardise the pH meter.

Slow acid dissociation reactions were followed at a fixed wavelength under pseudo 1st order conditions using a Zeiss DMR 10 spectrophotometer. Observed rate constants were computed by a least squares analysis using the equation¹

$$\ln \frac{A_t - A_\infty}{A_0 - A_\infty} = -kt \quad 7.1$$

where A_t = absorbance at any time 't'

A_0 = initial absorbance

A_∞ = absorbance at infinite time.
(more than seven half lives)

k = observed rate constant.

7.2 Magnetic Moment Measurements:-(a) The Gouy Method.

The magnetic moments of solid complexes, nitromethane solutions of complexes (tube filled inside a dry box) and the diamagnetic

susceptibility of solid LiClO_4 ($\chi = -0.178 \times 10^{-6}$ units/gm) were determined by the Gouy method² using $\text{Hg}[\text{Co}(\text{NCS})_4]$ as a standard. The mass susceptibility of 4.0 mol dm^{-3} LiClO_4 ($\chi = -0.533 \times 10^{-6}$ units/gm) was calculated, (assuming negligible change with temperature), by use of equation 7.2^{3, 4}

$$\chi_{\text{soln.}} = C_s \chi_s + (1 - C_s) \chi_w \quad 7.2$$

where $C_s = \frac{\text{weight of the solute}}{\text{total weight of solution}}$

and $\chi_{\text{soln.}}$, χ_w and χ_s being the susceptibility of solution, water and solute respectively. The diamagnetic corrections for elements, metals, etc., are well known.⁵ The corrections made for organic ligands were estimated from known values of simpler organic groups.

(b) The Evans' Method:-

The temperature dependent magnetic moment of $[\text{Ni}(\text{12aneN}_4)](\text{ClO}_4)_2$ in solution was determined by the Evans' method⁶ using precision co-axial n.m.r. tubes (wilmad) and a Bruker HX90E n.m.r. spectrophotometer for which temperature control accuracy was $\pm 0.3\text{K}$. Corrections were made for the experimentally determined density variation of the solutions with temperature. The magnetic moments of $[\text{Ni}(\text{12aneN}_4)](\text{ClO}_4)_2$ in water and nitromethane were determined by a Varian T60 spectrophotometer using 3% w/w tertiary butanol and tetramethyl silane as reference signals, respectively. Diamagnetic corrections were calculated from Pascal's constants. Magnetic moment was determined from the difference between the proton resonance frequency of tertiary butanol in the solution and the tertiary butanol in the capillary. The mass susceptibility, χ , of the dissolved substance is given by equation 7.3⁶

$$\chi = \frac{3\delta\nu}{2\pi\nu_0 m} + \chi_0 + \frac{\chi_0 (d_0 - d_s)}{m} \quad 7.3$$

where δv = frequency shift in hertz (Hz)
 ν_0 = the operating frequency (60 MHz or 90 MHz)
 m = mass of the substance contained in 1 cm³ of solution.
 χ_0 = mass susceptibility of the solvent
 d_0 = density of solvent
 d_s = density of solution.

For highly paramagnetic ions, Evans⁶ has shown that the last term in equation 7.3 can usually be neglected without serious error, thus

$$\chi = \frac{3\delta v}{2\pi\nu_0 m} + \chi_0 \quad 7.4$$

The effective magnetic moment (μ_{eff}) was calculated from χ in the following way:-⁷

$$\mu_{\text{eff}} = 2.84 \sqrt{T \cdot \chi_{\text{Mcorr.}}} \text{ B.M.} \quad 7.5$$

where χ_{M} = molar susceptibility

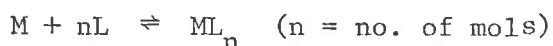
χ_{Mcorr} = corrected paramagnetic molar susceptibility
 = $\chi_{\text{M}} + / \Delta /$, Δ being computed by adding diamagnetic susceptibilities of all the constituent groups or atoms of the substance.

T = absolute temperature of measurement

B.M = Bohr magnetons.

7.3 Job's Method of Continuous Variation:-

If, to a solution of metal ion (M), ligand solution (L) is added, a complex may be formed according to the following equation



The composition of the complex ML_n formed in solution can be determined by Job's method^{8,9} of continuous variation using a uv/visible spectrophotometer provided the complex exhibits a suitable spectra. Solutions of approximately equimolar concentrations of

'M' and 'L' were prepared separately at a constant ionic strength. The following solution mixtures were then prepared with different volume ratios (M : L) of 'M' and 'L'

M:L 0:10, 1:9, 2:8, 3:7, 4:6, 5:5, 6:4, 7:3, 8:3, 9:1, 10:0.

The solution mixtures were left at a fixed temperature for attainment of final equilibrium and the uv/visible spectra were then recorded. A wavelength was selected where the ligand and metal ion absorbed to a negligible state in comparison with the absorbance of the complex. The total absorbance of each mixture at that fixed wavelength was then determined for each spectrum. This absorbance is denoted A_{measured} . If there had been no interaction between 'M' and 'L', then the absorbance at the same wavelength ($A_{\text{calculated}}$) would have been given by

$$A_{\text{calculated}} = \epsilon_M C_M t + \epsilon_L C_L t$$

where ϵ = molar extinction co-efficient of 'M'

C_M = concentration of 'M'

ϵ_L = molar extinction coefficient of 'L'

C_L = concentration of 'L'

t = path length of the cell.

Let Y be the difference between A_{measured} and $A_{\text{calculated}}$

i.e. $Y = A_{\text{measured}} - A_{\text{calculated}}$.

The values of Y are then plotted against the mol fraction of

'L' $\left(\frac{[\text{ligand}]}{[\text{ligand}] + [\text{metal salt}]} \right)$. The maxima in these curves will occur at mol fraction, $\frac{n}{1+n}$, of 'L', thus the formula of the complex present in solution can be deduced.

7.4 Oxygen-17 n.m.r. Measurements:-

Oxygen-17 n.m.r. measurements were carried out at 13.2, 11.5 and 5.75 MHz on a variable field n.m.r. spectrometer. The ^{17}O resonances were observed in the absorption mode and the half width at half

maximum amplitude, W , was derived through a computer fit of the Lorentzian line shape. Sample temperature control was adjustable to within $\pm 0.1\text{K}$ and the ^{17}O water was 10% ^{17}O (normalised in H content). Water exchange rate constants on $[\text{Ni}(\text{12aneN}_4)(\text{OH}_2)_2]^{2+}$ were determined in dilute solutions of this ion from the changes in transverse relaxation rates and chemical shifts of the bulk water ^{17}O nuclei according to the following equations:-¹⁰

$$T_{2p}^* = \frac{\tau_M \left((1/T_{2M} + 1/\tau_M)^2 + \Delta\omega_M^2 \right)}{n\chi_p (1/T_{2M}^2 + 1/T_{2M}\tau_M + \Delta\omega_M^2)} \quad 7.6$$

$$Q = \chi_p \cdot \left[\frac{n(T\Delta\omega_M/\omega_o)}{\tau_M^2 [(1/T_{2M} + 1/\tau_M)^2 + \Delta\omega_M^2]} + Q_o \right] \quad 7.7$$

where $\tau_M (= 1/k_{\text{H}_2\text{O}})$ = mean life time of a water molecule bound to $[\text{Ni}(\text{12aneN}_4)(\text{OH}_2)_2]^{2+}$, T_{2M} is the ^{17}O transverse relaxation time of that water molecule and $\Delta\omega_M$ is its chemical shift, χ_p is the mol fraction of nickel (II) in the high-spin state, Q_o is the contribution to Q from outside the first co-ordination sphere, T_{2p}^* and Q being relaxation and shift based parameters, n is the number of water molecules (assumed 2) in the complex.

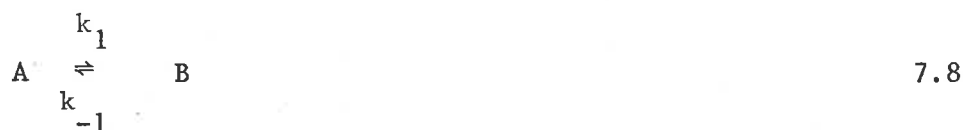
7.5 The Temperature Jump Method:-

(a) The Relation between relaxation time and rate constants:-

In the temperature jump method a reaction mixture at equilibrium is suddenly perturbed by a temperature rise brought about by discharging an electric current from a capacitor through the reaction mixture which also contains inert electrolyte. If the equilibrium constant depends upon the temperature,^{11, 12} the subsequent re-equilibration at the higher temperature can be followed spectrophotometrically. During chemical re-equilibration, in general, one or more relaxation processes may be observed if the spectrophotometer signal is

followed as a function of time and is stored as an oscilloscope trace.

For simplicity, the following reversible 1st order reaction¹³ represented by



may be considered to illustrate the method. At a fixed temperature, the concentrations of the reactants and the products will remain constant. Let a_0 be the initial concentration of A, b_0 be the initial concentration of B and at any time 't', the concentrations of 'A' and 'B' are 'a' and 'b', respectively. A new equilibrium is then established by a rapid rise of temperature, at time $t = 0$, where \bar{a} and \bar{b} are the new equilibrium concentrations at the higher temperature of 'A' and 'B', respectively. So, we may write

$$y = a - \bar{a} = \bar{b} - b \quad 7.9$$

where y is the difference between actual values and equilibrium values at any time 't' from the temperature rise. At any time 't', the rate of change of a is given by

$$-\frac{da}{dt} = k_1 a - k_{-1} b$$

$$\text{hence } -\frac{dy}{dt} = k_1 a - k_{-1} b \quad 7.10$$

where k_1 and k_{-1} are the forward and the backward rate constants.

At equilibrium,

$$k_1 \bar{a} - k_{-1} \bar{b} = 0 \quad 7.11$$

$$\text{hence } -\frac{dy}{dt} = (k_1 + k_{-1})y \quad 7.12$$

(from equations 7.9, 7.10 and 7.11)

The overall 1st order rate constant, k, is then defined by

$$k = (k_1 + k_{-1}) \quad 7.13$$

Integration of equation 7.12 using equation 7.13 results in equation 7.14

$$\frac{y}{y_0} = e^{-kt} = e^{-t/\tau} \quad 7.14$$

where y_0 is the value of y immediately after the temperature jump.

A plot of $\ln \frac{y}{y_0}$ vs time gives a straight line of slope $= -1/\tau$

Let us consider another reaction of the type¹³



with a temperature dependent equilibrium where complex formation and ion association results. At any time 't' after the temperature jump,

$$y = b - \bar{b} = c - \bar{c} = \bar{d} - d \quad 7.16$$

where b, c, d and $\bar{b}, \bar{c}, \bar{d}$ are the concentrations of B, C, D at any time 't' and at equilibrium, respectively, y being the difference between actual values and equilibrium values at any time 't'.

At any time 't', the net forward rate is given by

$$-\frac{dy}{dt} = k_1 bc - k_{-1} d \quad 7.17$$

and at equilibrium,

$$k_1 \bar{b}\bar{c} = k_{-1}\bar{d} \quad 7.18$$

with the help of equations 7.16, 7.17 and 7.18, neglecting y^2 terms as they will be negligible compared with y terms, the net forward rate results as

$$-\frac{dy}{dt} = [k_1(\bar{b} + \bar{c}) + k_{-1}] y \quad 7.19$$

which represents a 1st order approach to equilibrium, the terms within square brackets being a constant. Therefore considering

equation 7.15 as a 1st order process for small displacements, the relaxation time, τ , is related to the rate constant, k , as follows:-

$$\tau^{-1} = k = k_1(\bar{b} + \bar{c}) + k_{-1} \quad 7.20$$

Integration of equation 7.19 making use of equation 7.20 gives

$$\frac{y}{y_0} = e^{-kt} = e^{-t/\tau} \quad 7.21$$

and as before a plot of $\ln \frac{y}{y_0}$ vs time gives a straight line of slope $= -1/\tau$.

Only the single step mechanism is discussed above. In case of multistep systems, n independent concentration variables give n independent rate equations and solutions of various transformation matrices¹⁴ are necessary. Computer calculations of the multistep processes are listed by I. Amdur and G. G. Hammes.¹⁵

(b) The magnitude of the displacement of equilibrium concentration:-

The perturbation of a reaction mixture at equilibrium by altering the temperature of the system suddenly and using a fast recording device to follow the re-equilibration, is as has been explained, the basic principle of this method.^{13, 16, 17} The method can thus be applied to reactions for which the equilibrium constant depends upon temperature according to the Van't Hoff¹⁶ equation, $\Delta H^0 \neq 0$

$$\left(\frac{d \ln K}{dt} \right)_p = \frac{\Delta H^0}{RT^2} \quad 7.22$$

for a small change,

$$\frac{\Delta K}{K} + \frac{\Delta H^0}{RT^2} \Delta T \quad 7.23$$

A temperature rise of a few degrees produces an equilibrium shift resulting in a measurable concentration change provided ΔH^0 is not very small or zero. The equilibrium constant should be close to unity for the maximum effect. The magnitude of the concentration changes when the equilibrium is shifted by a temperature rise depends

upon the values of ΔH° and K_{eq} as well as on initial concentrations of the reactant species.

(c) Experimental Considerations:-

The time constant for the heating process depends upon the resistance of the solution in the cell (R) and the capacitance (C) of the discharge condenser as follows:

$$\text{Time constant for heating } (\tau_{\text{heating}}) = \frac{RC}{2}$$

thus where C = 0.1 microfarad (capacitance of condenser) and R = 27 ohms (resistance of a solution of NaClO_4 in the cell),

$$\tau_{\text{heating}} = 1.35 \mu\text{sec.}$$

The temperature jump of the reaction mixture on discharging may be computer as follows^{18, 19}

$$V_t = V_o e^{-t/RC} \quad 7.24$$

t = time from start of discharge

V_o = initial voltage,

R = cell resistance

C = capacitance.

The amount of energy E dissipated in time dt is

$$dE = \frac{V_t^2}{R} dt \quad 7.25$$

$$\Delta T(t) = \int_0^t \frac{V_o^2}{V\rho C_p R} e^{-2t/RC} \quad 7.26$$

where ΔT = temperature rise after time t

C_p = heat capacity of solution in the cell at constant pressure

ρ = density of solution

V = volume of solution

A temperature rise¹⁸ of 10.33K was measured for a small cell containing approximately 1.5 cm^3 at a capacitor voltage setting of

25kV (V_0). The heating time for a 10.33K temperature jump ($\leq 2 \mu\text{s}$ in the 2.0 to 4.0 mol dm^{-3} aqueous LiClO_4 solutions) was determined using phenol red in trizma base buffer at pH 7.21. Approximate optical densities (for 1 cm cell) of the solution were 0.96 and 0.89 at 288.2K and 298.2K, respectively. The change in absorbance with temperature was measured spectrophotometrically at 555 nm and the photographs were analysed to obtain the heating time. A chemical relaxation process may be more rapid than the heating time for a fast reaction and therefore the heating time must be determined to ensure that the observed chemical relaxation times are greater than τ_{heating} . Longer heating times (more than 2 μs) were observed for aqueous solutions less than 2.0 mol dm^{-3} in LiClO_4 and hence no relaxation studies were carried out using such solutions. Under the experimental conditions, cavitation effects did not arise. The temperature jump apparatus was constructed in a similar manner to that described in the literature.²⁰ In order to minimise electrical and magnetic disturbances, both the charging resistor and the condenser were shielded from the remaining circuitry by means of aluminium and iron boxes. The 0.1 microfarad condenser was charged from a Brandenburg E.H.T. generator type MR50/R. The electrical energy was discharged manually by closing a spark gap and a 500 m Ω charging resistor is incorporated in series with the capacitor. The schematic diagram is shown in Figure 7.1. The signal from the photomultiplier after passing through the cathode follower, enters into the Tektronix type 549 storage oscilloscope. Two 1.35 volt mercury batteries in series were used to back off the signal. The photomultiplier, type E.M.I. 6256/S, employs either five or seven dynodes, powered from a Nuclear Enterprises Ltd type N.E. 5307 E.H.T. supply. A Philips type 7023 (100 watt, 12 volt) quartz iodide lamp is the spectrophotometric

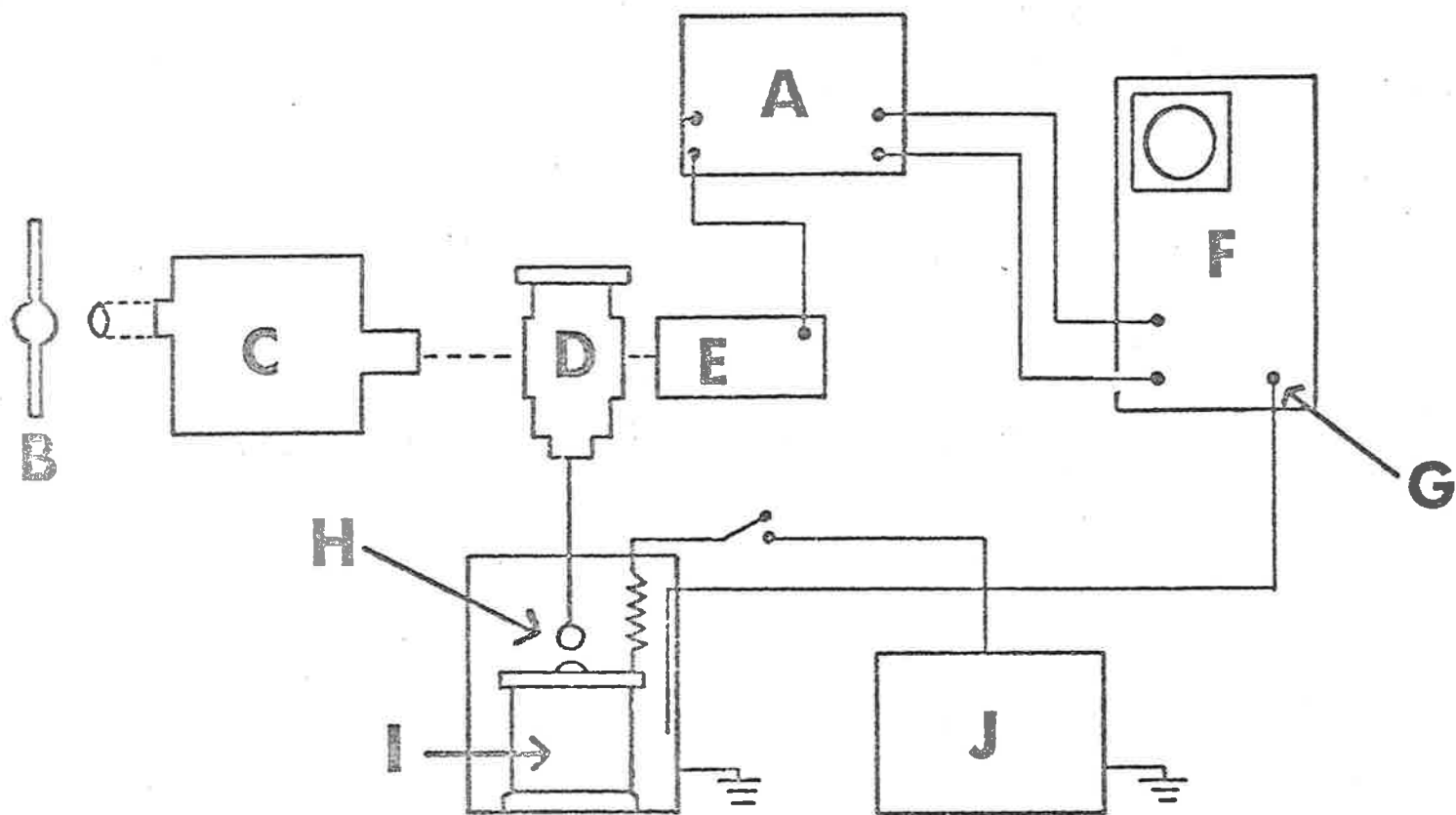


Figure 7.1

Schematic diagram of the temperature jump apparatus

A = Cathode follower

E = Photomultiplier type E.M.I. 6256/S

I = 35 kV - 0.1 μ F capacitor

B = Xe-Hg arc lamp

F = Tektronix type 549 storage oscilloscope

J = 0-50 kV power supply

C = Bausch and Lomb high intensity monochromator

G = External trigger

D = Cell assembly

H = Moveable spark gap

(Diagram from P.R. Collins's Ph.D. thesis, University of Adelaide, 1979)

light source while a Bausch and Lomb high intensity grating monochromator (1350 grooves/mm) is the source for monochromatic light. The ratio of entrance to exit slit width was about 1.8 for these studies. An iris diaphragm regulated the width of the beam of light entering the solution in the cell assembly. The cell assembly contains a volume of about 1.5 cm^3 and is filled through two narrow capillary inlets taking care that no air bubble is formed inside the cell. All solutions were degassed by the 'freeze pump thaw' method and filtered through a millipore filter before filling the cell to minimise bubble formation. The filled cell is placed in a cell jacket which is thermostated by passing water from a water bath. The cell may be rotated manually to maximise the intensity of the light passing through the solution. To prevent any spark, the cell body was made of perspex, using high grade stainless steel electrodes smoothly chamfered at the edges. Also, it was necessary to buff the electrodes periodically to remove any surface film.

(d) Analysis of the Photographs:-

A base line was drawn on each photograph corresponding to the voltage of infinite time. The photographs were measured using a digital micrometer device, built by Dr. G. S. Laurence in this department. The vertical displacement of the trace is related to an electrical signal in millivolts whereas the horizontal displacement is a measure of time. The displacement (x) of the trace between the relaxation curve and the base line was measured at various horizontal distances ' d ' (cm) from the origin of the trace. A plot of $\ln x$ vs d gives a straight line of a slope which when multiplied by a factor $\frac{0.888}{(\text{time/cm})}$ gives the true relaxation time (τ). The factor allows for the magnification of the oscilloscope camera. At least four

photographs were analysed for each solution and the mean value was used. The standard deviation (S.D) of the mean value was obtained as follows:-

$$\text{S.D.} = \sqrt{\frac{\sum x_i^2 - (\sum x_i)^2/n}{n - 1}} \quad 7.27$$

where n = number of values

x_i = individual values.

7.6 The Stopped Flow Method:

Two different stopped flow instruments were used.

(a) Principle of the stopped flow method:

The stopped flow method^{13, 16} is used for determining kinetic parameters within the typical time range of 10^2 to 10^{-3} seconds. Two solutions, each containing one of the reactants, flow rapidly through mixing chamber. The solutions having mixed, the flow is very rapidly stopped, so abruptly that the fall in velocity to zero is rapid compared to the delay time, which is the time between mixing and observation. If two reactants solutions A and B travel a distance 'd' cm, after mixing (Figure 7.2) before being observed, with a velocity 'V' metres per second, then the delay time 't₀' is simply

$$t_0 = \frac{d}{100V} \text{ sec} = \frac{10d}{V} \text{ millisecc.}$$

For a velocity of 5 metres per second which is easily obtained and for a distance 'd' 0.5 cm, the solution is 1 millisecond old when one observes the reaction. It is necessary to use a rapid method, usually spectrophotometric or fluorimetric, to observe the changes due to the reaction. There are many varieties of stopped flow spectrophotometer, each having their own experimental limitations.

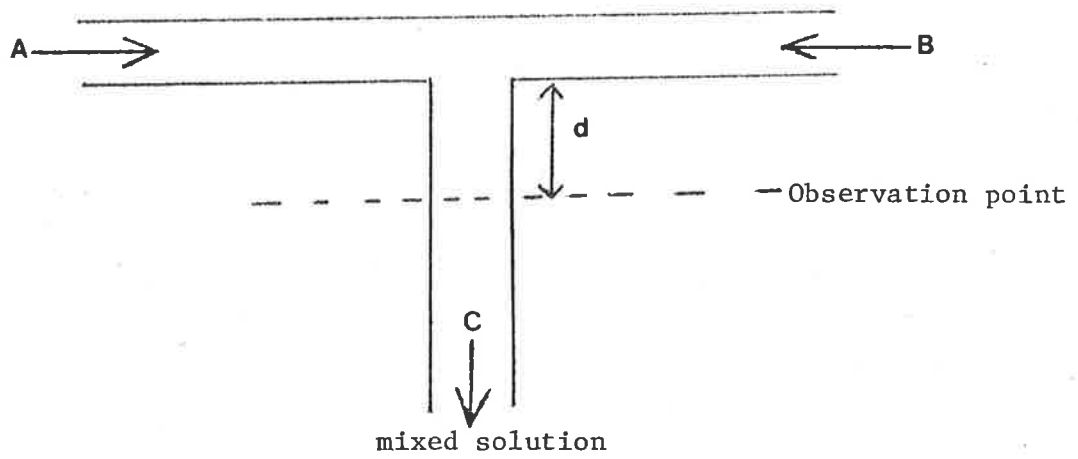


Figure 7.2 Principle of Flow Method

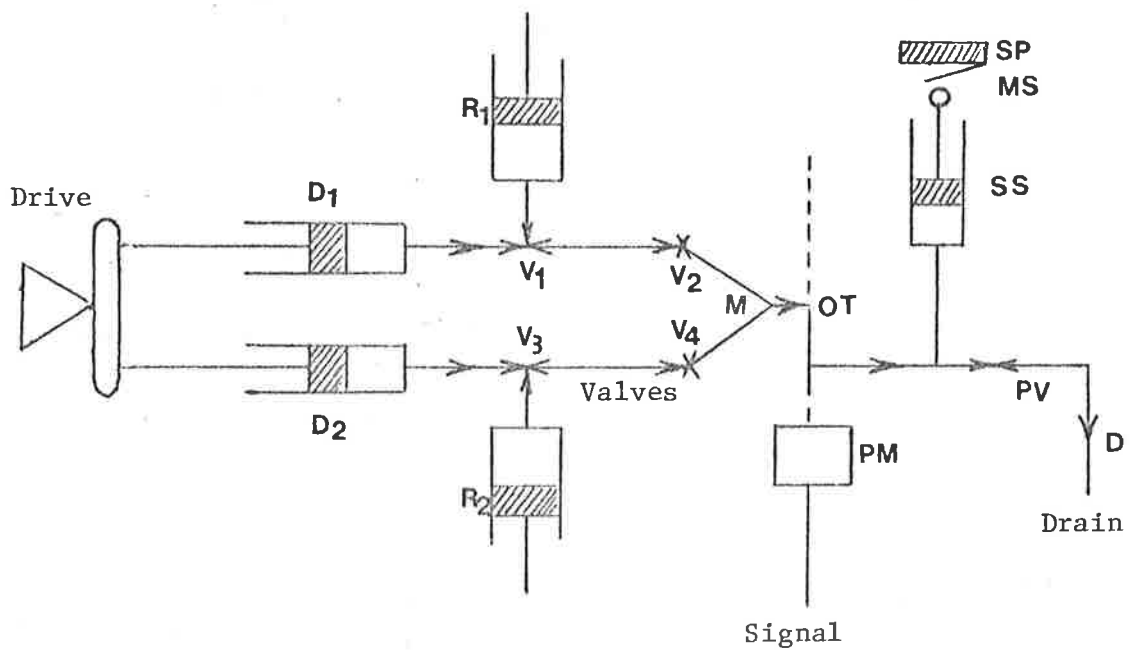


Figure 7.3 Stopped Flow Apparatus

(diagram from Dr. G.S. Laurence, "Instructions for using the stopped flow apparatus", University of Adelaide, 1976).

(b) The Stopped Flow Apparatus:-

The stopped flow apparatus was assembled in this department, using a rapid mixing device devised by Dr. P. Moore, University of Warwick. The apparatus is mounted in a water bath for controlling the temperature. The reactant solutions from reservoir syringes $[R_1, R_2]$ (Figure 7.3) are introduced into the 2.0 cm^3 driving syringes $[D_1, D_2]$ using the valves V_1 and V_3 . Valves V_1 and V_3 are closed, V_2 and V_4 are set about half a turn from fully closed position and the reagents are driven together rapidly into the specially designed mixer $[M]$ by a hydraulic piston acting on the plungers of the driving syringes. The path length of the cell is two centimetres. During a run, the mixed solution leaves the observation tube $[OT]$ and enters the 2.0 cm^3 stopping syringe $[SS]$. As soon as the plunger of the stopping syringe hits the stopping plate $[SP]$, the flow is abruptly stopped, the microswitch $[MS]$ is closed and sends a trigger pulse to the trigger input of the recorder (a biomatron 610 digital recorder in this case). The monitoring light beam, supplied by a tungsten lamp through a monochromator to select an appropriate wavelength, is focussed into the centre of the observation tube $[OT]$ and the light transmitted is detected continuously by the photomultiplier. The signal from the photomultiplier is fed into the Biomatron transient recorder, then to an oscilloscope and finally to a Rikendenshi chart recorder.

If the intensity of the light transmitted through the observation tube is I , then

$$V = CI$$

7.28

where V = voltage from photomultiplier

C = constant for a fixed photomultiplier voltage

When solvent alone is in the observation tube, then

$$V_o = CI_o \quad 7.29$$

(V_o and I_o are the solvent voltage and intensity, respectively).

The absorbance (A) at any time for the species being monitored can be calculated from the voltage derived from the photomultiplier when that species is present in the observation tube.

$$A = \log_{10} \frac{I_o}{I} = \log_{10} \frac{V_o}{V} \quad 7.30$$

and the variation of the voltage with time as the reaction proceeds can be analysed to give the kinetic data.

The Biomation transient recorder samples the photomultiplier voltage at frequent intervals and stores a digital record of the voltage from each sampling in its memory. The resultant record of voltage versus time is displayed as a much reduced speed as an oscilloscope trace and on the Rikendenshi chart recorder. The sample interval should be chosen so that one half life = 50 x sample interval. Appropriate settings of sample interval and volts full scale switches are determined in trial runs. The photomultiplier voltage is set to give an output voltage of about 0.50 to 5.0 volts on the signal voltmeter. The filter time constant is normally set to 1 msec but can be increased for slower reactions if necessary. The reaction should be followed for at least five half lives (97% reaction) to be sure that the final voltage which is read out from signal voltmeter when it is steady at the end of each run, is close to that for 100% reaction. Figure 7.4 shows the schematic diagram of power supply and signal connections.

(c) Analysis of Stopped Flow Traces:-

A reaction causing an increase in absorbance is accompanied by a fall in the voltage signal and less light transmission whereas a decrease in absorbance is accompanied by a rise in the voltage signal

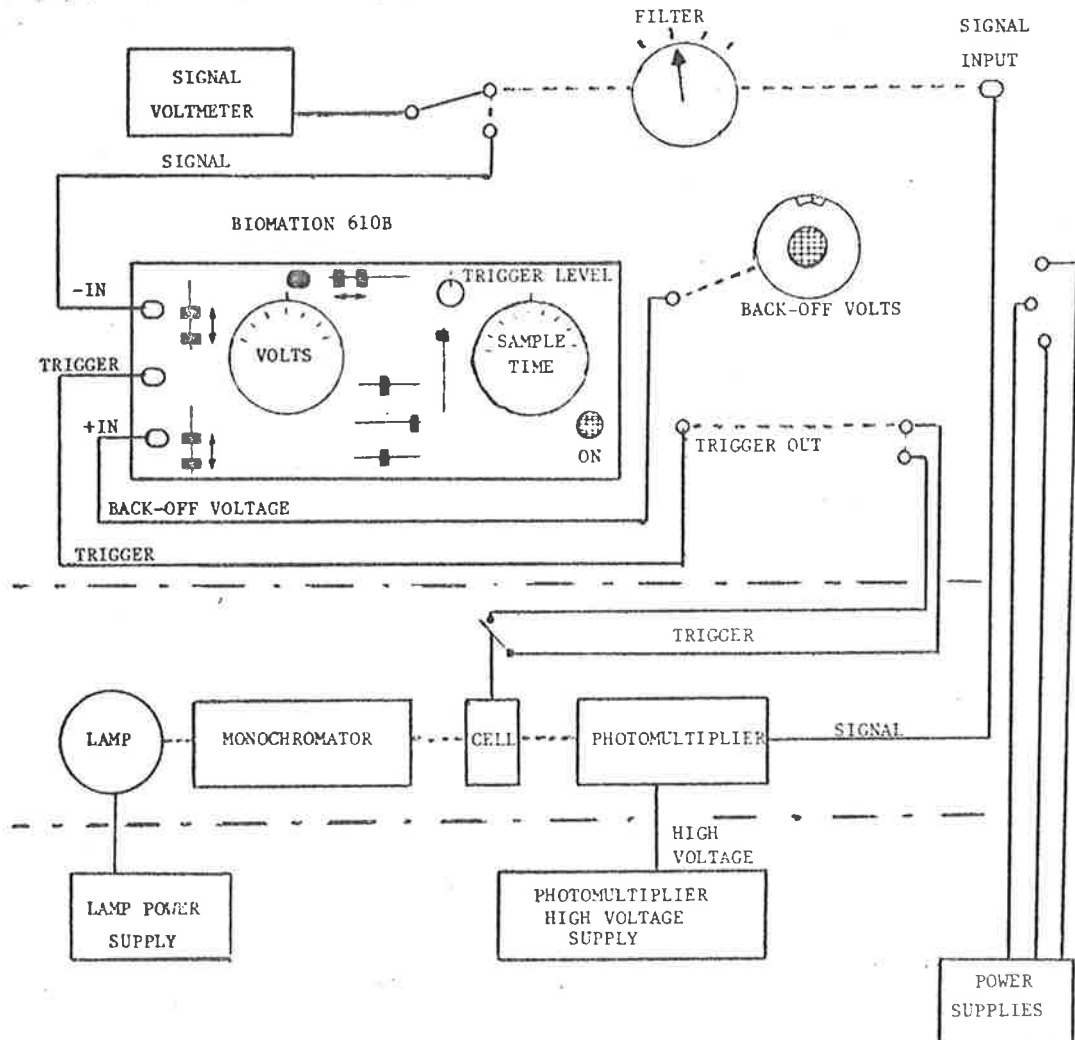


Figure 7.4

Schematic diagram of power supply and signal connections
 (diagram from Dr. G.S. Laurence, "Instructions for using the
 stopped flow apparatus", University of Adelaide, 1976).

and therefore more light transmission. The trace shown in Figure 7.5 is a case in which the absorbance decreases during the reaction. If various values of y_t are read from the trace relative to y_∞ , then we have

$$V_t = V_{\text{meter}_\infty} + \frac{y_t \times \text{volts full scale}}{\text{Full width of paper}} \quad 7.31$$

$$\text{and } V_o = V_{\text{meter}_\infty} + \frac{y_o \times \text{volts full scale}}{\text{Full width of paper}} \quad 7.32$$

where V_t = voltage at time 't',

V_{meter_∞} = voltage at time infinity

V_o = initial voltage

(V_{meter_∞} , V_o , V_t and V_∞ are negative)

For an increase in absorbance, the curve is inverted with respect to that shown in Figure 7.5, the positive sign in equations 7.31 and 7.32 must be replaced by a negative sign.

(d) Estimation of the rate constant for the 1st Order Process:-

The reactions were studied under pseudo 1st order conditions in which one reactant is at least ten times higher concentrated than the other. All solutions were degassed using a water pump. For a reaction where A_o , A and A_∞ are the absorbances at zero, 't' and infinite time, respectively, then for a rate constant k , it is shown²¹ that

$$\ln [(A - A_\infty)/(A_o - A_\infty)] = -kt \quad 7.33$$

$$\text{or } \log_{10} [(A - A_\infty)/(A_o - A_\infty)] = -\frac{kt}{2.303} \quad 7.34$$

Again, we know

$$A = \log \frac{V_o}{V} \quad 7.35$$

$$\text{So } A - A_\infty = \log_{10} \frac{V_\infty}{V_t} \quad \text{if } A > A_\infty \quad 7.36$$

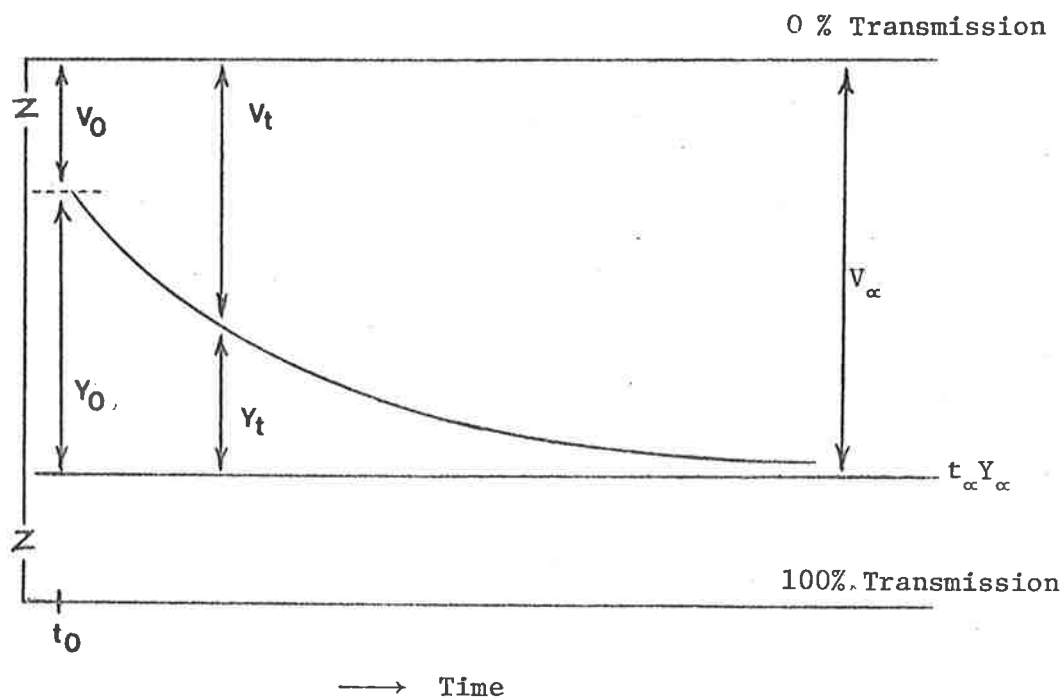


Figure 7.5

Typical stopped flow trace for a reaction with decreasing absorbance
(not to scale)

(diagram from Dr. P. Moore, "Stopped Flow, An Experimental Manual",
University of Warwick, 1972).

$$A_{\infty} - A = \log_{10} \frac{V_t}{V_{\infty}} \quad \text{if } A < A_{\infty} \quad 7.37$$

and inserting these into the equation 7.34, we have finally,
eliminating V_{∞}/V_0 :

(i) for a decrease in absorbance

$$\log_{10} \left[\log_{10} \left(\frac{V_{\infty}}{V_t} \right) \right] = C - \frac{kt}{2.303} \quad 7.38$$

(ii) for an increase in absorbance

$$\log_{10} \left[\log_{10} \left(\frac{V_t}{V_{\infty}} \right) \right] = C - \frac{kt}{2.303} \quad 7.39$$

A least squares programme was used to estimate a slope which when multiplied by -2.303 will be the rate constant for the reaction. At least three traces were analysed for each reaction mixture and the mean value was used. The formula used for the standard deviation of the mean value is as follows:-

$$S.D = \sqrt{\frac{\sum xi^2 - (\sum xi)^2/n}{n-1}} \quad 7.40$$

where n = number of values,

xi = individual value.

(e) Estimation of the Apparatus dead time:-

An approximate value of the dead time can be estimated in the following way.²² Two reactions, one slow and one fast, should be carried out for the determination of the dead time. For a reaction involving decrease in absorbance, the initial absorbance, A_1 , for the slower reaction will be greater than the initial absorbance, A_2 , for the faster reaction. Since the dead time for the slower reaction will be negligible, A_1 can be taken as A_0 (absorbance at zero time) for the faster reaction. Then the dead time can be determined from equation 7.41

$$\text{dead time} = \frac{\ln [(A_1 - A_{\infty}) / (A_2 - A_{\infty})]}{k} \quad 7.41$$

the value of k for the faster reaction being estimated as described in section 7.6(d). For example, the dead time could be measured by following potassium ferrocyanide ($K_4Fe(CN)_6$) and ascorbic acid reactions, one at very low concentration (slower reaction) and the other at very high concentration (faster reaction).

(f) Second Variety of Stopped Flow Apparatus:-

The second type of stopped flow apparatus shown in Figure 7.6, is based on the concept of E. Faeder.²³ The reactant solutions, stored in thermostated drive syringes are driven into the mixing chamber by means of a piston to which pressure is to be applied from a nitrogen gas cylinder at about 6 p.s.i. pressure. The piston is connected to a rod with a threaded cylindrical mechanical stop which is to be wound back about six revolutions before applying the pressure by a valve switch on the pressure line. The piston, on application of pressure, moves forward introducing about 0.2 cm^3 solution from each syringe into the mixing chamber. The flow stops when the solution enters into waste syringe and the mechanical stop actuates a microswitch thus triggering the storage oscilloscope. The drive syringes can be filled by means of two "three" position luer lock valves from reservoir syringes. An eight jet¹⁷ tangential mixer, employed for efficient and fast mixing, leads to the observation chamber by two millimetre diameter tubes. The path length of the cell is 2.0 cm. The output from the photomultiplier which is fed into the input of a Data Lab 905 transient recorder and is backed off against a 2.0 voltage supply. Stored traces can be displayed on an oscilloscope. The Data Lab 905 is also connected to a chart recorder and the trace may be recorded on the chart paper. If the

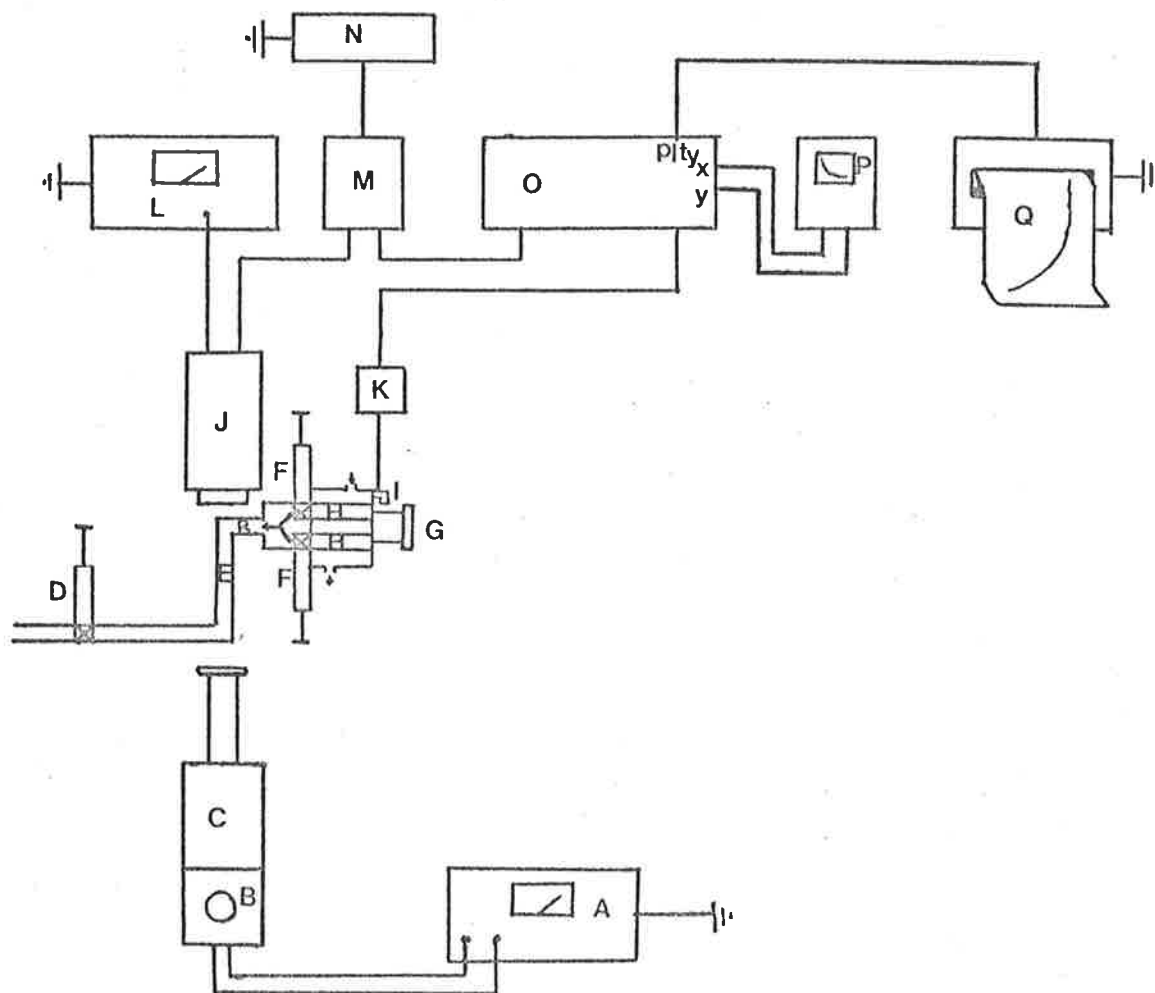


Figure 7.6

Schematic diagram for the stopped flow apparatus

- | | |
|-------------------------------|----------------------------------|
| A = light source power supply | J = 7 dynode photomultiplier |
| B = light source | K = trigger voltage source |
| C = monochromator | L = photomultiplier power supply |
| D = waste syringe | M = back off voltage supply |
| E = observation cell (2cm) | N = digital voltmeter |
| F = reservoir syringes | O = data lab DL905 |
| G = nitrogen pressure push | P = oscilloscope |
| H = drive syringes | Q = H.P. stripchart recorder |
| I = trigger microswitch | R = mixing chamber |

(diagram from B.G. Doddridge, University of Adelaide).

reaction is very slow, the trace can be directly recorded on the chart paper without the use of the Data Lab. Most of the traces were recorded onto the chart paper using oscilloscope and data lab. The equation used for calculation of observed rate constant was already described in section 7.6(d) and kinetic data were obtained using the L.S.I. 11 computer.²⁴

The observation cell must be located very close to the mixing chamber to minimise the time between mixing and observation. The light source is a quartz iodide lamp, enclosed in a light proof housing and connected to a constant voltage supply. The light passes through the entrance and exit slit of a Bausch and Lomb high intensity grating monochromator. A diaphragm was used to regulate the width of the light beam. This is a more accurate instrument than the other instrument and all non-aqueous experiments were carried out using this instrument. The instrument was set up inside the fume hood and all other precautionary measures were taken when using the toxic solvent dmf. The dead time of the instrument was found to be 4 ms by B. G. Doddridge, University of Adelaide. Some substitution reactions in aqueous solution were also studied using this instrument. In order to simplify the mathematical treatment, all experiments were carried out under pseudo 1st order conditions.

REFERENCES FOR CHAPTER SEVEN

1. S. Glasstone and D. Lewis, "Elements of Physical Chemistry", second edition, Macmillan and Co. Ltd., London, (1963).
2. B. N. Figgis and J. Lewis, "Modern Co-ordination Chemistry", edited by J. Lewis and R. G. Wilkins, Interscience, New York, (1960).
3. S. S. Bhatnagar and K. N. Mathur, "Physical Principles and Applications of Magnetochemistry", Macmillan, London, (1935).
4. P. W. Selwood, "Magnetochemistry", 2nd edn., Interscience, New York (1956).
5. R. C. Weast, Ed., "Hand Book of Chemistry and Physics", The Chemical Rubber Co., 57th edition, (1976-77).
6. D. F. Evans, J. Chem. Soc., 2003 (1959).
7. F. A. Cotton and G. Wilkinson, Advanced Inorganic Chemistry, 3rd ed., second Wiley Eastern reprint, (1978).
8. D. M. Adams and J. B. Raynor, "Advanced Practical Inorganic Chemistry", John Wiley, London, (1965).
9. P. Job, Ann. Chim., Paris, 9, 113 (1928).
10. T. J. Swift and R. E. Connick, J. Chem. Phys., 37, 307 (1962); 41, 2553 (1964).
11. C. H. Bamford and C. F. H. Tipper edited "Comprehensive Chemical Kinetics", Vol. 1, "The Practice of Kinetics", Elsevier, Amsterdam (1969).
12. E. M. Eyring and D. L. Cole in "Fast Reactions and Primary Processes in Chemical Kinetics", S. Claesson, Ed., Interscience, (1967).
13. E. F. Caldin, "Fast Reactions in Solution", Oxf Blackwell Scientific Pubs. (1964).
14. G. H. Czerlinski, "Chemical Relaxation", Dekker, New York, (1966).
15. I Amdin and G. G. Hammes, "Chemical Kinetics, Principles and Selected Topics", McGraw-Hill, New York (1966).
16. C. F. Bernasconi, "Relaxation Kinetics", Academic Press, New York, (1976).

17. S. L. Freiss, Techniques of Organic Chemistry, Vol. VIII, Investigation of Rates and Mechanisms of Reactions, Part II, 2nd ed. (1961)
18. P. R. Collins, Ph.D. thesis, University of Adelaide (1979).
19. G. Czerlinski and M. Eigen, Zeit Electrochem., 63, 652 (1959).
20. J. E. Erman and G. G. Hammes, Rev. Sci. Instr., 37, 746 (1966).
21. A. A. Frost and R. G. Pearson, "Kinetics and Mechanisms", Wiley, New York, 31 (1961).
22. P. Moore, Stopped Flow, an Experimental Manual, Molecular Sciences, University of Warwick. (1972).
23. E. J. Faeder, Ph.D. thesis, Cornell University, Ithaca, New York, (1970).
24. A computer programme, "SFTRN" written for stopped flow trace analysis by B. G. Doddridge, University of Adelaide.

PUBLICATION FROM THIS WORK

Oxygen-17 Magnetic Resonance and Temperature-Jump Spectrophotometric Study of the Square Planar-Octahedral Equilibrium in the 1,4,7,10-tetraazacyclododecanenickel(II) System.

John H. Coates, Dewan A. Hadi, Stephen F. Lincoln*, Harold W. Dodgen and John P. Hunt*.

Inorganic Chemistry, 20, 707-711 (1981).